Delft University of Technology

Shifting the limits of nut coke use in the ironmaking blast furnace

A fundamental study on the behaviour of ferrous raw material bed mixed with nut coke

Gavel, Dharm Jeet

DOI
10.4233/uuid:f2aeb72a-f68f-480d-a811-3093055e9320

Publication date
2020

Document Version
Final published version

Citation (APA)
Gavel, D. J. (2020). *Shifting the limits of nut coke use in the ironmaking blast furnace: A fundamental study on the behaviour of ferrous raw material bed mixed with nut coke*. [Dissertation (TU Delft), Delft University of Technology]. https://doi.org/10.4233/uuid:f2aeb72a-f68f-480d-a811-3093055e9320

Important note
To cite this publication, please use the final published version (if applicable).
Please check the document version above.

Copyright
Other than for strictly personal use, it is not permitted to download, forward or distribute the text or part of it, without the consent of the author(s) and/or copyright holder(s), unless the work is under an open content license such as Creative Commons.

Takedown policy
Please contact us and provide details if you believe this document breaches copyrights.
We will remove access to the work immediately and investigate your claim.

This work is downloaded from Delft University of Technology.
For technical reasons the number of authors shown on this cover page is limited to a maximum of 10.

Shifting the limits of nut coke use in the ironmaking blast furnace

A fundamental study on the behaviour of ferrous raw material bed mixed with nut coke

Dharm Jeet Gavel

Shifting the limits of nut coke use in the ironmaking blast furnace

A fundamental study on the behaviour of ferrous raw material bed mixed with nut coke

Dissertation

for the purpose of obtaining the degree of doctor
at Delft University of Technology
by the authority of the Rector Magnificus prof.dr.ir. T.H.J.J. van der Hagen,
chair of the Board for Doctorates,
to be defended publicly on
Wednesday 11 March 2020 at 10:00 o'clock

by

Dharm Jeet Gavel

Master of Materials Science and Engineering,
Indian Institute of Science, Bangalore, India
Born in Balco Korba, Chhattisgarh, India.

This dissertation has been approved by the promotors.

Composition of the doctoral committee:

Rector Magnificus,	chairperson
Dr. Y. Yang	Delft University of Technology, promotor
Prof.dr.ir. J. Sietsma	Delft University of Technology, promotor

Independent members:

Prof.dr. J. Dik	Delft University of Technology
Prof.dr.ir. J. Schenk	Montanuniversität Leoben, Austria
Prof.dr. T. Fabritius	University of Oulu, Finland
Dr.ir. W. Husslage - van Kaam	Tata Steel Europe, Netherlands
Prof.dr. M. Santofimia Navarro	Delft University of Technology (reserve member)

Other member:

Prof.dr. R. Boom	Delft University of Technology, member

Keywords:	Ironmaking; blast furnace; nut coke; reduction; softening; melting; dripping; permeability.
Printed by:	Ipskamp printing
Cover:	Various benefits potentials of nut coke use in the blast furnace, presented in the classical Delft blue tiles.
Cover design:	Harald Pieper (In Zicht Ontwerp) and Chandrakanta Gavel

Copyright © 2020 by Dharm Jeet Gavel
E-mail: dj.gavel10@gmail.com

ISBN 978-94-028-1969-4
An electronic version of this dissertation is available at http://repository.tudelft.nl

To my mother

Late. Smt. Khageshwari Devi Gavel

TABLE OF CONTENTS

1. Introduction

1.1 Background

Steel is an essential material for the development of a sustainable society. World crude steel production has increased from 189 million tonnes per annum in the year 1950 to 1808 million tonnes per annum in the year 2018 [1]. It is expected to grow with a steady rate in the time to come. Alloy of iron and carbon (0.05 - 2.14 % C) is steel, which is primarily produced by the decarburisation of pig iron (3.5 - 4.5 % C). To meet the future iron demand for the production of steel, the blast furnace (BF) is expected to remain a dominant ironmaking technology [2].

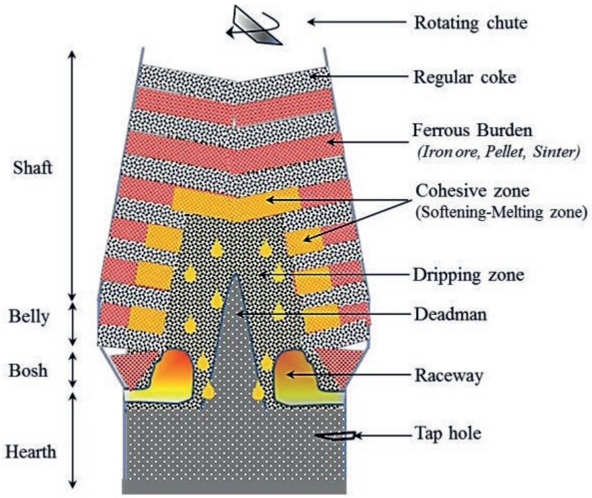

Fig. 1.1 Schematic of the ironmaking blast furnace (˜40 m tall).

The ironmaking blast furnace is a countercurrent reactor in which the solid raw materials (ferrous ore burden and coke) are charged from the top and oxygen-enriched air is introduced from the lower part of the furnace (Fig. 1.1). During the downward movement, the ferrous raw materials (iron ore, pellet and sinter) are reduced, soften and melt to reach the hearth of the blast furnace. Thereafter, the liquid iron, called hot metal or pig iron is tapped out for further processing in the steelmaking plant.

Since a blast furnace is a countercurrent reactor, it requires gas permeability at all levels. In the shaft of the furnace, permeability is achieved by using raw materials with large size and high strength. For ferrous burden, the optimum size is 8-30 mm, allowing it to be reduced to wüstite (FeO) before it reaches the high-temperature zone of the furnace [3].

For the chemical reduction of the ferrous burden, reducing gas is required, which is generated by the partial combustion of the carbon. In the lower part of the blast furnace, this carbon source acts as an iron carburiser and supplies heat to meet the energy demand of the endothermic reactions. Additionally, it is a requirement for this carbon source to be mechanically stable and possess temperature-based reactivity to sustain the blast furnace conditions. To meet these stringent requirements, metallurgical coke is produced by heating coal in the absence of air inside the coke ovens. When the coal is heated, its volatile matter vaporises due to which the coal shrinks and cracks. After about 18 hours of heating, coke is ready to be pushed out of the oven.

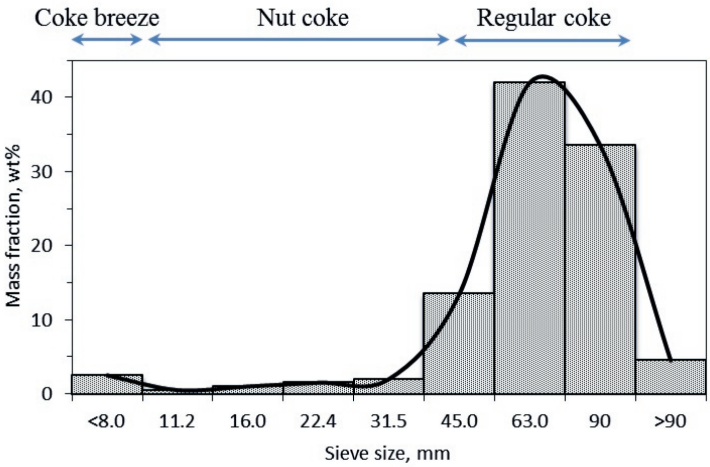

Fig. 1.2 Coke size distribution, adapted from Jenkins et al. [4].

The normal distribution of the coke particle size prepared from the oven is shown in Figure 1.2. Only coke size in the range of 40-80 mm (regular coke) is suitable for direct utilisation in the blast furnace. The small-sized coke tends to fill up the interstitial voids around the coarse ones, which results in a reduced porosity of the packed bed. Thus, the applied coke range is kept narrow to avoid tight packing of the bed. Due to this strict size demand for the regular coke in the blast furnace, a large fraction of under-sized coke is generated in the coke production process. The coke size less than 40 mm is divided into two size fractions: coke breeze (below 8 mm) and nut coke (8-40 mm). Because of the fine size, coke breeze finds its use in the sinter plant. However, the “Nut coke” lacks potential use inside or outside the steel plant.

Regular coke (40-80 mm) cannot be mixed with small sized ferrous burden (8-30 mm). As the ferrous burden softens and melts in the high-temperature zone (cohesive zone) of the furnace, it becomes practically impermeable for the gas flow. A passage for gas is required to continue the process, which is sustained by the presence of coke slits. Therefore, the ferrous raw material and regular coke are charged in alternate layers in the blast furnace.

Blast furnace productivity and process stability are strongly dependent on the gas permeability [3]. Furthermore, high permeability will increase the gas inlet capacity of the blast furnace, which will enhance the reaction kinetics to improve productivity. As the gas moves up in the blast furnace, the raw material resists the gas flow, which limits productivity. In the dry zone, i.e., in the shaft, around 35 % of the total pressure drop occurs [5]. This is primarily due to the gas resistance at the interface between the ferrous and coke layers [6]. Interfacial resistance cannot be avoided in blast furnaces with the conventional raw materials and layer charging style.

Furthermore, in the cohesive zone, around 25 % of the total pressure drop occurs [5], which is due to the presence of an impermeable (semi-fused) ferrous layer. It is believed that the size and location of the cohesive zone govern the gaseous (indirect) reduction reactions of the ferrous burden, controlling the fuel efficiency of the furnace. Therefore, several efforts have already been made to improve the dimension [7] and the position of the cohesive zone by changing the ferrous burden chemistry [8-10]. However, these have resulted in only marginal process improvement.

Therefore, with the aim to substantially improve the blast furnace productivity by enhancing gas permeability, mixing nut coke with the ferrous burden was proposed [11]. Mixed charging will provide an excellent opportunity to utilise the nut coke generated from the coke making process. Additionally, the nut coke utilisation will improve the process efficiency, reducing the coke demand for metal production [12]. Therefore, effective utilisation of the nut coke as a replacement of the regular coke will give an economic and environmental (lower CO_2 emission) advantage to the iron makers.

Therefore, a fundamental understanding of the nut coke mixed ferrous raw material (pellet and/or sinter) bed behaviour is of utmost importance to effectively utilise the nut coke in the blast furnace. In modern blast furnaces, the ferrous burden is generally a mixture of 2-4 types (pellets and sinters) of prepared iron oxides and/or raw iron lump ore. These raw materials are utilised in different proportions to satisfy the economic and chemical trade offset. The interactions among these chemically diverse raw materials naturally affect the blast furnace performance. Moreover, the level of interaction varies with the chemistry and added proportion of these raw materials. The nut coke mixing with ferrous burden further complicates the interaction behaviour in the bed.

Though nut coke is expected to improve the reaction kinetics, its net effect on the length and temperature range of the thermal reserve zone is not apparent [13]. Additionally, the influence on the softening and melting properties is not straightforward [14]. Particularly, the bed permeability with nut coke addition is not studied systematically [15-16] .

Under blast furnace conditions, the freshly reduced (solid) iron first carburises, later melts and drips away from the cohesive zone. While dripping out from the coke bed, the liquid (metal and slag) interacts with coke in a specific manner. Considering the stochastic nature of the liquid dripping from the bed in the absence of nut coke [17], it is essential to understand the carburisation, melting and dripping properties in the presence of the nut coke.

Furthermore, the nut coke is utilised as a partial replacement of the regular coke in the blast furnace. As a result of the replacement, the regular coke layer becomes thinner in the blast furnace, which is consequently speculated to have a negative impact on the overall furnace permeability [18].

Moreover, with higher auxiliary fuel/reductant (coal, plastics or H_2-gas) injections and regular coke replacement with the nut coke, a complete mixing scenario for ferrous raw materials with coke could arise in the near future of the ironmaking blast furnace. Hence, it is interesting to explore the concept and the bed behaviour and performance of complete nut coke mixed (100 % replacement of the regular coke) charging with the ferrous burden in the blast furnace.

Therefore, for effective utilisation of the nut coke, it is highly important to evaluate the physicochemical effects induced by variation in added nut coke concentration, on the furnace performance.

1.2 Principal question and method

The aim of this PhD thesis is to understand the physicochemical behaviour of nut coke mixed ferrous bed under blast furnace conditions. In the present study, a Reduction Softening and Melting (RSM) furnace is utilised to simulate blast furnace conditions in the laboratory. The RSM furnace was developed during a previous PhD project at Delft University of Technology [6] in close cooperation with Tata Steel Europe and Materials innovation institute (M2i).

RSM furnace is a type of experimental blast furnace simulator, and it is possible to vary the temperature and gas inlet composition with time, which provides the ability to simulate the blast furnace conditions in a stationary bed of raw material. The thermal and gas profile followed during the experiments are based on the information derived from the vertical probing of the blast furnace [19]. The blast furnace load condition is simulated by applying a load on top of the sample bed.

1.3 Objectives and structure of the thesis

Chapters (2, 4, 5, 6, 7 and 8) in this thesis are based on scientific articles which are either published or prepared for the submission in an international journal. Consequently, these chapters are partially similar to the published work and partly adapted to augment the understanding. Therefore, readers might find some degree of recurrence in some part of these chapters. The thesis consists of 9 chapters they are structured as follows.

In **Chapter 2,** a comprehensive review is presented on the state of the art of the use of nut coke at various blast furnaces around the world. The expected effects of the nut coke use on the permeability, thermal reserve zone (TRZ), reduction kinetics, softening and melting behaviour are discussed in reference to the laboratory and blast furnace trials performed globally. Challenges and scope for higher nut coke utilisation are identified via a systematic review.

To develop an understanding of the ferrous bed behaviour under mixed charge condition, high-temperature experiments are performed under simulated blast furnace conditions in the Reduction Softening and Melting (RSM) apparatus. In **Chapter 3,** the background and design of the high temperature (20 – 1550 ^{o}C) experiments are described. The facilities utilised for the present studies and operational procedure are introduced. The method for the result analysis (bed contraction, pressure drop and gas analysis) and interpretation are elucidated in detail.

In **Chapter 4,** the results are discussed of characterisation studies performed on the quenched sample bed from the previous PhD project [6]. The detailed characterisation studies were performed on the iron ore pellets quenched during sintering, softening and before complete melting. The principal role played by the nut coke is discussed in close comparison with the case when nut coke was absent in the bed.

Then, a series of high-temperature experiments (20-1550 ^{o}C) was performed in the RSM apparatus to investigate the effects of nut coke addition in the pellet bed. In **Chapter 5,** the physicochemical effects caused by the nut coke addition in the iron ore pellet bed are described. The influences of nut coke addition (0-40 wt%, as replacement of regular coke) on various stages of the bed shrinkage and permeability are discussed systematically. The effects of added nut coke size (10-15 mm, 15-20 mm and 20-25 mm) are explained and quantified.

Under the simulated blast furnace conditions, the iron ore pellets are reduced, soften, melt, and then drip out of the coke bed. The effect of nut coke on the melting and dripping behaviour of iron ore pellets is discussed in **Chapter 6**. The iron ore pellet beds were quenched at high temperatures to bring a clear understanding of the prime cause of the bed melting. This investigation further extends to develop an understanding of the liquid dripping pattern and chemical interaction at the time of liquid dripping in the presence of nut coke. To bring a clear contrast on the effect of nut coke mixing, results are compared with the case when nut coke is absent in the bed.

Thereafter, the effect of nut coke mixing with the ferrous burden (pellet and/or sinter) is discussed in **Chapter 7**. The effect of nut coke addition (20 and 40 wt%) is compared with the individual and mixed conditions. The effects on the critical temperatures and permeability are discussed statistically. Fundamentals of mixed burden interaction and effect of nut coke addition are explained by the characterisation of quenched sample beds.

Finally, the idea of complete mixing of the nut coke with the ferrous burden is explored in **Chapter 8**. The effect on gas permeability due to complete nut coke mixed charging as a replacement of the regular coke is scrutinized in the experiments. Impact of complete mixing on the physicochemical properties of the iron ore pellet and/or sinter bed was investigated. The principal functions of the coke and the consequences of regular coke replacement with nut coke in the blast furnace are discussed.

In **Chapter 9,** it is concluded that nut coke charging mixed with the ferrous burden increases the gas permeability, which will enhance the blast furnace productivity. Furthermore, the improved physicochemical properties of the ferrous bed in the presence of nut coke will enhance the efficiency of the blast furnace ironmaking process. In this chapter, other principal outcomes of the project and recommendations for further research are also conveyed.

1.4 References

[1] World Steel in figures 2019, www.worldsteel.org, 2019.

[2] J.P. Birat, Global technology roadmap for CCS in industry: Steel sectoral report, Amsterdam, 2010.

[3] A.K. Biswas, Principles of blast furnace iron making - theory and practice, Cootha Publishing House, Brisbane, Australia, 1981.

[4] D.R. Jenkins, D.E. Shaw, M.R. Mahoney, Fissure formation in coke. 3: Coke size distribution and statistical analysis, Fuel. 89 (2010) 1675–1689.

[5] M. Geerdes, R. Chaigneau, I. Kurunov, O. Lingiardi, J. Ricketts, Modern blast furnace ironmaking : an introduction, IOS Press, under the imprint of Delft University Press, Amsterdam, 2015.

[6] Q. Song, Effect of nut coke on the performance of the ironmaking blast furnace, PhD Thesis, Delft University of Technology, 2013.

[7] S. Ueda, T. Kon, H. Kurosawa, S. Natsui, T. Ariyama, H. Nogami, Influence of shape of cohesive zone on gas flow and permeability in the blast furnace analyzed by DEM-CFD model, ISIJ Int. 55 (2015) 1232–1236.

[8] K. Higuchi, T. Orimoto, F. Koizumi, H. Furuta, Y. Takamoto, T. Sato, K. Shinagawa, Quality improvement of sintered ore in relation to blast furnace operation, Nippon Steel Tech. Rep. 94 (2006) 36–41.

[9] K. Higuchi, M. Naito, M. Nakano, Y. Takamoto, Optimization of chemical composition and microstructure of iron ore sinter for low-temperature drip of molten iron with high

permeability, ISIJ Int. 44 (2004) 2057–2066.

[10] C.E. Loo, Important acid ferrous burden properties in the cohesive zone of a blast furnace, Miner. Process. Extr. Metall. 125 (2016) 187–196.

[11] V.I. Loginov, A.L. Berin, S.M. Solomatin, Effect of mixing burden with coke on blast furnace fluid mechanics and operation parameters, Stal. 5 (1977) 391–394.

[12] A. V. Kuzin, Effect of introducing different sizes of nut coke into the ore layer on the degree of reduction of iron oxides, Metallurgist. 57 (2014) 783–791.

[13] D.J. Gavel, A review on nut coke utilisation in the ironmaking blast furnaces, Mater. Sci. Technol. 33 (2017) 381–387.

[14] Q. Song, Y. Yang, R. Boom, Effect of nut coke on the reduction behavior in iron-making blast furnace, Baosteel Tech. Res. 9 (2015) 8–16.

[15] T. Kon, S. Natsui, S. Matsuhashi, S. Ueda, R. Inoue, T. Ariyama, Influence of cohesive zone thickness on gas flow in blast furnace analyzed by DEM-CFD model considering low coke operation, Steel Res. Int. 84 (2013) 1146–1156.

[16] S. Matsuhashi, H. Kurosawa, S. Natsui, T. Kon, S. Ueda, R. Inoue, T. Ariyama, Evaluation of coke mixed charging based on packed bed structure and gas permeability changes in blast furnace by DEM-CFD model, ISIJ Int. 52 (2012) 1990–1999.

[17] W.M. Husslage, M.A. Reuter, R.H. Heerema, T. Bakker, A.G.S. Steeghs, Flow of molten slag and iron at 1500 °C to 1600 °C through packed coke beds, Metall. Mater. Trans. B. 36B (2005) 765–776.

[18] K. Ichikawa, Y. Kashihara, N. Oyama, T. Hirosawa, J. Ishii, Evaluating effect of coke layer thickness on permeability by pressure drop estimation model, ISIJ Int. 57 (2017) 254–261.

[19] R. Chaigneau, H. Sportel, J. Trouw, R. Vos, J. Droog, Blast furnace burden quality: laboratory simulation, Ironmak. Steelmak. 24 (1997) 461–467.

2. Nut coke for the ironmaking blast furnace

As introduced in Chapter 1, nut coke as an inexpensive reductant can be utilised in the mixture with the ferrous burden to improve the blast furnace productivity. To mark the current status of the nut coke usage in blast furnaces around the world, a survey and overview are required. Additionally, a summary of the global trend in the research and developments concerning the nut coke use is necessary to identify the principal research questions for the effective utilisation of the nut coke. Therefore, in this chapter, a systematic review is presented of the current status of nut coke usage in various blast furnaces around the world. The level of nut coke mixing achieved and the corresponding effects realised are discussed quantitatively. The scientific challenges are identified and discussed in relation to various indicators of blast furnace performance like the shaft permeability, reduction kinetics, thermal reserve zone temperature and cohesive zone properties.

For effective utilisation of the nut coke, a scope of correlational research is identified which should incorporate the effects of the burden chemistry, carbon ordering, coke ash content, coke quality, reactivity and the burden distribution. To conclude the chapter various studies are discussed, which marks the limiting factors for the utilisation of nut coke in the blast furnaces.

This chapter is based on the published scientific paper

Dharm Jeet Gavel, “A review on nut coke utilisation in the iron making blast furnaces”, Materials Science and Technology, 33 (2017) 381-387.

2.1 Background

In the blast furnace route of ironmaking, metallurgical coke is used for three main purposes: first (chemical) to act as a reducing agent and iron carburiser, second (thermal) to fulfil the energy demand of the endothermic reduction reactions and for heating and melting of the raw materials and products, third (physical) to maintain the structure and permeability inside the furnace. In the conventional ironmaking practice, ferrous burden (iron ore, sinter and pellets) and regular coke are charged in alternate layers. For consistent blast furnace operation, the desired regular coke size range is 40–80 mm. This strict size and quality demand for regular coke results in a surplus of undersize coke (smaller than 40 mm), which is broadly divided into two size ranges. Coke particles from 8-40 mm known as “nut coke” and the coke below 8 mm as “coke breeze”. The nut coke definition is less strict, it varies with raw material management policy of different companies. It can be 8-25 mm, 8-30 mm or 8-35 mm. The coke breeze, due to its smaller size is efficiently utilised in iron ore sintering. On the other hand, nut coke is not able to utilise effectively inside and outside the steel industry.

It was suggested to utilise a small amount of nut coke with the ferrous burden to improve the reduction kinetics and gas permeability in the blast furnace [1-2]. The positive effect of nut coke mixing was also found on the Thermal Reserve Zone (TRZ) temperature and softening and melting properties of the ferrous burden [3-4]. However, there are some factors which could limit the nut coke use in the blast furnace. They are: (1) Coke layer thickness, as the nut coke is charged as the replacement of regular coke, the coke layer thickness diminishes, which could result in reduced overall furnace permeability [5]; and (2) drainage in hearth, higher nut coke utilisation could lead to improper hearth permeability due to the presence of fine unconsumed coke and coal particles in the deadman [6]. Therefore, nut coke should be utilised in the optimum concentration. This requires a fundamental understanding of nut coke interaction with the ferrous burden. Furthermore, quantified information of various effects is necessary for effective nut coke utilisation.

Therefore, a survey is required to know the current state of nut coke use in the ironmaking blast furnace. Thus in this chapter, the scope of effective utilisation of nut coke is explored by a systematic review of the scientific literature.

2.2 State of the art - nut coke utilisation

To improve the reduction kinetics and gas permeability in the blast furnace, Loginov et al. [1] first suggested the idea of mixed charging of nut coke with the ferrous burden. Additionally, the utilisation of the cheaper reductant (nut coke) in place of expensive regular coke has provided an economic advantage to the iron and steel industry. Thus, the idea of nut coke charging mixed with the ferrous burden is widely accepted among the iron-makers. The nut coke usage as a replacement of the regular coke for different blast furnaces around the world is shown in Figure 2.1. Detailed information about the blast furnace location is given in Table 2.1. The optimum nut coke concentration is not apparent from the literature. The nut coke usage was observed to vary from a few to 140 kilograms per ton hot metal (kg/thm).

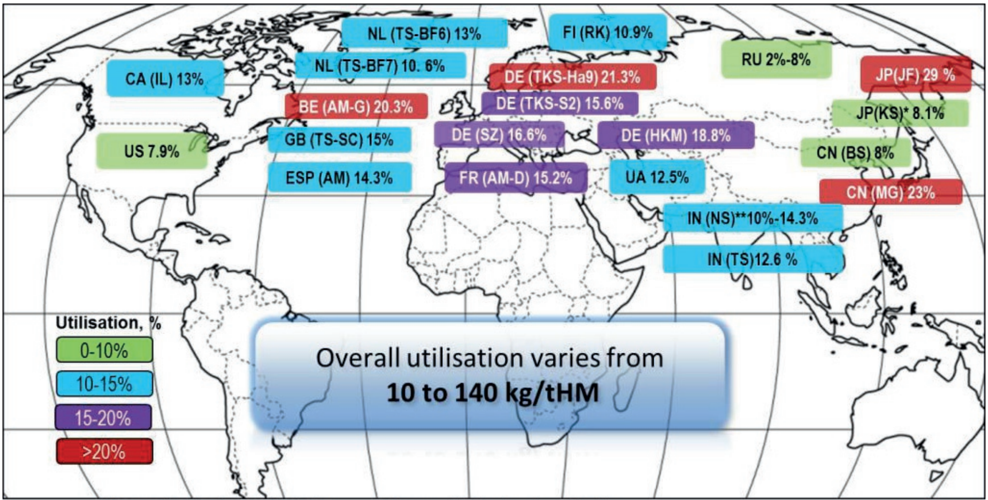

*Assumed total coke rate 370kg/thm **Assumed total coke rate 420kg/thm

Fig. 2.1 Nut coke utilisation in different blast furnaces around the world [7-16].

Possible reasons for variation in the nut coke utilisation are: (a) blast furnace operation philosophy differs with the company; (b) burden chemistry varies with the region, and (c) fundamental understanding of nut coke interaction with burden is limited.

2.3 Effect of nut coke on blast furnace performance

2.3.1 Shaft permeability

The blast furnace productivity can be enhanced by improving blast (gas) intake capacity [17]. Due to the resistance offered by the burden to the gas flow, a pressure drop occurs. Based on a series of cold model experiments, Babich et al. [18-19] and Song [13] recommended that the use of nut coke in a mixture with the ferrous burden could enhance the gas permeability in the dry zone of the blast furnace. It was estimated that the beneficial effect on the gas permeability of the ferrous burden layer diminishes with an increase in nut coke addition at higher levels (Fig. 2.2) [18]. It was suggested that by the use of 10 wt% and 20 wt% nut coke with the ferrous burden, the blast furnace productivity could be enhanced by 1.5 % and 2.5 %, respectively [19].

Table 2.1. Current state of nut coke utilisation in ironmaking blast furnaces.

Region (2 letter ISO code)	Company (abbreviation)	Blast furnace/ places	Nut coke consumption (kg/thm)	Regular coke (kg/thm)	Nut coke utilisation, %	Reference
China (CN)	Baosteel (BS)	Shanghai	26.0	300	7.9 %	[9]
	Magang (MG)	-	83.0	278	22.9 %	[9]
Belgium (BE)	ArcelorMittal (AM)	Gent	66.5	262	20.3 %	[8]
France (FR)	ArcelorMittal (AM)	Dunkirk	47.8	266	15.3 %	[8]
Finland (FI)	Ruukki (RK)	Rahe	39.0	319	10.9 %	[8]
Germany (DE)	ThyssenKrupp (TKS)	Ha	70.9	262	21.2 %	[8]
		S2	53.5	290	20.0 %	[8]
	HKM	-	66.8	289	18.8 %	[8]
	SZFG	BF A and B	75.0	375	16.6 %	[14]
Japan (JP)	Kobe Steel (KS)	Kakogawa	17-30	-	-	[10]
	JFE	BF 6, Chiba	116.0	279	29.4 %	[15]
Netherlands (NL)	Tata Steel (TS)	BF6	35.3	246	12.5 %	[8]
		BF7	32.1	271	10.6 %	[8]
Spain (ESP)	ArcelorMittal (AM)	BF A and B	50.0	350	12.5 %	[14]
Canada (CA)	ILVA	BF 2/ Toranto	45.0	325	12.2 %	[14]
United States (US)	-	-	30.0	380	7.3 %	[8]
Russia (RU)	-	-	6-24	-	-	[13]
Ukraine (UA)	Konstantinvovka	Donetsk	120-140	880	12-13.8 %	[12]
United Kingdom (GB)	Tata Steel (TS)	Scunthorpe	52.0	276	15.9 %	[12]
India (IN)	Neco (NS)	Raipur	40-60	-	-	[11]
	Tata Steel (TS)	G BF, JSR	55	383	12.6 %	[16]

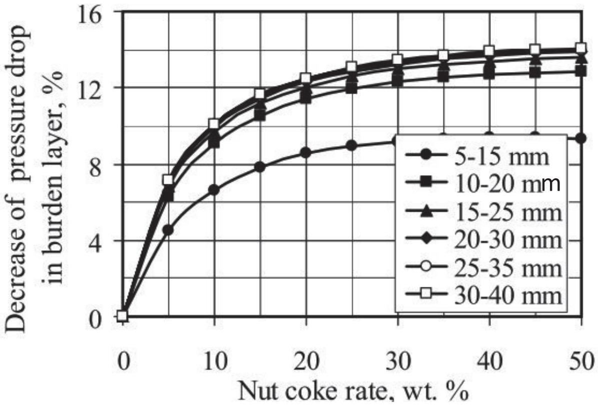

Fig. 2.2 Estimated effect of nut coke addition of various sizes on the pressure drop across the ferrous bed [18].

In single ferrous layer experiments, the bed permeability was observed to increase almost linearly with nut coke addition (Fig. 2.3) [13]. However, the increase in the pressure drop was also noted with increasing the number of alternating layers (Fig. 2.4). Thus, to investigate this phenomenon, a Computer Tomography (CT) scan of the packed bed (glass balls and coke) was performed (Fig. 2.5). The glass balls were observed to fill the interstitial voids around the coke to decrease the porosity at the interfaces. As a result, with the increase in the number of the layers and thus the interfaces, the overall permeability decreases.

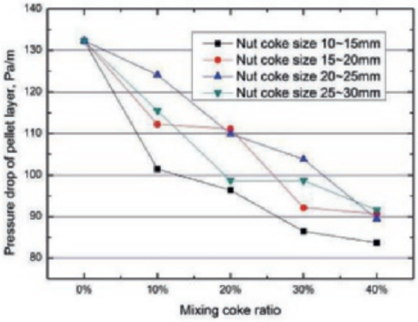

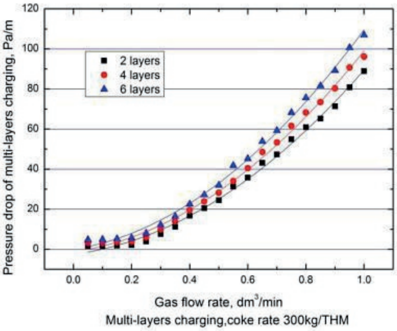

Fig. 2.3 Effect of nut coke size on the pressure drop across the packed bed (for a gas flow rate of 1 dm^3/min) [13].

Fig. 2.4 Effect of layers on the pressure drop across the packed bed [13].

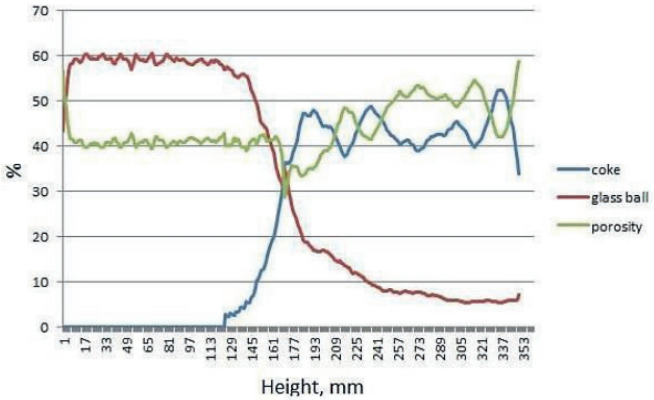

Fig. 2.5 Change in volume fraction along the bed height [13].

Song [13] recommended that nut coke mixing ratios of 20 % and 30 % will enhance the permeability of the ferrous bed. These findings were based on experiments performed at room temperature. However, in a real blast furnace, the burden encounters very high temperature, which will certainly affect the physicochemical properties of the bed. Therefore for effective utilisation of nut coke, detailed understanding of the bed behaviour under blast furnace conditions is essential.

2.3.2 Reduction kinetics

A higher reduction rate for ferrous burden is required for the improvement of blast furnace productivity [17]. Based on the reduction experiments of iron oxides in the temperature range from 900 °C to 1200 °C, Fruehan [20] found that the oxidation of carbon controls the rate of reduction reactions. The reduction of iron oxide takes place in three stages. First, it is reduced from hematite (Fe_2O_3) to magnetite (Fe_3O_4), in the second stage, it reduces further from magnetite (Fe_3O_4) to wüstite (FeO) and in the third stage wüstite (FeO) to metallic iron (Fe). The reduction of wüstite (FeO) to metallic iron (Fe) is the rate-controlling reaction. The freshly reduced iron (Fe) does not catalyse the oxidation reaction of carbon. Moreover, towards the final stage of iron ore reduction, the reaction rate further decreases due to the formation of fayalitic ($FeO.SiO_2$) slag, which causes the 'reduction retardation' phenomena [21].

By mixed charging of nut coke with the ferrous burden, reduction retardation can be minimised. Mixed charging will increase the contact area between the ferrous burden and the carbon (nut coke), which will improve the carbon (nut coke) oxidation. Furthermore, CO-rich gas will be able to penetrate deeper into the ferrous burden to improve the reduction kinetics.

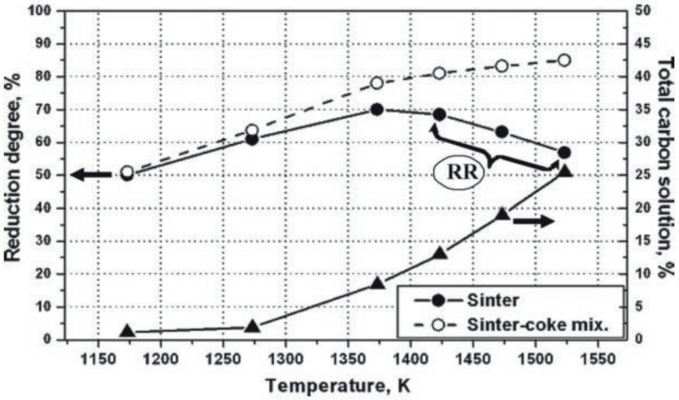

Fig. 2.6 Effect of nut coke addition on reduction degree of iron ore sinter [22].

Mousa et al. [2,22-23] confirmed that at high temperatures (above 1100 °C) ferrous burden without mixed nut coke suffers from reduction retardation, whereas in the burden mixed with nut coke this phenomenon was not observed (Fig. 2.6). In the sample bed mixed with nut coke, the micropores inside the ferrous burden were accessible for the reduction reactions, whereas in the sample bed without nut coke, the pores were blocked due to the sintering between the ferrous burden materials (Fig. 2.7). Song [13] noticed that in the presence of nut coke, the Boudouard reaction and water-gas reactions were promoted, which resulted in the higher reduction rate. Kuzin [24] suggested that for further improvement in the reduction kinetics, the size of nut coke should be comparable to or smaller than that of ferrous burden (iron ore, pellet and sinter).

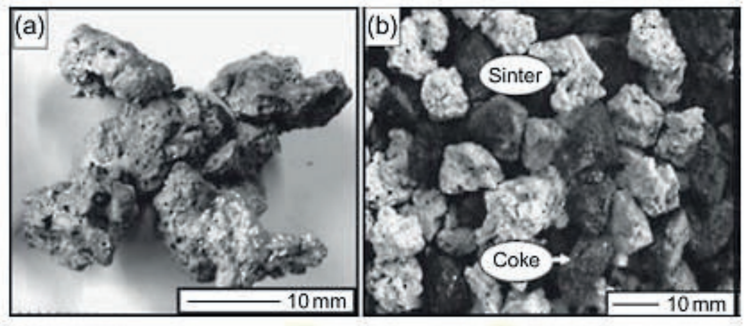

Fig. 2.7 Photograph of sinter (a) without and (b) with mixed nut coke [25].

2.3.3 Cohesive zone permeability

A uniform permeability and low-pressure drop over the burden layers are desired for the smooth function of the blast furnace. A typical pressure drop profile that evolves along the height of the blast furnace is shown in Figure 2.8. In the cohesive zone, due to the softening and melting of the ferrous burden, about 25 % of the total pressure drop occurs [5]. Based on DEM-CFD modelling, Kon et al. [26] found that the permeability in the cohesive zone can be increased by nut coke mixed charging with the ferrous burden. In another study, Matsuhashi et al. [27] predicted that by equal mixing of nut coke with the ferrous burden, the total pressure drop could be reduced to 20 % compared to the case when nut coke was absent.

Based on interrupted high temperature tests in the Reduction Softening and Melting apparatus (RSM), Song [13] has shown that the ferrous burden mixed with nut coke undergoes less contraction to result in a lower pressure drop. The nut coke acted as the skeleton to maintain the structure and permeability in the bed (Fig. 2.9).

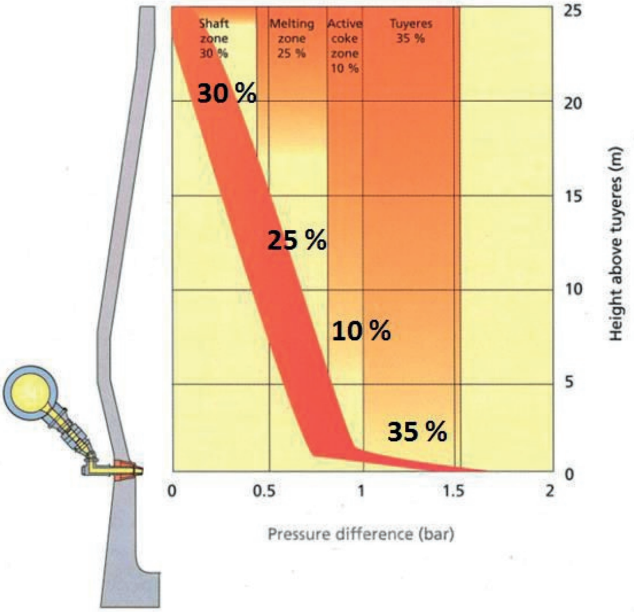

Fig. 2.8 Pressure drop profile along the height of the blast furnace [5].

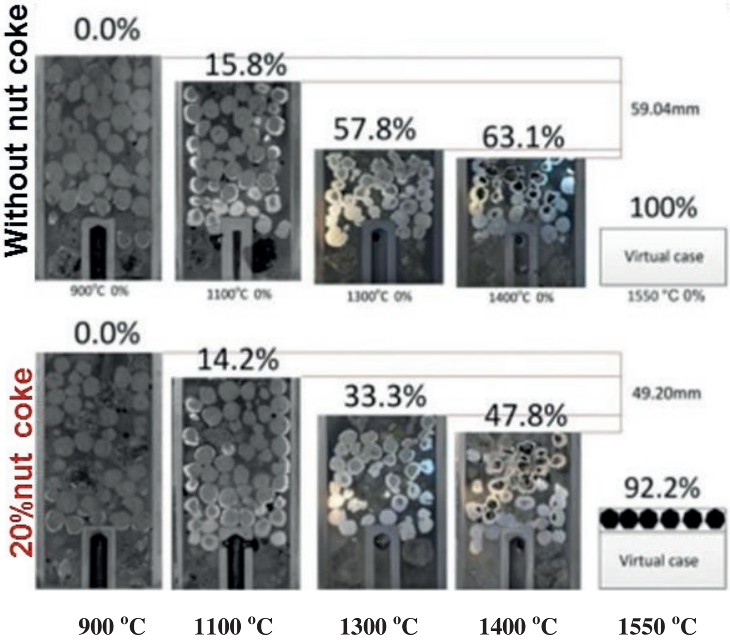

Fig. 2.9 Quenched sample bed with and without mixed nut coke [13].

2.3.4 Softening and melting temperature

A thinner cohesive zone is desired for better permeability (lower pressure drop) in the blast furnace [26]. This can be achieved with the ferrous burden that has a smaller temperature difference between its softening and melting. For given ferrous raw materials, the nut coke addition has shown the ability to alter the cohesive zone temperature range. Song [13] found that by 20 wt% nut coke mixing with the ferrous burden, the softening and melting temperatures increased by 86 °C and 15 °C, respectively. Consequently, the cohesive zone temperature range was decreased by 71°C (Fig. 2.10).

In another study, it was found that the softening, melting and dripping properties of the vanadium-titanium rich ferrous burden can be improved by 20 % nut coke addition [28]. However, when nut coke was added in higher quantity (50 wt%), the slag dripping properties deteriorated due to the formation of V and Ti carbide.

It was indicated that the melting of ferrous burden in the blast furnace is limited by the direct reduction reaction,

$$FeO(l) + C(s) \rightarrow Fe(s) + CO(g) \qquad (2.1)$$

which occurs on the surface of the reductant [29]. Thus, the nut coke utilisation in the mixture with ferrous burden increases the interfacial area to accelerate the direct reduction reaction.

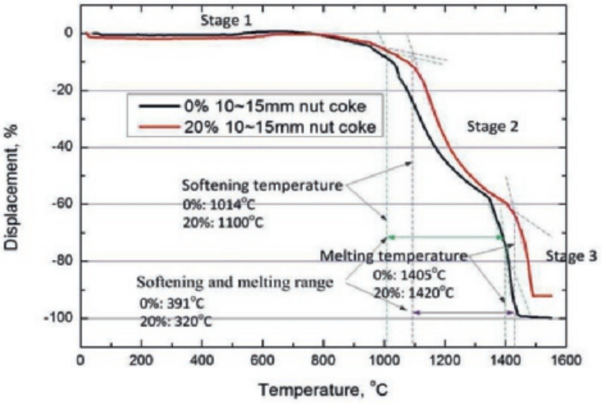

Fig. 2.10 Effect of nut coke (20 wt%) addition on softening and melting temperature [13].

These effects of the nut coke addition on the ferrous bed are desirable for furnace productivity. However, the optimum nut coke concentration is not apparent from the previous studies. Therefore, a series of high temperature experiments are required under blast furnace conditions to understand the different effects of nut coke mixing.

2.3.5 TRZ temperature

In the Thermal Reserve Zone (TRZ), indirect reduction of ferrous burden (iron oxides with CO or H_2 gas) occurs. The longer the length of the TRZ inside the blast furnace, the higher is the probability for wüstite (FeO) to be reduced by an indirect reduction reaction (Fig. 2.11) [17]. Consequently, the fuel efficiency of the blast furnace can be increased. Lowering TRZ temperature has a direct benefit in reducing the reductant demand for metal production (Fig. 2.12) [30]. After industrial trials, Sato et al. [31] reported that the TRZ temperature decreased by 50 °C when the nut coke rate was increased from 30 kg/thm to 100 kg/thm. Considering the magnitude of increase in nut coke in the blast furnace, the beneficial effect on the TRZ temperature was observed to be relatively low.

Therefore for further improvement in the TRZ temperature range, there are two possibilities: first enhancing the reactivity of the coke (or carbonaceous materials), second increasing the degree of contact among the particles. Kasai et al. [30] chose both options to prepare a new agglomerate, carbon composite of iron ore (CIO-B). It was prepared by hot briquetting of the fine coal and iron ore of similar particle size (~40 µm). The differential thermal analysis of CIO-B revealed that by the use of CIO-B agglomerates, the TRZ temperature could be reduced by ~270 °C. Similarly, Hirosawa et al. [32] suggested the use of Carbon Iron Composite (CIC, 70 % iron ore, 30 % coal), which resulted in the reduction of TRZ temperature by ˜140 °C.

In another attempt to reduce the TRZ temperature, Kowitwarangkul et al. [33] recommended the use of Self-Reducing Pellets (SRP) which were prepared by the pelletisation of the charcoal and iron ore fines of size 45–90 µm. SRP usage has the potential to decrease the TRZ temperature by 100 °C. Nomura et al. [34] selected the route of enhancing the nut coke reactivity by doping with calcium oxide (CaO) and iron oxide as a catalyst. This doped nut coke reduced the TRZ temperature by 100 °C [34].

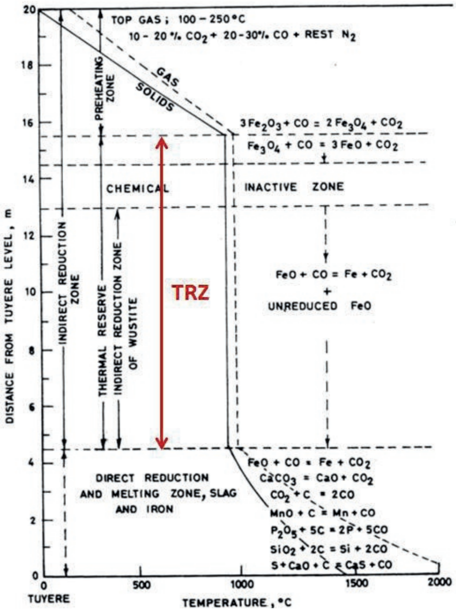

Fig. 2.11 The thermal profile of solid and gas along the height of the blast furnace with reactions [17].

Specially prepared iron ore agglomerate and catalyst doped nut coke have the ability to lower the TRZ temperature. However, their preparation will add to the extra cost of metal production. Thus, a detail financial case study is mandatory before the commercialisation implementation of special agglomerate and doped nut coke for the blast furnace.

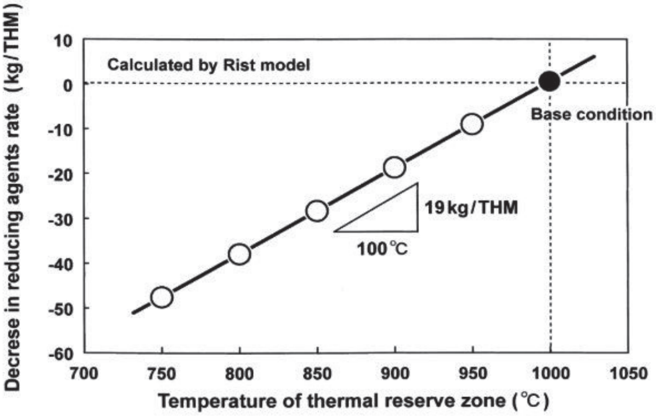

Fig. 2.12 A relationship between thermal reserve zone temperature and reducing agent rate [30].

2.4 Correlational research with nut coke

2.4.1 Effect of burden chemistry

The burden composition has a strong influence on its softening, melting and dripping properties. Under blast furnace conditions, the iron ore pellet visualised with X-ray revealed that the initial deformation is due to the softening of the formed metallic (iron) layer only [35]. However, the melting and dripping temperature are observed to be affected by the chemistry and reduction degree of the pellets [36]. Nogueira et al. [36] studied the effect of burden chemistry on the softening and melting properties. It was found that close to the softening temperature, a sharp increase in the liquid fraction occurs for both acidic and basic pellets [37]. It was stated that the reduction degree achieved on the acidic pellet decides its softening and melting properties, whereas in the case of basic pellets it has low significance. Due to the low melting point of slag and viscosity, the slag from acid pellets exudes first compared to the basic pellets. When acid and basic pellets are mixed together, interaction occurs only at high temperature, at low temperature these pellets behave independently. The mixture has similar softening and melting properties to that of basic pellets alone because the exuded slag from acid pellets interacts with the basic pellet surface to result in high viscosity, which stops the liquid flow (dripping). Consequently, for the mixed bed, the dripping temperature was observed to be high [36].

The nut coke mixed charging with the ferrous burden of various chemistry will certainly affect the bed properties. Therefore, a thorough investigation is required to understand the bed behaviour under nut coke mixed charged conditions. Furthermore, to develop an understanding of the optimal nut coke concentration for the ironmaking blast furnace some isothermal and interrupted experiments are required with and without nut coke mixing.

2.4.2 Carbon ordering and ash content in coke

The carbon ordering and an ash content of the coke have an effect on its reactivity. It was found that coke with high order (graphitisation degree) and ash content has lower strength and reactivity [38]. In the same study, it was also indicated that the coke with high iron content has high graphitisation degree [38]. Gupta et al. [39] further revealed that the coke ash content has a direct relationship with its dissolution in liquid iron. The coke ash content was found to hinder the contact between the carbon and iron and thus to affect the temperature of initial liquid formation (Fig. 2.13) [40]. Consequently, the liquid formation temperature was observed to decrease with the reduction in coke ash content. By industrial trials, Kardas [40] found that the coke with low ash content resulted in better furnace performance and hot metal quality.

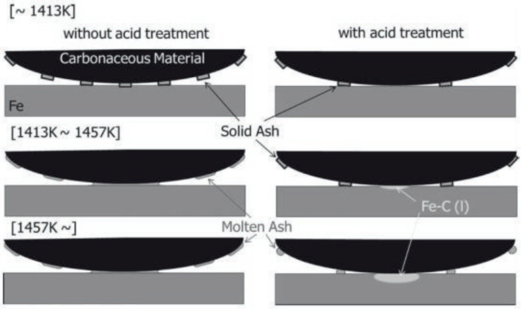

Fig. 2.13 Schematic illustration on the role of the ash content on Fe-C liquid formation [40].

Gupta et al. [39] revealed that reaction kinetics are strongly affected by coke ash content, slag chemistry and temperature. It was indicated that the coke ash content derives the coke reactivity [42]. On the contrary, by the characterisation of the coke collected from tuyeres Dong et al. [43] indicate that the degree of carbon ordering controls the reactivity of the coke. Thus, the ash content and carbon ordering are suggested to affect the reactivity of the coke. However, which factor is dominant is not apparent. Therefore to effectively utilise the coke (regular coke and nut coke) in the blast furnace, it is essential to quantify the effect of coke ash and ordering on its reactivity.

2.4.3 Coke Quality

In modern blast furnaces due to high injection rate and low coke rate operation, the prime function of the coke has changed. The coke functions of reductant and heat source are less important than its function of iron carburiser and maintainer of the gas permeability. To fulfil such requirements, a high-quality coke is required in the blast furnace [44-45]. After the blast furnace trials, it was indicated that with the use of good quality regular coke, a higher nut coke replacement ratio could be achieved [46-47]. In a comparative study between dry and wet quenched nut coke, qualities like hot (Coke Strength after Reaction, CSR) and cold strength, carbon content and its reactivity (Coke Reactivity Index, CRI) were observed superior for the dry quenched coke [48].

For adequate nut coke use in a mixture with the ferrous burden, its interaction relation with respect to the coke physical and chemical quality is relevant. This will give operational guidelines to the blast furnace operator for the effective utilisation of nut coke.

2.4.4 Nut coke reactivity

The concept of active nut coke and passive regular coke use in the blast furnace is introduced in the recent past [34,49-54]. The reactivity of nut coke is enhanced for its preferential dissolution in the mixed burden layer. The reactivity of nut coke can be enhanced by the addition of dopants (Fe_2O_3 and CaO) [54]. The use of passivating agents like B_2O_3, TiO_2, SiO_2 and Al_2O_3 is suggested in the literature for the passivation of the regular coke [49]. In the simulated blast furnace conditions, this has resulted in higher reduction kinetics, gas permeability, gas utilisation and lower thermal reserve zone temperature [49]. In another study, the use of microwaves was suggested to passivate the regular coke [55]. Microwave treatment of the coke will increase the graphitisation degree. As a result, the reactivity of the coke in a CO_2 atmosphere will decrease [55].

Trials were reported at an experimental blast furnace in MEFOS with the activated nut coke, in which a nut coke rate of about 150 kg/thm was achieved [54]. The utilisation of lime (CaO) and magnetite (Fe_3O_4) activated nut coke resulted in lowering of reductant consumption by 4 kg/thm and 6 kg/thm, respectively [54]. In Japan, industrial trials were reported with the catalyst (CaO) doped reactive nut coke [56]. This nut coke had higher reactivity and strength to sustain the blast furnace conditions. The utilisation of this coke in a mixture of ferrous burden improved the fuel efficiency by lowering the reductant consumption by 10 kg/thm [56]. In India, at Tata Steel (Jamshedpur) trials were conducted with iron ore fines coated nut coke, in which a 200 kg/thm of nut coke rate was achieved [57].

In another study, the benefits in narrowing the cohesive zone temperature (50 ^{o}C) were reported with the use of specially prepared briquettes called Iron Coke Hot Briquette (ICHB) [58]. ICHB was prepared by briquetting and carbonisation of the iron ore and coal fines (Fig. 2.14). In mixed charge conditions, the ICHB will get preferentially consumed to protect the regular coke in the blast furnace.

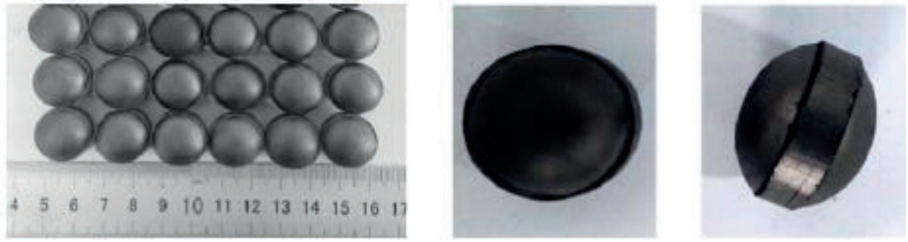

Fig. 2.14 Photograph of the iron coke hot briquettes (ICHB) [58].

2.5 Burden distribution for nut coke mixed charging

Mixing of the nut coke in a ferrous burden layer has beneficial effects. However, if not appropriately distributed, it has a negative impact on furnace productivity. Due to the density difference between the nut coke and the ferrous burden, there is a risk of segregation during the charging of the mixed burden [59-61]. By simulations (DEM), Kim et al. [60] concluded that fast nut coke discharge from the storage bin would result in the segregation of nut coke towards the periphery. It can be controlled by altering the charging sequence and by using the stone box at the furnace top hopper (Fig. 2.15) [60].

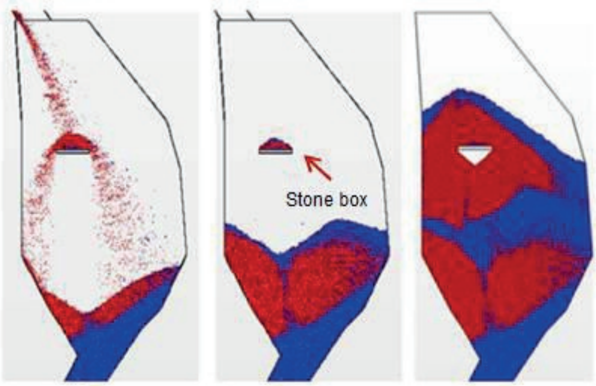

Fig. 2.15 DEM simulation to demonstrate the effect of stone box addition on the segregation behaviour in the top hopper, blue particle - nut coke and red particle – ore [60].

By industrial trials, it was suggested to simultaneously charge the coke and ferrous burden to avoid segregation (Fig. 2.16). Simultaneous charging provided an opportunity to enhance the nut coke use in the blast furnace (JFE, BF 6) from 60 kg/thm to 116 kg/thm. As a result, the metal quality (Si lowered from 0.35 to 0.15%) and gas permeability (Fig. 2.17) were improved to enhance the furnace productivity by 0.33 t/m^3/day [15].

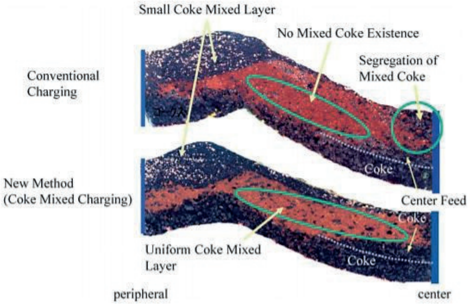

Fig. 2.16 Mixed burden distribution with conventional and new simultaneous charging method [15].

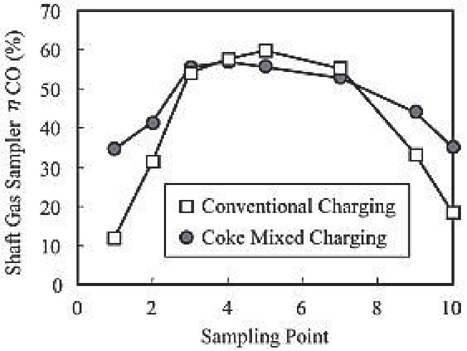

Fig. 2.17 Gas utilisation profile with conventional and mixed charging method [15].

To further improve the distribution, the filling sequence of nut coke in the upper and lower bunker of the bell-less top system was altered (Fig. 2.18) [62]. This new charging style allowed the nut coke to charge away from the wall (Fig. 2.19). As a result, good permeability was maintained for higher gas utilisation, which lowered the coke requirement for metal production (Fig. 2.20).

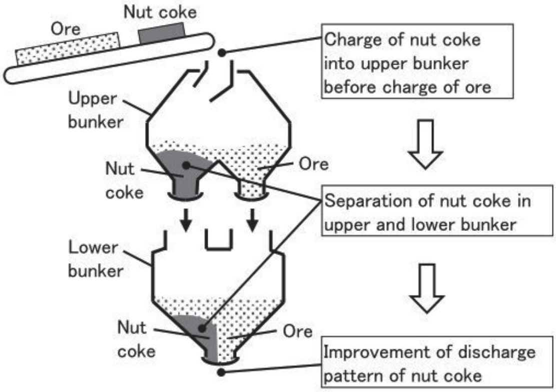

Fig. 2.18 New charging method [62].

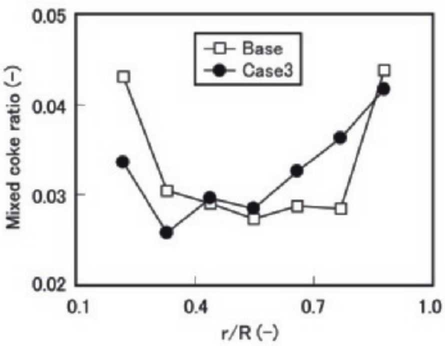

Fig. 2.19 Radial distribution of the mixed burden [62].

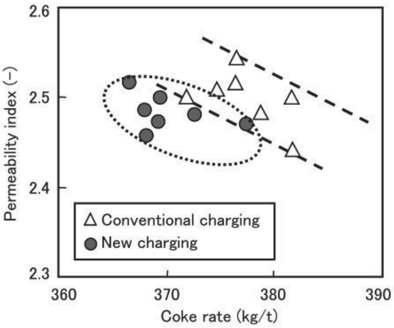

Fig. 2.20 Effect of new charging method on permeability and coke rate [62].

In another study, it was suggested to alter the charging order to obtain the uniformity in nut coke distribution [63]. It was proposed to first charge 70 % sinter at the bottom of the hopper, then nut coke followed by 30 % sinter, then at last pellets were charged. It was reported that this charging style improved the indirect reduction, hearth permeability and the slag properties in the blast furnace [63].

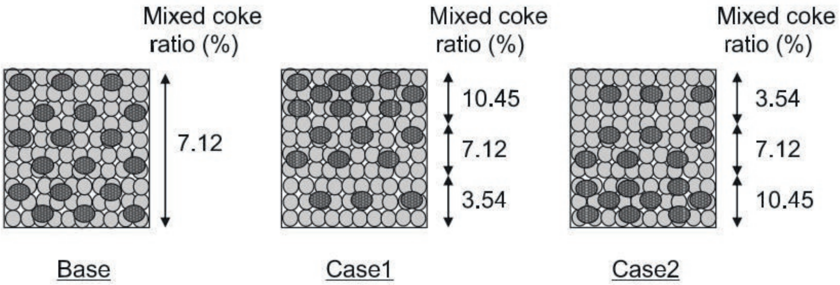

Fig. 2.21 Schematic of the nut coke mixing style [65].

Through simulation studies, Natsui et al. [64] found that the coke-ore-mix layer from bottom to the top showed a proper gas utilisation and reduction kinetics. Similarly, by experiments and blast furnace trials, Kashihara et al. [65] recommended that mixing the nut coke in the upper part of the ore layer (Fig. 2.21, case 1) could contribute to a higher reduction degree compared to the case of mixing at the lower part (Fig. 2.21, case 2) and uniform (Fig. 2.21, base case) mixing in the ferrous burden layer (Fig. 2.21). The peripheral and overall gas utilisation was also observed to increase with this distribution style. It was also recommended to decrease the particle size difference between the nut coke and sinter to avoid segregation [14].

The coke burning rate varies in the radial direction inside the blast furnace. In general nut coke was recommended to be charged away from the wall. However, the exact ideal radial location for effective nut coke utilisation is not finalised. Therefore, for effective utilisation of the nut coke, its dissolution ability in the ferrous burden needs to be linked with the distribution style.

2.6 Limiting factors for higher nut coke utilisation

2.6.1 Coke layer thickness (CLT)

In the blast furnace, gas rising from the tuyeres to the furnace top is distributed by the regular coke layers. For adequate gas flow, a minimum coke (regular) layer thickness is required [5]. High coal injection as a replacement of regular coke is common in the modern blast furnaces, which has resulted in thinning of the regular coke layer. Furthermore, with the utilisation of nut coke in mixture with the ferrous burden, the coke layer thickness decreases further (Fig. 2. 22), which could create a detrimental effect on an overall gas permeability in the blast furnace.

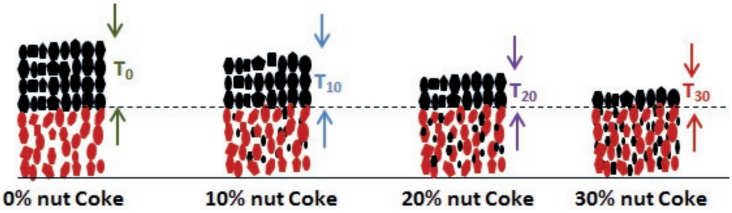

Fig. 2.22 Schematic effect of nut coke charging on the coke layer thickness.

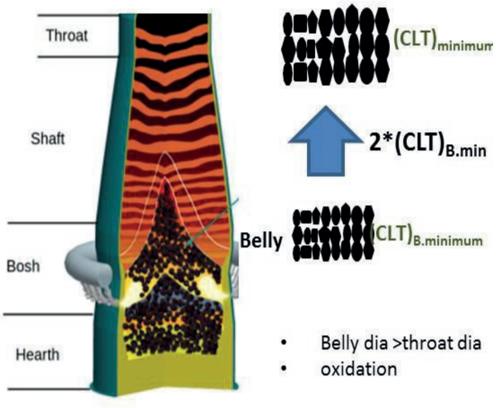

Fig. 2.23 Schematic minimum coke layer thickness at blast furnace belly and throat. (CLT-coke layer thickness)

From operational experience, Geerdes et al. [5] suggested that at least three discrete particle layers of regular coke are required at the belly level of the blast furnace. Now, as the belly diameter is bigger than the furnace throat and the coke oxidised before reaching the belly, the minimum coke layer thickness at the throat was suggested to be twice that at the belly. Therefore, the minimum coke layer thickness at the furnace throat and belly are six times and three times, respectively, of the average regular coke diameter (Fig. 2.23).

In another study, Ichikawa et al. [66] found that a minimum of two discrete layers of coke particles are required for adequate permeability. Below this critical coke layer thickness, the pressure drop increases sharply, which may cause operational irregularities in the blast furnace (Fig. 2.24). Therefore, a minimum of two discrete coke particle layers was recommended for smooth blast furnace operation.

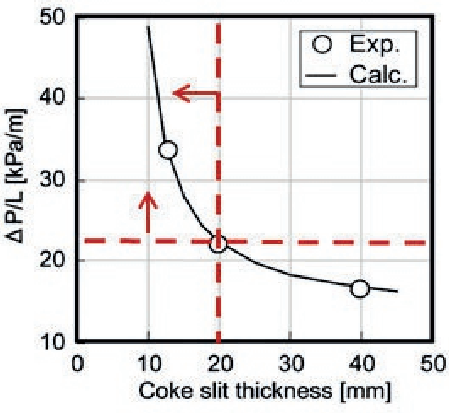

Fig. 2.24 Effect of coke slit thickness on pressure drop at 1400 ^{o}C [66].

However, these suggestions were made without considering the effect of nut coke addition. It will be interesting to understand the effect of nut coke addition of different size and concentration on minimum coke layer thickness.

2.6.2 Nut coke in the lower part of the furnace

Higher regular coke replacement with nut coke is desirable. However, with higher usage of nut coke, there is always a risk of the unconsumed nut coke reaching the lower part of the blast furnace, which could result in clogging of deadman and hearth. By mathematical modelling and experiments, Kashihara et al. [6] suggested that when the nut coke rate is low (less than 45 kg/thm), it will be consumed entirely by the gasification reactions (Fig. 2.25). However, when the nut coke mixing rate is high (more than 45 kg/thm), it will not be consumed completely (Fig. 2.25). It will continue to exist in the lower part of the furnace to cause an increase in the pressure drop.

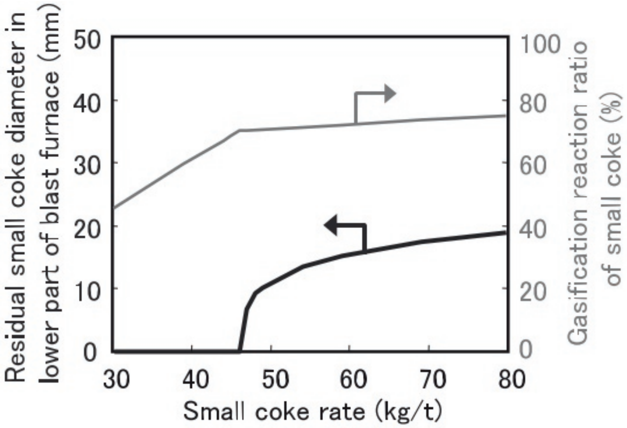

Fig. 2.25 Effect of nut coke addition on the residual nut coke size at the lower part of the blast furnace (initial size, regular coke-45mm and nut coke-25 mm) [6].

In another study to evaluate the amount of nut coke consumed up to 1300°C, Song [13] found that only about 40 wt% of the total charged nut coke (19 grams) was consumed (Fig. 2.26). This amount was similar to that observed by Mousa et al. [22] in a similar experiment up to 1227 °C (Fig. 2. 27). These give an indication that about 60 wt% of the total charged nut coke will not be consumed until the cohesive zone (~1300 °C) is reached. These unconsumed fine coke may cause irregularities in the blast furnace hearth.

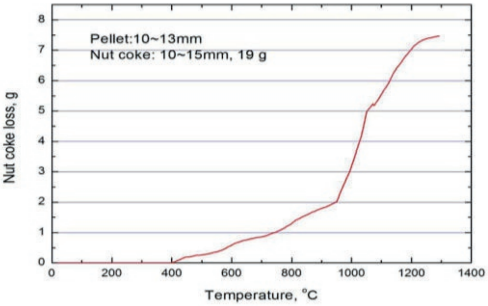

Fig. 2.26 Nut coke consumption under simulated blast furnace conditions [13].

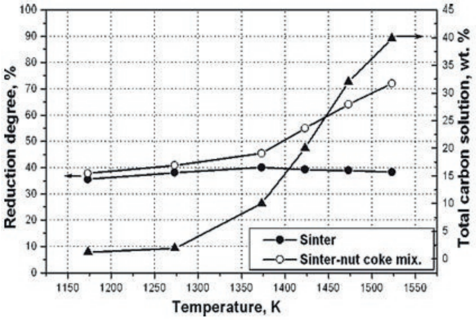

Fig. 2.27 The carbon loss and reduction degree under simulated blast furnace conditions [22].

Based on the blast furnace operational experiences, Logachov et al. [46] observed that increase in the nut coke addition beyond a certain optimum concentration could lead to poor smelting rate and improper hearth operation which lowers the furnace productivity. Fines generation and its accumulation are not desirable for the permeability of the deadman. In another simulation study of the blast furnace hearth, Nogami et al. [67] revealed that voidage is of higher importance than the coke diameter in the deadman zone.

The low voidage in the deadman could cause less penetration of the hot gases and will develop a low-temperature zone.

Therefore, a surplus addition of nut coke should be avoided in the blast furnace. Nut coke utilisation with ferrous burden has positive effects on the burden permeability, softening melting properties, TRZ temperature and reduction kinetics. However, its optimum utilisation in ironmaking is a function of variables such as burden (coke and ferrous) chemistry, burden quality, size, concentration and distribution style. It is essential to identify the optimum replacement ratio of regular coke with the nut coke. To further push the nut coke utilisation, fundamental understanding of the effects of nut coke on the minimum coke layer thickness and its behaviour in the lower part of the furnace is crucial. The option of nut coke reactivity enhancement with additive can also be explored.

2.7 Summary

The nut coke utilisation in a mixture with the ferrous burden, to a certain extent, was proven beneficial in many ironmaking blast furnaces. Its utilisation was observed to vary from several kilograms per ton hot metals (kg/thm) to as high as 140 kg/thm. Nut coke usage enhances the shaft and cohesive zone permeability by acting as a skeleton to maintain the ferrous bed structure. Consequently, by nut coke use the reduction kinetics was enhanced to avoid the ‘reduction retardation’ phenomena. Its utilisation improves the softening and melting properties of the burden.

For the optimum utilisation of the nut coke in the blast furnace, understanding of its reaction behaviour with different burden chemistry (acidic and basic) is essential. Co-relational research is important to understand the effect of coke quality and distribution style. Furthermore, it is worth to examine the effect of carbon ordering and ash content on the coke reaction ability with the ferrous burden.

Nut coke reactivity can be improved for its preferential consumption in place of regular coke. This can be achieved by coating nut coke with various dopants like Fe_3O_4, CaO, etc. This catalyst doped nut coke lowers the TRZ temperature to support the fuel and reductant efficiency of the blast furnace. For higher nut coke utilisation, the challenges such as coke layer thickness and unconsumed nut coke, need to be addressed systematically. Therefore, fundamental research with nut coke usage is highly required under blast furnace conditions.

2.8 References

[1] V.I. Loginov, A.L. Berin, S.M. Solomatin, Effect of mixing burden with coke on blast furnace fluid mechanics and operation parameters, Stal. 5 (1977) 391–394.

[2] Z. Yang, J. Yang, Effect of coke-ore mixed charging on reduction and gas flow characteristics in the softening-melting zone, Ironmak. Steelmak. 22 (1995) 191–195.

[3] E.A. Mousa, D. Senk, A. Babich, H.W. Gudenau, Influence of nut coke on iron ore sinter reducibility under simulated blast furnace conditions, Ironmak. Steelmak. 37 (2010) 219–228.

[4] S.N. Pishnograev, A. V. Chevychelov, V.A. Gostenin, N.S. Shtafienko, V.P. Gridasov, Using coke fines in the blast furnaces at OAO MMK, Steel Transl. 39 (2010) 878–881.

[5] M. Geerdes, R. Chaigneau, I. Kurunov, O. Lingiardi, J. Ricketts, Modern blast furnace ironmaking : an introduction, IOS Press, under the imprint of Delft University Press, Amsterdam, 2015.

[6] Y. Kashihara, Y. Iwai, T. Sato, N. Ishiwata, M. Sato, Effect of unconsumed mixed small coke on permeability in lower part of blast furnace, ISIJ Int. 55 (2015) 1237–1244.

[7] D.J. Price, Scunthorpe steelworks 1973–2006: a history of continuous development Part 2 – Process and product developments, Ironmak. Steelmak. 34 (2007) 389–402.

[8] I.F. Kurunov, Blast-furnace smelting in China, Japan, North America, Western Europe and Russia, Metallurgist. 54 (2010) 114–126.

[9] Z. Liu, J. Zhang, T. Yang, Low carbon operation of super-large blast furnaces in China, ISIJ Int. 55 (2015) 1146–1156.

[10] A. V. Kuzin, Effect of introducing different sizes of nut coke into the ore layer on the degree of reduction of iron oxides, Metallurgist. 57 (2014) 783–791.

[11] D. Singh, A.K. Sinha, M.P. Singh, S.K. Swain, A journey towards excellence in the blast furnace performance at Jayaswals Neco limited, Steel World. (2006) 15–22.

[12] S.L. Yaroshevskii, V.A. Nozdrachev, A.P. Chebotarev, V.A. Rudenko, S.A. Feshchenko, A.M. Kuznetsov, V.P. Padalka, N.S. Khlaponin, A. V. Kuzin, Efficiency of using coke fractions smaller than 40 mm in a blast furnace, Metallurgist. 44 (2000) 598–605.

[13] Q. Song, Effect of nut coke on the performance of the ironmaking blast furnace, PhD Thesis, Delft University of Technology, 2013.

[14] H. Atsumi, H. Horikoshi, Y. Kashihara, I. Yuki, K. Fukada, H. Matsuno, Development of new charging technique for mixing coke in ore layer at blast furnace with center feed, in: 8th Int. Congr. Sci. Technol. Ironmkaing, Vienna, 2018: pp. 646–653.

[15] S. Watakabe, K. Takeda, H. Nishimura, S. Goto, N. Nishimura, T. Uchida, M. Kiguchi, Development of high ratio coke mixed charging technique to the blast furnace, ISIJ Int. 46 (2006) 513–522.

[16] M. Agarwal, K.R.K. Rao, M.K.G. Choudhary, R.V. Ramna, Increase in production by increasing double through operation through straight campaign of through repair at G blast furnace, Tata Steel Jamshedpur, in: 8th Int. Congr. Sci. Technol. Ironmak., Vienna, 2018: pp. 634–640.

[17] A.K. Biswas, Principles of blast furnace iron making - theory and practice, Cootha Publishing House, Brisbane, Australia, 1981.

[18] A. Babich, D.G. Senk, S.L. Yaroshevskiy, N.S. Chlaponin, V. V. Kochura, A. V. Kuzin, Effect of nut coke on blast furnace shaft permeability, in: Scanmet, Lulea, Sweden, 2008: pp. 227–236.

[19] A. Babich, D. Senk, H.W. Gudenau, Effect of coke reactivity and nut coke on blast furnace operation, Ironmak. Steelmak. 36 (2009) 222–229.

[20] R.J. Fruehan, The rate of reduction of iron oxides by carbon, Metall. Mater. Trans. B. 8B (1977) 279–286.

[21] T. Bakker, Softening in the blast furnace process: local melt formation as the trigger for softening of ironbearing burden materials, TU Delft, 1999.

[22] E.A. Mousa, A. Babich, D. Senk, Effect of nut coke-sinter mixture on the blast furnace performance, ISIJ Int. 51 (2011) 350–358.

[23] E. Mousa, D. Senk, A. Babich, Reduction of pellets-nut coke mixture under simulating blast furnace conditions, Steel Res. Int. 81 (2010) 706–715.

[24] A. V Kuzin, Effect of introducing differenct sizes of nut coke into the ore layer on the degree of reduction of iron oxides, Metallurgist. 57 (2014) 783–791.

[25] A. Babich, D. Senk, Recent developments in blast furnace iron-making technology, Elsevier Ltd., 2015.

[26] T. Kon, S. Natsui, S. Matsuhashi, S. Ueda, R. Inoue, T. Ariyama, Influence of cohesive zone thickness on gas flow in blast furnace analyzed by DEM-CFD model considering low coke operation, Steel Res. Int. 84 (2013) 1146–1156.

[27] S. Matsuhashi, H. Kurosawa, S. Natsui, T. Kon, S. Ueda, R. Inoue, T. Ariyama, Evaluation of coke mixed charging based on packed bed structure and gas permeability changes in blast furnace by DEM-CFD model, ISIJ Int. 52 (2012) 1990–1999.

[28] W. Zhao, M. Chu, H. Wang, Z. Liu, J. Tang, Z. Ying, Effect of introducing coke into ore layer on softening-melting-dropping characteristics of vanadium-titanium mixed burden under simulating BF conditions, ISIJ Int. (2018).

[29] M. Geerdes, P. Warren, How iron melts, part 2: role of coke and nut coke, in: 8th Int. Congr. Sci. Technol. Ironmak., 2018: pp. 380–385.

[30] A. Kasai, Y. Matsui, Lowering of thermal reserve zone temperature in blast furnace by adjoining carbonaceous material and iron ore, ISIJ Int. 44 (2004) 2073–2078.

[31] A. Sato, M. Aritsuka, Y. Yamagata, Y. Miyakawa, T. Goto, I. Mizuguchi, The operation with larger amount of nut coke under high pulverized coal rate, CAMP-ISIJ. 8 (1995) 1064.

[32] T. Hirosawa, A. Murao, N. Oyama, S. Watakabe, M. Sato, Advanced blast furnace reaction simulator combining a calculation model and experimental furnace, ISIJ Int. 55 (2015) 1321–1326.

[33] P. Kowitwarangkul, A. Babich, D. Senk, Reduction kinetics of self-reducing pellets of iron ore, in: AISTech 2014, Indianapolis, USA, 2014: pp. 611–622.

[34] S. Nomura, T. Tahara, S. Matsuzaki, M. Naito, H. Ayukawa, S. Koizumi, T. Abe, H. Kitaguchi, T. Tahara, Improvement in blast furnace reaction efficiency through the use of catalyst-doped highly reactive coke, Nippon Steel Tech. Rep. 94 (2006) 109–114.

[35] P.F. Nogueira, R.J. Fruehan, Blast furnace burden softening and melting phenomena: Part I. Pellet bulk interaction observation, Metall. Mater. Trans. B. 35 (2004) 829–838.

[36] P.F. Nogueira, R.J. Fruehan, Blast furnace burden softening and melting phenomena: Part II. Evolution of the structure of the pellets, Metall. Mater. Trans. B. 36 (2005) 583–590.

[37] P.F. Nogueira, R.J. Fruehan, Blast furnace burden softening and melting phenomena: Part III. Melt onset and initial microstructural transformations in pellets, Metall. Mater. Trans. B. 37B (2006) 551–558.

[38] S. Gupta, V. Sahajwalla, J. Burgo, P. Chaubal, T. Youmans, Carbon structure of coke at high temperatures and its influence on coke fines in blast furnace dust, Metall. Mater. Trans. B. 36B (2005) 385–394.

[39] S. Gupta, D. French, R. Sakurovs, M. Grigore, H. Sun, T. Cham, T. Hilding, M. Hallin, B. Lindblom, V. Sahajwalla, Minerals and iron-making reactions in blast furnaces, Prog. Energy Combust. Sci. 34 (2008) 155–197.

[40] K. Ohno, S. Tsurumaru, A. Babich, T. Maeda, D. Senk, Effects of ash amount and molten ash's behavior on initial Fe – C liquid formation temperature due to iron carburization reaction, ISIJ Int. 55 (2015) 1245–1251.

[41] E. Kardas, The effect of selected properties of coke on the quality of coke and indicators of blast furnace process, in: Acta Metall. Slovaca-Conference, 2014: pp. 31–39.

[42] V. Sahajwalla, T. Hilding, S. Gupta, B. Björkman, R. Sakurovs, M. Grigore, N.S. Chaudhury, Study of gasification reaction of cokes excavated from pilot blast furnace, in: Scanmet, Lulea, Sweden, 2004: pp. 1–12.

[43] S. Dong, N. Paterson, S.G. Kazarian, D.R. Dugwell, R. Kandiyoti, Characterization of tuyere-level core-drill coke samples from blast furnace operation, Energy & Fuels. 21 (2007) 3446–3454.

[44] H.W. Gudenau, D. Senk, K. Fukada, A. Babich, C. Froehling, Coke behavior in the lower part of BF with high injection rate, in: Int. BF Low. Zo. Symp., Wollongong, 2002: pp. 1–12.

[45] S. Gupta, Z. Ye, R. Kanniala, O. Kerkkonen, V. Sahajwalla, Coke graphitization and degradation across the tuyere regions in a blast furnace, Fuel. 113 (2013) 77–85.

[46] G.N. Logachov, S.N. Pishnograev, V.A. Gostenin, A. V. Chevychelov, V.P. Gridasov, Evaluating the effectiveness of using coke breeze in blast-furnace smelting, Metallurgist. 56 (2012) 87–90.

[47] S.N. Pishnograev, A. V. Chevychelov, V.A. Gostenin, N.S. Shtafienko, V.P. Gridasov, Using coke fines in the blast furnaces at OAO MMK, Steel Transl. 39 (2009) 878–881.

[48] S.K. Sibagatulin, A.S. Kharchenko, E.O. Teplykh, E.N. Stepanov, D.A. Mezin, V.B. Fetisov, Quality comparison of coke nuts, Coke Chem. 55 (2012) 62–65.

[49] H. Zhao, Y. Bai, S. Cheng, Effect of coke reaction index on reduction and permeability of ore layer in blast furnace lumpy zone under non-Isothermal Condition, J. Iron Steel Res. Int. 20 (2012) 6–10.

[50] S. Nomura, H. Kitaguchi, K. Yamaguchi, M. Naito, The characteristics of catalyst-coated highly reactive coke, ISIJ Int. 47 (2007) 245–253.

[51] S. Nomura, M. Naito, K. Yamaguchi, The post-reaction strength of catalyst-doped highly reactive coke, ISIJ Int. 47 (2007) 831–839.

[52] B. Tuo, J. Wang, Y. Yao, J. Yang, Influence of coke reactivity on softening-melting dropping behavior of iron bearing burden, Steel Res. Int. 86 (2015) 1028–1036.

[53] B. Tuo, J. Wang, Y. Yao, L. Han, Z. Liu, X. Hu, Influence of coke reactivity improved on high temperature properties of iron-bearing burden, ISIJ Int. 55 (2015) 1859–1865.

[54] L.S. Ökvist, C. Brandell, M. Lundgren, Impact of activated nut coke on energy efficiency in the blast furnace, in: AISTech - Iron Steel Technol. Conf. Proc., Association for Iron and Steel Technology, AISTech, 2014: pp. 663–672.

[55] C. Tian, Q.H. Pang, Z.J. He, J.H. Zhang, X.T. Zhao, Effect of microwave irradiation on reactivity of metallurgical coke in CO_2 atmosphere, Metalurgija. 57 (2018) 19–22.

[56] S. Nomura, S. Matsuzaki, M. Naito, Improvement in blast furnace reaction efficiency through the use of catalyst-doped highly reactive coke, Nippon Steel Tech. Rep. 94 (2006) 109–114.

[57] 106th Annual report 2012-2013, Tata Steel, 2012.

[58] H. Wang, M. Chu, W. Zhao, R. Wang, Z. Liu, J. Tang, Fundamental research on iron coke hot briquette – A new type burden used in blast furnace, Ironmak. Steelmak. 43 (2016) 571–580.

[59] S. Watakabe, A. Murao, S. Goto, Application of high ratio coke mixed charging technique to blast furnace, 2009.

[60] J. Kim, Y. Lee, C. Baek, Distribution control of nut coke in blast furnace burden, in: Metec 2nd Estad, Dusseldorf, 2015: pp. 1–5.

[61] H. Mio, S. Komatsuki, M. Akashi, A. Shimosaka, Y. Shirakawa, J. Hidaka, M. Kadowaki, H. Yokoyama, S. Matsuzaki, K. Kunitomo, Analysis of traveling behavior of nut coke particles in bell-type charging process of blast furnace by using discrete element method, ISIJ Int. 50 (2010) 1000–1009.

[62] Y. Kashihara, Y. Iwai, N. Ishiwata, N. Oyama, H. Matsuno, H. Horikoshi, K. Yamamoto, M. Kuwabara, Development of new charging technique for mixing coke in ore layer at blast furnace with center feed type bell-less top, ISIJ Int. 57 (2017) 665–672.

[63] S.K. Sibagatullin, A.S. Kharchenko, G.N. Logachev, The rational mode of nut coke charging into the blast furnace by compact trough-type charging device, Int. J. Adv. Manuf. Technol. 86 (2016) 531–537.

[64] S. Natsui, R. Shibasaki, T. Kon, S. Ueda, Effect of high reactivity coke for mixed charge in ore layer on reaction behavior of each particle in blast furnace, ISIJ Int. 53 (2013) 1770–1778.

[65] Y. Kashihara, Y. Morikawa, T. Sato, N. Ishiwata, M. Sato, Development of charging technique for controlling mixed coke distribution in ore layer, ISIJ Int. 55 (2015) 1165–1171.

[66] K. Ichikawa, Y. Kashihara, N. Oyama, T. Hirosawa, J. Ishii, Evaluating effect of coke layer thickness on permeability by pressure drop estimation model, ISIJ Int. 57 (2017) 254–261.

[67] H. Nogami, P.R. Austin, J. Yagi, K. Yamaguchi, Numerical investigation on effects of deadman structure and powder properties on gas and powder flows in lower part of blast furnace, ISIJ Int. 44 (2004) 500–509.

3. High-temperature experiments and characterisation techniques

As discussed in the second chapter, systematic parametric studies are required for the effective utilisation of the nut coke in the iron making blast furnace. This requires equipment which can simulate the blast furnace conditions (gas, temperature and mechanical load) and records the process performance through the laboratory experiments. Additionally, clear definitions are required to correlate the results from the simulator with the blast furnace performance indicators.

This chapter explains the design of the blast furnace simulator and the methods to interpret the experimental results with the real blast furnace performance. In this chapter first, the design of an in-house developed blast furnace simulator (Reduction Softening and Melting apparatus) is explained. Then, the experimental approach and the methods adopted for the result characterisation and analysis (bed contraction, pressure drop and gas analysis) are discussed. The chapter concludes with discussing the interpretation of RSM experiment results in relation to the blast furnace performance indicators.

3.1 Blast furnace simulator

The ironmaking blast furnace is a counter-current high temperature reactor, which produces liquid iron [1]. The Blast Furnace Simulators (BFS) are designed in such a way to mimic the three important conditions of blast furnace: (i) reducing gas profiles (ii) high temperature profiles, and (iii) the mechanical load present in a real ironmaking blast furnace. In most of the BFS, these conditions are simulated for a stationary bed [2]. In BFS, the gas, temperature and load profiles are varied in such a way that it imitates the downward movement of the burden in the real blast furnace.

The reduction, softening and melting of the ferrous raw materials and oxidation of the coke (carbon) takes place during the downward movement in the blast furnace. Similarly, in the BFS, these phenomena take place in a stationary bed but with varying gas composition and temperatures, which is computer controlled and detected with the help of several sensors. Additionally, the off-gas coming out after interaction with the sample bed is analysed to identify the key reactions and the rate of reaction occurring at different temperatures. Later, these recorded data are further analysed to understand the physicochemical behaviour of the raw materials under blast furnace conditions. In industry and research laboratories, it is a standard practice to test the new raw materials in BFS to understand its behaviour under the blast furnace conditions.

A comprehensive review of different type of BFS present around the world is presented in the references [2-3]. The BFS utilised for the present Ph.D. study is discussed in detail in section 3.2.

3.2 Reduction Softening and Melting (RSM) apparatus

The Reduction Softening and Melting (RSM) apparatus was developed in the course of the previous Ph.D. project titled “Effect of nut coke on the performance of the ironmaking blast furnace” [3]. It has been established at the Delft University of Technology in close cooperation with Tata Steel Europe (IJmuiden) and Materials innovation institute (M2i) in the Netherlands. The RSM was employed for the previous project work [3], following this it has been modified and adapted to suit the current research. The RSM furnace is replaced with the new high temperature furnace with the ability to heat up to 1800 ^{o}C. Additionally, the lower flange attached to the furnace is adapted to improve the sample weighing capability during the high temperature tests in RSM.

The RSM facility is intended to examine the reduction, softening, melting and dripping behaviour of the ferrous raw materials under simulated blast furnace conditions. A schematic view is shown in Figure 3.1. The blast furnace condition is simulated by varying the temperature and gas conditions for a stationary sample bed arranged inside the crucible, which is placed inside the furnace. Various physicochemical phenomena occurring during the test are measured with the help of the sensors. A thermocouple is placed on the top of the sample bed inside the crucible to monitor the sample temperature. The change in sample bed height during the swelling, softening and melting is measured with the displacement transducer. The pressure drop across the sample bed is recorded with a differential pressure transducer. The mass flow controllers of different gases (CO, CO_2, H_2 and N_2) are employed to control the composition and amount of gas, which is injected to the sample bed. After interaction with the sample bed, the gas passes through the filter. Thereafter, gas analysis is performed for respective gases (CO, CO_2, H_2 and H_2O) in the gas analyser panel. The gas analysis is logged (every 10 seconds) in the computer and is utilised for further analysis. After the analysis, the exhaust gas is sent to the ventilation hood. The flanges present at both ends of the furnace are water cooled to protect the rubber gaskets, which ensures the gas tightness.

Once the ferrous material is reduced significantly and the high temperature is attained, the melting of the ferrous material takes place. Thereafter, the liquid drips out of the sample crucible and get collected in the cups arranged in the sample collector (Fig. 3.1). The event of liquid dripping is viewed and a video is recorded from the two glass windows present in the sample collector to provide dripping information along time. Based on the experimental requirement, these cups are rotated to collect the liquid (metal and slag) over the time and temperature range. These collected samples are later chemically analysed.

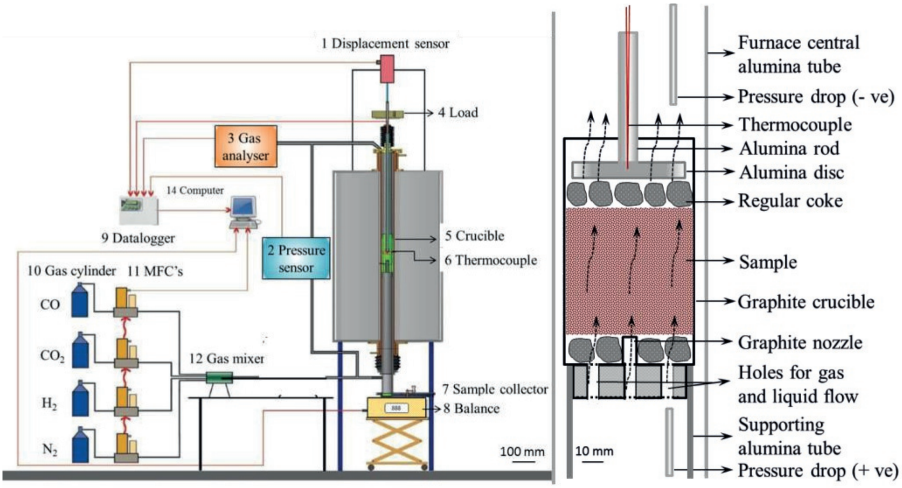

Fig. 3.1 Schematic of Reduction Softening and Melting (RSM) apparatus [3-4].

Various parts and functions of the RSM are briefly discussed below.

High temperature furnace: The RSM is installed in a new high temperature furnace (Carbolite), which has a capacity to attain high temperature up to 1800 °C. This furnace has six heating elements, which are symmetrically arranged around the central alumina tube for homogeneous heating. The heating profile is controlled by a thermal controller, which responds to the in-built thermocouple.

Crucible: Specially designed high-grade graphite crucibles are utilised for the experiments (Fig. 3.2). The inner and outer diameter of the crucible is 64 mm and 76 mm, respectively. The crucible is fitted with the graphite nozzle to ensure proper gas distribution inside the sample bed. Additionally, six identical holes of 10 mm diameter are present at the bottom of the crucible to allow the liquid dipping.

Mass flow controller: Brooks mass flow controller for carbon monoxide (CO), carbon dioxide (CO_2), hydrogen (H_2) and nitrogen (N_2) gas are utilised to control the gas inlet composition during the experiments. These mass flow controllers for different gases are connected with the computer and controlled with a LabVIEW program, specially written for this project.

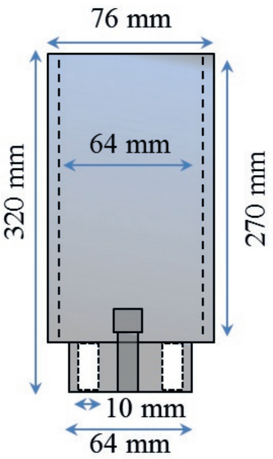

Fig. 3.2 High-grade graphite crucible utilised in the experiments.

Gas mixer: A gas mixer (Verdermix, VMX static mixer) is installed in the gas panel. After passing through their respective mass flow controllers, the gas is passed to the mixer to ensure the proper mixing of the inlet gases before it enters the sample bed.

Gas analyser: A gas analyser panel is utilised during the experiments (Fig. 3.3a). The off-gas after interaction with the sample is filtered to enter the analyser. The panel is fitted with the separate gas analysers of carbon monoxide (CO), carbon dioxide (CO_2), hydrogen (H_2), and moisture (H_2O). The measured concentration is summed up and balance is assumed for nitrogen (N_2) gas. These gas analysers are calibrated for gases with known composition. Then, one hour prior to the start of the experiment, the gas analyser is switched on and flushed with nitrogen gas to ensure the stability in the gas analysis.

At the later phase of the project, a new mass spectrometer (Hiden, HPR-20) is utilised for the gas analysis (Fig. 3.3b). This gas analyser has the capability to identify the unknown evolved gas with atomic mass up to 300 amu and with the composition detection level up to 5 ppb.

(a). Gas analyser panel (b). Mass spectrometer

Fig. 3.3 Gas analysers utilised in the project.

Displacement sensor: A displacement transducer (RDP, ACT2000C) is attached with the tripod stand on the top of the RSM furnace (Fig. 3.1). The displacement sensor is calibrated to accurately (error < ±0.5 mm) measure the change in sample bed height up to 100 mm. As the sample is placed inside the crucible and load is applied from the top, any volume change will result in a change of the bed height. The sample swelling will result in an increase of bed height, which is measured as a positive change in bed height. The sample shrinkage, softening and melting will result in a decrease of the bed height, which is measured as a negative change in bed height. The change in bed height is logged every 10 seconds for the entire experiment.

Pressure drop sensor: A differential pressure transducer (Honeywell, KZ) is employed in the RSM to measure the pressure difference across the sample bed (Fig. 3.1). This has the capacity to measure the change in pressure difference up to 6000 Pa. It gives a direct indication of the state of sample bed permeability. As the softening and melting of the sample will change the permeability in the burden bed, the pressure difference between the lower and upper chamber across the sample bed will change. It is measured by the pressure drop transducer with the help of tubes attached to these two chambers. The rate and change in the pattern of pressure drop across the sample bed are inferred as a signature of different physical phenomena occurring inside the sample bed (Section 3.7.2). The change in pressure difference across the sample bed is measured and logged every 10 seconds during the experiment.

Thermocouple for sample temperature: A standard B-type thermocouple is utilised to measure the sample temperature. To accurately monitor the sample temperature, it is attached inside of the alumina piston, which is rested on the top of the sample bed (Fig. 3.1).

Balance: As a result of coke gasification and reduction reaction of iron oxide, the sample weight changes. To measure the change in sample weight during the experiment, a weighing balance (AND, GP61K) is employed (Fig. 3.1). This balance has the capacity to measure the weight from 0.1 g to 61 kg with an accuracy of 0.1 g.

Datalogger: An advance 16 channel data logger (Atal, ATM-05) is used for the recording of process data during the experiment (Fig. 3.1). The output of the employed transducers for the measurement of displacement, pressure drop, gas analysis and temperature are connected with the input of the data logger. The output of the data logger is connected with the computer to display and record the experiment data.

Computer: The computer controls and records the process data during the test. RS232 cable is utilised to connect the computer with the mass flow controller and the datalogger. A specially written program in LabVIEW software was utilised to control and monitor the gas flow rate during the experiment.

Load: A mechanical load is applied on the top of the sample bed to simulate the load conditions of the iron-making blast furnace, A constant weight of 25 kg is applied with the help of the alumina piston. This represents a load of 0.98 kPa on the sample bed.

Sample collector: It is located at the bottom of the RSM furnace (Fig. 3.1). The sample collector is fitted with 12 metal cups to collect the dripping liquid from the sample crucible (Fig. 3.4a). This can be rotated during the experiment to collect the liquid over time and temperature range. It is also fitted with two glass windows to view and record the event of liquid dripping (Fig. 3.4b).

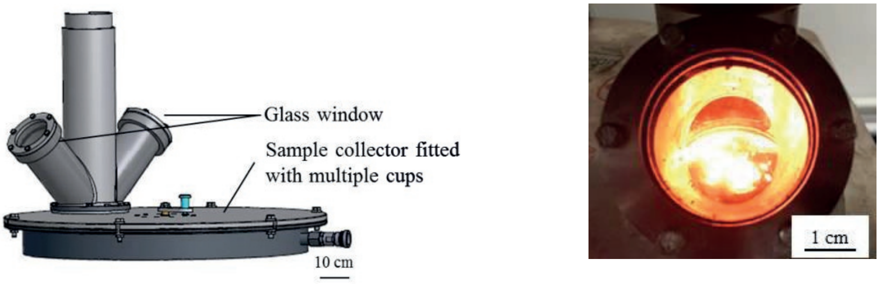

(a). Sample collector

(b). Glass window of the sample collector

Fig. 3.4 Sample collector and event of first liquid drop visualised from the gas window.

Support jack: The central assembly of the RSM is rested on the support jack. The sample crucible is loaded and unloaded in the RSM furnace with the help of a support jack.

A photograph of the RSM apparatus present at the Department of Materials Science and Engineering at the Delft University of Technology is shown in Figure 3.5.

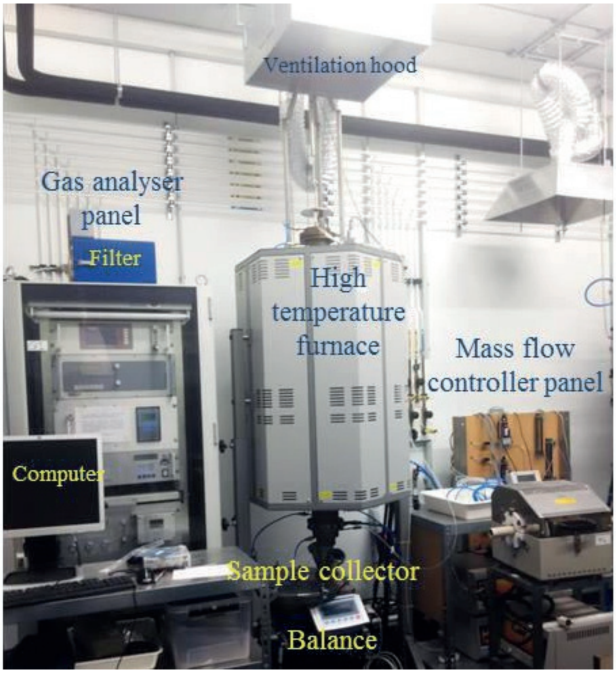

Fig. 3.5 Photograph of Reduction Softening and Melting (RSM) apparatus.

3.3 Raw materials

Commercially supplied iron ore pellets and sinter of size range 10-15 mm are used in the present study (Table 3.1). In the case of pellet-only burden, pellet type 1 is utilised for the experimental studies. In the case of ferrous burden, the pellet type 1, pellet type 2 and sinter are mixed utilised in 20:40:40 ratio. During the test, the coke of size 10-15 mm, 15-20 mm and 20-25 mm is utilised as the nut coke. Nut coke and ferrous burden are mixed (stochastically), then charged in the crucible. Due to the crucible size (inner diameter 64 mm) limitation, the nut coke of size 20-25 mm is applied as the regular coke. Hematite is the principal phase present in all examined ferrous raw materials (Fig. 3.6). However, in iron ore sinter, the magnetite and magnesioferrite phases are also noted in the X-ray diffraction pattern due to their significant presence (Fig. 3.6). The nut coke (10-15 mm) chemical and coke ash analyses are given in Table 3.2 and Table 3.3, respectively.

Table 3.1. Chemical analysis of the ferrous burden (XRF) wt%.

Sample	Fe(T)	FeO	CaO	SiO_2	MgO	Al_2O_3	TiO_2	MnO	P_2O_5	K_2O
Pellet type 1	64.94	1.20	0.37	3.70	1.21	1.06	0.26	0.30	0.08	0.04
Pellet type 2	66.46	0.60	0.45	2.22	1.38	0.27	0.16	0.07	0.06	0.04
Sinter	57.42	9.80	11.50	4.31	1.24	1.19	0.16	0.43	0.10	0.03

Figure 3.7 shows the schematic of the sample bed arrangement inside the graphite crucible. In the sample without nut coke, the ferrous raw material layer is sandwiched between the two regular coke layers, similar to the blast furnace layered structure. In the case of sample mixed with nut coke, the regular coke layer is proportionally removed and the coke layer becomes thinner (Fig. 3.7). The regular coke is equally distributed between the top and bottom layers.

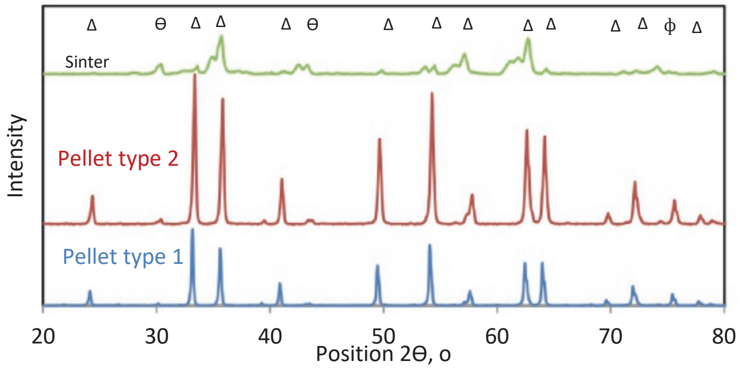

Fig. 3.6 X-ray diffraction (XRD) pattern of ferrous raw materials (Δ- Hematite, ϕ-Magnetite, Θ-Magnesioferrite).

Table 3.2 Chemical analysis of the 10-15 mm sized nut coke (ultimate analysis).

Component	Carbon	Nitrogen	Sulphur	Hydrogen	Ash
wt%	85.5	1.48	0.61	0.25	12.16

Table 3.3 Chemical analysis of the 10-15 mm sized nut coke ash.

Component	SiO_2	Al_2O_3	Fe_2O_3	CaO	TiO_2	K_2O	P_2O_5	MgO	Na_2O	MnO
wt%, in ash	58.70	26.80	5.90	2.48	1.93	1.47	1.24	0.84	0.30	0.04

All experiments in the RSM are carried out with a constant bed weight of ferrous burden (pellet and/or sinter mixture) (500 g) and coke (100 g), which represents a coke ratio of

300 kg/t of hot metal (kg/tHM) in the blast furnace equivalent. The blast furnace is assumed to operate with a pulverised coal injection (PCI) rate of 200 kg/tHM.

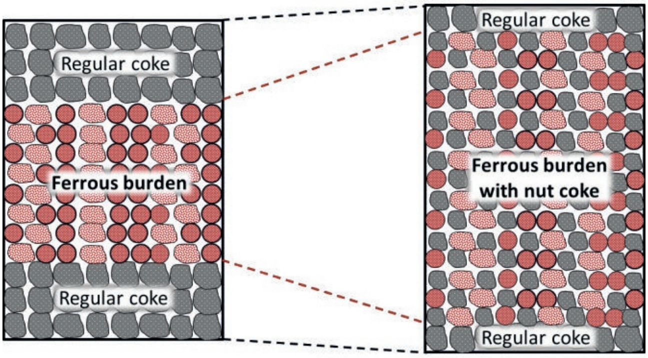

(a). Sample bed without nut coke (b). Sample bed with mixed nut coke

Fig. 3.7 Schematic of the sample bed arrangement inside the crucible.

3.4 Experimental procedure

The Reduction Softening and Melting (RSM) apparatus (Fig. 3.1) is utilised to perform the experiments under simulated blast furnace conditions. The sample bed arranged inside the graphite crucible is placed inside the RSM furnace (Fig. 3.1). Then the lower flange is installed. Thereafter, all the sensors, gas and water cooling connections are made. Then, the nitrogen gas is passed into the system and leak detection liquid (Swagelok snoop) is used to detect the gas leakage from the system. After ensuring no gas leakage, the gas analyser and the furnace is switched on and the furnace tube is flushed with nitrogen gas (5 Litre Per Minutes, litre/min) for an hour.

The mass flow controller of the respective gases (CO, CO_2, H_2 and N_2) is employed to control the gas flow rate. These gases are pre-mixed in the gas mixing station through a mass flow controller. Thereafter, the gas mixture flows upwards inside the reactor tube of the high temperature furnace from the inlet present at the bottom flange. Then, this mixture enters the crucible (height of 270 mm; internal diameter of 64 mm) from six holes and a nozzle located at the bottom of the crucible. For all experiments, a graphite nozzle of 5 cm high is fitted at the bottom of the crucible for the gas distribution (Fig. 3.2). After interaction with the sample, the gas is filtered and the chemistry is analysed and recorded.

3.5 Experimental conditions

During the experiments, the blast furnace conditions are simulated by varying the gas and temperature conditions with time for a stationary sample bed. In the blast furnace, as the material travels from top to bottom the load on the raw material bed increases. Additionally, the stress on the raw material varies in the radial direction inside the blast furnace. Thus, it is difficult to measure the real stress on the raw material bed inside the blast furnace. However, an estimation can be made for stress with Janssen equation [5]. Figure 3.8 shows the stress estimated by Yamaguchi et al. [6] using Janssen equation. This shows that the stress increases as the raw materials travel from furnace top to the lower part. However, in reality, the effect of load on burden becomes apparent when the materials reach a high temperature zone to start the burden softening. Thus, a common practice is to apply a constant load of 96 kPa on the sample bed for test under simulated blast furnace conditions [7-8]. In the present case, a fixed load of 25 kg is applied on the top of the sample bed during the experiment to effectuate this load.

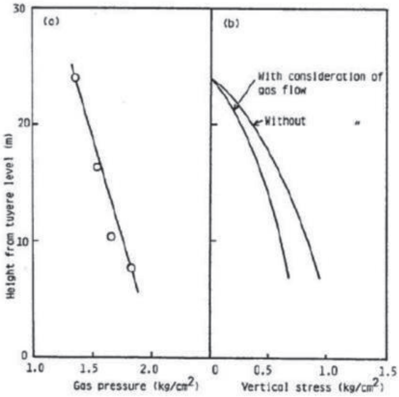

Fig. 3.8 Calculated pressure and stress distribution in the blast furnace [6].

A displacement transducer is employed to measure the sample bed contraction during softening and melting. The pressure drop across the sample bed is measured by a differential pressure transducer. The sample bed temperature is measured by the B-type thermocouple. The gas analysis, pressure drop and bed contraction are logged every 10 seconds and recorded in the datalogger (Atal, ATM05).

The experiment is performed following the heating and gas profile derived from the vertical probing of a real blast furnace [9]. The thermal and gas composition profiles followed during the experiments are given in Table 3.4. The gas velocity inside the crucible is also presented in Table 3.4. It is estimated by gas flow rate to the inner cross-sectional area of the crucible. In the blast furnace, the gas velocity is expected to change with the temperature and bed porosity. The effect of temperature on the gas velocity is incorporated by assuming the ideal gas behaviour (Table 3.4). For the estimation of gas velocity, the crucible is considered empty (porosity, $\varepsilon = 1$). However, in the real blast furnace scenario, the bed porosity will be much less than 1 due to the presence of raw materials for iron production. Additionally, bed porosity will change with temperature. Especially during softening and melting of the ferrous raw materials, the bed porosity will decrease dramatically. Consequently, the gas velocity will increase, resulting in higher pressure drop across the pellet bed. Furthermore, the mass flow rate of the total gas within the blast furnace may also change due to reduction reactions and gasification of coke. Inside the blast furnace, the pressure also changes along the height. All these should be taken into account when calculating the real local gas velocities.

A detailed matrix of the experiments planned for the current project is given in Table 3.5. For detailed investigation on the reduction, softening, melting and dripping behaviour of the nut coke mixed ferrous bed, the following three sets of experiments are performed.

Smelting experiments: High temperature (20-1550 ^{o}C) experiments are carried out in RSM to realise the melting of the ferrous raw material. The thermal and gas profile followed during the smelting experiments are given in Table 3.4. The liquid (metal and slag) drips and is collected in cups located in the sample collector (Fig. 3.4). The event of first liquid dripping (T_{xf}) is recorded after visualising the droplet from the glass window located at the lower part of the RSM apparatus (Fig. 3.4b).

After the melting experiment, the dripped samples collected in the cup are removed. Thereafter, a portion of the sample is pulverised and magnetically separated (slag and metal). The slag (non-magnetic portion) is analysed (XRF) for the present elements, and metal (magnetic portion) is analysed for the carbon content (LECO, Carbon-Sulphur analyser).

Quenching experiments: The decision on the quenching temperature for the sample bed is made after a series of melting experiments. In order to understand the prime reason for the ferrous bed melting and liquid dripping, samples are quenched at designated temperatures. Sample beds are quenched at the start of bed melting. In order to understand the dripping behaviour in the presence of nut coke, the sample beds are also quenched at dripping temperature for some selected experiments.

Once the desired temperature is reached, the bed is quenched by purging nitrogen gas (7.5 liter/min) and the furnace is switched off. After cooling, the sample crucibles are cast using cold mounting resin and cut vertically into two halves for further characterisation and analysis.

Dripping experiments: The thermal and gas profiles during the dripping experiments are kept the same as for the melting experiments shown in Table 3.4. During the dripping experiments, the rotating sample collector located at the bottom of the RSM (Fig. 3.9) is utilised. The sample collector is fitted with multiple cups (12 pieces), which is rotated to collect the dripping liquid (metal and slag) over the time and temperature range. To compare the effect of nut coke addition, experimental results are closely compared for the case when nut coke is absent in the sample bed.

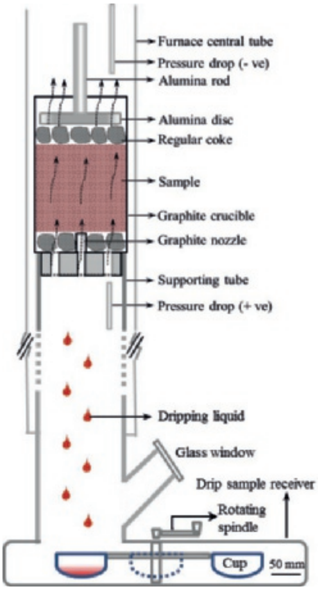

Fig. 3.9 Schematic of RSM, sample arrangement and dripped liquid collection system.

After the melting and dripping experiments, the coke present inside the crucible is collected and sorted. The size difference between the regular coke and nut coke is utilised for the separation. Then the sorted coke is weighed to estimate the fraction consumed during the experiments.

Table 3.4. Thermal and gas profiles followed during the experiments.

Step	Temperature range (°C)	Heating rate (°C/min)	CO(%)	CO_2 (%)	H_2 (%)	N_2 (%)	Gas flow rate (liter/min)	Real gas velocity range* x10^{-2} (m/sec)
Step 1	20 – 400	7.0	0	0	0	100	5	2.7 - 6.2
Step 2	400 – 600	5.0	25	20.5	4.5	50	15	18.6 - 24.1
Step 3	600 – 950	5.0	30	15.5	4.5	50	15	24.1 - 33.7
Step 4	950 – 1050	1.2	33	12.0	5.0	50	15	33.7 - 36.5
Step 5	1050 – 1550	5.0	42	0	8.0	50	15	36.5 - 50.3
Step 6	1550 – 20	-5.0	0	0	0	100	5	16.8 - 2.7

*Calculated for the empty crucible

Table 3.5 Matrix of the experimental plan.

A-series: RSM calibration.

- A few high temperature (20-1550 ^{o}C) experiments with pellets under N_2 gas.
- A few high temperature (20-1550 ^{o}C) experiments with the ferrous burden (pellet and sinter mixture) in reducing gas atmosphere.

B-series: Effect of nut coke concentration on physicochemical properties of the pellet bed.

- Iron ore pellets with 0 wt%, 10 wt %, 20 wt%, 30 wt% and 40 wt% nut coke (10 - 15 mm) under simulated blast furnace conditions of varying gas composition and temperature (20-1550 ^{o}C).
- Repetition of the above series of experiments.
- Quenching experiments for pellet bed at melting temperature (T_m), with (40 %) and without nut coke (10-15 mm).
- Quenching experiment for pellet bed mixed (40 wt%) with nut coke (10-15 mm) at dripping temperature (T_d).
- Dripping experiments with (40 %) and without nut coke (10-15 mm).

C-series: Effect of nut coke size on physicochemical properties of pellet bed.

- Iron ore pellet with 10% and 30% of nut coke size 10-15 mm, 15-20 mm and 20-25 mm under simulated blast furnace conditions of varying gas composition and temperature (20-1550 ^{o}C).

D-series: Effect of nut coke on the ferrous burden (Pellet and Sinter mixture) behaviour.

- Benchmarking with the individual ferrous burden of pellets and sinter with (40 wt%) and without nut coke (10-15 mm).
- The ferrous burden with 0 wt%, 20 wt% and 40 wt% nut coke, under simulated blast furnace conditions of varying gas composition and temperature (20-1550 ^{o}C).
- Repetition of the above series of experiments.
- Quenching of ferrous bed at the bed melting (T_m), with (40 %) and without nut coke (10-15 mm).

E-series: Effect of full replacement of regular coke with nut coke.

- Pellet mixed with 100 nut coke of size 10-15 mm, under simulated blast furnace conditions of varying gas composition and temperature (20-1550 ^{o}C).
- Pellet mixed with 100 nut coke of size 20-25 mm, under simulated blast furnace conditions of varying gas composition and temperature (20-1550 ^{o}C).
- Repetition of the above experiments.
- The ferrous burden with 100 % nut coke of size 10-15 mm under simulated blast furnace conditions of varying gas composition and temperature (20-1550 ^{o}C).
- Dripping experiment with 100 % nut coke (10-15 mm) mixed with ferrous burden under simulated blast furnace conditions of varying gas composition and temperature (20-1550 ^{o}C).

3.6 Analysis

The cross-sections of the selected samples before and after the experiments are visualised by an optical microscope (Keyence VHX-5000). The chemical analysis of the pellets, sinter, dripped metal and slag are examined with XRF (X-ray fluorescence, Panalytical, Axios Max).

The elemental distribution present in the quenched sample is investigated [10] with the help of the Energy Dispersive X-ray analysis (SEM-EDS, JSM-IT100) and Electron Probe Micro Analysis (EPMA- JEOL JXA 8900R). For the estimation of carbon in the dripped metal, the combustion infrared detection technique (LECO, Carbon-Sulphur analyser, CS744) is employed. The thermodynamics software 'Factsage 7.0' is utilised to estimate the carbon concentration in the formed iron metal.

3.7 Typical ferrous bed characteristics

3.7.1 Bed shrinkage

A typical trend of ferrous sample bed contraction under simulated blast furnace conditions is shown in Figure 3.10. Various stages of the bed contraction and parameters are described in Table 3.6. In the sample bed, three distinct stages of contraction can be observed. Under the blast furnace conditions, the ferrous sample layer evolves through these three stages [4,11].

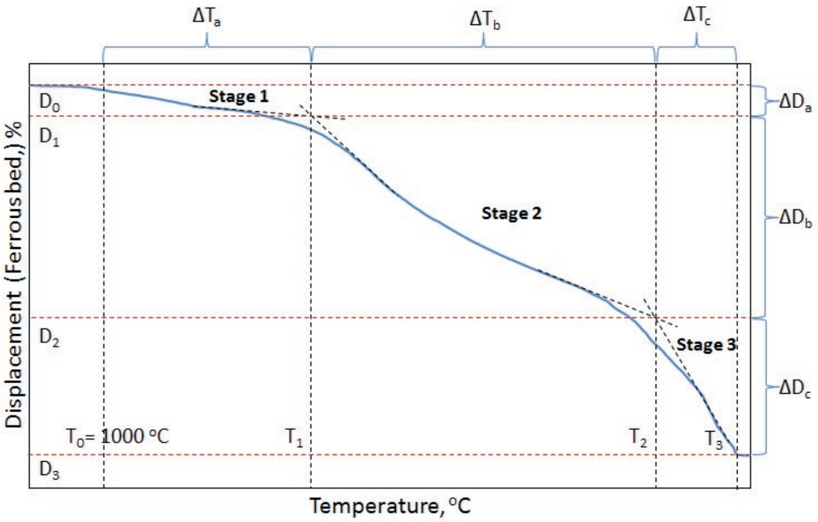

Fig. 3.10 Stages of sample bed contraction under simulated blast furnace conditions.

Table 3.6. Various parameters of sample bed contraction.

Symbol	Description	Unit
Stage 1	Individual ferrous raw material shrinkage due to reduction	-
Stage 2	Softening, sintering, and iron carburisation	-
Stage 3	Melting of ferrous burden and melts dripping (molten iron and slag)	-
T_0	=1000 ^{o}C, This temperature is defined as end temperature of the thermal reserve zone in the blast furnace [1] and is taken as 1000 ^{o}C.	^{o}C
T_1	First stage end temperature. Identified by the intersection point of tangents drawn to stage 1 and stage 2 behaviour. T_1 represents the start of bed softening.	^{o}C
T_2	Second stage end temperature. Identified by the intersection point of tangents drawn to stage 2 and stage 3 behaviour. T_2 represents the start of individual ferrous raw material melting in the bed.	^{o}C
T_3	Third stage end temperature. Identified as the point after which no further bed contraction occurs.	^{o}C
ΔT_a	$(T_1\text{-}T_0)$, the temperature interval between the thermal reserve zone and the end of stage 1.	^{o}C
ΔT_b	$(T_2\text{-}T_1)$, the temperature interval of stage 2. Softening temperature range.	^{o}C
ΔT_c	$(T_3\text{-}T_2)$, the temperature interval of stage 3. Melting and dripping temperature range.	^{o}C
D_0	Sample layer contraction at the start of an experiment (= 0 %).	%
D_1	Bed contraction at the end of stage 1. Identified by the intersection point of tangents drawn to stage 1 and stage 2.	%
D_2	Bed contraction at the end of stage 2. Identified by the intersection point of the tangents drawn to stage 2 and stage 3.	%
D_3	Bed contraction at the end of stage 3. Identified as the point after which no further contraction occurs.	%
ΔD_a	$(D_1\text{-D}_0)$, bed displacement in stage 1, occurs due to indirect reduction.	%
ΔD_b	$(D_2\text{-}D_1)$, bed displacement in stage 2, occurs due to burden softening.	%
ΔD_c	$(D_3\text{-}D_2)$, bed displacement in stage 3, occurs due to burden melting and draining.	%

Generally, the three principal phenomena responsible for bringing these three stages are indirect reduction, softening and melting. The complete list of different physicochemical phenomena which occur at these stages is given in Table 3.7.

Table 3.7. Physicochemical phenomena occurring at various stages of the sample bed contraction.

Physicochemical Phenomena	**Stage 1**	**Stage 2**	**Stage 3**
Swelling of individual ferrous raw material	✓	-	-
Indirect reduction (gaseous reduction)	✓	✓	-
Metal (iron) formation	✓	✓	-
Shrinking of individual ferrous raw material	✓	✓	-
Softening of the ferrous raw material	-	✓	-
Sintering of the ferrous raw material	-	✓	-
Iron carburisation (in solid state)	-	✓	✓
Burden deformation and collapse	-	-	✓
Melting and dripping	-	-	✓
Direct reduction	-	-	✓
Iron carburisation (in liquid state)	-	-	✓

3.7.2 Gas permeability

A typical pressure drop profile during the softening and melting of ferrous raw materials under blast furnace conditions is shown in Figure 3.11 and various parameters are described in Table 3.8. A steady pressure difference across the sample bed means that a large density of pores is present in the bed, facilitating the passage for gas flow. As the reduction reaction proceeds, the iron nuclei form on the ferrous raw materials. Then with an increase in the temperature, these ferrous raw materials start to sinter individually (shell sintering) and among the other raw materials. Consequently, the interior of the ferrous raw materials becomes inaccessible for reducing gases [12].

Later, the unreduced iron oxide (FeO) starts to melt along with other flux (CaO and MgO) and gangue oxides (SiO_2, Al_2O_3, etc.). Shortly after the start of melting, the gas starts to face resistance to flow across the bed. This is noticed by a gradual increase in pressure drop from the P_{Base} value at the bed softening temperature (T_s). The pressure drop continues to increase gradually as the sintering and local melting continue with an increase in the temperature.

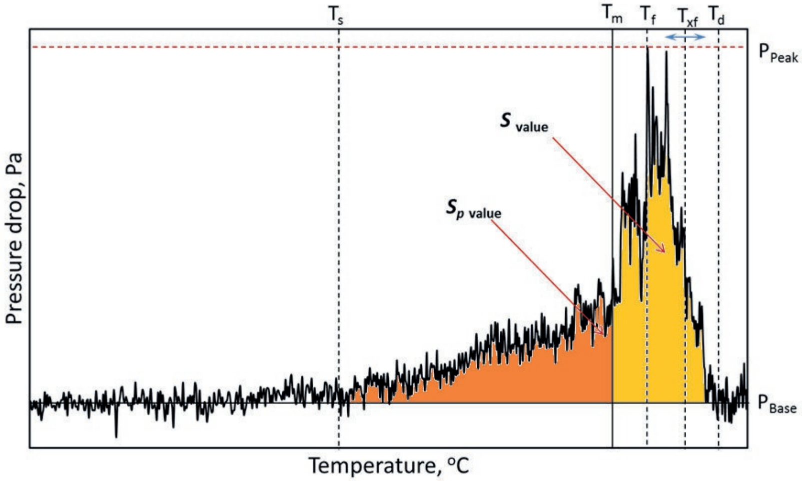

Fig. 3.11 A typical pressure drop profile during the softening and melting of the ferrous burden.

Table 3.8. Process parameters of pressure drop in the sample bed.

Symbol	Description	Unit
P_{Base}	The base value of pressure drop before the melting phenomenon.	Pa
P_{Peak}	The peak value of the pressure drop, the maximum pressure drop value observed during the test.	Pa
T_s	The softening point of the sample bed, the temperature at which the pressure drop value gradually increases above the P_{Base} value.	°C
T_m	The melting point of the sample bed, the temperature at which the pressure drop across the bed starts to increase steeply.	°C
T_f	The flooding point, the temperature at which the pressure drop reaches the maximum.	°C
T_{xf}	The first liquid drop point, the temperature at which the first liquid drop is visualised (from the glass window, Fig. 3.4) dripping out of the sample bed.	°C
T_d	The dripping point, the temperature at which the pressure drop value reaches back to the base value as before the softening and melting.	°C
S_p	The area under the pressure drop curve, in the softening range just before the start of melting temperature (T_m). It is a measure of resistance to the gas flow due to the burden softening [13].	Pa.°C
S_{value}	The complete area under the pressure drop curve, being a measure of the resistance offered by the sample to gas flow during softening and melting.	Pa.°C

Then, based on the carburisation level achieved on the reduced ferrous sample surface, melting occurs to cause the shell breakout. This is noted by a drastic increase in the pressure drop across the sample bed (T_m). Then, the liquid fills up the open pores and voids to cause the flooding in the bed (T_f). Thereafter, the liquid starts to move downward to drip out (T_{xf}) of the sample bed. Consequently, the pressure drop value starts to recover back to reach the P_{Base} at bulk dripping temperature (T_d). Thus, the total area under the pressure drop curve is a measure of overall resistance to the gas flow due to the softening and melting of the ferrous raw materials, which is denoted by '*S*-value'. The area under the pressure drop curve till the start of bed melting (T_m) is a measure of total resistance to the gas flow during softening, which is denoted by "S_p-value".

3.7.3 Reproducibility

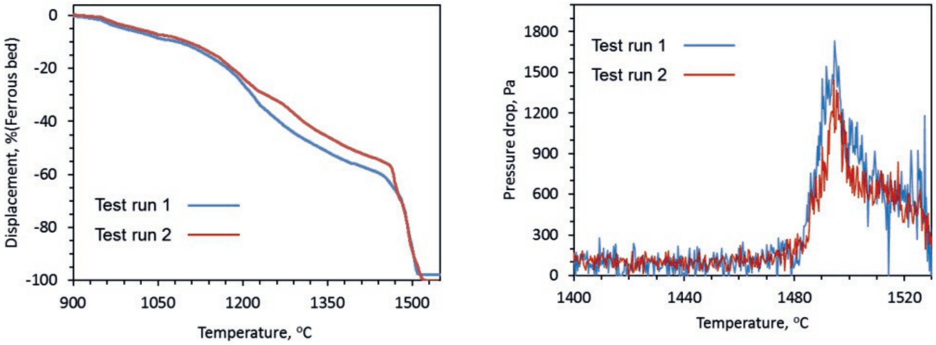

(a). Without nut coke, bed contraction (b). Without nut coke, pressure drop

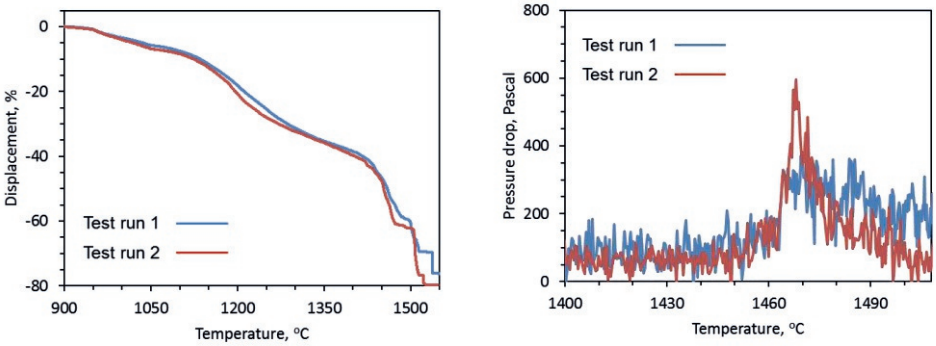

(a). With 40wt% nut coke, bed contraction (b). With 40 wt% nut coke, pressure drop

Fig. 3.12 Repeated experiments to check the reproducibility of the test in reduction softening and melting apparatus.

In order to check the result reproducibility, a series of experiments were repeated in RSM. A typical trend of the bed contraction and pressure drop profile evolved in the repeated experiment without nut coke and with 40 wt% mixed nut coke is shown in Figure 3.12. Interestingly, the bed characteristics temperature and displacement are observed to be in a close range for the repeated experiments. This shows the ability of RSM to provide reproducible results.

3.7.4 Degree of reduction (DOR)

The reduction degree achieved on the ferrous raw materials at any instant during the experiment can be represented by the oxygen to iron ratio. The initial oxygen and iron compositions are known from the chemical analysis of the ferrous raw materials (Table 3.1).

The degree of reduction is represented as DOR and it is calculated as follows:

$$DOR = \frac{m_O^{Rem}}{\mathrm{m}_O^{\mathrm{Raw}}} \tag{3.1}$$

where,

m_O^{Rem}: total mass of oxygen removed (g) from the sample at any instant during the experiment.

m_O^{Raw}: mass of oxygen present in ferrous raw materials (g) before the start of the experiment.

The oxygen balance between the gas inlet and outlet is used to estimate the amount of oxygen removed from the ferrous raw material. When the gas interacts with the ferrous sample, the reduction of iron oxide takes place by CO and H_2 gas. As a result, these gases convert into the CO_2 and H_2O (water vapour) and are analysed at the gas analyser panel (Fig. 3.3). However, this method for the calculation of DOR is not very accurate because the reduction of other oxides (MnO, SiO_2, TiO_2, etc.) which are usually present in the ferrous burden will also add to the removed oxygen (m_O^{Rem}) mass. However, considering the phase stability [1] and the amount of impurities (Table 3.1) present in the ferrous raw material, it is expected that this method will provide DOR value in a reasonable range.

The mass of removed oxygen at any instant during the experiments is given as:

$$\dot{\mathrm{m}}_O^{Rem} = \dot{\mathrm{m}}_O^{Outlet} - \dot{\mathrm{m}}_O^{inlet} \tag{3.2}$$

For the injected gas in RSM, the above equation can also be written as

$$\dot{\mathrm{m}}_{\mathrm{O}}^{\mathrm{Rem}} = \left\{\left(\frac{[CO]^{outlet} + 2[CO_2]^{outlet} + [H_2O]^{outlet}}{[N_2]^{outlet}}\right) - \left(\frac{[CO]^{inlet} + 2[CO_2]^{inlet} + [H_2O]^{inlet}}{[N_2]^{inlet}}\right)\right\} \frac{M_o\, x\, \theta_{N2}}{Vo} \tag{3.3}$$

Where,

$[x]$: Volume fraction of species x

θ_{N2} : Volume flow of N_2 gas, dm^3/min

M_o : Molar mass of oxygen, 16 g/mol

V_o : Standard volume of an ideal gas at room temperature, 22.4 dm^3/mol

Now, the mass of the oxygen removed can be estimated by integrating the oxygen removal rate over time.

$$m_O^{Rem} = \Sigma(\dot{m}_O^{Rem}) \tag{3.4}$$

The degree of reduction (DOR) can also be estimated with the help of the measured weight change of the sample bed during the experiment. The weight difference between the reduced and the initial weight of the ferrous raw material is due to the reduction reactions occurred on the burden. Thus, the ratio of a sample weight difference to the initial weight of oxygen in the sample represents the degree of reduction at any instant during the experiment.

In the present studies, due to the high noise and fluctuations in the measured sample weight mainly caused by the frictions at different locations of the system, this method for the estimation of the degree of reduction is not used.

3.7.5 Carbon mass balance

Under the blast furnace conditions, at low temperatures (below 700 °C), the carbon is deposited from the gas phase and at high temperatures (above 700 °C), the carbon is gasified from the solid phase according to the solution loss reaction [1].

$$CO_2 + C \rightarrow 2CO \tag{3.5}$$

The degree of this reaction can be estimated by the carbon balance. Similar to the estimation of DOR, carbon loss can be estimated by:

$$\dot{m}_C^{Rem} = \dot{m}_C^{inlet} - \dot{m}_C^{outlet} \tag{3.6}$$

$$\dot{m}_C^{Rem} = \left\{\left(\frac{[CO]^{inlet} + [CO_2]^{inlet}}{[N_2]^{inlet}}\right) - \left(\frac{[CO]^{outlet} + [CO_2]^{outlet}}{[N_2]^{outlet}}\right)\right\} \frac{M_C \, x \, \theta_{N2}}{Vo} \tag{3.7}$$

where,

M_C : Molar mass of carbon, 12 g/mol.

The total carbon loss can be estimated by integrating the carbon removal rate with time.

$$m_C^{Rem} = \Sigma(\dot{m}_C^{Rem}) \tag{3.8}$$

The positive value of m_C^{Rem} represents the carbon deposition and a negative value represents the carbon consumption during the experiment.

3.8 Objectives results

The experimental results from the Reduction Softening and Melting (RSM) apparatus are interpreted broadly in two categories as physical and chemical behaviour of the samples. These are discussed briefly in the section below.

Chemical behaviour: The analysis of the off-gas is performed to examine the chemical behaviour of the sample bed under blast furnace conditions. The time and temperature range for various key reactions like the reduction of iron oxide (direct and indirect reduction) and carbon (coke) gasification can be identified by the gas analysis. Additionally, the reaction between the liquid (metal and slag) and coke can also be identified by the off-gas analysis (Chapter 5).

Furthermore, the characterisation of the quenched sample bed at some key temperatures will help to verify the hypothesis. The chemical characteristics of the sample bed can be finalised after the investigation of the dripped liquid (metal and slag).

Physical behaviour: The physical behaviour of the sample bed is examined by the analysis of measured bed contraction and pressure drop across the sample bed under blast furnace conditions. The softening, melting and dripping of the ferrous raw materials occur at high temperature, which is noted by a specific pattern of bed displacement during the test in RSM (Fig. 3.10). The intermediately quenched samples will also give the physical status of the bed at different stages of the process.

The change in gas permeability is also a result of physical change occurring during the experiment under blast furnace conditions. It is observed by the change in a pressure drop across the sample bed. Various critical temperatures such as bed melting temperature (T_m), flooding temperature (T_f), and dripping temperature (T_d) can be identified by the nature of the pressure drop curve (Fig. 3.11, Table 3.8). The areas under the pressure drop curve also provide quantitative information about the resistance exerted by the sample bed during its softening and melting. Additionally, discussion of the liquid dripping pattern from the cohesive zone can also be made by the analysis of the video footage recorded from the glass window during the experiment.

3.9 References

[1] A.K. Biswas, Principles of blast furnace iron making - theory and practice, Cootha Publishing House, Brisbane, Australia, 1981.

[2] X. Liu, T. Honeyands, G. Evans, P. Zulli, D. O'dea, A review of high-temperature experimental techniques used to investigate the cohesive zone of the ironmaking blast furnace, Ironmak. Steelmak. (2018).

[3] Q. Song, Effect of nut coke on the performance of the ironmaking blast furnace, PhD Thesis, Delft University of Technology, 2013.

[4] D.J. Gavel, A. Adema, J. van der Stel, J. Sietsma, R. Boom, Y. Yang, Effect of nut coke addition on physicochemical behaviour of pellet bed in ironmaking blast furnace, ISIJ Int. 59 (2019) 778–786.

[5] U. Marini Bettolo Marconi, A. Petri, A. Vulpiani, Janssen's law and stress fluctuations in confined dry granular materials, Physica A. 280 (2000) 279–288.

[6] H. Yamaguchi, M. Maekawa, K. Narita, T. Uenaka, Properties of pellets, sinter and crushed pellet taken from cohesive zone in teh blast furnace, in: Ironmak. Conf. Proc., USA, 1983: pp. 531–540.

[7] P. Kaushik, R.J. Fruehan, Mixed burden softening and melting phenomena in blast furnace operation Part 3 – Mechanism of burden interaction and melt exudation phenomenon, Ironmak. Steelmak. 34 (2007) 10–22.

[8] P.F. Nogueira, R.J. Fruehan, Blast furnace burden softening and melting phenomena: Part I. Pellet bulk interaction observation, Metall. Mater. Trans. B. 35 (2004) 829–838.

[9] R. Chaigneau, H. Sportel, J. Trouw, R. Vos, J. Droog, Blast furnace burden quality: laboratory simulation, Ironmak. Steelmak. 24 (1997) 461–467.

[10] F. Robaut, A. Crisci, M. Durand-Charre, D. Jouanne, Practical aspects of carbon content determination in carburized steels by EPMA, Microsc. Microanal. 12 (2006) 331–334.

[11] J. Sternel, A.K. Lahiri, Contraction and meltdown behaviour of olivine iron ore pellets under simulated blast furnace conditions, Ironmak. Steelmak. 26 (1999) 339–348.

[12] D.J. Gavel, Q. Song, A. Adema, J. van der Stel, J. Sietsma, R. Boom, Y. Yongxiang, Characterization of the burden behaviour of iron ore pellets mixed with nut coke under simulated blast furnace conditions, Ironmak. Steelmak. (2018) 1–8.

[13] M. Bos, Effect of nut coke on cohesive zone properties of the ironmaking blast furnace, Masters thesis, Delft University of Technology, 2009.

4. Characterisation of iron ore pellets under mixed charge condition with nut coke

As described in the third chapter, the blast furnace conditions are simulated by means of Reduction Softening and Melting (RSM) apparatus, which was developed during the course of a previous Ph.D. project. After RSM installation, a series of high-temperature experiments were performed with nut coke (20 wt%) and without nut coke in the iron ore pellet bed. The pellet bed mixed with nut coke shows improved physicochemical properties, which resulted in the lower bed contraction. To understand the prime reason for improved bed properties, a detailed characterisation study is performed on the well preserved quenched sample beds from 1300 ^{o}C and 1400 ^{o}C.

In this chapter, the effect of nut coke addition is discussed in close comparison to the case when nut coke is absent in the bed. The mineralogical phases present in the representative sample are examined with the help of X-ray diffraction and scanning electron microscope. The microstructures are recorded and quantified using the image analysis tool. Then the quantified results are compared to understand the effect of nut coke addition during softening and before the melting stage. The chapter concludes by discussing the effect of nut coke mixing on the physicochemical properties of the pellet bed.

This chapter is based on the published scientific paper

Dharm Jeet Gavel, Qingshi Song, Allert Adema, Jan van der Stel, Jilt Sietsma, Rob Boom and Yongxiang Yang, “Characterization of the burden behaviour of iron ore pellets mixed with nut coke under simulated blast furnace conditions”, Ironmaking and Steelmaking, 2018. https://doi.org/10.1080/03019233.2018.1510873.

4.1 Introduction

In the blast furnace, the reduction of ferrous burden (iron ore, pellets and sinter) occurs during its descent from furnace top to the lower part. The reduction of ferrous raw materials experiences various steps, first hematite (Fe_2O_3) reduces to magnetite (Fe_3O_4), then magnetite to wüstite (FeO) and finally wustite reduces to metal iron (Fe). The kinetics of the reduction reactions varies for each step. Reduction of wüstite to iron is generally considered as the rate-controlling reaction [1]. Furthermore, the reduction kinetics is affected by the physicochemical phenomena occurring within and around the burden. As the burden descents in the furnace, the load experienced by the burden increases, which complicates the burden reduction and its interaction with surrounding materials.

The ferrous burden (iron ore, sinter, and pellet) reduction is accompanied by shrinkage, softening and melting in the cohesive zone. The cohesive zone starts with the softening and sintering of the ferrous burden and ends with the melting and dripping. Thus, high resistance to the gas flow is experienced in this zone [2]. This restricts the gas intake capacity of the blast furnace to limit productivity [1]. To improve the permeability in the cohesive zone, a method such as the addition of nut coke (10-40 mm, 2-23 wt%-replacement of regular coke) to ferrous burden has gained researchers and industrial attention [3]. Furthermore, the nut coke addition has the ability to improve the shaft permeability [4], enhance reduction kinetics [5], improve burden softening and melting properties [6] and extend the length of thermal reserve zone [3,7].

Under the nut coke mixed charged conditions, the changes in the ferrous burden properties with respect to a conventional burden without nut coke are the results of intrinsic changes. Therefore, to understand the fundamental reason for improved bed properties, a thorough comparative characterisation of the ferrous burden with and without nut coke is essential.

4.2 Materials and Methods

Iron ore pellets are a commonly used raw material for the iron production from the blast furnace route. Hence, commercially supplied iron ore pellets (olivine fluxed) are utilised in the present study. The chemical analysis with XRF (X-ray fluorescence, Pan-analytical, AxiosMax) of the raw pellet is given in Table 4.1. X-ray diffraction (Bruker D8 discover, WL=1.5406 Å) pattern of the raw iron ore pellet is shown in Figure 4.1, which reveals the hematite and magnetite as the major phases present in the iron ore pellets. The pellets and nut coke used are in size range of 10-13 mm and 10-15 mm, respectively.

Table 4.1 Chemical analysis of the iron ore pellets (wt%).

Fe (total)	SiO_2,%	CaO,%	Al_2O_3,%	MgO,%	MnO,%	TiO_2,%	ZnO,%
64.40	4.50	0.22	1.20	1.20	0.37	0.20	0.23

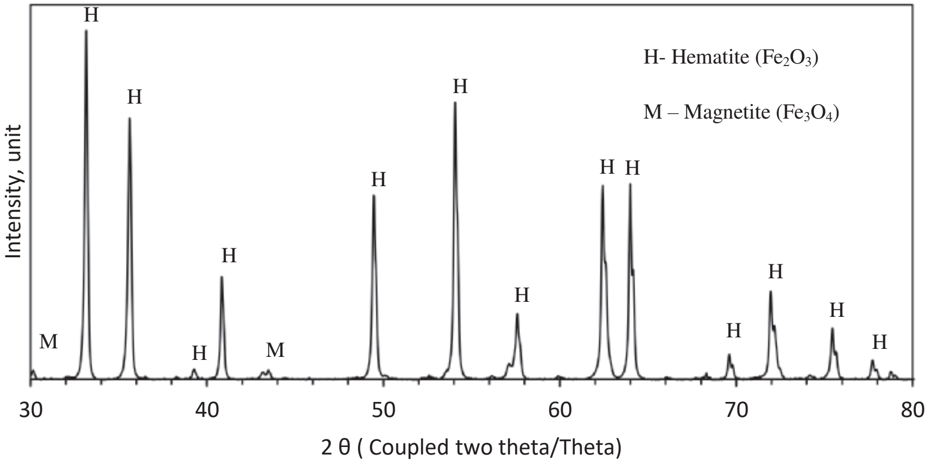

Fig. 4.1 X-ray diffraction (XRD) of the raw iron ore pellet.

In order to understand the effect of the nut coke addition on the ferrous burden, Song [6,8] has performed a series of experiments, both at room temperature and at high temperatures. His studies were intended to investigate the effect of nut coke addition on the bed permeability, reduction behaviour and softening-melting properties of the ferrous burden. These properties were found improving with the nut coke addition in the pellet bed. In order to further investigate the principal reasons for these improved burden properties, Song [6] has performed a series of quenching experiments under simulated blast furnace conditions. The thermal and gas profile followed during the experiments is given in Table 4.2, which is derived from the vertical probing of a real operating blast furnace [9]. Segment up to 9 and 10 were followed for sample bed heating up to 1300 °C and 1400 °C, respectively. Then sample bed were cooled (5 °C/min) in nitrogen gas atmosphere.

In the present work, the characterisation studies were further carried out. These well preserved quenched pellet beds were thoroughly investigated to characterise the microscopic development occurring during the shrinkage, softening and before the complete melting stage.

Similar to the blast furnace layered burden structure, iron ore pellets were sandwiched between the two regular coke layers inside the crucible. In the case of pellets mixed with nut coke, 20 wt% nut coke replacing the regular coke were mixed with the pellets before sandwiching in between the regular coke layers (Fig. 3.7). All the experiments were conducted with equal amounts of the pellets (500 g) and total coke (100 g). More information about the experimental set-up, procedure and condition can be found in chapter 3.

Table 4.2 Thermal and gas profile followed during the experiments.

Segment	Temperature (^{o}C)	Rate (^{o}C/min)	CO (%)	H_2 (%)	CO_2 (%)	N_2 (%)	Gas rate (litre/min)
1	20-250	7	0	0	0	100	5
2	250-400	7	25	4.5	20.5	50	
3	400-600	5	25	4.5	20.5	50	
4	600-800	5	30	4.5	15.5	50	
5	800-900	5	33	5	12	50	
6	900-950	5	33	5	12	50	15
7	950-1050	1.2	33	5	12	50	
8	1050-1100	5	42	8	0	50	
9	1100-1300	5	42	8	0	50	
10	1300-1400	5	42	8	0	50	

4.2.1 Sample selection

Compared to burden mass and volume in the blast furnace, the sample mass used in the study was very small. However, in the microscale, this burden experiences similar surroundings and atmosphere as in the blast furnace. Therefore, by the analysis of one or two representative pellets, the burden bed behaviour can be explained adequately.

In the study performed by Song [6], it was found that significant bed shrinkage occurs around 1300 ^{o}C, and sample melting occurs at a temperature above 1400 ^{o}C. Therefore, in the current study, detailed investigations are performed on the pellets quenched at 1300 ^{o}C and 1400 ^{o}C. In order to characterise the effect of nut coke addition, the sample beds with and without nut coke were closely compared. Photographs of the quenched sample beds are shown in Figure 4.2. The pellets located away from the graphite crucible wall and approximately cut through their centre are marked as representative pellets. In the case of pellets mixed with nut coke, to understand the effect brought by the nut coke addition, pellets located close to the nut coke were selected for the detailed analysis. Encircled pellets in Figure 4.2 are selected for detailed investigations. For the sample bed quenched at 1300 ^{o}C, the pellets look similar by brief observation under the microscope. Thus, one pellet was selected for the detailed analysis. In the case of sample quenched at 1400 ^{o}C, variation in the present phase appears among the representative pellets. Hence, two representative pellets were selected for the closer investigation.

(a). 1300 °C, without nut coke.

(b). 1400 °C, without nut coke.

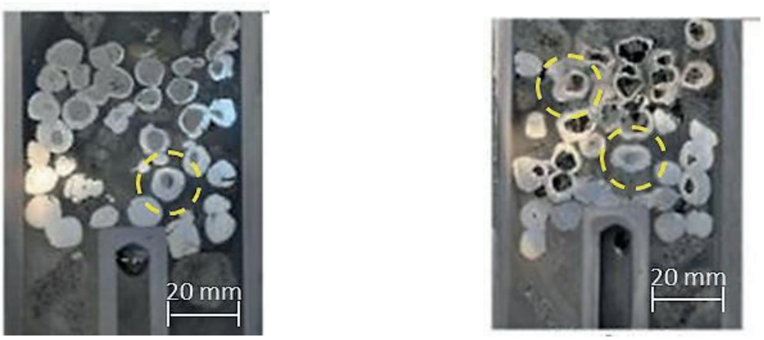

(c). 1300 °C, mixed with 20 wt% nut coke.

(d). 1400 °C, mixed with 20 wt% nut coke.

Fig. 4.2 Photographs of the sample bed quenched from high temperature [6,8]. Encircled pellets are selected for detailed analysis.

4.2.2 Phase identification

Phases (iron, wüstite, and slag), and pore distribution patterns were investigated in the sample pellets. Different phases present in the samples were determined by X-ray diffraction. XRD analyses were carried out with CoKα radiation (wavelength 1.5406 Å) with an accelerating voltage of 45 kV and a filament current of 25 mA. Parallel beam geometry was applied for the analysis. The scanning rate was 1.2 degree/min and the diffraction angle (2θ) was between 30° to 80°. Phases were analysed both at the pellet shells and core. Phase details and features were examined in a Field Emission Scanning Electron Microscope (FESEM, Joel 6500F). The composition of the phases was semi-quantitatively analysed using Energy Dispersive Spectroscopy (EDS). An acceleration voltage of 15 kV and 8 nA probe current were applied.

4.2.3 Phase quantification

For the phase quantification in the ferrous burden, advanced reflected light microscopes are generally used and their accuracy is stated to be high [10-11]. Thus in present studies, phases distribution in the pellet samples were logged by reflected light microscopy (Olympus BX60M) and quantified by image analysis techniques (Fig. 4.3). Two randomly selected diameters in the pellet cross-section were photographed from one end to the other, approximately 530 µm in each frame at 100 magnification. These micrographs were analysed for phase concentration and distribution with the help of ‘GIMP-2’ open-source image processing software [12]. The shape and contrast difference among the phases were used for the analysis. The number of pixels per phase was utilised to determine the volume percentage of different phases present in a micrograph.

To further enhance the accuracy in the examination of the features, SEM-EDS analysis were cross-referred. The pixels for the pores were estimated by subtracting the metal, wüstite and the slag pixels from the total micrograph pixels. These exercises were repeated for all the captured micrographs of the pellet. To view a complete cross-section of the selected pellet, a Keyence optical microscope (VHX-5000) was utilised in the ‘stitching’ mode.

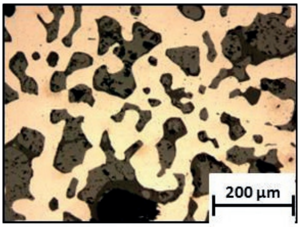

(a). Raw micrograph of the pellet section quenched at 1300 ^{o}C

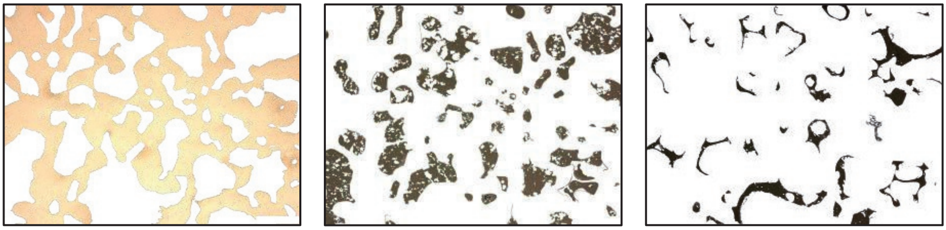

(b). Extracted metal (c). Extracted wüstite (d). Extracted slag

Fig. 4.3 Phase identification and quantification from the micrograph using image processing application (GIMP).

4.3 Results

4.3.1 Identified phases

For the detailed characterisation, the selected pellet from the sample bed is shown in

Figure 4.2. To identify the phases present in the pellet cross-section, XRD investigations were performed at the two positions on the selected pellets: shell and core. The diffraction patterns of the quenched pellets are given in Figure 4.4. A sharp peak of iron at the pellet periphery (shell) for all the selected samples shows that the reduction reactions is initiated at the surface, and proceeds to the centre.

In the samples quenched at 1300 °C, differences in the phases present between the pellet shell and core are observed (Fig. 4.4(a, b)). In the pellet without mixed nut coke, iron and wüstite are observed as the dominant phases present at shell and core, respectively (Fig. 4.4a). In the pellet mixed with 20 wt% nut coke, iron is observed as the primary phase at the shell. Additionally, a sharp peak of iron at the core along with wüstite indicates its presence in a significant fraction (Fig. 4.4b).

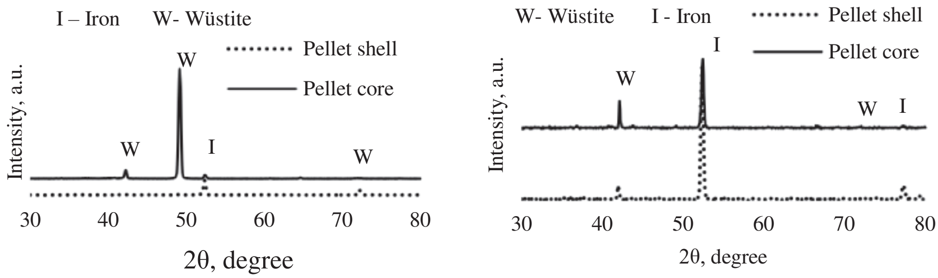

(a). Pellet quenched at 1300 °C without nut coke

(b). Pellet quenched at 1300 °C with 20 wt% nut coke

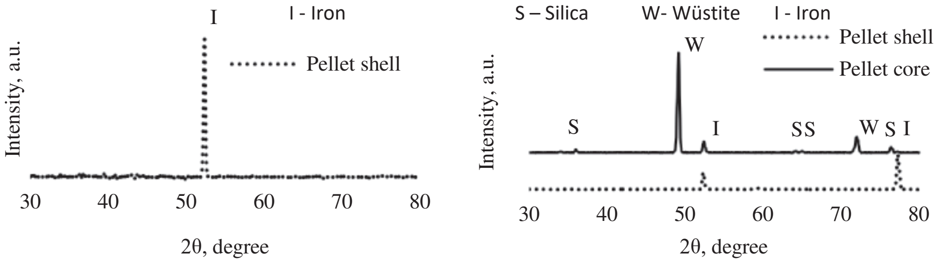

(c). Pellet quenched at 1400 °C without nut coke
Note: Analysed pellet core was hollow

(d). Pellet quenched at 1400 °C with 20 wt% nut coke

Fig. 4.4 XRD patterns of the quenched pellets.

In the sample quenched at 1400 °C, iron is observed at the pellet shell as the primary phase for both the cases (Fig. 4.4(c, d)). In the pellet mixed with nut coke, along with iron and silica, wüstite was observed as the leading phase at the core. On the other hand, in pellet without nut coke, the core was observed hollow, possibly due to the draining of the slag present in the pellet core (Fig. 4.4d).

In line with the XRD investigations, the identified phases are confirmed by the SEM-EDS analysis. For both cases and quenching temperatures (1300 °C and 1400 °C), the pellet shell consists of an iron matrix with entrapped partially reduced iron oxide (wüstite) and slag (Fig. 4.5(a, c)). In the sample quenched at 1300 °C with nut coke, the presence of iron nuclei at the pellet core is noted along with wüstite and slag (Fig. 4.5b). In the same pellet, at the core dispersed pores in size range of 10-100 µm are also observed.

As discussed earlier, the pellet core is hollow for the pellet without nut coke. However, strikingly in the core of pellet mixed with nut coke, iron is observed to be embedded in the wüstite matrix. In the same pellet, the presence of bigger size (100 – 400 µm) pores is also noted at the core (Fig. 4.5d).

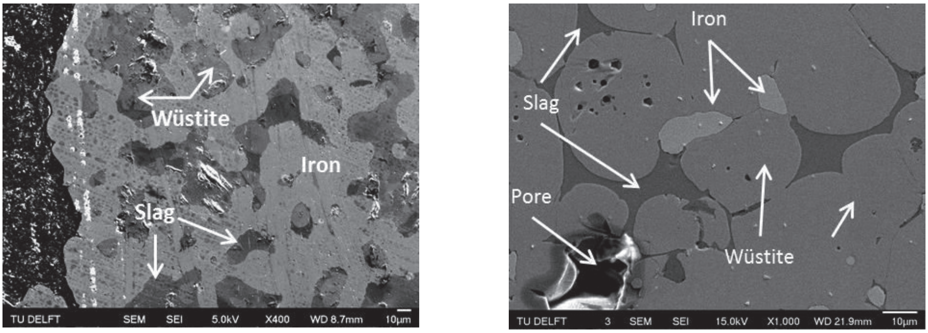

(a). Pellet shell at 1300 °C without nut coke

(b). Pellet core at 1300 °C with 20% nut coke

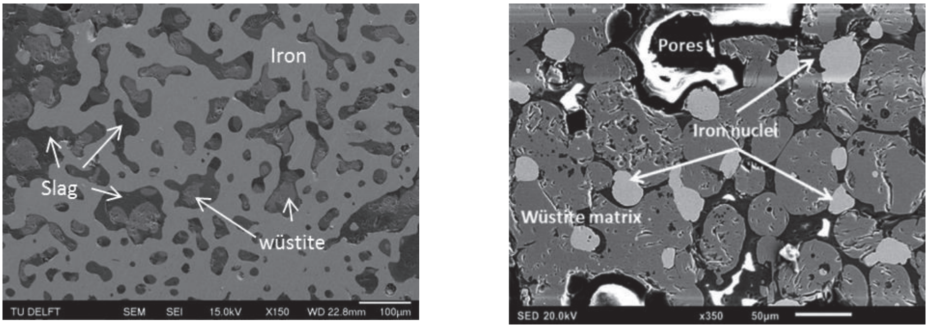

(c). Pellet shell at 1400 °C without nut coke

(d). Pellet core at 1400 °C with 20 % nut coke

Fig. 4.5 SEM-EDS micrographs of the quenched pellet sections.

4.3.2 Phase distribution

4.3.2.1 Pellets quenched at 1300 °C

Photographs of the pellet cross-sections quenched from 1300 °C are shown in Figure 4.6. In the pellet without mixed nut coke, close contact with surrounding pellets was observed (Fig. 4.6a). Reduced iron shells of the pellet are sintered with the neighbour pellets. In some instances, due to inadequate availability of the pellet surface for reduction and sintering at low temperatures (1050 °C) [13], pellets were seen connected even before the formation of an iron shell. This brings the situation of a common shell and connected core among two or more pellets (Fig. 4.6a). In the case of quenched pellets with 20 wt% nut coke, a uniform porous and a broader iron shell is seen. Furthermore, limited contact (sintering) among the pellets were observed. Quantified phase information for the pellets quenched at 1300 °C with and without nut coke is given in Figure 4.7. At the outer layer of both pellets, iron is observed as the dominant phase. The iron-rich region is thicker for the pellet mixed with nut coke compared to the pellet without nut coke. The total volume of unreduced iron oxide (wüstite) is observed to be large and concentrated at the core for pellet without mixed nut coke.

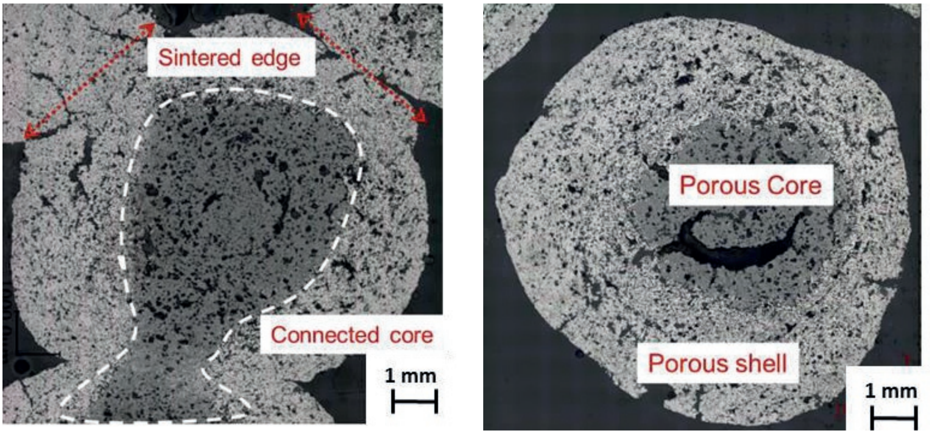

(a). Pellets from bed without nut coke (b). Pellet from bed mixed (20 wt%) nut coke

Fig. 4.6 Samples quenched from 1300 °C.

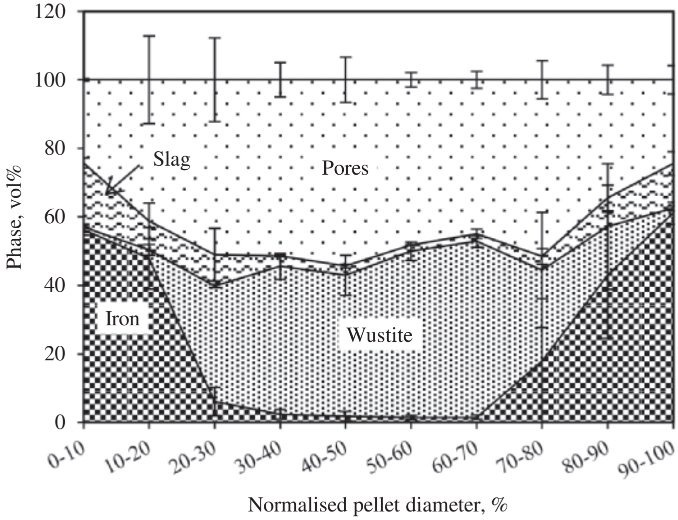

(a). Phase fractions in the pellet without mixed nut coke

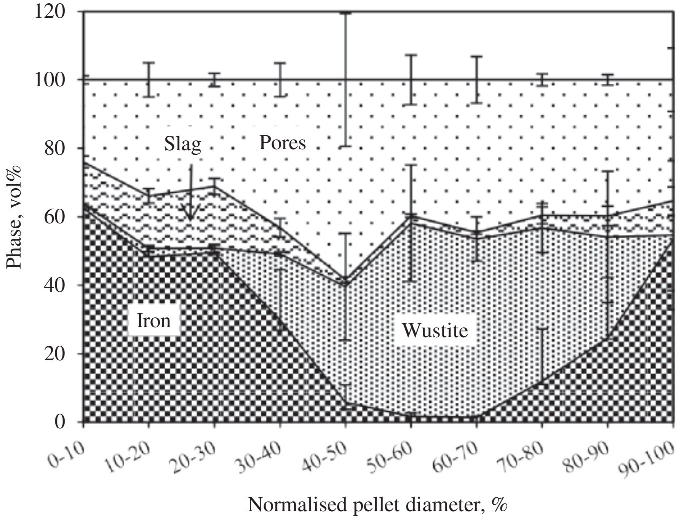

(b). Pellet with mixed (20 wt%) nut coke

Fig. 4.7 Distribution of phases and pores in the pellet quenched at 1300 °C.

4.3.2.2 Pellets quenched at 1400 °C

Pellets without nut coke mixing: Detailed observation in the microscope for pellets quenched at 1400 °C reveals significant variation in the features. Thus, for the pellets quenched at 1400 °C the investigations are performed on two representative pellets. Figure

4.8 shows the phase distribution within the pellet cross-section. Analysed results are plotted against the normalised pellet diameter. It is clear from Figure 4.8 that the central part of the pellet is hollow. The material concentration steeply decreases from about 90 vol% to 0 vol% by reaching nearly 40 % of the diameter from both ends of the pellet. Iron is present as a primary phase in the pellet shell. Within the shell, the presence of both wüstite and slag was observed in a similar range of 10-15 vol% and 15 vol% of pores were present at the shell. The metal concentration decreases from the shell to the core. It decreases sharply to 0 vol% at 40 % of its normalised diameter from both ends. Contrary to the metal phase, wüstite and slag concentrations (volume percentage) decrease in a gradual manner from pellet shell to the core. The pore volume is observed to increase continuously from the shell to core.

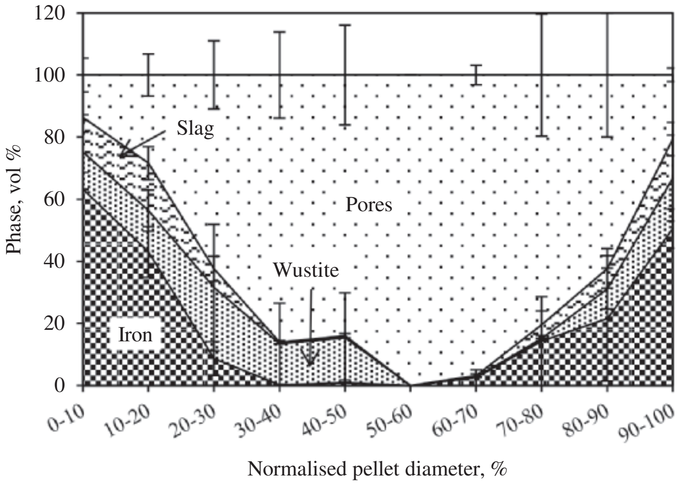

Fig. 4.8 Distribution of phases and pores in pellets quenched from 1400 °C without nut coke.

Pellets mixed with nut coke: Similar to the case when nut coke was absent, in the presence of (20 wt%) nut coke, a high material concentration is observed around the pellet periphery (Fig. 4.9). It decreases from about 90 vol% at the pellet edge to approximately 25 vol% around the core. The notable difference between the pellet with and without mixed nut coke at 1400 °C is the presence of approximately 25 vol% of materials at the pellet core in the pellets mixed with nut coke. Material at the core consists of about 5-15 vol% metal and 15-20 vol% wüstite along with the minimal quantity of the solidified slag.

Zooming into the section around the pellet core revealed that these materials are present in a network structure (Fig. 4.10). The matrix consists of wüstite with iron nuclei embedded in it. The iron nuclei are irregular in shape, present in a size range of 10-20 µm. The wüstite matrix thickness is inconsistent around the pellet core. The pore sizes are observed in a wide range of 100-400 µm.

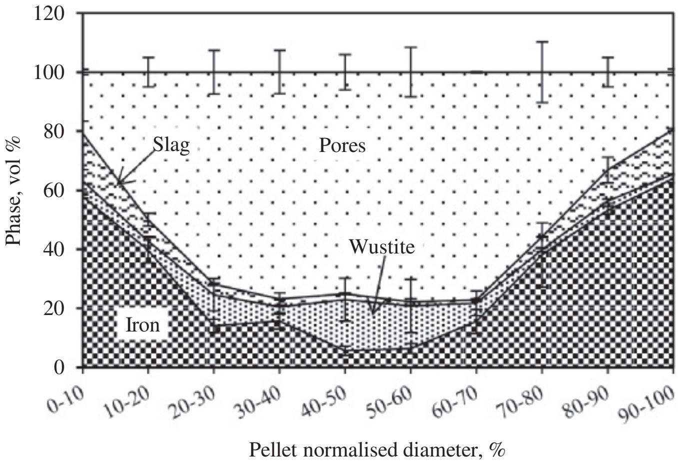

Fig. 4.9 Distribution of phases and pores in the pellets quenched from 1400 °C with nut coke (20 wt%).

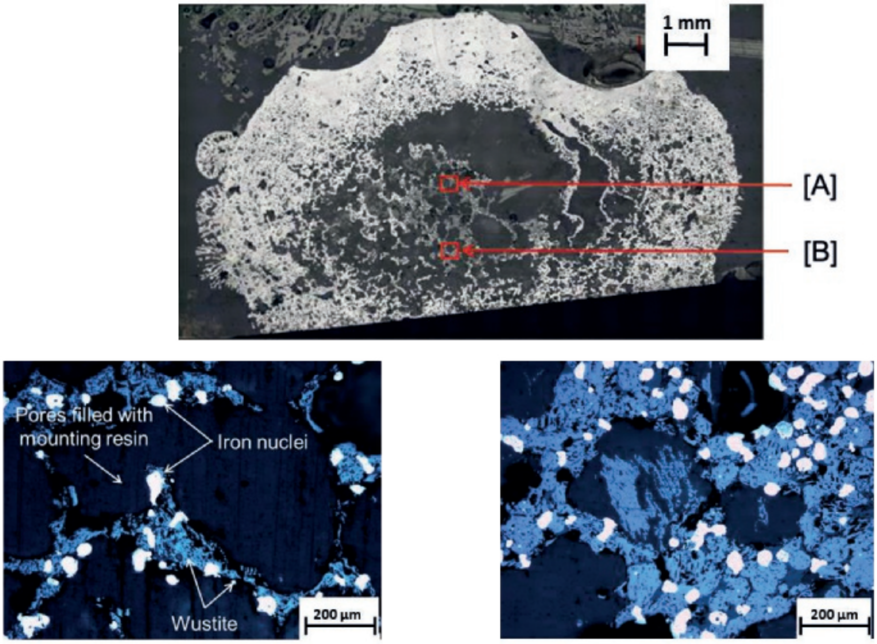

Location [A]:Thinner network of wüstite with few iron nuclei. (Iron nuclei-white colour, wüstite-grey colour and mounting resin-black colour)

Location [B]:Thicker network of wüstite with a large number of iron nuclei. (Iron nuclei-white colour, wüstite-grey colour and mounting resin-black colour)

Fig. 4.10 Reflected light microscopy of the pellet quenched from 1400 °C with 20 wt% mixed nut coke.

4.4 Discussion

4.4.1 Pellet behaviour in the absence of nut coke

Under blast furnace conditions, the topo-chemical reduction of iron ore pellets results in the formation of a product layer of iron metal at the periphery (shell). Due to the load on the burden and sintering at high temperature, this iron layer becomes dense and often turns out to be impermeable for the reducing gases. These phenomena hamper the reduction kinetics, leading to the formation of a partially reduced pellet core. As the pellet reaches the high-temperature zone inside the blast furnace, this partially reduced core together with fluxes and gangue minerals in and around the core melts to form the initial slag. This melt pool of slag tries to percolate or break the shell to pass on to its neighbour pellet or to the next available voids [14]. This leads to the formation of 'hollow icicles' in the pellet bed (Fig. 4.11).

Thereafter, with further increase in iron carburisation and temperature, the pellet shell ultimately collapses. This results in the filling of intrinsic pores and interstitial voids in the bed. Owing to the liquid filled in the pores and voids, a high pressure drop is experienced in this temperature zone inside the blast furnace. These series of events were explained by Gudenau et al. [14] after systematic experimentation. In the present study, corroborating the observation of Gudenau et al. [14], the hollow core is observed in the pellet bed without nut coke quenched at 1400 ^{o}C (Fig. 4.12). Observed pellets are connected to their neighbours and it appears that the liquid from the core has already transferred to the pellet located on the lower side.

As a result of close contact among the pellets, the probability of sintering among the pellets is high in the case of pellets without nut coke. The connection is observed to start even before core melting, as is evident from the pellets quenched at 1300 ^{o}C without nut coke (Fig. 4.6a). The shell and core seem to be connected because of close contact and sintering among the pellets. In the sintered pellet cluster, it is difficult for the reducing gases to penetrate inside the core, resulting in a large quantity of the leftover partially reduced iron oxide (wüstite) concentrated at the pellet core. Once melting initiates at high temperature, this situation further accelerates the melting to cause the 'physical core collapse' in the pellet, ultimately leading to the collapse and melting of the complete pellet bed.

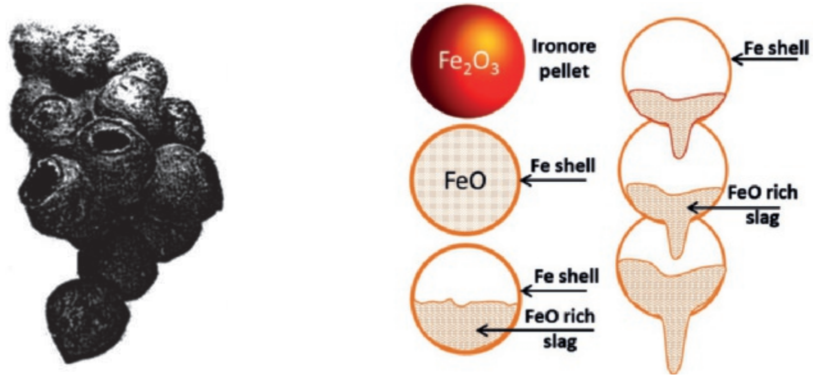

(a). Cluster of pellet shell with a hollow core. (b). Schematic of hollow icicles formation

Fig. 4.11 Hollow icicles formation in the cohesive zone, adapted from Gudenau et al. [14].

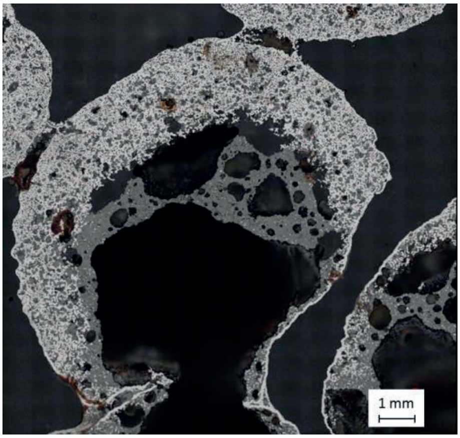

Fig. 4.12 Micrograph of the pellet quenched from 1400 °C without nut coke.

4.4.2 Pellet behaviour in the presence of nut coke

4.4.2.1 Reduction

Similar to the scenario without nut coke, the reduction reactions in the case of pellets mixed with nut coke progresses topo-chemically. The notable difference is the presence of a thicker iron product layer for the pellets mixed with nut coke for both examined temperatures (1300 °C and 1400 °C). Being a source of carbon, nut coke enhances both direct and indirect reduction reactions, resulting in a higher reduction degree [4]. In the presence of nut coke, the reduction reaction is controlled by chemical reaction and gas diffusion through the porous product iron layer. However, in the absence of nut coke, the reduction reaction was controlled by the solid-state diffusion (gas diffusion through a solid product layer).

Consequently, a comparatively smaller quantity of the wüstite is present at the pellet core (Fig. 4.7b). The wüstite (FeO) phase is known to form slag with gangue and additives at relatively low temperature (˜1200 °C). This means in the pellet mixed with nut coke, comparatively less raw materials (FeO) are available for the liquid (slag) formation. In the presence of more solid material at the core, a lower order of the deformation will occur. This delays the deformation and melts formation in the pellets to improve its high-temperature properties.

Furthermore, the presence of iron grains even at the core supports the argument of a higher reduction degree in the presence of nut coke, and on the contrary, no material is observed at the pellet core when nut coke is absent (Figs. 4.10 and 4.12). At the pellet core, iron nuclei are observed embedded in the matrix of wüstite and act as anchor points for the core structure.

The gasification reaction is faster for the nut coke scenario compared to the regular coke scenario because of the higher surface area (smaller size). This will result in bigger sized regular coke going to the hearth to maintain a *healthy* (permeable) blast furnace hearth operation.

4.4.2.2 Sintering

In the pellet bed mixed with nut coke, limited sintering among the pellets is witnessed (Fig. 4.2(c, d)). On the other hand, close contact and sintering among the pellets are noticed in the bed when nut coke is absent (Fig. 4.2(a, b), Fig. 4.6a, Fig. 4.12). In the representative pellets from the bed mixed with nut coke quenched from 1300 °C and 1400 °C, no sintering with the neighbour is noted (Fig. 4.10 and Fig. 4.6b). Nut coke brings the ‘spacer effect’ to physically hinder the contact among the pellets. By physical hindering, nut coke prevents the sintering among the pellets. Thus, at high temperatures, mixed nut coke particles limit the pellet cluster formation. As a result, more surface area and micropores on pellet surface are available for reduction reactions. Therefore, at high temperature nut coke enhances the reduction reactions to avoid ‘reduction retardation’ phenomenon [15], which is known to occur in the pellet bed.

4.4.2.3 Bed structure

In the pellet bed mixed with nut coke comparatively, less bed displacement was experienced at high temperatures [8]. In pellets with mixed nut coke, due to the presence of material (approximately 25 vol%) at the pellet cores, it offers higher resistance against the deformation. The reinforcement given to the core wüstite network structure with iron nuclei is clearly marked in the present study (Fig. 4.10).

Furthermore, to support the bed structure, nut coke acts as the *frame* for the pellet bed (Fig.

4.2(c,d)). Thus, the pellets undergo less sintering due to the support offered by the nut coke structure against the applied load on the top (Fig. 4.6b). This brings more reducing gases to the interior of the pellet to enhance the reduction process. Together with the network structured filled core, a wider iron product layer enhances the high temperature properties of the pellet. In the case of a pellet mixed with nut coke, a broader iron layer offers higher resistance against the deformation to increase the softening temperature. During melting of the pellets, the nut coke mixed in the bed is expected to support the structure and maintain gas permeability within the bed [8]. Additionally, this will prevent the sudden collapse of the pellet bed.

4.5 Conclusions

Based on a detailed characterisation of the quenched iron ore (olivine fluxed) pellets with (20 wt.%) and without nut coke, the following conclusions are drawn.

(1) In the pellet bed quenched from high temperature (1400 °C) without nut coke, the presence of a hollow pellet core was reconfirmed with the common understanding of pellet behaviour in the cohesive zone of the blast furnace.
Whereas, in the pellet bed mixed with 20 wt% nut coke (1400 °C), the core was observed to be filled with about 25 vol.% of material, which was unevenly distributed in a network structure. In the matrix of wüstite, iron nuclei reinforced the structure to bring additional strength to support the pellets against the deformation.

(2) In the case of pellets mixed with nut coke, for both quenching temperatures (1300 °C and 1400 °C), a broader outer iron layer (shell) and iron nuclei at the core was a clear result of the enhanced reduction kinetics offered by the presence of nut coke.

(3) It is experimentally confirmed that nut coke not only acts as a reducing agent when placed in close proximity of the iron ore pellets but also acts as a ‘spacer’ to physically hinder the contact of the pellets. Hence limits the sintering among the pellets.

Nut coke addition in mixture with the iron ore pellets has promised higher reduction degree, lower sintering among the pellets and stable bed structure.

4.6 References

[1] A.K. Biswas, Principles of blast furnace iron making - theory and practice, Cootha Publishing House, Brisbane, Australia, 1981.

[2] M. Geerdes, R. Chaigneau, I. Kurunov, O. Lingiardi, J. Ricketts, Modern blast furnace ironmaking : an introduction, IOS Press, under the imprint of Delft University Press,

Amsterdam, 2015.

[3] D.J. Gavel, A review on nut coke utilisation in the ironmaking blast furnaces, Mater. Sci. Technol. 33 (2017) 381–387.

[4] A. Babich, D. Senk, H.W. Gudenau, Effect of coke reactivity and nut coke on blast furnace operation, Ironmak. Steelmak. 36 (2009) 222–229.

[5] E.A. Mousa, D. Senk, A. Babich, H.W. Gudenau, Influence of nut coke on iron ore sinter reducibility under simulated blast furnace conditions, Ironmak. Steelmak. 37 (2010) 219–228.

[6] Q. Song, Y. Yang, R. Boom, Effect of nut coke on the reduction behavior in iron-making blast furnace, Baosteel Tech. Res. 9 (2015) 8–16.

[7] A. Sato, M. Aritsuka, Y. Yamagata, Y. Miyakawa, T. Goto, I. Mizuguchi, The operation with larger amount of nut coke under high pulverised coal rate, CAMP-ISIJ. 8 (1995) 1064.

[8] Q. Song, Effect of nut coke on the performance of the ironmaking blast furnace, PhD Thesis, Delft University of Technology, 2013.

[9] R. Chaigneau, H. Sportel, J. Trouw, R. Vos, J. Droog, Blast furnace burden quality: laboratory simulation, Ironmak. Steelmak. 24 (1997) 461–467.

[10] T. Kamesh, S. Kumar, M. Simonsson, N.N. Viswanathan, H. Ahmed, C. Andersson, B. Björkman, Establishing a novel methodology to correlate the macroscopic and microscopic degree of sintering in magnetite pellets during induration, Steel Res. Int. 89 (2018) 1–8.

[11] F. Nellros, Quantitative image analysis - A focus on automated characterization of structures in optical microscopy of iron ore pellets, Lulea University of Technology, 2013.

[12] Gimp.org, (2016). https://www.gimp.org/ (accessed November 20, 2016).

[13] J.P.S.G. de Alencar, V.G. de Resende, L.F.A. de Castro, Effect of temperature on morphology of metallic iron and formation of clusters of iron ore pellets, Metall. Mater. Trans. B. 47 (2016) 85–88.

[14] H.W. Gudenau, D. Senk, S. Wang, K. De Melo Martins, C. Stephany, Research in the reduction of iron ore agglomerates including coal and C-containing dust, ISIJ Int. 45 (2005) 603–608.

[15] E. Mousa, D. Senk, A. Babich, Reduction of pellets-nut coke mixture under simulating blast furnace conditions, Steel Res. Int. 81 (2010) 706–715.

5. Physicochemical behaviour of pellet bed mixed with nut coke

Mixing nut coke with iron ore pellets has shown the ability to improve the physicochemical properties of the bed by enhancing the pellet microstructure and by limiting the sintering among the pellets (Chapter 4). However, as the nut coke is utilised as a replacement of the regular coke, this will lead to thinning of the regular coke layer, and thus could affect the blast furnace performance. Furthermore, the nut coke size (10-15 mm, 15- 20 mm, 20-25 mm) can affect the bed properties differently. Thus, a parametric analysis is required to incorporate the effect of nut coke size and concentration (percentage replacement of the regular coke) on bed behaviour.

In the present chapter, the effect of nut coke size and mixing concentration on the iron ore pellet bed is described. To explore the behaviour of the nut coke mixed pellet bed, full temperature range (20-1550 ^{o}C) melting and dripping experiments were performed with the reduction softening and melting (RSM) apparatus. The added nut coke (10-15 mm) concentration is varied (0, 10, 20, 30 and 40 wt%). First, the effect of nut coke addition on various stages of the bed contraction and gas permeability (pressure drop and S-value) is explained. Then, the effect of mixing nut coke on the reduction degree and carbon utilisation is discussed. Finally, the chapter is concluded by explaining the effect of nut coke size (10-15 mm, 15-20 mm and 20-25 mm) on the physicochemical behaviour of the iron ore pellet bed.

This chapter is based on the published and prepared manuscript for submission in international peer reviewed journals

[1] Dharm Jeet Gavel, Allert Adema, Jan van der Stel, Jilt Sietsma, Rob Boom and Yongxiang Yang, “Effect of nut coke addition on physicochemical behaviour of the pellet bed in ironmaking blast furnace”, ISIJ International, 2019, 59 (5), 778-786.

[2] Dharm Jeet Gavel, Allert Adema, Jan van der Stel, Jilt Sietsma, Rob Boom and Yongxiang Yang, “Effect of nut coke size on the pellet bed behaviour under simulated blast furnace conditions”, (Manuscript prepared for submission in international peer reviewed journal).

5.1 Introduction

The ironmaking blast furnace is a counter-current reactor, in which reducing gases and solid raw material travel in opposite directions and exchange heat and mass efficiently. Hence, gas permeability is crucial at all levels of a blast furnace. About 25 % of the total (furnace) pressure drop occurs in the cohesive zone, which is due to the softening and melting of ferrous raw materials [1]. This zone of poor permeability has a negative impact on the productivity of the furnace. Gas permeability in this zone can be increased by mixing nut coke (10-40 mm) with the ferrous burden of pellets and/or sinter [2-4]. Furthermore, nut coke addition to the ferrous raw material has beneficial effects on enhancing the shaft permeability, lowering thermal reserve zone temperature and improving burden softening-melting properties [5].

Some studies were already performed to understand the influence of nut coke addition on the ferrous burden. For example, Babich et al. [6] reported the improvement in the shaft permeability, and therefore the furnace productivity was enhanced (1.5 % to 2.5 %) with the nut coke mixing (10 - 20 wt%). Mousa et al. [7-9] revealed that nut coke addition enhances reduction kinetics to avoid ‘reduction retardation’ phenomena, which occur at ˜1250 ^{o}C due to the formation of fayalitic ($2FeO\text{-}SiO_2$) slag. The softening and melting of the ferrous burden are known to occur at high temperatures (1250-1450 ^{o}C) [2,10]. As these studies were performed at a low temperature (below 1250 ^{o}C), no information was obtained on the effect of nut coke addition on the softening-melting properties of the ferrous burden. Additionally, when ferrous raw material reaches the cohesive zone, a massive pile of the burden rests on the top of the raw material bed; inevitably this will have an impact on the physical properties of this area of the furnace [11-12]. Since the loads were absent in those studies, the test condition was not representative for the blast furnace and only limited understanding was established.

Song [2] incorporated the gases, temperature, and load conditions to simulate the blast furnace conditions for the sample bed. Former studies [2,13] reported an increase in the softening and melting properties of the ferrous raw material when mixed charged with nut coke. However, these studies did not include the variation in the added nut coke size and concentration (performed only with 20 wt% of 10-15 mm size), and in-depth analysis is not provided.

Mostly, nut coke utilisation is driven by its generation during the coke making process. Despite being beneficial in the iron making process, nut coke is utilised in limited quantity (less than 30 wt%) [5,14]. It was also reported that nut coke addition might bring a negative impact on the overall gas permeability due to the regular coke layer thinning [1,15]. Therefore, considering the idea of nut coke use as the replacement of regular coke, it is of utmost importance to understand its impact on the gas permeability, when regular coke layer is thinned due to the higher replacement ratios (more than 20 wt% of the regular coke). It is clear from the literature that there is a lack of fundamental understanding of the bed behaviour at high temperatures when nut coke is added in higher concentration as a replacement of the regular coke.

In the present chapter, the effects of nut coke concentration (as a replacement of the regular coke) and size on the physicochemical properties of the iron ore pellet bed will be comprehensively evaluated and quantified.

5.2 Materials and method

5.2.1 Raw materials

In the present study, commercially supplied olivine fluxed iron ore pellets (type 1) with a size of 10-13 mm and nut coke with a size of 10-15 mm, 15-20 mm and 20-25 mm are used. The chemical analysis of the iron ore pellet sample, measured with XRF (X-ray fluorescence, Panalytical, Axios Max) is given in Table 3.1. The schematic of the sample arrangement inside the graphite crucible is shown in Figure 5.1. Due to the graphite crucible size limitation (inner diameter 64 mm), coke with a size of 20 to 25 mm is utilised as regular coke in the study. In the case of a sample bed without nut coke, a pellet layer is sandwiched between the two regular coke layers (Fig. 5.1a), similar to the blast furnace layered structure. In the case of pellets mixed with nut coke, the regular coke is proportionally removed, and the coke layer becomes thinner (Fig. 5.1b). The regular coke is equally distributed over the top and bottom layers. To avoid critical thinning of the regular coke layer, experiments are performed up to a maximum of 40 wt% nut coke mixing, the replacement ratio of normal-sized coke (called “nut coke concentration” in this study).

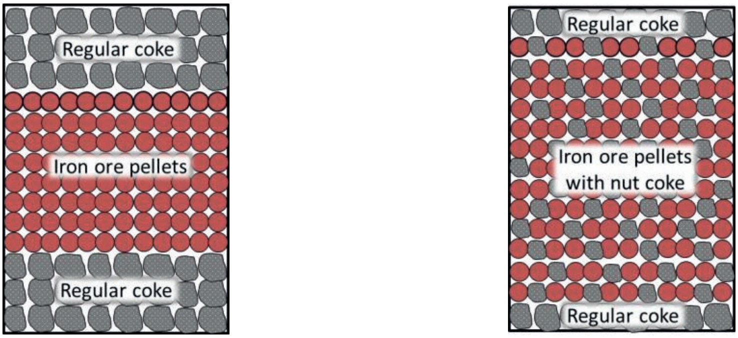

(a). Sample bed without nut coke.

(b). Sample bed with mixed nut coke.

Fig. 5.1 Schematic of sample bed arrangement inside the graphite crucible (internal diameter 64 mm).

For experiments with nut coke size 10-15 mm, its concentration is altered from 0 wt% to 40 wt% at intervals of 10 wt% and experiments are performed twice to check the reproducibility (3.7.3). For the nut coke size 15-20 mm and 20-25 mm, experiments are performed for 10 wt% and 30 wt% concentration only. All experiments are carried out with a constant bed weight of coke (100 g) and pellets (500 g), which represents a coke ratio of 300 kg/t of hot metal (kg/tHM) in the blast furnace equivalent. The blast furnace is supposed to operate with a pulverised coal injection (PCI) rate of 200 kg/tHM.

5.2.2 Experimental conditions

The sample bed is heated in the Reduction Softening and Melting (RSM) apparatus (Fig. 3.1), under simulated blast furnace conditions. During the experiments, the thermal and gas profiles followed the previously measured conditions of an operating blast furnace [16], and are given in Table 3.4. The mass flow controllers of the respective gases (CO, CO_2, H_2 and N_2) are employed to control the gas flow rate. These gases are pre-mixed in the gas mixing station and then passed to the preheating furnace. Thereafter, the gas mixture flows upwards inside the reactor tube of the high temperature furnace from the inlet at the bottom flange. Then, this mixture enters the crucible (height of 270 mm; internal diameter of 64 mm) from six holes and a nozzle located at the bottom of the crucible (Fig. 3.2). For all experiments, a graphite nozzle of 5 cm high is fitted at the bottom of the crucible for the gas distribution. After interaction with the sample, the gas composition is analysed and recorded.

During the tests, a load of 9.8 N/cm^2 is applied on the top of the sample bed (a total of 25 kg). To measure the sample bed contraction during softening and melting a displacement transducer (RDP, ACT2000C) is employed. The pressure difference across the sample bed is measured by a differential pressure transducer (Honeywell, KZ). The sample bed temperature is measured by the B-type thermocouple. The gas analysis, pressure drop and bed contraction are logged every 10 seconds and recorded in the datalogger (Atal, ATM05). More information about the experimental set-up, the crucible, the test procedure and conditions can be found in section 3.4 - 3.5. The thermodynamics software 'Factsage 7.0' is utilised to estimate the carbon concentration in the formed iron metal, produced from the above-mentioned iron ore pellets.

5.3 Result and discussion

5.3.1 Bed contraction

The sample bed contraction as a function of temperature for all experiments shows similar trends. Various stages of the bed contraction and different parameters are shown and defined in Figure 3.9 and Table 3.6, respectively.

5.3.1.1 General characteristics of pellet bed contraction behaviour

In the sample bed, three distinct stages of contraction occur (Fig. 3.9, Table 3.6). Under the blast furnace conditions, the sample layer always evolves through these three stages [11]. Generally, the three principal phenomena responsible for these three stages are an indirect reduction, softening and melting. The complete list of different physicochemical phenomena which occur at these stages is given in Table 3.7.

In the first stage, marginal bed contraction occurs (Fig. 3.9). Stage 1 occurs primarily due to shrinkage of individual pellets as a result of the gaseous (indirect) reduction. Pellets shrink due to the loss of the oxygen and sintering of gangue minerals [17]. Then the metallic iron forms during the complete reduction of the iron oxide (pellet). Due to topo-chemical reduction reactions, the iron forms first at the pellet periphery and grows into a shell [11,18].

This thin iron shell becomes dense due to the sintering under the load, which makes it difficult for reducing gases to reach the pellet core. Subsequently, with an increase in temperature, the partially reduced pellet core (rich in FeO) and other oxides (SiO_2, CaO, MgO, and Al_2O_3), start to melt and form a primary slag. This molten slag slowly fills the micropores present in the pellet to cause the softening that marks the start of the second stage of bed contraction and further hinders the reduction reactions to proceed.

Along with softening, due to the close contact among the pellets, sintering takes place to result in bed contraction [11,19]. At the start of the second stage, the rate of displacement is high, which later decreases due to the depletion of the micropores (Fig. 3.9). Simultaneously, the pellet shell (iron) carburises by the CO gas [20] and carbon from the regular coke present in the close vicinity [21]. Due to the close contact between the pellets and regular coke at the layer interface, the iron carburisation degree is high. Based on the carburisation degree achieved in the iron shell, melting occurs. Consequently, the pellet deforms and melting starts to mark the start of stage 3.

As the first layer of pellets melts away, the regular coke layer moves to the next pellet layer to carburise and thereafter melting proceeds. This continues layer-wise until all the pellets are molten and drained out. Because of the shell melting, the liquid present at the core is released, formed before or during the shell carburisation. Once this liquid (metal and slag) starts to flow over the coke, the metal rich portion picks up the carbon and slag (rich in FeO), is reduced first (direct reduction) and subsequently carburised. At the end of stage 3 due to the draining of liquid, the bed height becomes constant.

5.3.1.2 Effect of nut coke addition on pellet bed contraction

The sample bed contraction is recorded as a function of temperature for the full heating cycling of the experiment (Table 3.4). Influence of nut coke addition on various stages of the sample bed shrinkage is shown in Figure 5.2 and is discussed in detail in the next section.

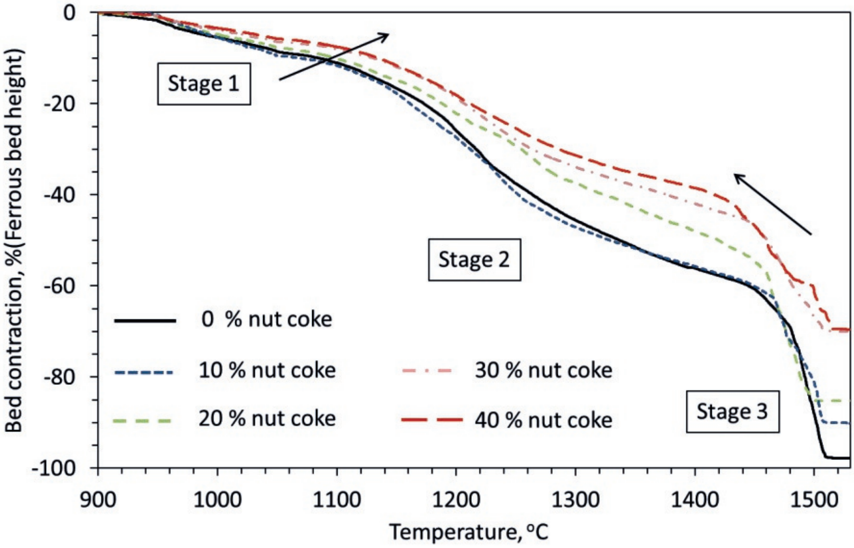

Fig. 5.2 Effect of nut coke addition on the sample bed contraction.

Effect of nut coke concentration on stage 1 behaviour:

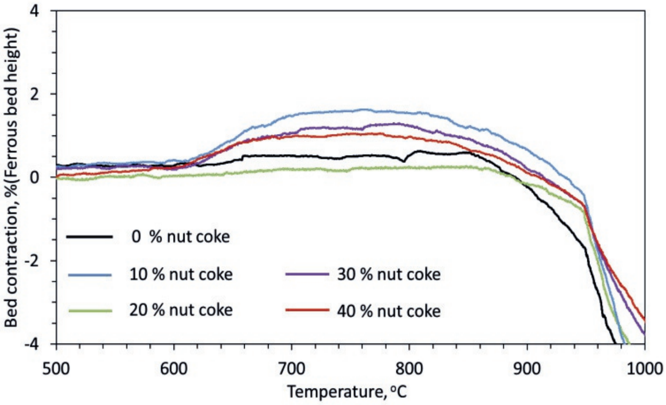

Fig. 5.3 Effect of nut coke addition on the swelling behaviour of the pellets.

Iron ore pellet swelling is known to occur in the temperature range between 600 °C and 1000 °C, which is inside the first stage [11,22-23]. However, in the present case due to the load (9.8 N/cm^2) on the top of sample bed and use of hydrogen (H_2) gas during the experiment, limited swelling (< 2%) is observed (Fig. 5.3). Due to the narrow swelling range, a clear relationship between the nut coke concentration and swelling behaviour is not established.

The point $T_{1,}$ which represents the start of pellet softening, shifts to a higher temperature with nut coke addition as a result of an increase in the reduction degree. Consequently, less liquid (slag) formation and limited sintering among the pellets occur in bed mixed with more nut coke (Fig. 5.2 and Fig. 5.4). Additionally, due to the extended stage 1 regime, the indirect reduction of the pellets further enhances. The first stage end temperature (identical to T_1) linearly increases from 1149 °C to 1165 °C up to 40 wt% nut coke addition (Fig. 5.4). T_1 increases by ˜4 °C for every 10 wt% nut coke addition in the pellet bed.

Despite the higher degree of reduction achieved in the presence of nut coke, the sample bed contraction decreases, i.e. by ˜2 % for 40 wt% nut coke mixing (Fig. 5.4). Additionally, the variance in the first stage displacement is observed to be high, which is possible due to the shape factor of the added material in the bed. Although the particle size is within a narrow range, the shape of the sample could vary, especially for the nut coke. This can bring fluctuations in the first stage of bed contraction. Now considering the trend and magnitude of the variance in the measured data for two experiments, a linear relationship is assumed between the nut coke addition and the contraction in the first stage of bed displacement.

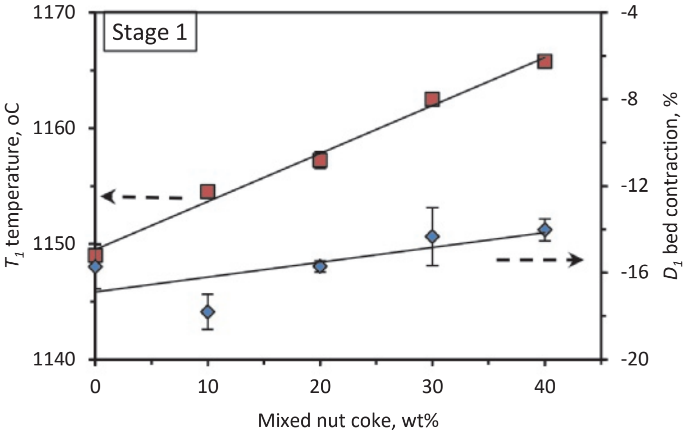

Fig. 5.4 Effect of nut coke mixing on stage 1 of bed contraction (individual pellet shrinkage) and start of pellet softening.

Effect of nut coke concentration on stage 2 behaviour: Nut coke addition has a substantial effect on stage 2 (Fig. 5.2 and 5.5), which is also known as softening stage. The stage 2 end temperature (T_2), which represents the start of individual pellet melting and collapse, decreases linearly from 1480 °C to 1436 °C upon the addition of 40 wt% nut coke in the pellet bed (Fig. 5.5). Consequently, the temperature difference between the start (T_1) and end of the second stage (T_2) decreases drastically, i.e. by 15 °C with every 10 wt% nut coke addition in the pellet bed. The bed contraction in stage 2 (D_2) decreases linearly from 70 % to 44 % (Fig. 5.5). D_2 decreases by 6.5 % for every 10 wt% nut coke mixing in the pellet bed.

One of the primary reasons for the bed contraction in the second stage is the sintering among the pellets [11]. Sintering not only results in larger bed contraction but also slows down the reducing gases to reach the unreduced portion of the pellets, which melts ($2FeO.SiO_2$) along with gangue at a relatively low temperature and causes reduction retardation [7,24]. These in-situ melt formation decreases the strength of the pellet to cause the softening. However, under mixed charge condition, nut coke hinders the sintering among the pellets and also facilitates the gases with a high reduction potential to reach the pellet core, thus minimizing the reduction retardation [7]. Consequently, the pellet strength and softening temperature increase.

Furthermore, direct contact between the coke and pellet (shell iron) enhances the kinetics of iron carburisation and thus decreases the melting point of the pellet shell (Fe-C). As a result, a decrease in the starting temperature of pellet melting is observed (Fig. 5.2 and 5.5). It is also evident from the iron-carbon phase diagram that with the increase in the carbon concentration in iron, the melting temperature (liquidus) decreases [25]. The kinetics for the reduction reactions, the rate of metal (iron) formation and iron carburisation are observed to increases with nut coke addition in the pellet bed.

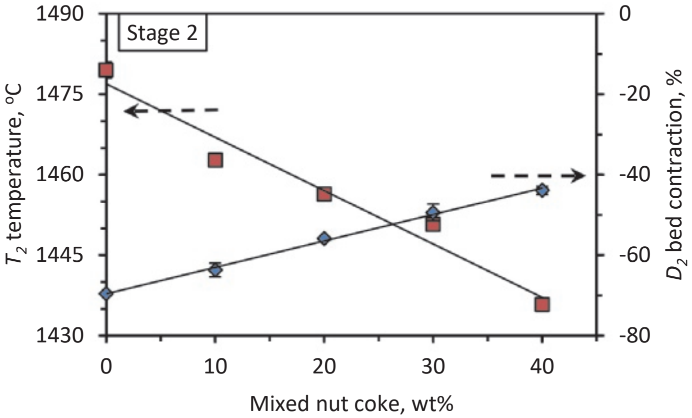

Fig. 5.5 Effect of nut coke addition on stage 2 of bed contraction and the end temperature of softening.

Effect of nut coke concentration on stage 3 behaviour: Stage 3 ends with melting and dripping of the ferrous material when maximum possible bed contraction is achieved. The stage 3 end temperature (T_3) is observed in the range between 1505 °C to 1520 °C for the pellets mixed with and without nut coke (Fig. 5.2 and 5.6). It shows that T_3 increases with the nut coke addition in the pellet bed. Due to the higher reduction degree achieved on the pellets, a thicker iron shell is formed [19]. This shell takes comparatively longer time and higher temperature for carburisation, melting and dripping.

As a result of nut coke mixing, the initial sample bed height (pellets + nut coke) increases. During the experiment, the iron ore pellets melt and drain out to leave the unconsumed nut coke in the sample bed. Consequently, due to the presence of unconsumed nut coke in the bed, the final bed displacement (D_3) decreases with the nut coke addition. A linear relationship is found between D_3 and nut coke addition (Fig. 5.6).

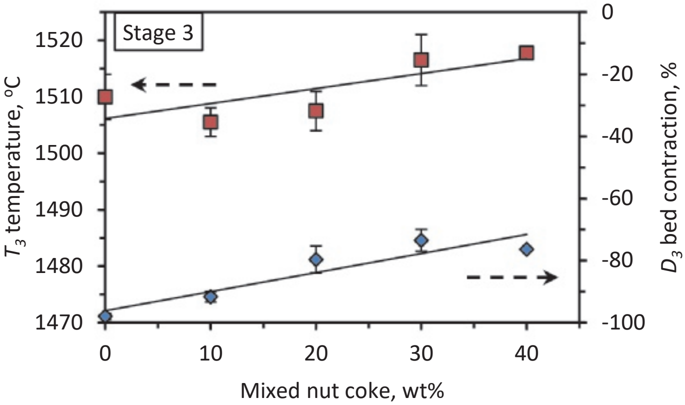

Fig. 5.6 Effect of nut coke mixing on stage 3 of bed contraction and the end temperature of the melting.

Effect of nut coke concentration on bed displacement and temperature range: From Figure 5.7, it can be seen that the effect of nut coke addition is most significant in the stage of softening (second stage). Temperature range for the first (ΔT_a) and third (ΔT_c) stages increases with the nut coke mixing (Fig. 5.7a). Nut coke, being a source of carbon placed in close vicinity of the pellets (iron oxide), enhances reduction kinetics. The second stage temperature range strongly depends on the kinetics of reduction and carburisation of the pellet shell (iron). Nut coke causes higher rate of carburisation for the freshly reduced iron, present at the pellets periphery. This results in the earlier melting of the shell (Fe-C) to shorten the second stage temperature range (ΔT_b) by 60 °C upon 40 wt% nut coke addition. In the softening stage, the nut coke hinders the direct contact between the pellets and therefore slows down sintering among the other pellets to decrease the bed contraction. Nut coke also acts as a frame in the softening pellet bed to resist the load on the top.

Consequently, in the second stage, the bed displacement decreases substantially, i.e. by 24 % upon 40 wt% nut coke addition (Fig. 5.7b).

In the presence of nut coke, ΔT_a increases due to the delay in the softening of the pellets, which is induced by the less liquid (slag) formation and limited sintering among the pellets (Fig. 5.7b). In the third stage, displacement occurs due to the melting and draining of ferrous material from the bed. Therefore, before reaching the third stage, due to softening and sintering the maximum possible compaction has already been achieved in the bed. With the nut coke addition, in the third stage, a marginal increase in the bed displacement is observed. The higher utilisation of added nut coke in the bed for iron carburisation and reduction of FeO rich slag in the liquid state cause this change in the third stage.

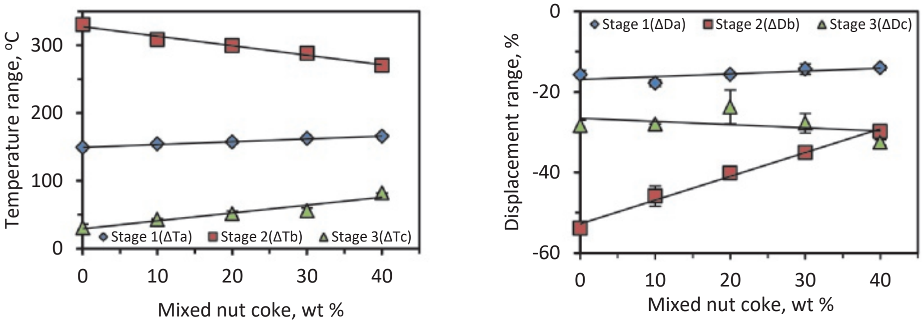

(a). Temperature ranges of three stages.

(b). Bed displacement of three stages.

Fig. 5.7 Effect of nut coke on bed displacement and temperature ranges of different stages.

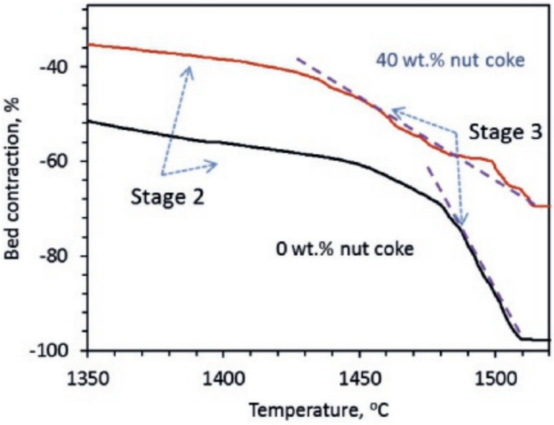

Fig. 5.8 Effect of nut coke addition on the slope of the third stage of bed contraction.

As discussed earlier, a thicker layer of iron forms at the pellet periphery in the presence of nut coke [19]. To carburise and melt this thick iron (Fe-C) layer more time and higher temperature are required. Therefore in the third stage for only ˜30 % displacement (Fig. 5.7b), a relatively long temperature interval means a sluggish rate of bed contraction (Fig. 5.2). This slow rate of bed contraction is evident from the third stage slopes, which are compared for two extreme cases is shown in Figure 5.8. Additionally, nut coke being solid at the time of pellet melting supports the bed structure to slow down the collapse.

5.3.2 Gas permeability

A typical pressure drop profile measured during the softening, melting and dripping of the ferrous burden is shown in Figure 3.10 in Chapter 3. Various characteristics are defined in Table 3.8.

5.3.2.1 General characteristics of gas permeability across the pellet bed

A steady pressure difference between the gas inlet and outlet means that a high density of pores is available in the sample bed for the gas flow. As described in the earlier section, due to the liquid formation, pellet softening occurs (second stage of bed contraction). The formed liquid is mostly entrapped in the pellet core and in the micro-pores present in the pellet. As the iron shell melts and breakout occurs, this liquid slag and metal comes out and starts to fill the interstitial voids. Consequently, the pressure drop across the sample bed increases drastically. Therefore, the temperature at which the pressure drop starts to increase sharply from the base value (P_{Base}) is considered as the melting temperature for the sample bed (T_m) (Fig. 3.10). After that, flowing liquid floods the bed to cause the maximum pressure drop P_{Peak} across the bed at temperature T_f. Then the downward flow of the melt starts, and as a result, new space becomes available for the gas flow. Therefore, the pressure drop decreases after the flooding point (T_f).

In the case of pellet bed without nut coke, the pressure drop continues to be high due to the layer-wise melting and presence of liquid in the bed. Once this liquid drains out sufficiently, the pressure drop recovers to the base value (P_{Base}, Fig. 3.10). The temperature at which the pressure drop returns to the base value is defined as the dripping point (T_d).

5.3.2.2 Effect of nut coke on gas permeability

Permeability variation: The pressure drop across the sample bed is measured and recorded at intervals of 10 seconds for the complete experiment (Table 3.4). It is found that the pressure drop across the sample bed is dynamic and varies in a narrow range before the start of macroscopic melting in the sample bed (Fig. 5.9). It is evident from the measured pressure drop profile that with the increase in nut coke concentration, the variance in the measured pressure drop across the sample bed decreases. The presence of the nut coke in the pellet bed provides the pores and voids for the gas to flow through. Consequently, the number and density of the pores and void increases with the increase in mixed nut coke concentration. This eases the gas flow through the sample bed at the time of burden softening. Consequently, less variation in the pressure drop occurs for the sample bed mixed with higher nut coke content.

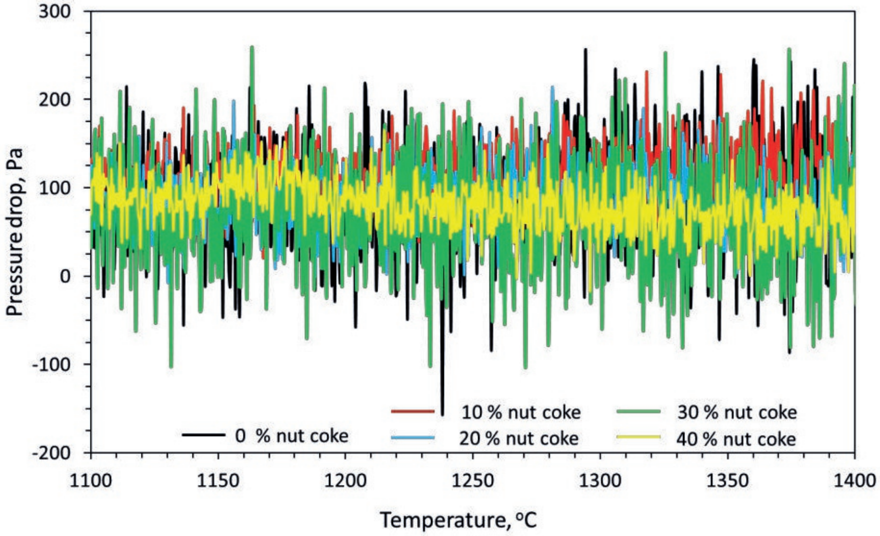

Fig. 5.9 Effect of nut coke addition on the variation in pressure drop during sintering and softening of the pellets.

Pressure drop and S-value:

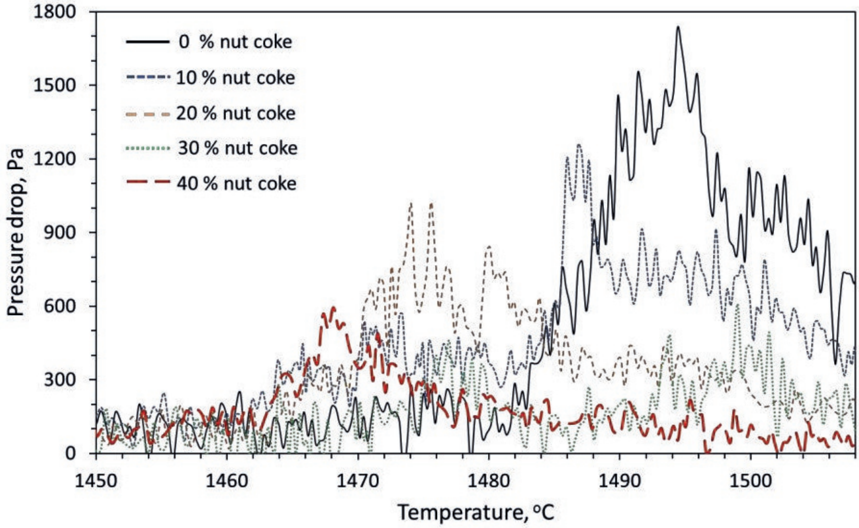

Fig. 5.10 Effect of nut coke addition on the gas permeability (represented by the pressure drop).

The pressure drop curves recorded during the experiments with and without nut coke are shown in Figure 5.10. Nut coke addition affects the gas permeability and key temperatures (T_m, T_f and T_d) of the sample bed (Fig. 5.10). The principal observed effects of nut coke addition in the pellet bed are quantified and discussed in this section.

The pressure difference between the gas inlet and outlet through the packed bed increases due to the resistance provided by the ferrous raw material during softening and melting [10]. Therefore, the complete area under the pressure drop curve is a measure of total resistance provided by the raw material during the softening and melting phenomena. It is represented as *'S - value'* (Table 3.8 and Fig. 3.10). At the point of highest pressure drop (T_f), a low density of voids is available for the gas flow. Thus, the higher the magnitude of pressure drop, the lower the number of pores available for the gas flow (Fig. 3.10 and Fig. 5.10).

The peak pressure drop (P_{Peak}) and *S*-value decrease with the nut coke addition (Fig. 5.11). Nut coke remains solid under the blast furnace cohesive zone temperature conditions. These provide additional micro (on nut coke), and macro (interstitial) pores for the gas flow to result in a comparatively lower pressure drop during the melting process (Fig. 5.11a). Melting and breakout of ferrous raw material occur in the third stage of bed contraction. As evident from stage 3 slope (Fig. 5.8), the rate of bed contraction decreases with the nut coke addition in the bed. Thus at any instant, the melt volume is comparatively small to fill the open pores. Therefore, a lower pressure drop is observed in the pellet bed mixed with the nut coke.

The decreasing trend of the peak pressure drop (P_{Peak}) with the nut coke addition is evident from Figure 5.10 and 5.11a. However, a large variance suggests that the internal sample arrangement has a strong influence on the pressure drop peak (P_{Peak}) (Fig. 5.11a). Nevertheless, the permeability (represented by P_{Peak} and *S*-value) is found to increase exponentially with the nut coke addition (Fig. 5.11).

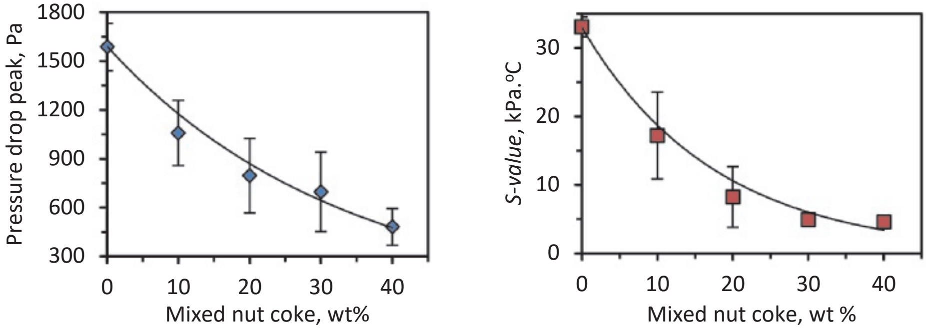

(a) (b)

Fig. 5.11 Effect of nut coke addition on (a). Pressure drop peak (P_{Peak}) and (b). *S-value*.

Pellet bed melting, flooding and dripping temperature: The temperatures of the pellet bed melting (T_m), flooding (T_f) and dripping (T_d) are examined according to the definition presented in Figure 3.10 and Table 3.8. T_m, T_f and T_d decrease linearly by ˜4 °C, 6 °C, and 11 °C, respectively, for every 10 wt% nut coke addition in the pellet bed (Fig. 5.12). The range between the bed melting temperature (T_m) and dripping temperature (T_d) decreases by 28 °C with the addition of up to 40 wt% nut coke.

The primary cause of the decrease in pellet bed melting temperature (T_m) is the high degree of iron carburisation achieved on the iron shell induced by the presence of nut coke. The nut coke promotes the reduction kinetics and carburisation of the pellets due to its larger surface area and close contact with the pellets [19].

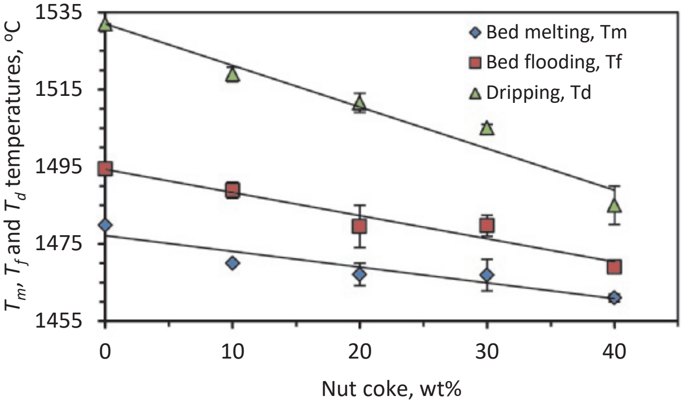

Fig. 5.12 Effect of nut coke addition on the bed melting (T_m), flooding (T_f) and dripping (T_d) temperature deduced from the pressure drop curve.

5.3.3 Effect of nut coke addition on the pellet bed characteristics

5.3.3.1 Pellet and bed melting temperatures

In the case of samples mixed with nut coke, the pellet bed (bulk) melting temperature (T_m, Table 3.8) is different from the individual pellet melting temperature (T_2, Table 3.6). The stage 2 end temperature (T_2) represents the start of the individual pellet melting, and the bed melting (T_m) denotes the temperature at which the melt has spread to the bed to pose a substantial resistance to the gas flow. As explained earlier, nut coke remains solid at the time of pellet softening and melting, providing interstitial space (macro-pores) to accommodate the deformation and melts from pellets. As a result, the temperature difference between T_2 and T_m increases (Fig. 5.13). A linear relationship is found between the nut coke addition and the difference between these two melting temperatures (T_m and

T_2). The difference in melting temperatures increases by 6 °C for every 10 wt% nut coke addition.

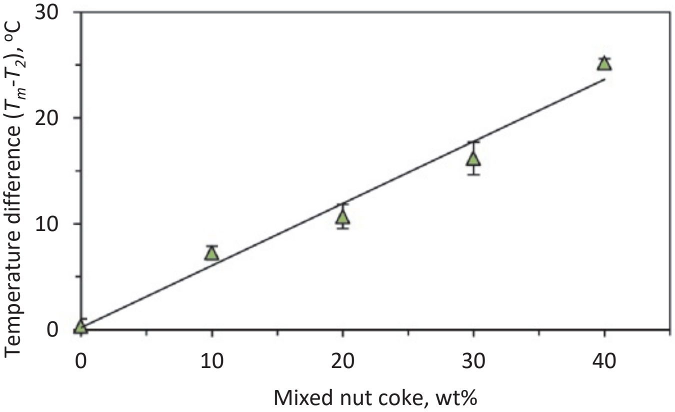

Fig. 5.13 Difference between the pellet bed melting temperature (T_m) and individual pellet melting temperature (T_2).

5.3.3.2 Softening and melting temperature range

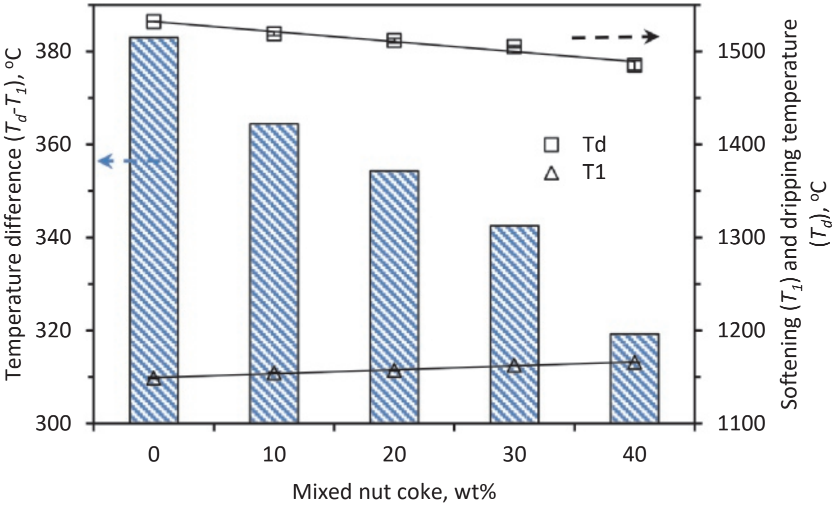

Fig. 5.14 Effect of nut coke addition on the softening and dripping temperatures (representing the cohesive zone temperature range in the blast furnaces).

In the blast furnace, the cohesive zone starts with softening of the ferrous burden and ends with the dripping of the melt [20]. In the related temperature range, the burden is known to exert substantial resistance against the gas flow. Therefore, it is desired in the blast furnaces to have this zone as narrow as possible [10]. During the experiments under simulated blast furnace conditions, the cohesive zone temperature range is represented by the difference between the starting temperature of the softening stage (T_1) and dripping temperature (T_d). It is observed from the experiments that this temperature interval decreases substantially, i.e. up to 64 °C upon 40 % nut coke addition. The T_1 and T_d temperatures along with the difference are plotted in Figure 5.14.

5.3.3.3 Iron carburisation

It is well known that carburisation can lower the melting temperature of the iron-carbon alloy below 4.3 wt%. Under the blast furnace conditions, the iron forms at the pellet periphery and is carburised by CO gas [20] and carbon (nut coke) present in the close vicinity [21]. At a certain temperature, the pellet shell (iron) melts due to the increase in the degree of the carburisation. As a result, a breakout occurs, releasing liquid from the pellet core. Mixing the nut coke into iron ore pellet burden results in a larger interface area of solid carbon with the pellets. Also, the relatively high permeability of the burden (voidage) creates a large gas-pellet interfacial area. Therefore, the carburisation degree of the pellet shell is expected to be higher with a burden of nut coke mixed charge. Correspondingly, pellet melting (T_2) and dripping (T_d) temperature will be lower with higher nut coke concentration.

It is generally referred that under the blast furnace conditions, the reactions evolve close to the equilibrium [20]. Therefore, the carbon present at the point of melting can be estimated using the iron-carbon equilibrium phase diagram. If we assume the pellet melting temperature (T_2) to be the liquidus temperature of the iron-carbon alloy, the equilibrium concentrations of the carbon in solidus and liquidus iron at T_2 can be estimated using Factsage 7.0 (Fig. 5.15). Notably, a steep increase in the liquidus carbon concentration is noted from 0.7 to 1.3 wt% upon 40 wt% nut coke addition (Fig. 5.15). As it is shown, the increase in carbon concentration leads to a linear decrease in pellet melting temperature.

Theoretically, once the carbon concentration of the pellet shell is within this range, the shell melting occurs. Moreover, it can be predicted that since it has sufficient fluidity for the deformation and liquid flow; the present carbon concentration might be close to its liquidus value rather than to the solidus concentration at the temperature of pellet melting (T_2).

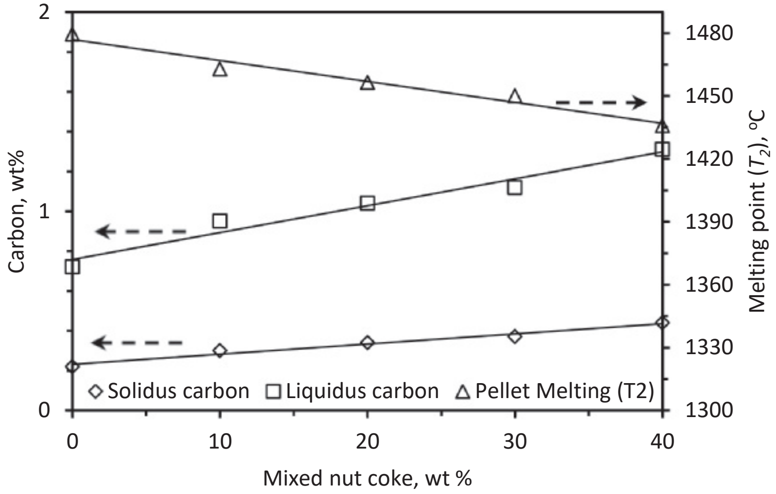

Fig. 5.15 Estimated effect of nut coke addition on the solidus and liquidus carbon concentration by using FactSage software.

5.3.3.4 Relationship with bed characteristics

Based on the series of experiments, the effect of nut coke addition on the various process parameters was studied in detail. The key relationships are summarised in Table 5.1. As discussed earlier, for temperature and displacement parameters, the effect of nut coke addition is linear either with a positive or a negative slope. Gas permeability (P_{Peak} and *S - value*) is observed to increase exponentially with the nut coke addition.

Table 5.1 Relationship summary on the effect of nut coke addition in the pellet bed characteristics.

Parameters	**Unit**	**Relationship**	**Equation** **X= nut coke concentration (wt%)**	**R^2**
Stage 1 temperature (T_1)	°C	Linear	$0.42X + 1150$	0.99
Stage 1 displacement (D_1)	%	Linear	$0.07X – 17$	0.53
Stage 2 temperature (T_2)	°C	Linear	$-0.99X + 1477$	0.96
Stage 2 displacement (D_2)	%	Linear	$0.66X – 70$	1.00
Stage 3 temperature (T_3)	°C	Linear	$0.27X + 1506$	0.59
Stage 3 displacement (D_3)	%	Linear	$0.61X – 96$	0.85
Bed melting temperature (T_m)	°C	Linear	$-0.41X + 1477$	0.87
Flooding temperature (T_f)	°C	Linear	$-0.60X + 1494$	0.94
Dripping temperature (T_d)	°C	Linear	$-1.08X + 1532$	0.96
(T_m-T_2)	°C	Linear	$0.59X + 0.20$	0.98
Pressure drop peak (P_{peak})	Pa	Exponential	$1590e^{-0.03X}$	0.97
Permeability (*S-value*),	Pa.°C	Exponential	$33e^{-0.06X}$	0.93

5.3.3.5 Coke consumption

The coke utilised during the experiments is given in Figure 5.16. In general, the variation in the nut coke utilisation is high, the irregular shape (variation in surface area) of the nut coke can possibly cause these variations. Furthermore, the stochastic nature [26] of the liquid dripping from the bed may change the reaction time of liquid iron and slag (FeO rich slag) to affect the coke utilisation.

The total coke utilisation is also observed to decrease with the nut coke addition in the pellet bed. First, a drastic drop in total coke utilisation is noted with 10 wt% nut coke addition in the pellet bed. Then a gradual decrease in the weight of the total consumed coke is noticed. Nevertheless, the nut coke is observed to be utilised in place of the regular coke (Fig. 5.16). Additionally, the fraction of the regular coke consumed is seen to decrease with the nut coke mixing in the pellet bed. This indicates that the nut coke is preferentially utilised to fulfil the chemical functions (reductant and iron carburiser) of the coke in the blast furnace conditions. Furthermore, less utilised regular coke will be of a bigger size, which will reach the blast furnace hearth to support the liquid permeability.

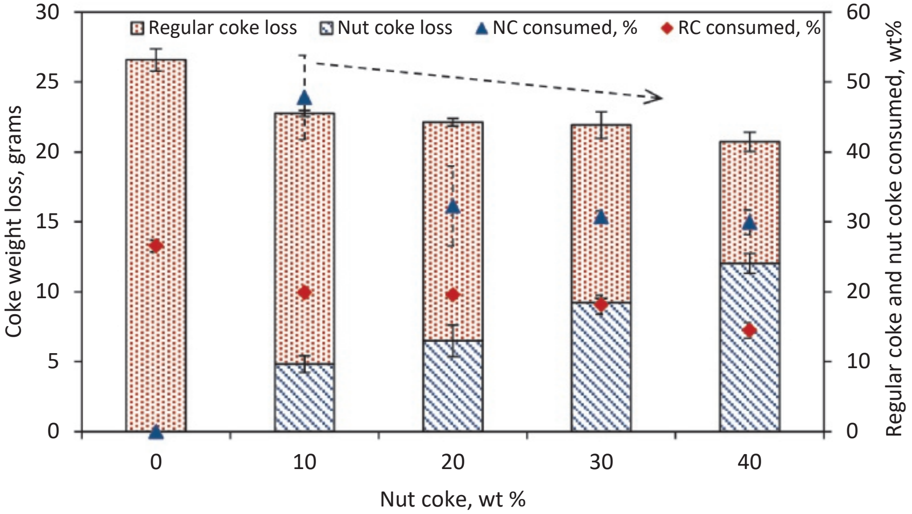

Fig. 5.16 Coke utilisation in the smelting and dripping experiments.

5.3.4 Gas characteristics

5.3.4.1 Graphite crucible

A crucible made of graphite is utilised for the experiment in RSM. Graphite has the ability to sustain the blast furnace conditions of high temperature, reducing gas and load.

However, graphite reacts with CO_2 gas at a high temperature to form CO gas by the Boudouard reaction [20].

$$CO_{2(g)} + C_{(s)} = 2CO_{(g)} \quad (5.1)$$

To limit this reaction from the crucible, high-grade graphite with high density and limited porosity is selected for the experiments.

Additionally, a benchmarking study is performed with a graphite crucible filled with alumina spheres. The experiment conditions are kept the same for smelting experiments (Table 3.4). The generated profile of various gases evolved from the benchmark study is utilised during the data analysis of experiments performed in RSM (Fig. 5.17). The graphite crucible was found to be stable and strong to sustain the simulated blast furnace conditions. Only a limited amount (2.4 grams) of crucible weight is lost during the experiment.

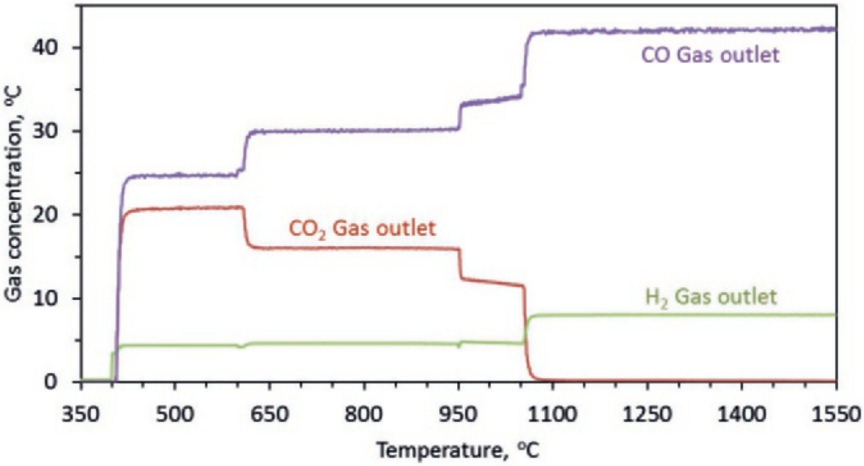

Fig. 5.17 Gas outlet profile for benchmarking test with alumina spheres. Graphite crucible weight loss (2.4 g).

5.3.4.2 Gas profile

A typical profile for the evolved gases during the experiment in RSM is shown in Figure 5.18. A significant difference between the gas inlet and outlet profile clearly indicates that a strong interaction between the gas and sample occurs during the experiment. It can be seen that CO_2 gas fraction measured in the outlet is always observed higher than in the inlet. Similarly, the concentration of CO gas outlet is observed to be lower than the inlet profile, below 1450 °C. In high temperature range ($T > 1450$ °C) a regime of high CO gas concentration is marked in the outlet profile. Additionally, a variation in the moisture (H_2O) content is noticed during the experiments. Possible reactions for bringing these changes in the gas outlet are discussed in the following section.

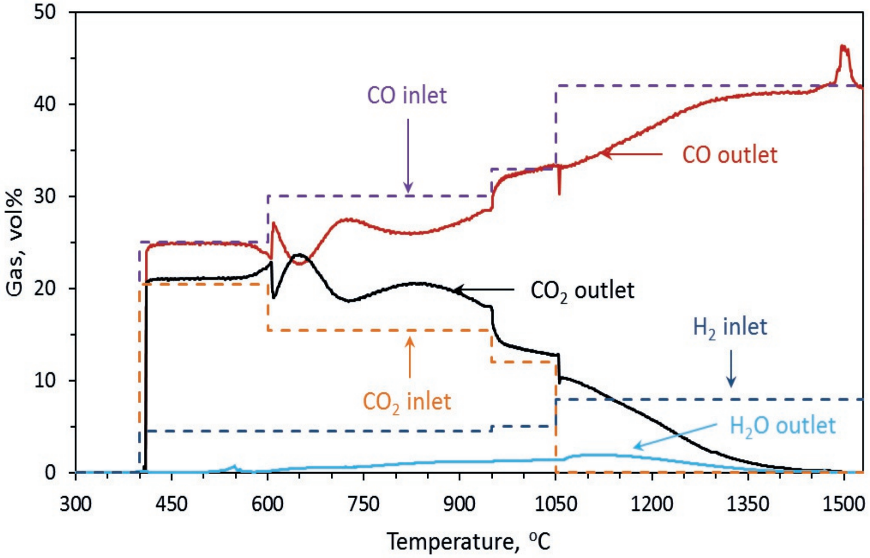

Fig. 5.18 A typical gas inlet and outlet profile during the experiments in RSM.

Reactions: Phase stability of iron and its oxides as a function of temperature and gas composition is shown in Figure 5.19. The iron ore pellet (iron oxide) interacts with the reducing gas to form metallic iron. As a result, the oxygen present in the iron ore pellet evolves in the form of CO, CO_2 and H_2O gas. The reactions are

$$3Fe_2O_{3(s)} + CO_{(g)} = 2Fe_3O_{4(s)} + CO_{2\,(g)} \tag{5.2}$$

$$Fe_3O_{4(s)} + CO_{(g)} = 3FeO_{(s)} + CO_{2\,(g)} \tag{5.3}$$

$$FeO_{(s)} + CO_{(g)} = [Fe]_{(s)} + CO_{2\,(g)} \tag{5.4}$$

As a result of these reactions, compared to gas inlet, a higher CO_2 concentration is reported in the off-gas analysis. Furthermore, this evolved CO_2 gas is regenerated by Boudouard reaction (5.1). Thus, the overall reaction (5.1 to 5.4) of iron oxide reduction with carbon monoxide can be written as

$$2Fe_2O_{3(s)} + 3C_{(s)} = 4Fe_{(s)} + 3CO_{2(g)} \tag{5.5}$$

During the experiment, a high CO gas regime emerges in the high temperature range (T>1450 °C). This temperature range is close to the start of pellet bed melting and dripping (Fig. 5.10). As a result of pellet melting, the liquid slag from the pellet core flows over the coke and is reduced by its direct interaction with solid coke.

$$FeO_{(l)} + C_{(s)} = Fe_{(l)} + CO_{(g)} \tag{5.6}$$

Consequently, a sharp rise in the CO gas concentration is noticed (Fig. 5.18). Furthermore, from the equilibrium diagram (Fig. 5.19), it is apparent that at high temperature, the CO gas is more stable than the CO_2 gas. Consequently, evolved CO gas is not regenerated to CO_2 gas.

Similar to the reduction reactions with CO gas, iron oxide is also reduced by the H_2 gas. The reactions are as follows

$$3Fe_2O_{3(s)} + H_{2(g)} = 2Fe_3O_{4(s)} + H_2O_{(g)} \tag{5.7}$$

$$Fe_3O_{4(s)} + H_{2(g)} = 3FeO_{(s)} + H_2O_{(g)} \tag{5.8}$$

$$FeO_{(s)} + H_{2(g)} = Fe\ (s) + H_2O_{(g)} \tag{5.9}$$

The evolved H_2O (moisture) from reaction (5.7) to (5.9) can be regenerated to H_2 gas by its interaction with carbon monoxide (water-gas reaction)

$$H_2O_{(g)} + CO_{(s)} = H_{2(g)} + CO_{2(g)} \tag{5.10}$$

At high temperature, this reaction shift to left to produce more CO gas and at low temperature shift to right to produce more H_2. However, in the present case due to the low content and stability of CO_2 gas at high temperature (above 1400 °C), limited reverse reaction occurs.

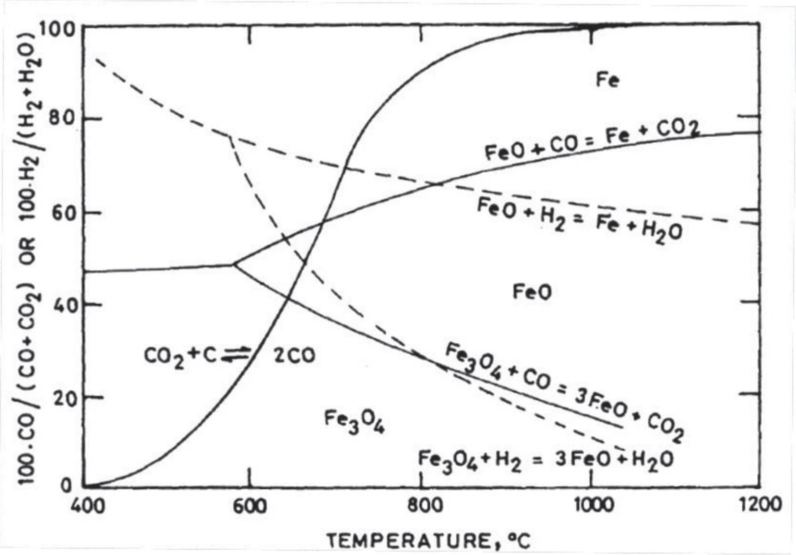

Fig. 5.19 Fe-O-C and Fe-O-H equilibrium profile superimposed with Boudouard reaction [20].

Effect of nut coke addition on the evolved gas chemistry: The nut coke is carbonaceous material actively involved in the reduction reaction of the iron ore pellets, which affects the off-gas chemistry. Furthermore, the off-gas chemistry might also be affected by the thinning of the regular coke layers. Figure 5.20 shows the comparison of the evolved gas composition during the experiments for the pellet bed without and with (40 wt%) mixed nut coke (as a replacement of the regular coke). An apparent difference in the gas chemistry at the outlet is noticed for the pellet bed with and without mixed nut coke. Especially in the high temperature range from 1050 °C – 1550 °C. Regimes of high CO_2 and CO gas concentration is observed from 1050 °C to 1250 °C and 1250 °C to 1500 °C, respectively. This is due to the active participation of the nut coke in the reduction and iron carburisation of the iron ore pellets. These off-gas composition profiles are further analysed to quantify the effect of the nut coke addition on the degree of reduction (DOR) of iron ore pellets and carbon utilisation during the experiments.

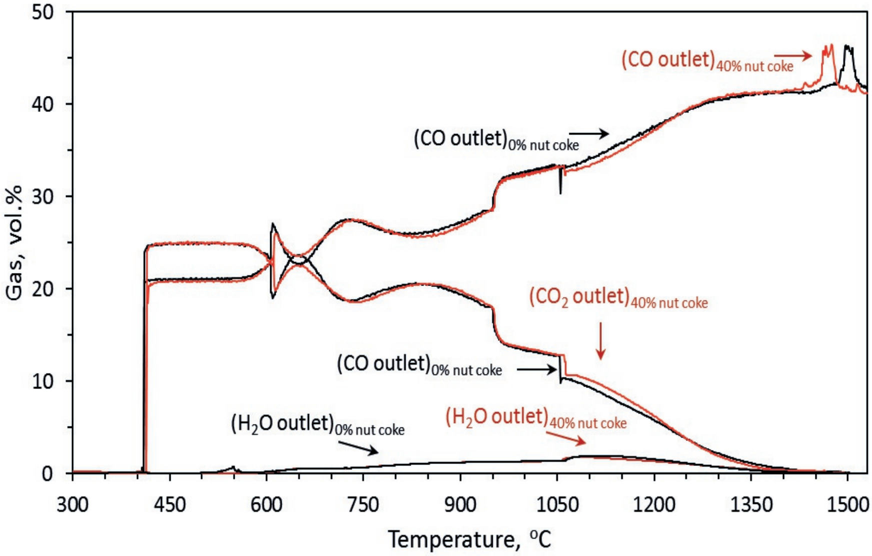

Fig. 5.20 Effect of nut coke (40 wt%, replacement of regular coke) addition on outlet gas profile.

5.3.4.3 Degree of reduction

The degree of reduction is estimated based on the weight of oxygen present in the raw iron ore pellets (Table 3.1) and the oxygen removed during the experiment (equation 3.4). Several shifts in the slope of the DOR curve are noticed during the experiment, which is due to the change in the heating rate at different temperature intervals (Table 3.4).

An apparent increase in the DOR is observed with the increase in temperature from 400 °C to 1300 °C for the pellet bed without nut coke (Fig. 5.21). The iron ore pellet reduces topo-chemically to form a metallic shell around the pellet. Now, as a result of sintering of iron present as shell, it becomes difficult for the reducing gas to reach the pellet core. Consequently, a regime of sluggish DOR increases from 1300 °C to 1480 °C. Then, as the temperature increases, a drastic increase in the DOR is marked as a result of pellet melting in the bed. Due to the melting of the pellet shell, the core, rich in FeO slag, comes in contact with the coke for direct reduction reaction (5.6). Then the melting and dripping of the liquid iron and slag occur from the sample bed.

The effect of nut coke addition (0-40 wt%) on the degree of reduction is shown in Figure 5.21. An increase in the DOR is noticed with the increase of nut coke concentration in the pellet bed. Especially, in the high temperature range (950 °C to 1550 °C) comparative higher rate (slope) of oxygen removal is observed for the pellet bed mixed with nut coke. The improved gas permeability (Fig. 5.9) in the presence of nut coke enhances the reduction kinetics of the iron ore pellets. Additionally, in the pellet bed mixed with nut coke, the reaction product of iron oxide reduction, i.e. CO_2 is regenerated by its reaction with nut coke in the mixed bed (5.1). Consequently, the reduction potential of the gas is enhanced in the presence of nut coke in the bed.

However, in the absence of nut coke, evolved CO_2 gas might not be able to regenerate inside the pellet bed. Thus, while passing across the top layer regular coke, the CO_2 rich gas from the pellet bed without nut coke is regenerated. This results in high CO gas content in the outlet of the pellet bed without nut coke (1050 °C to 1250 °C, Fig. 5.20). On the other hand, from the pellet bed mixed with nut coke, a high CO_2 gas fraction is evolved (1050 °C to 1250 °C). This occurs due to the presence of thinner regular coke layer, which results in limited CO_2 gas regeneration (Fig. 5.20 and Fig. 5.24). Additionally, the carburisation of the freshly reduced iron present as the pellet shell also results in the generation of the CO_2 gas (5.11) [27]. As a result, higher nut coke is utilised and limited regular coke is consumed from the nut coke fraction mixed pellet bed.

The nut coke supports the bed structure and limits the sintering in the pellet bed [19] (Fig. 4.2). Consequently, more pores are available for reducing gas to reach the interior of the iron ore pellet. Thus, an accelerated reduction occurs in the high temperature regime for pellet mixed with the nut coke. However, in the absence of nut coke, the iron present in the pellet periphery sinters to form a dense shell, which is difficult for the reducing gas to penetrate. Consequently, the reduction reaction in the absence of nut coke at high temperature is controlled by the solid-state diffusion mechanism [28].

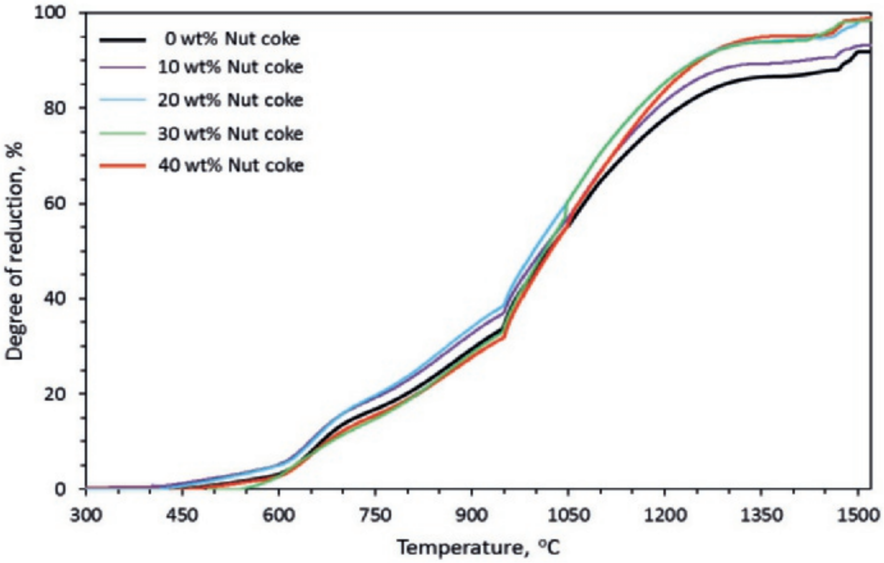

Fig. 5.21 Effect of nut coke addition on an estimated degree of reduction (DOR).

5.3.4.4 Carbon utilisation

The carbon utilised during the experiment is estimated by carbon mass balance between the gas inlet and outlet (3.5). Accumulated mass of carbon loss (3.8) from the sample bed during the experiment is shown in Figure 5.22. Similar to the DOR, many changes shifts in the slope of curve for carbon loss (utilisation) are apparent due to the change in heating rate (Table 3.4). At lower temperature (below 950 °C), a lower degree of carbon utilisation is observed in case of pellet bed mixed with nut coke, which might be a result of limited Boudouard reaction (5.1) occurring inside the bed (Fig. 5.19). As the temperature increases the rate of carbon utilisation increases (950 °C to 1550 °C). Moreover, a higher degree of carbon utilisation is apparent with the increase in the nut coke concentration (Fig. 5.22). The presence of carbon (nut coke) in the close vicinity of the iron ore pellet enhances the reduction reaction kinetics. The carbon utilisation in the presence of nut coke is enhanced by the increased rate of Boudouard reaction (5.1), water gas reaction (5.10) and by direct reduction of the FeO rich slag (5.6). Furthermore, before the bulk melting in the bed, the coke is also consumed in the carburisation of (solid-state) iron present as the pellet shell [29]. In this carburisation reaction, gas (CO_2) is evolving (5.11) [27].

$$2CO_{(g)} = [C]_{[\text{in Fe}]} + CO_{2(g)} \tag{5.11}$$

This is also accounted for in the carbon loss estimated by the gas analysis (3.6). However, the carbon loss due to the liquid state iron carburisation (5.12) cannot be estimated by the mass balance of carbon between the inlet and evolved gas. The liquid state carburisation occurs once the liquid iron flows over the solid coke particles, which occurs at high temperature (above 1450 °C) towards the end of the heating cycle (Table 3.4).

$$C_{(s)} = [C]_{[l]} \quad (5.12)$$

Thus, an exact amount of the coke utilised by the liquid state carburisation is difficult to estimate. However, an estimation can be made by comparing the weight difference between the carbon loss from the gas analysis and the actual weight of carbon loss from the coke collected after the experiments.

This shows that compared to the estimated weight loss according to the gas analysis, a larger amount of carbon is lost during the experiments (Fig. 5.23). This unaccounted mass loss is found decreasing with the increase in the nut coke concentration. It is assumed that this is due to the liquid state iron carburisation. As in the case of nut coke mixed pellet bed, the liquid iron flows over a relatively thin regular coke layer having less time to carburise. Consequently, a smaller amount of coke is consumed in the liquid state. This is further evident from the lower level of carbon in the dripped iron from the pellet bed mixed with nut coke (Fig. 6.16) [30].

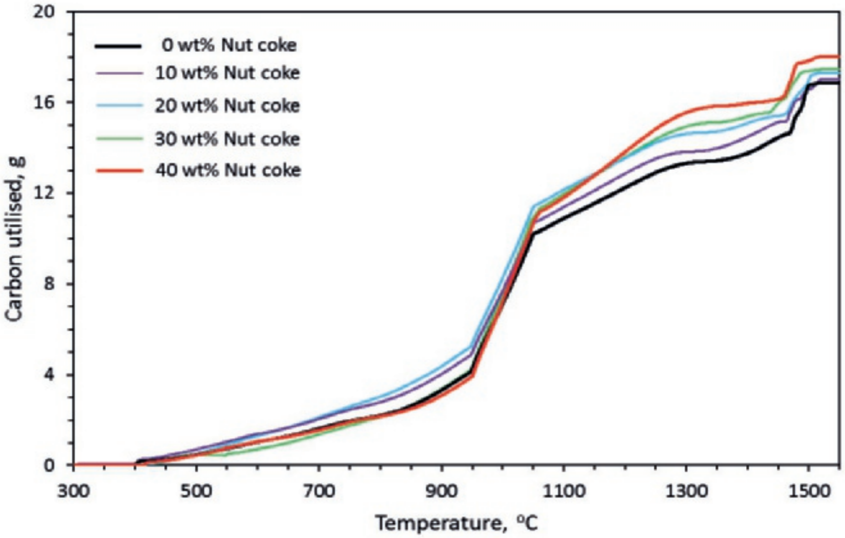

Fig. 5.22 Effect of nut coke addition on the carbon utilisation.

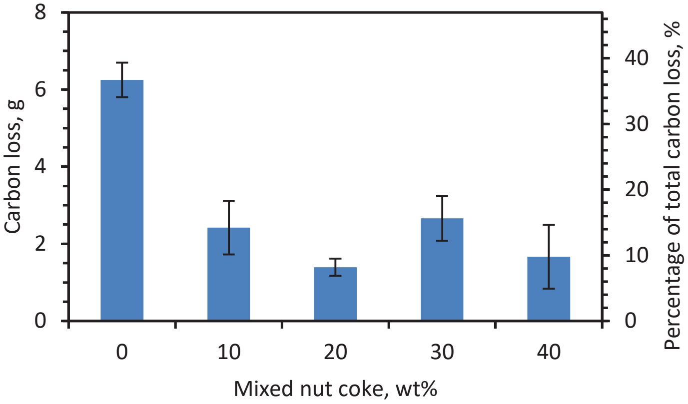

Fig. 5.23 Effect of nut coke addition on carbon loss due to the liquid state carburisation (estimated).

Various reactions occurring in the sample bed with and without nut coke before and after the start of melting are illustrated in Figure. 5.24. The coke present in the sample bed is utilised principally in three ways: first in the reducing gas generation – Boudouard reaction (5.1), second by carburising the iron (5.11) and (5.12) and third by reducing the FeO rich slag in the liquid state – direct reduction (5.6).

The nut coke present inside the iron ore pellet bed enhances the reduction degree of the pellets by supplying the CO-rich reducing gas. This CO-rich gas reacts with the iron oxide to form CO_2 and later in its reaction with the nut coke present in the bed is converted to the CO gas again via Boudouard reaction (Fig. 5.24). Therefore, the chemical function of coke to reduce the iron oxide is enhanced in the presence of nut coke in the bed. This is a dominant mechanism of nut coke utilisation under mixed charged conditions.

Then after reaction in the bed, the gas moves out of the ferrous burden to react with the regular coke present in the top layer (Fig. 5.24). Now, in the case of nut coke mixed bed due to the presence of thinner regular coke layer, less conversion of the carbon dioxide (CO_2) to carbon monoxide (CO) (Fig. 5.20) will occur. As a result, less regular coke from the top layer is consumed.

The nut coke added in the pellet bed not only enhances the reduction degree but also increases the degree of iron carburisation (Fig. 5.24), which results in the earlier melting of the pellet bed (Fig. 5.10). Then after melting, when this liquid percolates through the thinner regular coke layer at the bottom to drip out of the sample bed, less carburisation in the liquid state takes place (Fig. 6.16) [30]. This results in limited consumption of the regular coke present below the ferrous bed layer. As a result, when nut coke is added as a replacement of the regular coke, limited regular coke is consumed.

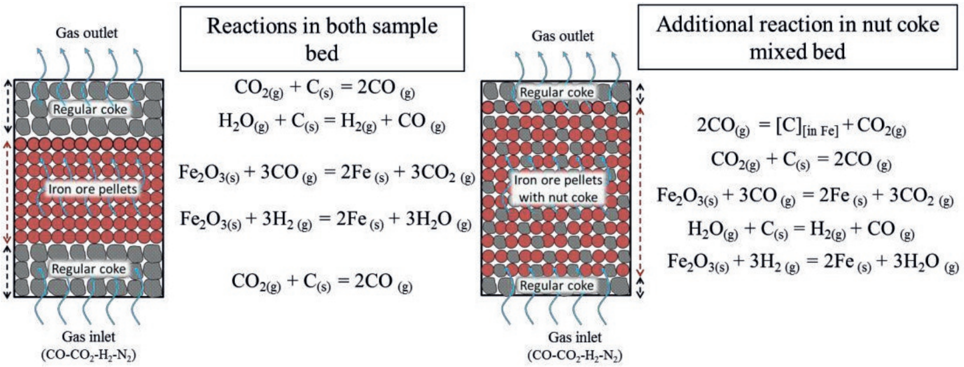

(a.) Sample bed before melting

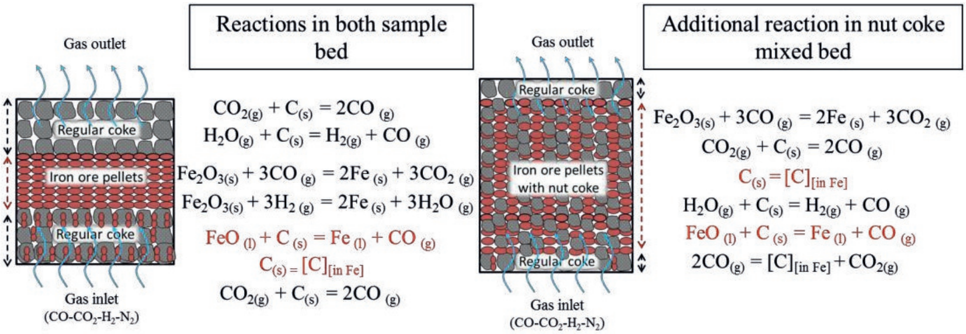

(b). Sample bed after the start of bulk melting

Fig. 5.24 Various reactions occurring in the iron ore pellet bed with and without nut coke.

5.3.5 Effect of nut coke size

Generally, it is indicated that the coke size ranges from 40-80 mm is regarded as the regular coke [31]. In the big blast furnace, the regular coke size is kept as narrow as possible, as the reaction and heat exchange efficiency decreases by 0.2 % and 3 %, respectively, by just 1 mm increase in the regular coke size [32]. Therefore, it is suggested that regular coke size should be maintained around 50 mm to avoid flooding at the tuyeres level in the blast furnace [32]. As a result, a significant amount of the undersize coke (nut coke) is being generated at the coke-making site.

Nut coke utilisation in the mixture with the ferrous burden has given an opportunity to replace the expensive regular coke [5,33]. However, similar to the regular coke size range, nut coke particle size also has a wide range, from 8 to 40 mm. Upon mixing with iron ore pellet bed, different nut coke size might differently affect the physicochemical properties of the bed Thus, in the present study, the effect of different nut coke size is systematically investigated for nut coke size ranges of 10-15 mm, 15-20 mm and 20-25 mm. Due to the crucible size limitation, studies are not extended beyond 25 mm mixed nut coke size.

It is suggested elsewhere that for enhancing the reduction kinetics, mixed nut coke size should be of similar size as the ferrous burden [33,34]. Thus, the effect of nut coke size of 10-15 mm is first studied extensively in section 5.3 to 5.6. Now, the effect of nut coke size range of 15-20 mm and 20-25 mm on the physicochemical properties of the bed are discussed in this section.

5.3.5.1 Bed characteristics with 15-20 mm mixed nut coke

The sample bed contraction and the pressure drop recorded for the pellet bed mixed with 15-20 mm sized nut coke is shown in Figure 5.25.

Bed contraction: Similar to 10-15 mm sized mixed nut coke in the pellet bed, in the sample bed mixed with 15-20 mm sized nut coke, a limited swelling is noticed. Then, the three stages of sample bed contraction are experienced during the experiments (Fig. 5.25a). It is also noticed that with the increase in nut coke concentration, the temperature and displacement range for the second stage shrinks. The first stage end temperature (T_1) is increased due to the higher reduction degree [19,28] achieved on the iron ore pellets. Additionally, the presence of nut coke in the iron ore pellet bed enhances the carburisation [29,30] of the freshly reduced iron present as the pellet shell. As a result, the melting temperature for the pellets decreases with the nut coke addition. In the third stage of bed contraction (melting and dripping stage) due to the support provided by the nut coke to the sample bed, a gradual bed shrinkage occurs, which is contrary to the drastic shrinkage in the absence of nut coke in the bed (Fig. 5.25a).

Bed permeability: The pressure drop profile for the sample bed during melting and dripping of the pellet bed with and without nut coke is shown in Figure 5.25b. Similar to the case of 10-15 mm size nut coke, with 15-20 mm sized mixed nut coke, the high pressure-drop regime is noticed to shift to the lower temperature. This occurs primarily due to the higher degree of iron carburisation in the presence of nut coke in the pellet bed [30], which decreases the melting point of the iron-carbon alloy present at the pellet shell. Additionally, the area under the pressure drop curve and peak (P_{Peak}) is noticed to decrease drastically with the nut coke addition in the pellet bed.

The principal effect brought by the nut coke addition of size 15-20 mm on the various bed characteristics is given in Table 5.2 in the next section.

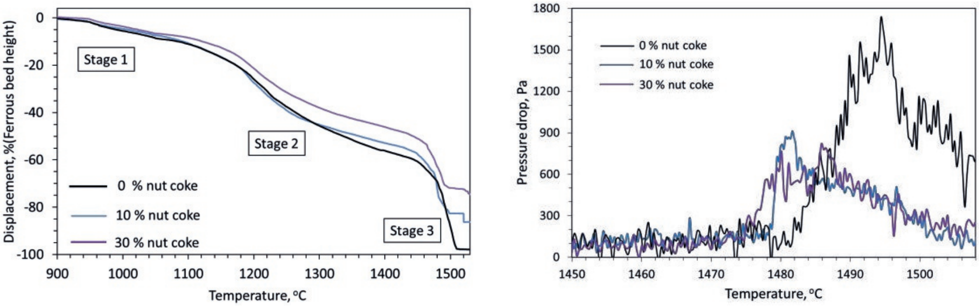

(a). Bed contraction (b). Pressure drop

Fig. 5.25 Effect of nut coke (15-20 mm) addition on sample bed characteristics.

5.3.5.2 Bed characteristics with 20-25 mm mixed nut coke

The sample bed contraction and the pressure drop recorded for the pellet bed mixed with 20-25 mm sized nut coke are shown in Figure 5.26.

Bed contraction: After limited swelling, the three stages of the bed contraction are observed for pellet bed mixed with 20-25 mm sized nut coke. The stage 1 end temperature (T_1) increases, and the stage 2 end temperature (T_2) decreases with the nut coke mixing in the pellet bed (Fig. 5.26a). This indicates that similar to the pellet bed mixed with 10-15 mm and 15-20 mm sized nut coke, the reduction degree of the iron ore pellet and the carburisation degree of the freshly reduced iron is improved by mixing of 20-25 mm sized nut coke in the pellet bed. However, the bed contraction profile with mixed nut coke of size 20-25 mm does not appear smooth as that is realised with the 10-15 mm and 15-20 mm sized mixed nut coke. This might be a result of the large size difference between the nut coke (20-25 mm) and the iron ore pellets (10-13 mm), which causes the alignment of smaller pellets around the bigger nut coke. This would cause a non-smooth bed contraction during the softening and melting of the pellet in the mixed bed.

Bed permeability: For the sample bed mixed with 20-25 mm nut coke, similar pressure drop profile is observed as that for the bed mixed with 10-15 mm and 15-20 mm sized mixed nut coke (Fig. 5.26b). The pressure drop peaks and the area under the curve (*S-value*) are observed to decrease drastically with the nut coke addition in the pellet bed (Table 5.2). However, with the increase in nut coke concentration, only a marginal shift in the bed melting temperature (T_m) is observed. This could be the result of lower iron carburisation in case of pellet mixed with larger sized nut coke.

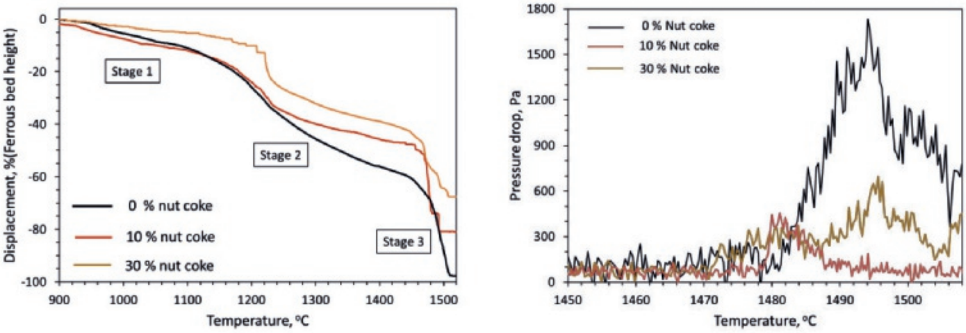

(a). Bed contraction (b). Pressure drop

Fig. 5.26 Effect of nut coke (20-25 mm) addition on sample bed properties.

Table 5.2 Effect of nut coke size and concentration bed characteristics.

Nut coke size, (mm)	Nut coke Conc, (wt%)	T_m, °C	T_f, °C	T_d, °C	P_{Peak}, Pa	S value, kPa.°C	T_1, °C	D_1, %	T_2, °C	D_2, %	T_3, °C	D_3, %	T_d-T_1, °C	T_d-T_m, °C	P_{Peak}, Pa
0	0	1479	1494	1534	1732	35	1148	-16	1479	-69	1509	-98	386	55	1732
10-15	10	1470	1488	1518	1258	17	1155	-17	1463	-64	1505	-90	363	48	1050
10-15	30	1465	1477	1505	442	4	1165	-14	1450	-50	1516	-70	340	40	700
15-20	10	1477	1482	1517	912	14	1151	-17	1474	-59	1521	-86	365	40	912
15-20	30	1475	1480	1506	765	12	1157	-13	1464	-54	1529	-75	349	31	765
20-25	10	1477	1482	1517	443	3	1152	-17	1471	-52	1493	-81	365	40	443
20-25	30	1475	1480	1506	695	26	1166	-8	1465	-47	1509	-68	340	31	695

5.3.5.3 Effect of nut coke size on bed contraction

Mixed bed with 10 wt% nut coke: For 10 wt% added nut coke concentration, the effect of nut coke size on the sample bed shrinkage is shown in Figure 5.27. The effect of added nut coke size is marginal on the first stage characteristics (T_1 and D_1). Its effect becomes apparent in the second and the third stage, where a lower bed contraction is noticed with the increase in the nut coke size (Fig. 5.27). The bigger nut coke strongly supports the sample bed structure to undergo less contraction, especially at the time of softening and melting of iron ore pellets.

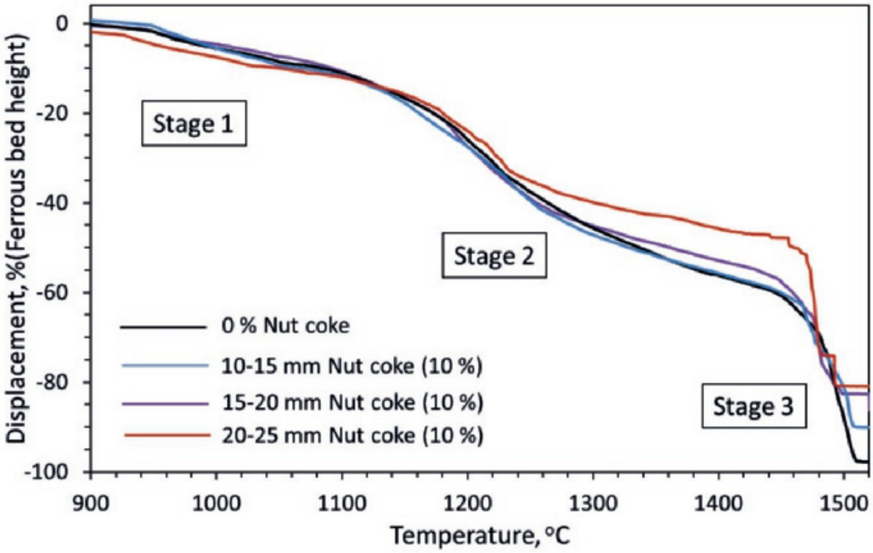

Fig. 5.27 Effect of nut coke size (10 wt%) on sample bed shrinkage characteristics.

Mixed bed with 30 wt% nut coke:

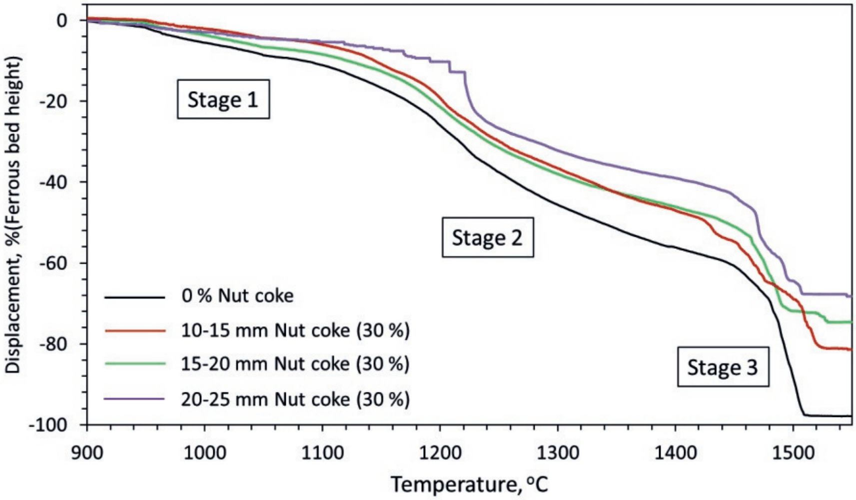

Fig. 5.28 Effect of nut coke size (30 wt%) on sample bed shrinkage characteristics.

The effects of the nut coke size and concentration on the bed characteristics derived from the bed displacement curves are shown in Figure 5.29.

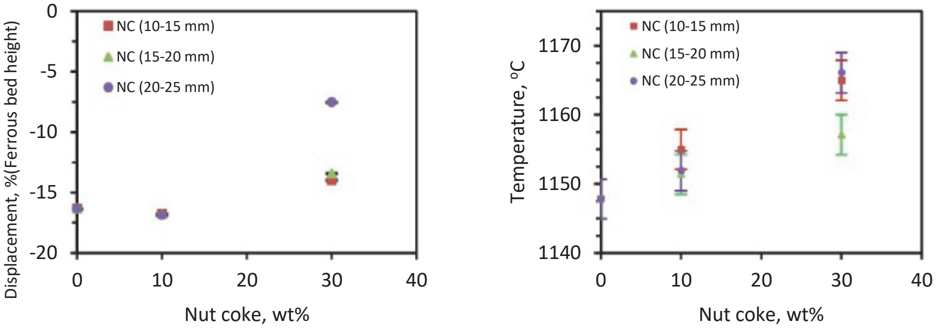

(a). First stage bed displacement, D_1

(b). First stage temperature, T_1

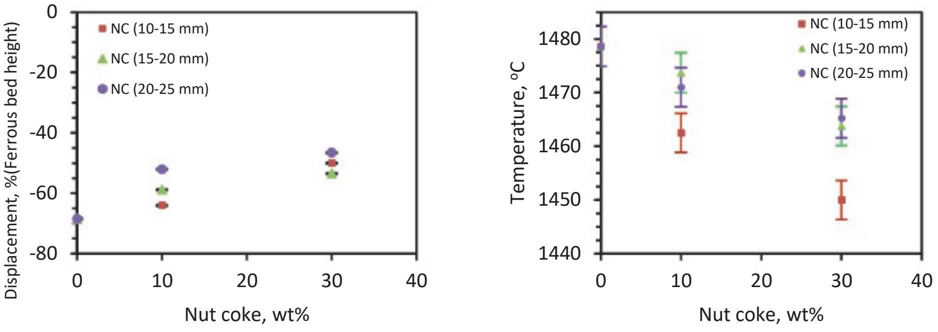

(c). Second stage bed displacement, D_2

(b). Second stage temperature, T_2

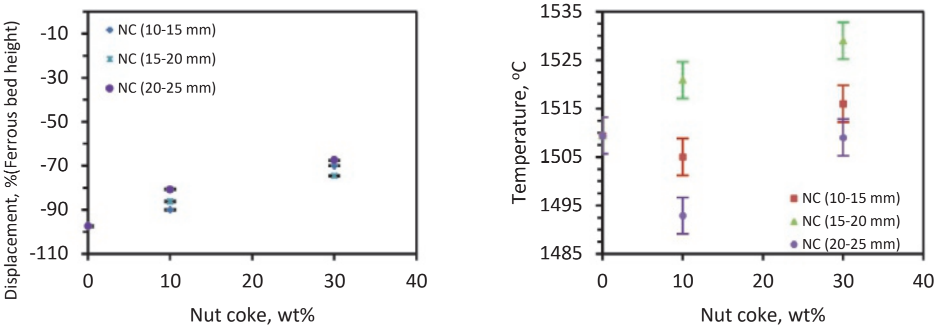

(e). First stage bed displacement, D_3

(f). Third stage temperature, T_3

Fig. 5.29 Effect of nut coke size and added concentration on the sample bed characteristics.

In the case of 30 wt% added nut coke concentration, the effect of nut coke size on the sample bed shrinkage is shown in Figure 5.28. Similar to 10 wt% mixed nut coke concentration, for the bed mixed with 30 wt% nut coke, the effect of nut coke size becomes apparent in the second and third stage of bed contraction. The support provided by the bigger nut coke results in lower sample bed contraction. During the melting and dripping phenomena in the third stage, the bed displacement is not smooth compared to that in bed without nut coke, which is due to the resistance provided by the solid nut coke particles present in the melting bed of iron ore pellets.

5.3.5.4 Effect of nut coke size on bed permeability

Variations in measured pressure drop: Before the start of macroscopic melting in the sample bed, the pressure drop varies in a narrow range across the bed. The measured pressure drop profiles for the sample bed during the softening of the pellet bed are shown in Figure 5.30. The pressure drop profiles are plotted for different nut coke size ranges, mixed with 30 wt% nut coke as a replacement of the regular coke. A decrease in the variance of measured pressure drop profile is noticed with the increase in nut coke size (Fig. 5.30). The voids and pores density in the bed is expected to decrease with the increase in the nut coke size. However, the void size will increase with the nut coke size. Consequently, a wide passage for the gas is available, which results in a decrease of the variance in the measured pressure drop across the sample bed. Under the assumption that continuous pores or channels are available for the gas flow, this illustrates that the size of the pores in the bed has a stronger influence on the pressure drop than the density of voids. Thus, the physical function played by the nut coke to support the bed structure and to provide the voids in the softening bed of the pellet increases with the nut coke size for the examined cases.

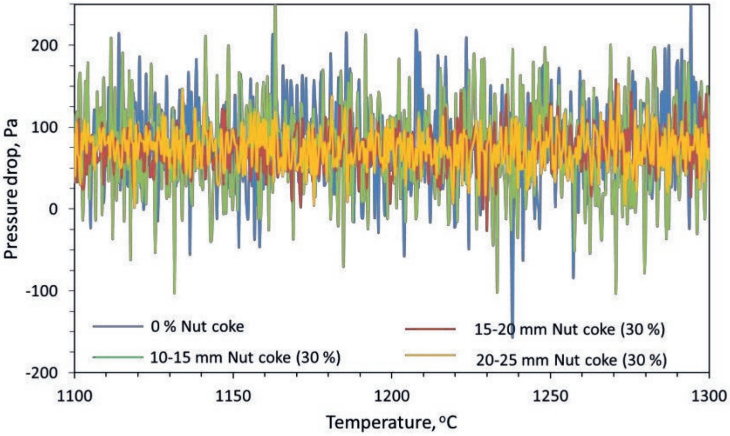

Fig. 5.30 Effect of added nut coke size on the variance in measured pressure drop profile during softening.

Mixed bed with 10 wt% nut coke: For 10 wt% nut coke mixing, the effect of nut coke size on the gas permeability is shown in Figure 5.31. It is noticed that with an increase in added nut coke size, the bed melting temperature increases. This is due to the lower degree of iron carburisation achieved on the reduced iron ore pellet shell [25]. The number of added nut coke particle decreases with the increase in nut coke size for any given concentration. Consequently, the contact area between the coke and pellet decreases, which decreases the degree of iron carburisation to increase the melting point [25] of the pellet bed.

However, the physical role played by the nut coke to provide pores and voids improves with the nut coke size. As a result, the pressure drop peak (P_{Peak}) and the area under the pressure drop curve (*S-value*) are noticed to decrease with the increase in the nut coke size (Fig. 5.31).

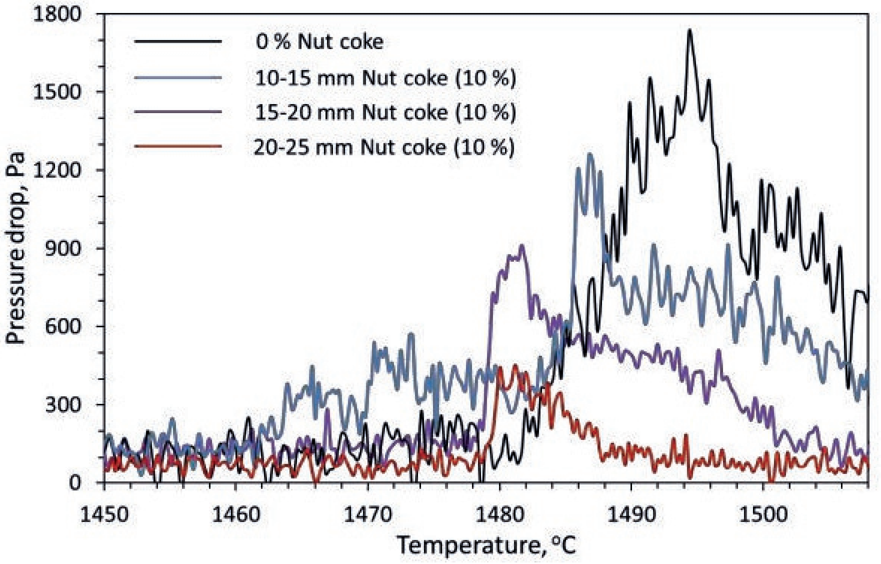

Fig. 5.31 Effect of nut coke size (for 10 wt%) on the gas permeability (pressure drop).

Mixed bed with 30 wt% nut coke: For 30 wt% mixing, the effect of nut coke size on gas permeability is shown in Figure 5.32. Only a marginal effect of nut coke size is noticed on the bed melting temperature (T_m). For all the examined nut coke size ranges, the mechanical function of providing the pores and voids for the gas to flow is appropriately performed by the nut coke. As a result, a lower pressure drop peak (P_{Peak}) and less resistance to the gas flow (*S-value*) during melting and dripping is observed (Fig. 5.32). However, a clear relationship of nut coke size on bed characteristic temperature is not observed, which is possibly due to the dynamic nature of gas flow from multiple voids present in the case of higher (30 wt%) mixed nut coke concentration.

The quantified effect of nut coke size and concentration on the gas permeability characteristics is shown in Figure 5.33.

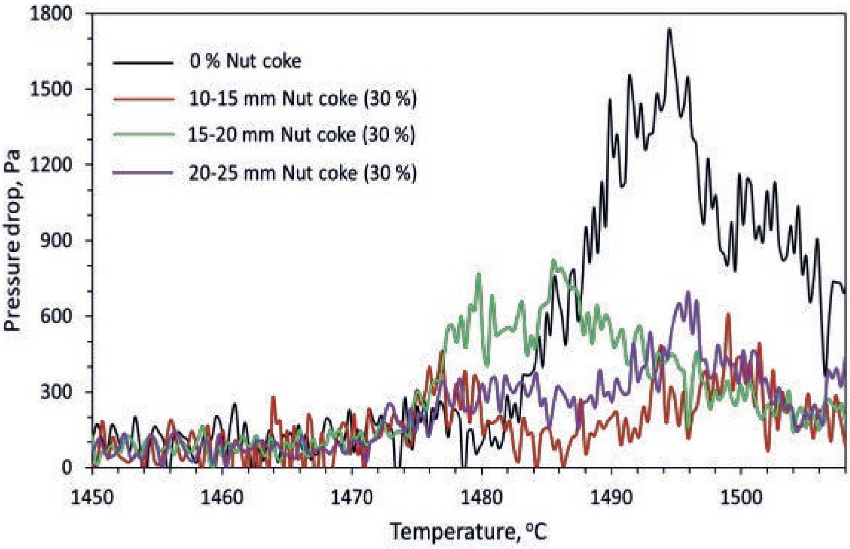

Fig. 5.32 Effect of nut coke size (for 30 wt%) on the gas permeability (pressure drop).

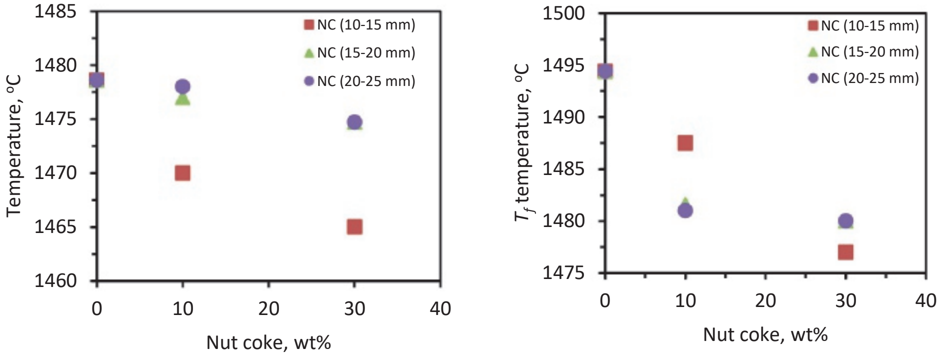

(a) Bed melting temperature, T_m

(b). Flooding temperature, T_f

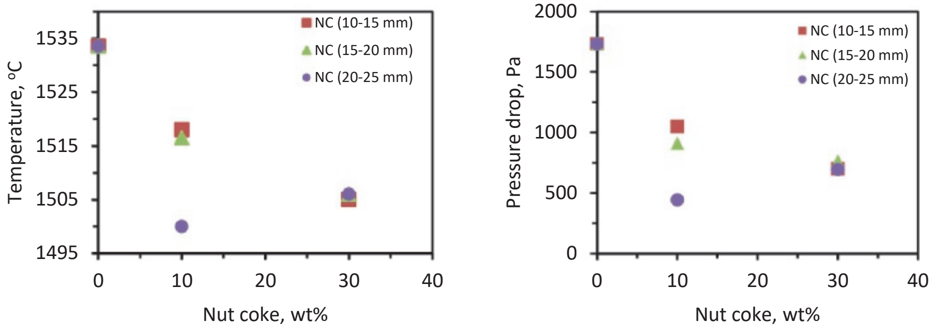

(c). Dripping temperature, T_d

(d). Pressure drop peak (P_{Peak})

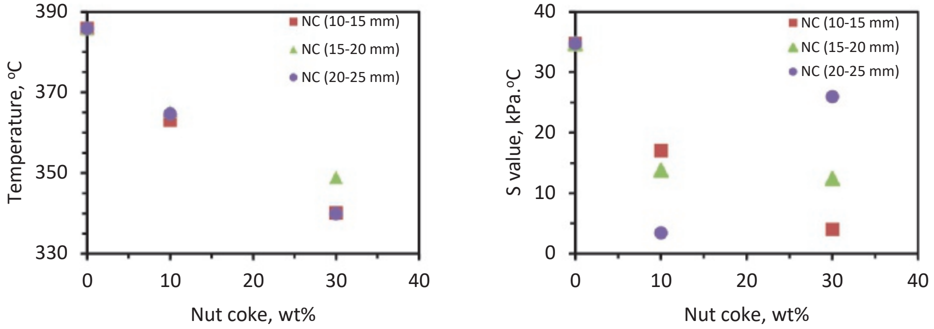

(e). Softening melting temperature range (T_d-T_1)

(f). *S-value*

Fig. 5.33 Effect of nut coke size and concentration of the sample bed characteristics.

5.3.5.5 Effect of nut coke size on coke utilisation

The remaining coke after the experiment is collected from inside the crucible. The difference in the coke size is utilised to separate the nut coke from the regular coke. After separation, this coke is weighed to estimate the total coke consumed during the experiments.

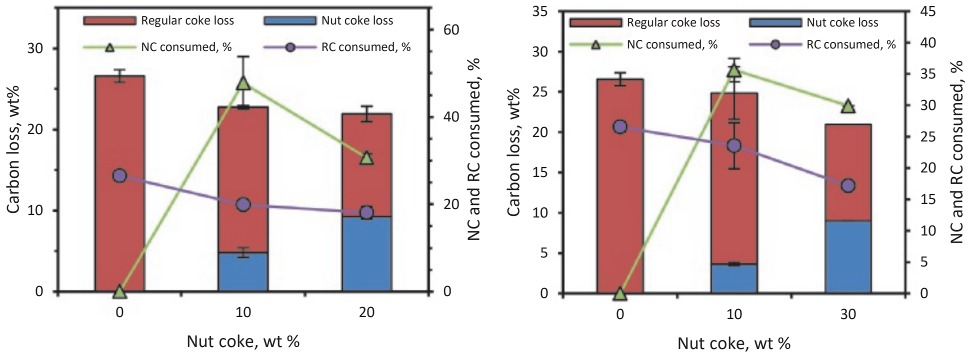

(a). Coke utilisation for pellet bed mixed with 10-15 mm nut coke

(b). Coke utilisation for pellet bed mixed with 15-20 mm nut coke

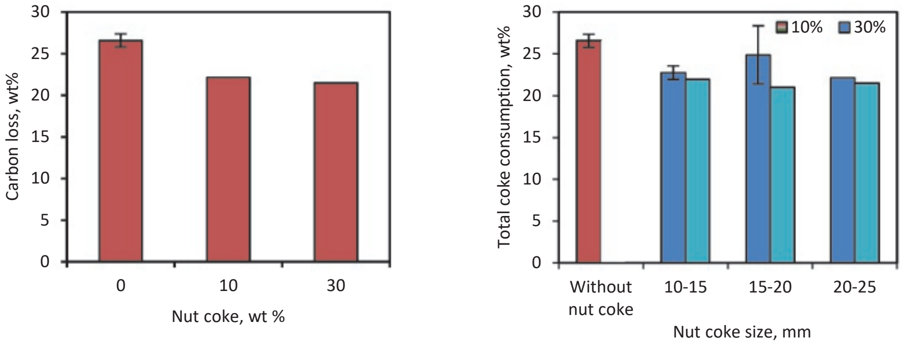

(c). Coke utilisation for pellet bed mixed with 20-25 mm nut coke

(d). Effect of nut coke size and concentration on total coke consumption

Fig. 5.34 Effect of nut coke size and concentration on coke utilisation.

From the experiments with 10-15 mm and 15-20 mm nut coke size, it is found that the nut coke can be utilised as a replacement of the regular coke. Additionally, the total amount of coke consumed during the experiments decreases with the increase in mixed nut coke concentration (Fig. 5.34). The regular coke and nut coke utilisation are noticed to decrease with the increase in the mixing concentration.

In the present series of experiments, the nut coke of size 20-25 mm is utilised as the regular coke. Thus, in the case of mixed nut coke of size 20-25 mm, it is difficult to identify and separate the nut coke with the regular coke. Therefore, all the coke collected after the experiment is weighed together to find the total amount of coke consumption. It is found that the total amount of coke consumed during the experiments decreases with the increase in the mixed nut coke concentration (Fig. 5.34), irrespective of nut coke size.

5.3.5.6 Effect of nut coke size on gas characteristics

The effect of nut coke concentration and size on the DOR and carbon utilisation is shown in Figure 5.35 and 5.36.

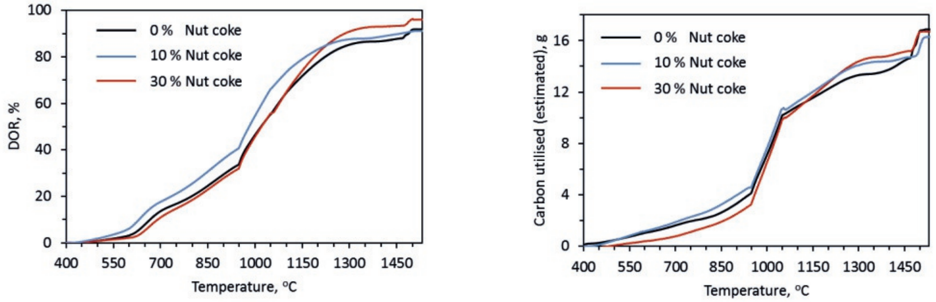

(a). Degree of reduction (DOR,%), pellet bed mixed with 15-20 mm nut coke

(b). Carbon utilisation, pellet bed mixed with 15-20 mm nut coke

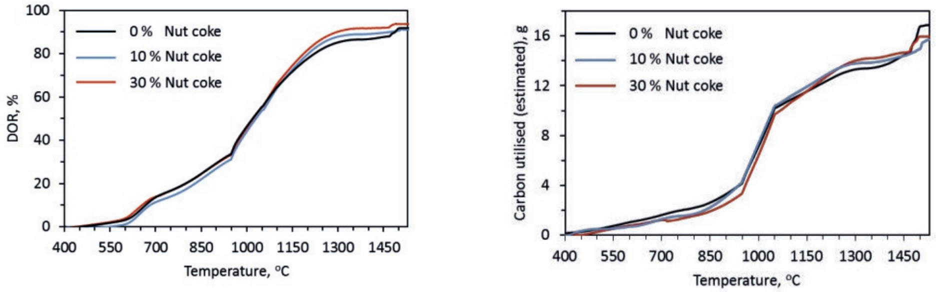

(c) Degree of reduction (DOR,%), pellet bed mixed with 20-25 mm nut coke

(d). Carbon utilisation, pellet bed mixed with 20-25 mm nut coke

Fig. 5.35 Effect of nut coke concentration on sample bed gas characteristics (nut coke 20-25 mm).

Similar to the pellet bed mixed with 10-15 mm sized nut coke, for the pellet bed mixed with 15-20 mm and 20-25 mm sized nut coke, an increase in DOR and carbon utilisation is observed with the increase in nut coke concentration (Fig. 5.35). Furthermore, the ability to perform the chemical function of reduction and carbon utilisation is noticed to increase with the decrease in the nut coke particle size. This is due to the increase in specific surface area of the mixed nut coke in the pellet bed, which promotes the Boudouard reaction (5.1), water gas reaction (5.10) and iron carburisation (5. 1 and 5.12).

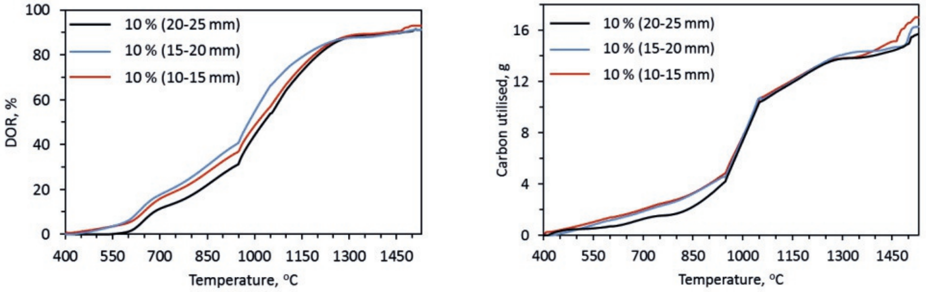

(a). Degree of reduction (DOR,%), pellet bed mixed with 10 wt% nut coke.

(b). Carbon utilisation, pellet bed mixed with 10 wt% nut coke.

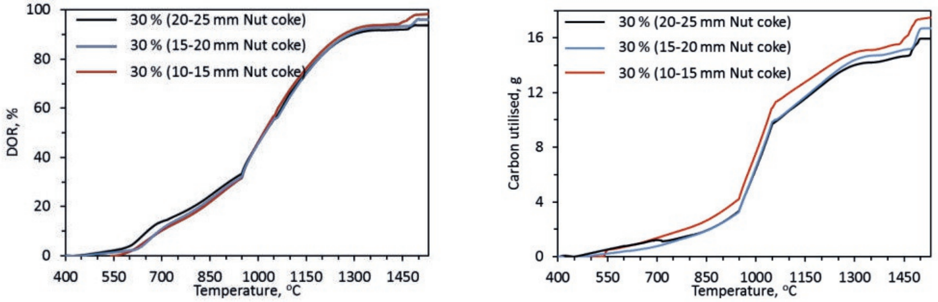

(c). Degree of reduction (DOR,%), pellet bed mixed with 30 wt% nut coke.

(d). Carbon utilisation, pellet bed mixed with 30 wt% nut coke.

Fig. 5.36 Effect of nut coke size on sample bed gas characteristics (nut coke mixing 30 %).

5.4 Conclusions

The impact of nut coke addition at various size and concentration on an iron ore pellet bed is studied under simulated blast furnace conditions in a reduction softening and melting (RSM) apparatus. Based on the series of experiments, the following conclusions can be drawn.

(1) Three distinct stages of bed contraction are observed during the bed heating under simulated blast furnace conditions. In the first stage, an indirect reduction of the iron ore pellet takes place. Sintering, softening and carburisation of the iron shell evolve in the second stage. Thereafter, in the third stage, pellet melting and dripping occurs.

(2) Nut coke mixing with the iron ore pellet affects all three stages of bed contraction. The second stage is affected the most, which is shortened due to the enhanced reduction kinetics, limited sintering, lower softening and high degree of carburisation achieved on the iron ore pellets. Consequently, the cohesive zone temperature range (T_1 to T_d) narrows by the nut coke addition in the pellet bed.

(3) At the time of bed softening, the pores provided by the nut coke decrease the variation in the gas permeability (represented by pressure drop and *S-value*). Furthermore, by keeping the voids open for the gas flow at the time of bed melting and dripping, nut coke drastically increases the gas permeability.

(4) In the presence of nut coke, the degree of reduction (DOR) of the iron ore pellets increases in the high temperature range.

(5) Due to the increased kinetics of reduction and iron carburisation, the carbon utilisation increases with the nut coke addition in the pellet bed. However, the total coke consumption decreases due to the limited liquid state carburisation assisted by the presence of thinner regular coke layer, when nut coke is added as a replacement of the regular coke.

(6) Quantified effects of nut coke addition of size 10-15 mm on the pellet bed behaviour are as follows:

   a. In the second stage, the bed displacement and temperature linearly decrease from 70 % to 44 % (6.5 % per 10 wt% nut coke mixing) and 1480 °C to 1436 °C (11 °C per 10 wt% nut coke mixing), respectively, upon 40 wt% nut coke addition.

   b. The pellet bed melting (T_m), flooding (T_f) and dripping (T_d) temperature, decrease linearly by 19 °C, 25 °C and 47 °C, respectively, upon 40 wt% nut coke addition.
   c. The cohesive zone temperature range (T_1 to T_d) narrows by 64 °C upon 40 wt% of nut coke addition.
   d. An exponential relationship is found between the increase in gas permeability (represented by pressure drop peak and *S-value*) and the nut coke addition in the pellet bed (examined up to 40 wt% as replacement of regular coke).
   e. In the high temperature range (950 °C to 1550 °C), the kinetics of iron ore reduction reactions and carbon utilisation increases with the nut coke addition.

(7) For all examined nut coke sizes and concentrations, nut coke was able to effectively utilise as a replacement of the regular coke. The nut coke is consumed in preference to the regular coke. Additionally, the total coke consumption is noticed to decrease with the nut coke mixing in the pellet bed.

(8) Similar physicochemical behaviour is noticed for the pellet bed mixed with 10-15 mm, 15-20 mm and 20-25 mm sized nut coke. However, the ability to limit the bed contraction and to enhance the bed permeability increases with the nut coke size. The chemical function to reduce the iron oxide and to carburise iron decreases with the increase in nut coke size.

5.5 References

[1] M. Geerdes, R. Chaigneau, I. Kurunov, O. Lingiardi, J. Ricketts, Modern blast furnace ironmaking : an introduction, IOS Press, under the imprint of Delft University Press, Amsterdam, 2015.

[2] Q. Song, Effect of nut coke on the performance of the ironmaking blast furnace, PhD Thesis, Delft University of Technology, 2013.

[3] T. Kon, S. Natsui, S. Matsuhashi, S. Ueda, R. Inoue, T. Ariyama, Influence of cohesive zone thickness on gas flow in blast furnace analyzed by DEM-CFD model considering low coke operation, Steel Res. Int. 84 (2013) 1146–1156.

[4] S. Matsuhashi, H. Kurosawa, S. Natsui, T. Kon, S. Ueda, R. Inoue, T. Ariyama, Evaluation of coke mixed charging based on packed bed structure and gas permeability changes in blast furnace by DEM-CFD model, ISIJ Int. 52 (2012) 1990–1999.

[5] D.J. Gavel, A review on nut coke utilisation in the ironmaking blast furnaces, Mater. Sci. Technol. (United Kingdom). 33 (2017) 381–387.

[6] A. Babich, D. Senk, H.W. Gudenau, Effect of coke reactivity and nut coke on blast furnace operation, Ironmak. Steelmak. 36 (2009) 222–229.

[7] E. Mousa, D. Senk, A. Babich, Reduction of pellets-nut coke mixture under simulating blast furnace conditions, Steel Res. Int. 81 (2010) 706–715.

[8] E.A. Mousa, D. Senk, A. Babich, H.W. Gudenau, Influence of nut coke on iron ore sinter reducibility under simulated blast furnace conditions, Ironmak. Steelmak. 37 (2010) 219–228.

[9] E.A. Mousa, A. Babich, D. Senk, Effect of nut coke-sinter mixture on the blast furnace performance, ISIJ Int. 51 (2011) 350–358.

[10] B. Nandy, S. Chandra, D. Bhattacharjee, D. Ghosh, Assessment of blast furnace behaviour through softening–melting test, Ironmak. Steelmak. 33 (2006) 111–119.

[11] J. Sternel, A.K. Lahiri, Contraction and meltdown behaviour of olivine iron ore pellets under simulated blast furnace conditions, Ironmak. Steelmak. 26 (1999) 339–348.

[12] A.A. El-Geassy, M.I. Nasr, M.H. Khedr, Reduction behaviour of iron ore fluxed pellets under load at 1023-1273 K, ISIJ Int. 44 (2004) 462–469.

[13] Q. Song, Y. Yang, R. Boom, Effect of nut coke on the reduction behavior in iron-making blast furnace, Baosteel Tech. Res. 9 (2015) 8–16.

[14] S. Watakabe, K. Takeda, H. Nishimura, S. Goto, N. Nishimura, T. Uchida, M. Kiguchi, Development of high ratio coke mixed charging technique to the blast furnace, ISIJ Int. 46 (2006) 513–522.

[15] K. Ichikawa, Y. Kashihara, N. Oyama, T. Hirosawa, J. Ishii, Evaluating effect of coke layer thickness on permeability by pressure drop estimation model, ISIJ Int. 57 (2017) 254–261.

[16] R. Chaigneau, H. Sportel, J. Trouw, R. Vos, J. Droog, Blast furnace burden quality: laboratory simulation, Ironmak. Steelmak. 24 (1997) 461–467.

[17] G. Wang, Q. Xue, J. Wang, Volume shrinkage of ludwigite/coal composite pellet during isothermal and non-isothermal reduction, Thermochim. Acta. 621 (2015) 90–98.

[18] M. Iljana, A. Kemppainen, T. Paananen, O. Mattila, E.-P. Heikkinen, T. Fabritius, Evaluating the reduction-softening behaviour of blast furnace burden with an advanced test, ISIJ Int. 56 (2016) 1705–1714.

[19] D.J. Gavel, Q. Song, A. Adema, J. van der Stel, J. Sietsma, R. Boom, Y. Yang, Characterization of the burden behaviour of iron ore pellets mixed with nut coke under simulated blast furnace conditions, Ironmak. Steelmak. (2018) 1–8.

[20] A.K. Biswas, Principles of blast furnace iron making - theory and practice, Cootha Publishing House, Brisbane, Australia, 1981.

[21] K. Nagata, R. Kojima, T. Murakami, M. Susa, H. Fukuyama, Mechanisms of pig-iron making from magnetite ore pellets containing coal at low temperature., ISIJ Int. 41 (2001) 1316–1323.

[22] T. Sharma, R.C. Gupta, B. Prakash, Effect of reduction rate on the swelling behaviour of iron ore pellets, ISIJ Int. 32 (1992) 812–818.

[23] F.W. Frazer, H. Westenberger, K.H. Boss, W. Thumm, The relationship between basicity and swelling on reduction of iron-ore pellets, Int. J. Miner. Process. 2 (1975) 353–365.

[24] T. Bakker, Softening in the blast furnace process: local melt formation as the trigger for softening of iron bearing burden materials, PhD Thesis, Delft University of Technology, 1999.

[25] O.K. Goldbeck, Iron-Carbon, in: Iron-Binary Phase Diagrams, Springer, Berlin, 1982: pp. 23–26.

[26] W. Husslage, Dynamic distribution - sulphur transfer and flow in a high temperature packed coke bed, PhD Thesis, Delft University of Technology, 2004.

[27] H. Kim, D.J. Min, S.M. Jung, A kinetic study on carburization of Fe by using 13 CO isotope gas, ISIJ Int. 53 (2013) 199–206.

[28] E. Mousa, D. Senk, A. Babich, Reduction of pellets-nut coke mixture under simulating blast furnace conditions, Steel Res. Int. 81 (2010) 706–715.

[29] D.J. Gavel, A. Adema, J. van der Stel, J. Sietsma, R. Boom, Y. Yang, Effect of nut coke addition on physicochemical behaviour of pellet bed in ironmaking blast furnace, ISIJ Int. 59

(2019) 778–786.

[30] D.J. Gavel, A. Adema, J. van der Stel, C. Kwakernaak, J. Sietsma, R. Boom, Y. Yang, Melting behaviour of iron ore pellet bed under nut coke mixed charge conditions, ISIJ Int. 60 (2020).

[31] A.V. Kuzin, Determination of the optimum size of skip coke, Metallurgist. 57 (2013) 481–486.

[32] J.K. Chung, S.M. Lee, M.S. Shin, Effect of Coke size on reducing agent ratio (RAR) in blast furnace, ISIJ Int. 58 (2018) 2228–2235.

[33] A.V. Kuzin, Effect of introducing different sizes of nut coke into the ore layer on the degree of reduction of iron oxides, Metallurgist. 57 (2014) 783–791.

[34] M. Naito, A. Okamoto, K. Yamaguchi, T. Yamaguchi, Y. Inoue, Improvement of blast furnace reaction efficiency by temperature control of thermal reserve zone, 2006.

6. Melting and dripping behaviour of the pellet bed mixed with nut coke

The previous chapter has shown that the use of nut coke can improve the gas permeability and high-temperature properties of the iron ore pellet bed under blast furnace conditions (Chapter 5). The softening and melting temperature range decrease due to the substantial shift in melting temperature of the pellet bed. This was thought to occur due to the higher iron carburisation in the presence of nut coke in the bed. However, clear evidence for this has not been produced so far in the thesis. Furthermore, when the liquid drips out of bed, it reacts with coke to be reduced (FeO in the slag) and carburised (iron). Consequently, this influences the liquid dripping pattern to affect the blast furnace performance.

Therefore, in the present chapter, the effect of nut coke addition on the melting and dripping properties of the pellet bed will be explained. The results of quenching, melting and dripping experiments are analysed systematically. First, the pellet beds are quenched around the melting temperature and characterised to examine the prime reason of the melting, for the scenarios of both with (40 wt%) and without mixed nut coke. Then the dripped samples collected after the smelting experiments are analysed to find the effect of nut coke on the dripped metal and slag chemistry. Finally, the chapter concludes by explaining the effect of nut coke mixing on the profile of the weight and chemistry of the dripped liquid over the temperature range.

This chapter is based on the accepted manuscript for publication in the ISIJ international journal.

Dharm Jeet Gavel, Allert Adema, Jan van der Stel, Cees Kwakernaak, Jilt Sietsma, Rob Boom and Yongxiang Yang, "Melting behaviour of iron ore pellet bed under nut coke mixed charge conditions", 2020, 60(3).

6.1 Introduction

The ability of nut coke to improve the physicochemical behaviour of the iron ore pellet bed is shown in the previous chapters (4 to 5). It was found that the nut coke addition in the pellet bed substantially increases the bed permeability. Furthermore, the cohesive zone temperature range was observed to reduce by 16 ^{o}C for every 10 wt% nut coke addition. In the study, it was suggested that along with enhanced reduction kinetics, the higher iron carburisation would be the main cause for such behaviour. However, the complete characterisation was not presented and discussions were not made about melting pattern in the presence or absence of nut coke in the pellet bed.

On one hand nut coke addition provides multiple contact points of coke with the ferrous raw material; on the other hand, the regular coke layer becomes thin due to the replacement. This might have an impact on the melting and liquid dripping pattern from the ferrous bed. The melting and dripping pattern from the cohesive zone derives the burden decent and affect the gas permeability in the active coke zone of the blast furnace. Thus, an understating of the melting and liquid dripping behaviour is important. Especially when nut coke is added as a replacement of the regular coke this becomes even more critical. To understand the dripping behaviour some simulation studies [1-3] have been performed. However, in those studies either nut coke addition was not considered or the chemical interaction (reduction of FeO slag and iron carburisation) at the time of melting and dripping was ignored, which makes these studies of limited use.

In the present chapter, a thorough investigation is performed to understand the effect of nut coke addition on the melting and dripping behaviour of the iron ore pellet bed. The study is extended to examine the effect of nut coke addition on the iron carburisation, in both solid and liquid state.

6.2 Materials and method

6.2.1 Raw materials

Commercially supplied iron ore pellets and nut coke of size range of 10 to 13 mm and 10 to 15 mm, respectively, are utilised in the present study. The coke size of 20 to 25 mm is applied as the regular coke due to the crucible size limitations (inner diameter 64 mm). The chemical analysis of the pellet (type 1) is given in Table 3.1.

Figure 5.1 depicts a schematic of the sample bed arrangement inside the graphite crucible. In the sample without nut coke mixing, the pellet layers are sandwiched between the two regular coke layers (Fig. 5.1a). In the case of samples mixed with nut coke, the regular coke layer is proportionally reduced. As a result, the layer thickness of the regular coke decreases (Fig. 5.1b). In the experiment with nut coke, a maximum of 40 wt% replacement is used in the mixture to avoid critical thinning of the regular coke layers.

6.2.2 Experimental conditions

To investigate the effect of nut coke addition on the melting and dripping behaviour of the pellet bed, a series of smelting, quenching and dripping experiments are performed in the RSM. Experimental conditions, data and sample analysis procedures are discussed in Chapter 3 (3.3-3.6). The thermal and gas inlet profile followed during the experiments is given in Table 6.1.

6.2.2.1 Quenching experiments

The quenching temperature for the sample bed was determined based on a series of high-temperature smelting experiments (Chapter 5) [4]. In order to understand the prime reason of the pellet bed melting, samples were quenched from a temperature close to the bed melting temperature. Additionally, to understand the liquid flow behaviour in the presence of nut coke, the sample bed was quenched at the dripping temperature.

For the case of pellet bed without mixed nut coke, the bed was quenched at 1480 ^{o}C (Table 6.1). The sample bed mixed with nut coke two quenching experiments were performed. In the first experiment, the sample bed was quenched closed to bed melting temperature of 1450 ^{o}C and in the second experiment the sample bed was quenched close to dripping temperature of 1500 ^{o}C (Table 6.1).

Table 6.1 Thermal and gas profile followed during the experiments.

Step	Temperature range (^{o}C)	Heating rate (^{o}C/min)	CO (%)	CO_2 (%)	H_2 (%)	N_2 (%)	Gas flow rate (litre/minute)
Step 1	20 – 400	7.0	0	0	0	100	5
Step 2	400 – 600	5.0	25	20.5	4.5	50	15
Step 3	600 – 950	5.0	30	15.5	4.5	50	15
Step 4	950 – 1050	1.2	33	12.0	5.0	50	15
Step 5	1050 – 1450	5.0	42	0	8.0	50	15
Step 6	1450 – 1480	5.0	42	0	8.0	50	15
Step 7	1480 – 1500	5.0	42	0	8.0	50	15
Step 8	1500 – 1550	5.0	42	0	8.0	50	15
Step 9	1550 – 20	-5.0	0	0	0	100	5

6.2.2.2 Dripping experiments

The thermal and gas profile followed during the dripping experiments is shown in Table 6.1. During the dripping experiments, the rotating sample collector located at the bottom of the RSM (Fig. 3.4) was utilised. The sample collector is fitted with multiple cups (12 pieces), which was rotated to collect the dripping liquid (metal and slag) over the time and temperature range. To compare the effect of nut coke addition, one experiment without nut coke and another with 40 wt% nut coke replacement ratio were performed.

6.3 Results and discussion

6.3.1 Effect of nut coke addition on the pressure drop

The effect of nut coke addition on the pellet bed contraction and pressure drop was discussed comprehensively in Chapter 5 [4]. In the present study, the fundamentals of pellet bed melting and dripping are investigated. These phenomena are analysed for the cases with and without mixed nut coke (40 wt%) in the pellet bed.

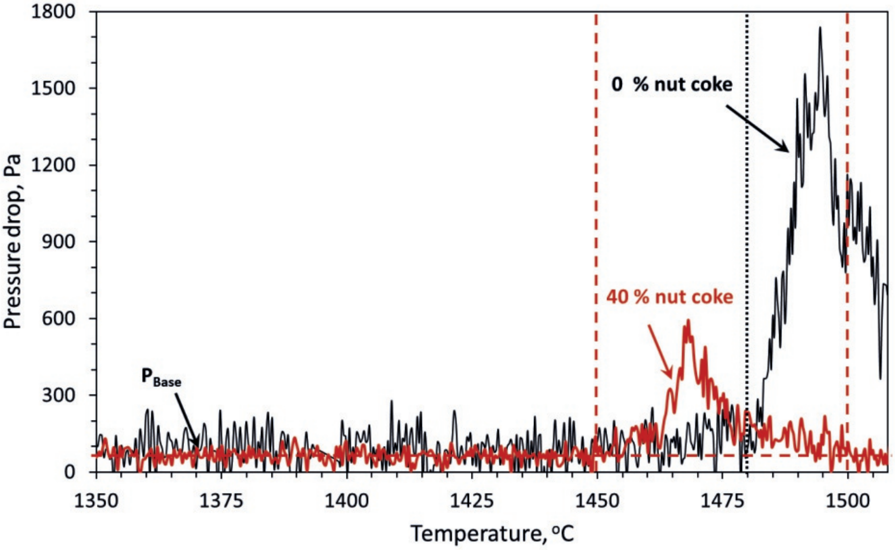

Fig. 6.1 Pressure drop curves and identified quenching temperatures for the sample bed without (1480 °C) and with (40 wt%) mixed nut coke (1450 °C and 1500 °C).

The pressure drop curves for the sample beds without nut coke and with 40 % nut coke for the temperature range up to 1550 °C are shown in Figure 6.1. It is observed that upon nut coke addition, the maximum pressure drop decreases and shifts towards lower temperatures. In order to investigate the prime reasons for such behaviour, iron ore pellet beds are quenched at various key temperatures. The pellet beds with and without mixed nut coke were quenched close to the bed melting temperatures, i.e., 1450 °C and 1480 °C, respectively. To further investigate the effect of nut coke addition on the sample chemistry during dripping, the bed with 40 wt% nut coke was quenched at 1500 °C.

6.3.2 Pellet bed in the absence of nut coke

The cross-section of the sample bed without nut coke, quenched at 1480 °C, is shown in Figure 6.2. The layer arrangement of the reduced pellets is apparent from the photograph. In earlier our work [4], it is suggested that the start of pellet bed melting is the prime reason for the sharp rise in the pressure drop. The broken top layer of the pellets in the present experiment (Layer 1 in Fig. 6.2) suggests that melting has just started in the pellet bed. On the other hand, the pellets located in other layers are not broken and retain their shape. It also appears that after breaking the top layer of the pellets, the regular coke layer from the top penetrates into the second layer of pellets due to the applied load.

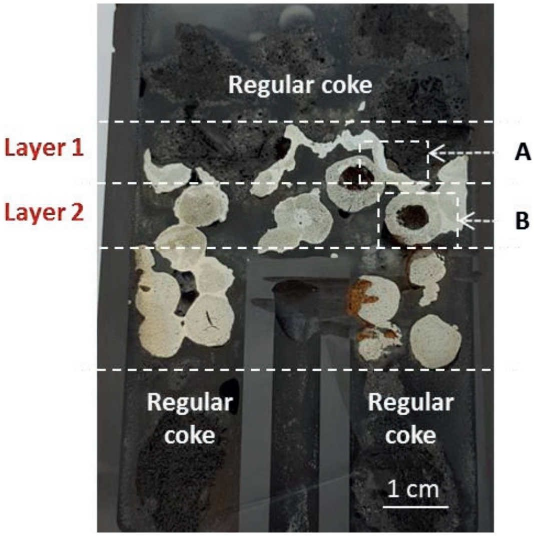

Fig. 6.2 Sample bed without nut coke quenched at 1480 °C.

The layer interface between the regular coke layer and the broken pellet layer was visualised with the optical microscope. In the region A (Fig. 6.2), a clear wetted interface between the coke and the pellet can be seen (Fig. 6.3). It appears that the regular coke from Layer 1 indents the pellet shell, breaking the pellets present in the first layer. As a consequence, the pellets lose their strength under direct contact with the regular coke. The iron (pellet shell) carburisation occurs under direct contact with the regular coke, which results in the local melting and breaking of the pellets.

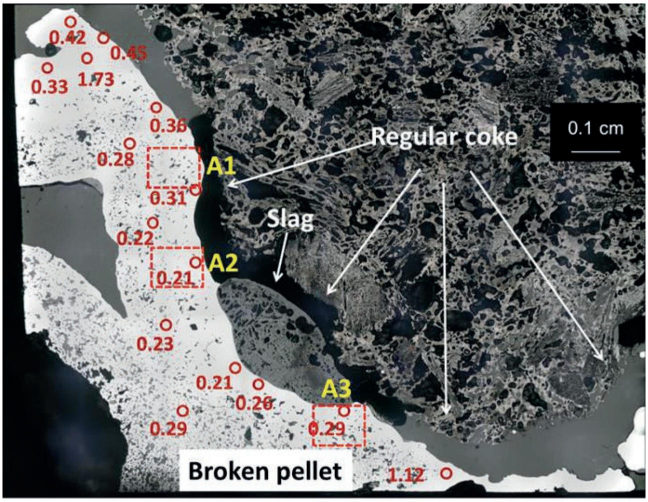

Fig. 6.3 Micrograph of the region A selected from pellet bed without nut coke, quenched at 1480 °C (broken first layer pellet, Figure 6.2)

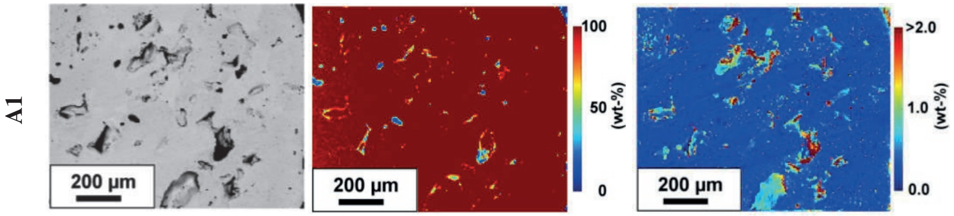

(a). Electron (BSE) image (b). Iron distribution (EPMA) (c). Carbon distribution (EPMA)

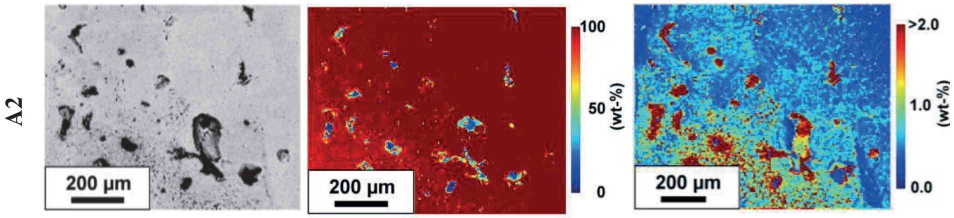

(d). Electron (BSE) image (e). Iron distribution (EPMA) (f). Carbon distribution (EPMA)

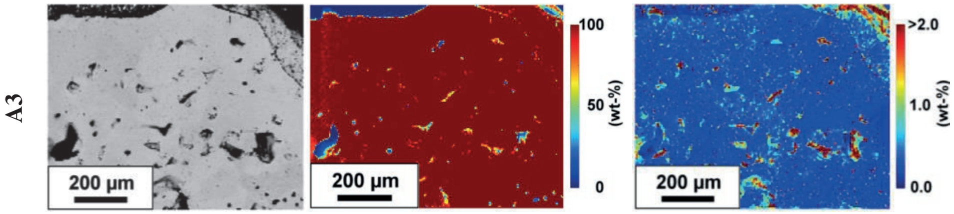

(g). Electron (BSE) image (h). Iron distribution (EPMA) (i). Carbon distribution (EPMA)

Fig. 6.4 EPMA (Electron Probe Micro-analyser) scan at location A1, A2 and A3 from Figure 6.3.

To check the level of iron carburisation on the selected pellet of the first layer, EPMA point and area analyses were performed (Fig. 6.3). The numbers next to the points (**o**) in Figure 6.3 represent the carbon content (in wt%) present at the examined spots (0.2 μm^2). For most of the spots, the local carbon content is in the range of 0.20 to 0.40 wt%. However, for some sites, the carbon concentration is as high as 1.73 wt%. Therefore, to investigate the reason for the variation in the carbon distribution, an EPMA scan was performed on selected areas (Fig. 6.3 and Fig. 6.4). This reveals that the carbon is present in diverse ranges (0 to 1.25 %) inside the iron matrix. Some spots of very high carbon concentration (>2 %) can also be observed inside the pores, which is due to the presence of mounting resin. Nevertheless, the carbon is mostly distributed in a similar range (˜0.30 wt%) in the iron matrix as examined by point analysis.

A similar analysis was performed on the pellet selected from Layer 2 (Fig. 6.2, region B). The carbon concentration obtained by EPMA (Fig. 6.5) is approximately 0.03 wt.%. In the second layer pellet, the carbon concentration is significantly lower (8-10 times) than in the broken first pellet layer. The EPMA elemental area analysis (Fig. 6.6) further confirms the results from the point analysis. However, in the small areas close to the surface or in pores, the carbon is distributed with higher concentration (B1, B2 and B3) due to the presence of polymeric mounting resin (Fig. 6.6). However, generally the carbon concentration is observed significantly lower than in the pellet from the first layer.

The differences in the carbon content of the reduced iron of the pellet in the first and second layer demonstrate that iron matrix carburisation results from direct contact with the regular coke. Subsequently, based on the iron carburisation level, melting of the first pellet layer occurs. After this melting, the interface between the regular coke and pellet moves to the second layer for further iron carburisation and melting thereafter. Consequently, layer-wise melting occurs in the pellet bed without nut coke. These phenomena continue until all the pellets become molten and drip out of the sample bed.

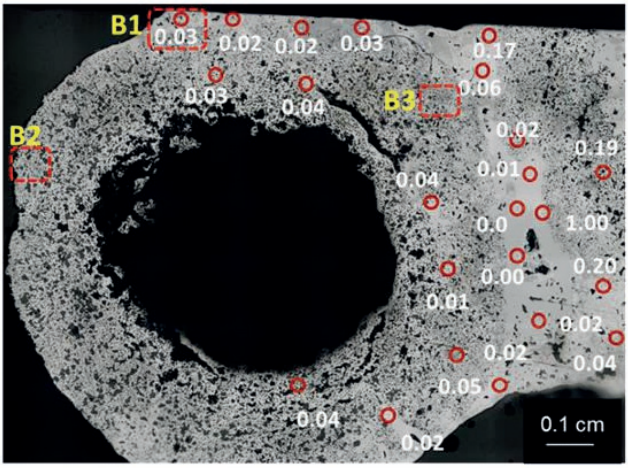

Fig. 6.5 Micrograph of the region B (Fig. 6.2) selected from the pellet bed without nut coke, quenched at 1480 ^{o}C, carbon concentration (wt%) indicated in white text.

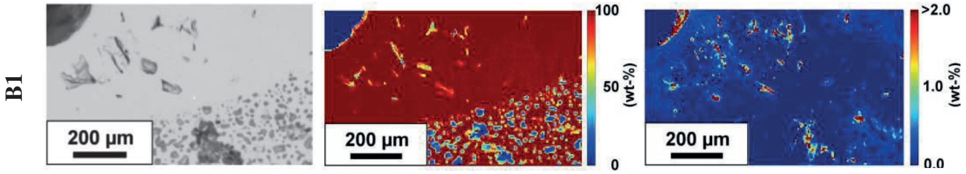

(a). Electron (BSE) image (b). Iron distribution (EPMA) (c). Carbon distribution (EPMA)

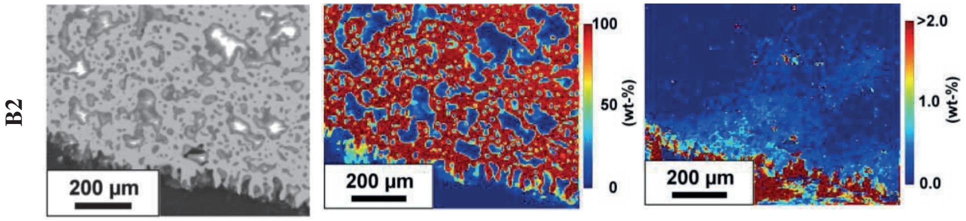

(d). Electron (BSE) image (e). Iron distribution (EPMA) (f). Carbon distribution (EPMA)

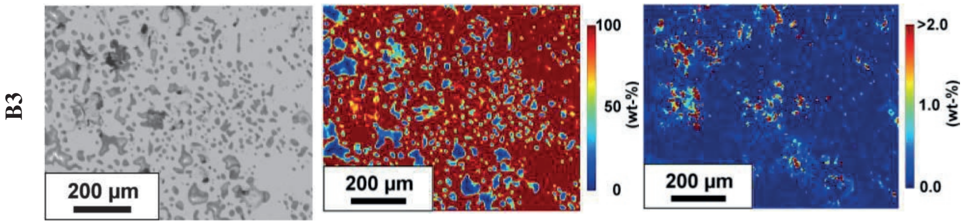

(g). Electron (BSE) image (h). Iron distribution(EPMA) (i). Carbon distribution (EPMA)

Fig. 6.6 EPMA area scan at locations B1, B2 and B3 from Figure 6.5.

6.3.3 Pellet bed mixed with nut coke

6.3.3.1 Pellet bed quenched from 1450 ^{o}C

It is observed that the pellet bed melting temperature decreases with the nut coke addition (Fig. 6.1) [4]. In order to investigate the principal reason for the decrease in the bed melting temperature, pellet bed mixed with nut coke (40 wt%) is quenched close to the bed melting temperature of 1450 ^{o}C. The cross-section of the quenched sample bed with 40 wt% nut coke mixing is shown in Figure 6.7. From the photograph, it is apparent that the nut coke acts as a frame to support the bed structure by physically hindering the sintering among the pellets [5]. Thus, the pores are instrumental for the gas to flow in the pellet bed during melting. It is also noted that most of the pellets are deformed, especially the pellets located close to the coke (nut coke and regular coke). This is due to the start of melting in the bed.

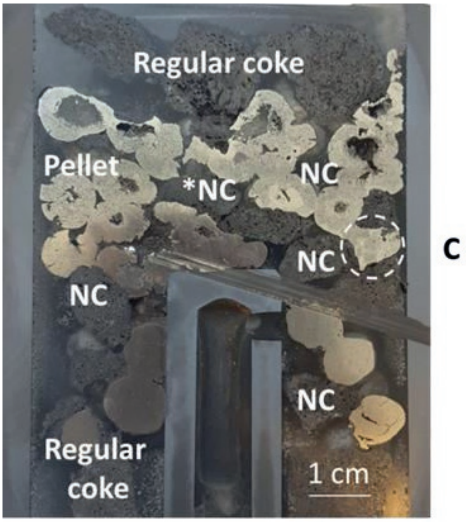

* NC- Nut Coke

Fig. 6.7 Sample bed with nut coke (40 wt%) quenched at 1450 ^{o}C.

From the quenched pellet bed, a representative pellet is selected (Figs. 6.7 and 6.8) to examine the effect of nut coke addition on the pellet chemistry. The EPMA point analysis on the pellet reveals a wide variation (0.00 - 1.26 wt%) in carbon content. Nevertheless, the average carbon concentration is observed to be higher than in the case where nut coke is absent in the pellet bed. To further investigate this phenomenon, selected pellet areas are scanned for the presence of carbon (Fig. 6.8 and 6.9). In the peripheral region (C1 and C3), the segregation of carbon is noticed in the form of grains; the carbon concentration is found to be distributed in the range of 0.60 - 0.80 wt% in the matrix of iron (Fig. 6.9). The area around the pellet core is also reduced. However, the carbon concentration is observed to be insignificant close to 0.00 wt% in area C2). This suggests that similar to the reduction reactions, the iron carburisation also progresses topo-chemically in the reduced pellets.

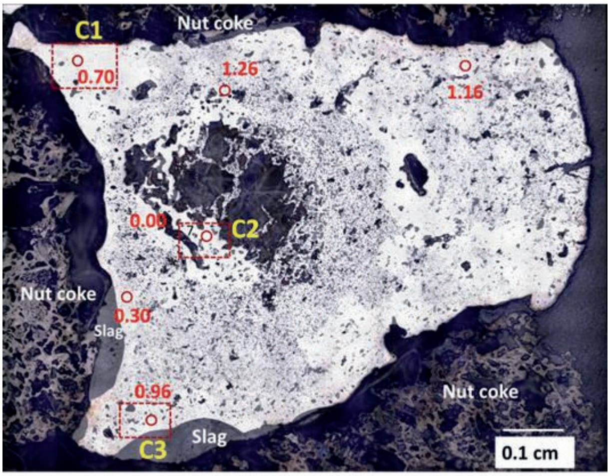

Fig. 6.8 Micrograph of the region C selected from the pellet bed mixed with (40 wt%) nut coke, quenched at 1450 °C (Figure 6.7), carbon concentration (wt%) indicated in red.

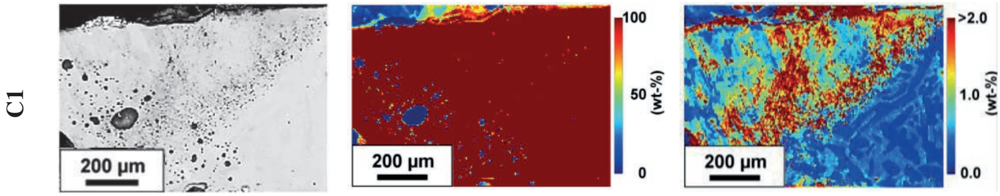

(a). Electron (BSE) image (b). Iron distribution (EPMA) (c). Carbon distribution (EPMA)

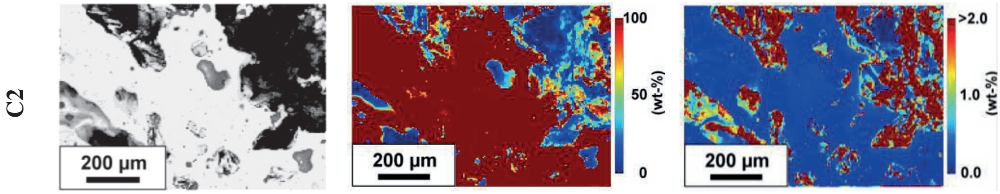

(d). Electron (BSE) image (e). Iron distribution (EPMA) (f). Carbon distribution (EPMA)

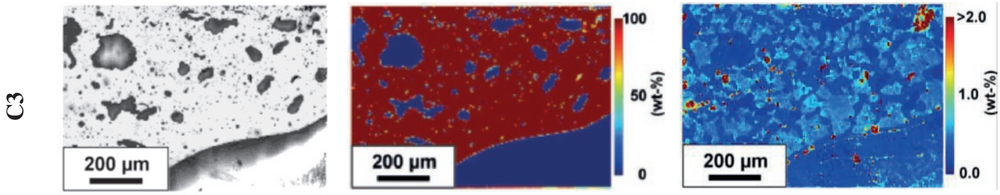

(g). Electron (BSE) image (h). Iron distribution (EPMA) (i). Carbon distribution (EPMA)

Fig. 6.9 EPMA area scan at location C1, C2 and C3 from Figure 6.8.

In the pellet bed mixed with nut coke, the CO-rich gas is able to flow inside the bed, invoking a higher level of carburisation (5.11) of the pellets [6]. Additionally, by direct contact of the pellet iron shell with coke (regular coke and nut coke), iron carburisation occurs throughout the pellet bed. As a result, the pellet shell starts to melt and loses its shape at many spots inside the bed (Fig. 6.7). Thus, in the pellet bed mixed with nut coke, simultaneous iron carburisation occurs. It results in simultaneous melting in the bed mixed with nut coke contrary to the layer-wise melting in the absence of nut coke.

6.3.3.2 Pellet bed quenched from 1500 °C

In the case of nut coke mixed pellet bed, a lower rate of bed deformation is noticed during the melting and dripping stage (third stage of bed contraction) [4]. The sample bed was quenched at 1500 °C to investigate the effect of nut coke addition during simultaneous melting and dripping (Fig. 6.10). Nut coke supports the bed structure to resist the deformation and provides pores for the gas flow. Additionally, due to the higher reduction degree realised on the iron ore pellets in the presence of nut coke, a thicker iron shell will form around the pellets. This will take a relative long time to carburise and melt out of the bed. Consequently, the rate of bed contraction is decreased in the presence of nut coke.

In the quenched sample bed, it is observed that the pellet shape is deformed significantly due to the melting. The solid metallic areas in the quenched bed are the re-solidified liquid iron melts (Fig. 6.10).

EPMA analysis is performed on such metallic locations to determine the level of iron carburisation (Fig. 6.11). The analysis reveals that the carbon is heterogeneously (0.22-2.21 wt%) distributed in the melting sample. The segregated profile of the carbon-rich dendrites or grains is apparent from the scanned areas (Fig. 6.12). The average carbon concentration (˜0.97 wt%) is higher than in the case of the pellet bed quenched from 1450 °C (˜0.73 wt%). This is due to the increase in temperature, which enhances the kinetics of iron carburisation [7]. Furthermore, when the liquid iron flows over the coke, the carburisation reaction rate increases due to the direct contact between the coke and the liquid iron.

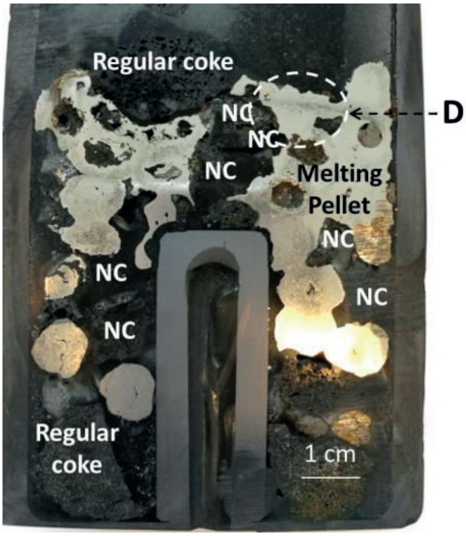

Fig. 6.10 Pellet bed mixed with 40 wt% nut coke, quenched at 1500 ^{o}C.

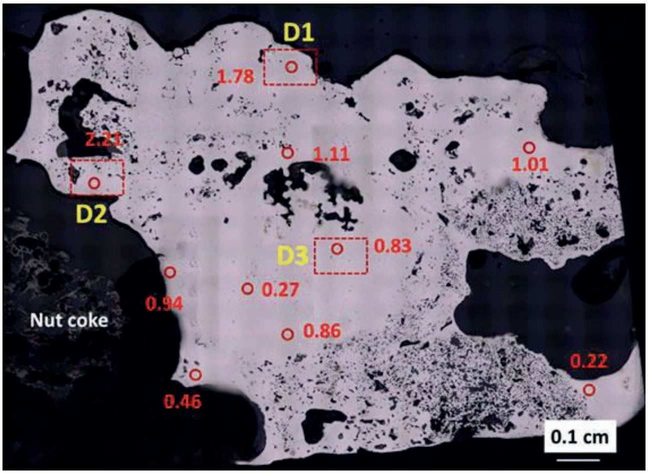

Fig. 6.11 Micrograph of the region D selected from the pellet bed mixed with (40 wt%) nut coke, quenched at 1500 ^{o}C (Figure 6.10), carbon concentration (wt%) indicated in red.

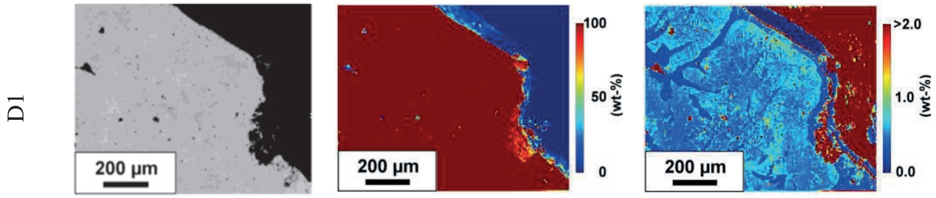

(a). Electron (BSE) image (b). Iron distribution (EPMA) (c). Carbon distribution(EPMA)

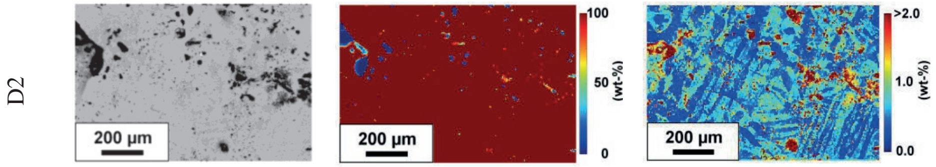

(d). Electron (BSE) image (e). Iron distribution (EPMA) (f). Carbon distribution (EPMA)

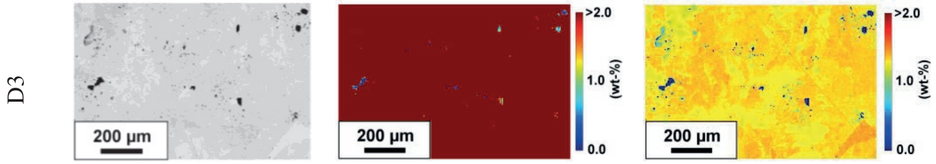

(g). Electron (BSE) image (h). Iron distribution (EPMA) (i). Carbon distribution (EPMA)

Fig. 6.12 EPMA area scan at location D1, D2 and D3 from Figure 6.11.

As the temperature increases during the experiment, based on the carburisation level achieved on the pellets, the melting begins. The melting starts from the location of the highest carbon content, provided that the carbon concentration is less than 4.3% [8] in the pellet, which is at the point of contact between the coke and iron (shell). Consequently, the melting starts from there, then it spreads to the individual pellet.

6.3.4 Effect of nut coke on liquid dripping

In the blast furnace, the liquid drips out from the cohesive zone and flows through the active coke zone to reach the hearth. While the liquid is dripping out of the cohesive zone, many relevant reactions occur such as the direct reduction of FeO rich slag, liquid iron carburisation, sulphur and silicon transfer [9]. Furthermore, the dripping pattern of the liquid is strongly linked to the gas intake capacity and therefore to the productivity of the blast furnace [9].

It is expected that nut coke addition will have an impact on the liquid dripping pattern. On the one hand, nut coke use results in thinning of the regular coke layer, which might affect the residence time (reaction) of liquid. On the other hand, nut coke enhances the area of contact between the liquid and the coke to affect the reaction and dripping behaviour.

Therefore, it is crucial to understand the nature of liquid dripping in the presence of nut coke in the iron ore pellet bed.

6.3.4.1 Dripping temperature

The liquid drips out of the sample crucible and is collected in the cup located at the sample receiver (Fig. 3.4). The time and the temperature (T_{xf}) of the first liquid drop are marked after visualising the event from the glass window located at the receiver (Fig. 3.4b). The liquid is observed to drip in the form of rivulets. A variation in the dripping frequency is due to the stochastic nature of the liquid dripping from the coke bed [10]. The variation in liquid dripping is a result of the liquid (slag and metal) and solid interaction (coke). For example, the liquid iron turns from wetting (contact angle of 50^o for 0 wt% C) to non-wetting (130^o for 5 wt% C) with an increase in the carbon concentration [11]. The wetting nature of the liquid iron during melting and dripping in the pellet bed quenched from 1500 ^{o}C can be clearly seen in Figure 6.13.

It is observed that the temperature of the first liquid drop (T_{xf}) is in the narrow range of 1495-1510 ^{o}C (Fig. 6.14). On the other hand, the dripping temperature (T_d) derived from the pressure drop curve is observed to decrease with the nut coke addition in the pellet bed (Fig. 6.14). In the blast furnace, the temperature T_d is crucial because at this temperature the regime of high resistance to the gas flow ends by the pressure drop returning to the base value (P_{Base}) (Chapter 5). By this temperature, a significant number of voids are regained after the liquid flows through the bed.

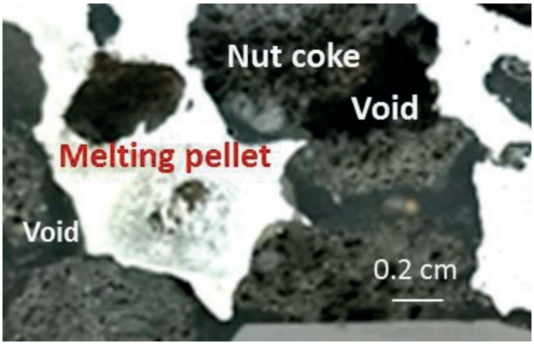

Fig. 6.13 Wetting nature of liquid iron, quenched at 1500 ^{o}C, with 40 wt% mixed nut coke.

The temperature difference between the dripping temperature (T_d) and actual first drop liquid dripping (T_{xf}) decreases with the nut coke addition in the pellet bed (Fig. 6.14). This represents the faster recovery of the voids for the gas flow, which principally occurs due to the simultaneous melting of the pellets in the presence of the nut coke in the bed.

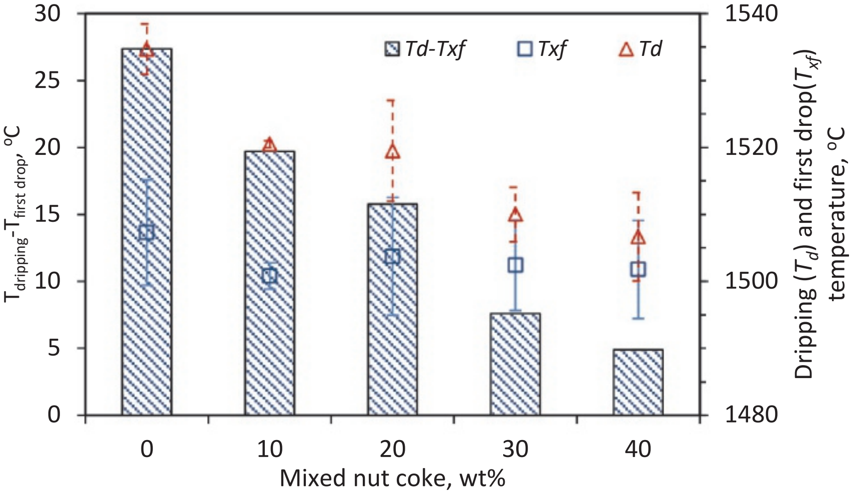

Fig. 6.14 Effect of nut coke addition on the dripping temperatures (T_d and T_{xf}).

6.3.4.2 Drip liquid composition

During the liquid flows over the coke, the reduction of liquid FeO rich slag and carburisation of iron takes place. For all the melting experiments, the carbon concentration in dripped metal is observed in the range of 2.5 to 3.5 wt% (Fig. 6.15a) and the FeO fraction in the slag is observed in the range 3 wt% to 4 wt% (Fig. 6.15b). Considering the high carbon concentration in the pellet quenched in the presence of mixed nut coke (Fig. 6.8 - 6.12), it is expected for the dripped liquid to have higher carbon concentration in iron and low FeO fraction in the slag. However, no clear trend for the dripped metal and slag composition is observed. Additionally, a high variation in the metal-carbon content and slag FeO fraction is observed. This indicates the complex nature of the liquid dripping. Furthermore, the uncertain nature [1] of liquid dripping from the coke bed can possibly result in variation in the reaction time for the liquid with the coke. Additionally, the dripping history of the analysed sample is unknown, since the liquid from one experiment is collected in one cup. This makes it difficult to understand the effect of nut coke addition of liquid dripping profile.

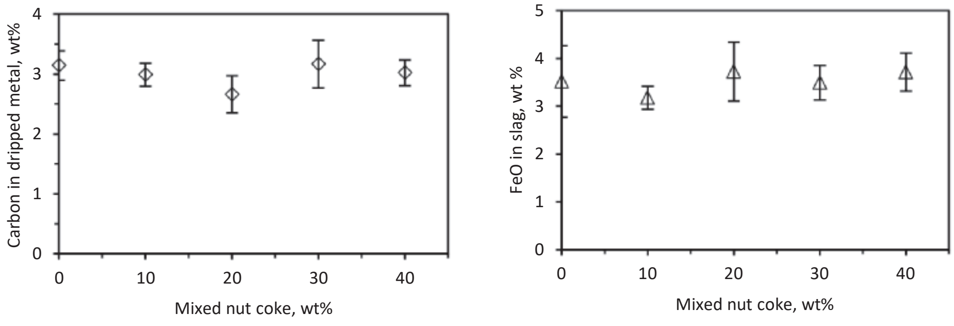

(a) (b)

Fig. 6.15 Effect of nut coke mixing on (a) carbon in the dripped metal and (b) FeO in the slag.

Therefore, to investigate the effect of nut coke addition on the dripped liquid mass and composition (carbon and FeO contents), experiments are performed in which the liquid is collected over the time and temperature range. The results are discussed in the following section.

6.3.4.3 Dripping profile

Two control experiments were performed — first without nut coke and second with 40 wt% nut coke mixing in the pellet bed. The dripped liquid was collected in different cups to study the effect of dripping time and temperature on the liquid chemistry (metal and slag) and mass distribution (Fig. 6.16). The temperature range and the collected weight of the samples are given in Table 6.2.

It is noticed from both the experiments (with and without nut coke) that first only molten metal drips out of bed, which indicates that the melting and dripping phenomena are controlled by the melting of the metal (iron). Thereafter, metal and slag simultaneously drip out of bed. Dripping from the sample bed mixed with nut coke starts at a lower temperature (1500 ^{o}C) compared to the case when nut coke is absent (1518 ^{o}C). It is observed for both experiments that the liquid drips in the form of rivulets. The dripping frequency is seen to vary in a close weight range (˜35 g/min) for the pellet bed mixed with nut coke, whereas, for the pellet bed without nut coke a significant fraction of liquid drips (˜50 wt%) at higher temperature (˜1550 ^{o}C). This delay in liquid dripping from the pellet bed without nut coke indicates that the iron is lean in carbon at the start of melting [8]. Then, as the temperature increases, the liquefaction occurs in the bed to continue the dripping.

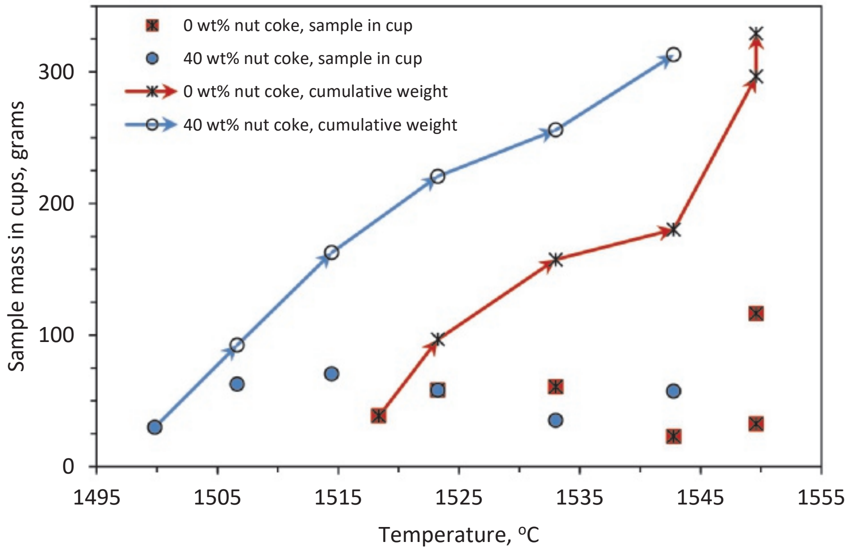

Fig. 6.16 Distribution of the dripped liquid mass collected over the temperature range.

Table 6.2 Sample weight after the dripping experiments.

	Cup no.	Temperature range, °C		Weight, g		Material nature	Remarks
		From	To	Liquid weight	Total		
Without nut coke	1	1518	1523	38.4	38.4	Metal	-
	2	1523	1533	58.2	96.6	Metal and Slag	-
	3	1533	1543	60.8	157.3	Metal and Slag	-
	4	1543	1550	22.8	180.2	Metal and Slag	-
	5	1550	1550	116.4	296.6	Metal and Slag	Hold for 5 min
	6	1550	20	32.5	329.0	Metal and Slag	During cooling cycle
With 40 wt% nut coke	1	1500	1507	29.8	29.8	Metal	-
	2	1507	1515	62.6	92.3	Metal and Slag	-
	3	1515	1523	70.4	162.8	Metal and Slag	-
	4	1523	1533	57.9	220.7	Metal and Slag	-
	5	1533	1543	35.1	255.8	Metal and Slag	-
	6	1543	1550	57.2	312.9	Metal and Slag	-

Iron carburisation: The carbon content of the dripped iron melt is shown in Figure 6.17. The average carbon content of the dripped metal from the pellet bed without nut coke is higher (3.40 wt%) compared to the case when nut coke (40 wt%) is present (2.75 wt%) in the bed. Considering enhanced solid-state carburisation (Fig. 6.9) in the pellet bed mixed with the nut coke, this is contrary to the expectation. There are two possible reasons for such behaviour in the pellet bed without nut coke. First, the dripping at high temperature supports the kinetics of the iron carburisation in the liquid state. Second, when the liquid iron flows over the thicker regular coke layer at high temperature, it possibly accumulates more carbon from the coke.

In the case of a pellet bed without nut coke, the carbon content in the iron is observed to increase with temperature up to 1533 °C. Then, it is observed similar for the collected metal up to 1542 °C. Thereafter, the carbon content is decreased by 0.5 wt%, which is due to the large volume of liquid dripped around this temperature (Fig. 6.17). As a result, the liquid does not have sufficient time to be carburised by the regular coke [12]. After that, some liquid drips out of the crucible at the start of the cooling cycle. This liquid drips out due to its high carbon content which decreases the liquidus temperature and lowers the viscosity by providing the available superheating.

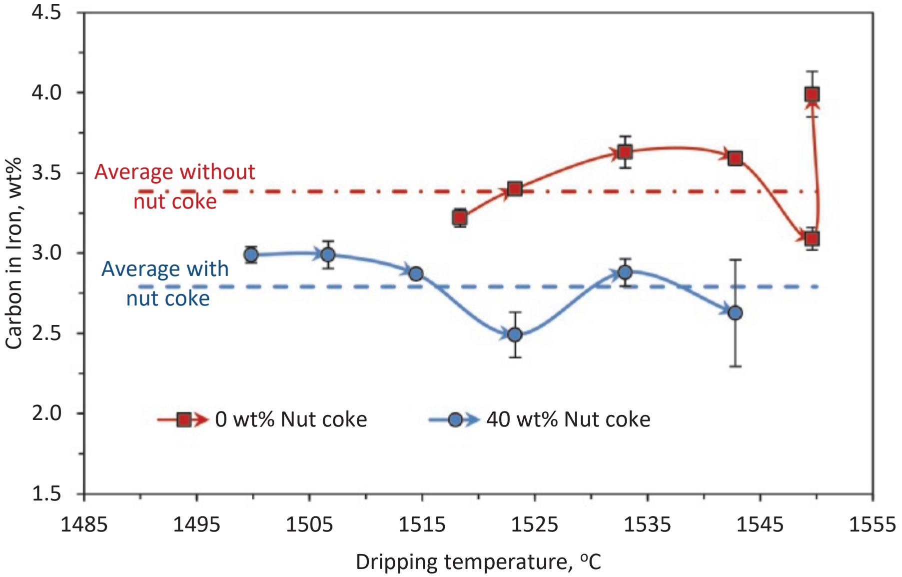

Fig. 6.17 Variation of carbon concentration of the dripped iron metal collected at different temperatures and time.

On the contrary, in the pellet bed mixed with nut coke, the carbon content in the dripped iron is observed to be in a close composition range (2.50 - 3.00 wt%). However, a mild fluctuation in the carbon concentration is the observed in samples collected at high temperature (T > 1523 °C), and this might be a result of a hold-up and stochastic dripping nature [10]. As the temperature increases, the more iron-carbon alloy will liquefy which will flow over a thinner layer of regular coke compared to the bed without nut coke. As a result, liquid iron has less time to interact with the regular coke to accumulate the carbon. Nevertheless, the carbon concentration in the dripped liquid is in a close range (˜2.75 wt%). This is possibly due to the steady dripping of the liquid from the bed when nut coke is present.

FeO in the dripped slag: The average FeO content in the dripped slag for the nut coke mixed case is observed to be low (3.8 wt%) compared to the case in which the nut coke is absent (4.6 wt%) in the pellet bed (Fig. 6.18). The lower level of FeO in dripped slag indirectly indicates that a higher reduction degree is achieved in the case of pellet mixed with nut coke.

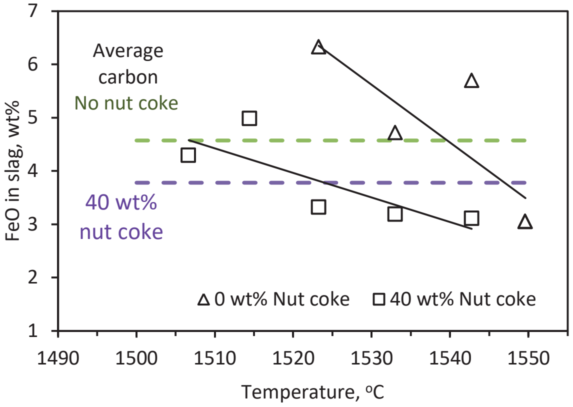

Fig. 6.18 FeO in the dripped slag.

For both cases, the dripped slag reaches a final FeO level of ˜3.1 wt% (Table 6.3). In the case of pellets mixed with nut coke, this FeO level is achieved at a lower temperature than in the case of pellet without nut coke. In the case of pellet mixed with nut coke, after some initial variation, the FeO concentration eventually reaches the final level (3.1 wt%) whereas in the case of pellet bed without nut coke, slag drips at a high temperature (above 1542 ^{o}C) and has a stable level of FeO. This final FeO content in slag might be the result of stable complex oxide formation with other oxides (CaO, SiO_2, Al_2O_3, MgO), which need longer interaction time with coke for further reduction. The complete slag analysis is given in Table 6.3.

Table 6.3 The dripped liquid slag chemistry (XRF).

Temperature, °C Start	Temperature, °C End	Cup	SiO_2 wt%	FeO wt%	MgO wt%	Al_2O_3 wt%	MnO wt%	CaO wt%	TiO_2 wt%	V_2O_5 wt%	K_2O wt%
Sample without nut coke											
1523	1533	2	47.4	6.3	13.2	14.5	4.7	5.5	4.7	0.3	1.0
1533	1543	3	47.7	4.7	12.9	17.3	4.2	5.2	4.5	0.3	1.1
1550	1550	4	43.9	5.7	12.5	15.2	6.4	6.0	5.8	0.3	1.2
1550	1550	5	49.6	3.1	13.2	17.2	3.9	5.3	4.5	0.2	1.1
1550	-	6	49.8	3.1	13.2	15.9	4.0	5.6	4.8	0.1	1.1
Sample with 40 wt% mixed nut coke											
1507	1515	2	49.3	4.3	13.9	13.7	4.4	5.8	4.9	0.3	1.1
1515	1523	3	47.6	5.0	12.6	17.0	4.3	5.2	4.5	0.3	1.3
1523	1533	4	50.1	3.3	14.0	14.0	4.3	5.9	4.9	0.2	1.2
1533	1543	5	50.6	3.2	13.7	14.7	3.9	5.8	4.7	0.1	1.1
1543	1550	6	49.5	3.1	14.2	14.9	3.7	6.0	5.0	0.1	1.2

6.4 Conclusions

Based on the detailed examination of the samples from a series of specially designed quenching and dripping experiments under simulated blast furnace conditions, the following conclusions can be drawn.

1. In the melting bed of iron ore pellets, nut coke is present as a frame to maintain the passage for the gas flow.
2. By direct contact with the coke, the formed iron shell of the pellets becomes carburised first and then eventually melts. In the case of the pellet bed without nut coke, this starts from the first top layer and progresses layer-wise, whereas, in the pellet bed mixed with nut coke, melting proceeds simultaneously due to the presence of multiple points of contact between the coke (nut coke and regular coke) and pellets across the whole bed.
3. The higher iron carburisation achieved in the presence of the nut coke is observed to be the prime reason for the decrease in the melting temperature of the pellet bed.
4. The difference between the first liquid drop temperature (T_{xf}) and the derived dripping temperature (T_d) is observed to decrease with the increase of the nut coke mixing in the pellet bed.
5. In the case of the pellet mixed with nut coke (40 wt%), the liquid dripping starts earlier, i.e. at a lower temperature (˜1500 °C) than in the case when nut coke is absent (1518 °C). In the nut coke mixed pellet bed a steady rate of liquid dripping occurs,

whereas from the pellet bed without nut coke a significant amount of liquid drops at higher temperature (above 1542 °C).

6. A substantial degree of iron carburisation occurs in the liquid state, which is indicated by the difference in the carbon level of quenched pellet and the dripped metal.
   In the case of sample bed without nut coke, a higher degree of carburisation takes place when liquid iron flows over the thicker regular coke layer, whereas in the pellet bed mixed with nut coke the liquid state carburisation is observed to be low due to the presence of the thinner regular coke layer.

6.5 References

[1] W.M. Husslage, M.A. Reuter, R.H. Heerema, T. Bakker, A.G.S. Steeghs, Flow of molten slag and iron at 1500 °C to 1600 °C through packed coke beds, Metall. Mater. Trans. B. 36B (2005) 765–769.

[2] T. Kon, S. Natsui, S. Ueda, R. Inoue, T. Ariyama, Numerical simulation of dripping behavior of droplet in packed bed using particle method, ISIJ Int. 52 (2012) 1565–1573.

[3] H. Jin, S. Choi, J. Yagi, J. Chung, Dripping liquid metal flow in the lower part of a blast furnace, ISIJ Int. 50 (2010) 1023–1031.

[4] D.J. Gavel, A. Adema, J. van der Stel, J. Sietsma, R. Boom, Y. Yang, Effect of nut coke addition on the physicochemical behaviour of the pellet bed in ironmaking blast furnaces, ISIJ Int. 59 (2019).

[5] D.J. Gavel, Q. Song, A. Adema, J. van der Stel, J. Sietsma, R. Boom, Y. Yang, Characterization of the burden behaviour of iron ore pellets mixed with nut coke under simulated blast furnace conditions, Ironmak. Steelmak. (2018) 1–8.

[6] T. Murakami, H. Fukuyama, K. Nagata, Mechanisms of carburization and melting of iron by CO gas, ISIJ Int. Vol. 41 (2001) 416–421.

[7] S.T. Cham, R. Sakurovs, H. Sun, V. Sahajwalla, Influence of temperature on carbon dissolution of cokes in molten iron, ISIJ Int. 46 (2006) 652–659.

[8] O. K. Goldbeck, Iron-Carbon, in: Iron-binary phase diagrams, Springer, Berlin, 1982: pp. 23–26.

[9] A.K. Biswas, Principles of blast furnace iron making - theory and practice, Cootha Publishing House, Brisbane, Australia, 1981.

[10] W. Husslage, Dynamic distribution - sulphur transfer and flow in a high temperature packed coke bed, PhD Thesis, Delft University of Technology, 2004.

[11] M. Humenik, D.W. Hall, R.L. Van Alsten, Graphite-base cermets- a new material for bearing, electrical high temperature applications, Met. Progr. 81 (1962) 101.

[12] V. Shatokha, O. Velychko, Study of softening and melting behaviour of iron ore sinter and pellets, High Temp. Mater. Process. 31 (2012) 215–220.

7. Ferrous bed (pellet and sinter) behaviour under nut coke mixed charge conditions

The effect of nut coke mixing on the ferrous raw material bed of iron ore pellets was discussed in Chapters 4-6. In the blast furnace, the ferrous burden is generally a mixture of lumpy iron ore, pellets and sinter. The mixing proportion of this ferrous burden is selected to satisfy the chemistry and economic trade offset. Due to the difference in chemistry, these different forms of ferrous burdens interact with each other under blast furnace conditions. Additionally, when nut coke is mixed with a mixture of these ferrous raw material in the bed, it could change the bed shrinkage, permeability and gas utilisation properties. Thus, for effective utilisation of the nut coke in the blast furnace, it is essential to understand the effect of nut coke mixing on the ferrous raw material bed properties.

Therefore, the effect of nut coke addition on various physicochemical properties of the ferrous bed of pellet and sinter mixture is discussed in this chapter. First, the behaviour of the individual components of the ferrous burden is briefly presented. Then the properties of the ferrous burden (pellet and sinter mixture) are discussed in the absence of nut coke. Thereafter, various effects brought by the nut coke addition on the bed contraction and permeability of ferrous burden is discussed. The difference between the ferrous bed with and without nut coke is discussed by the characterisation of the quenched sample beds. Subsequently, the melting and dripping behaviour of the nut coke mixed ferrous bed are described. Finally, the chapter concludes by discussing the effect of nut coke on the dripped liquid chemistry, gas and the coke utilisation.

This chapter is based on prepared manuscripts for submission in peer-reviewed international journals.

[1] Dharm Jeet Gavel, Allert Adema, Jan van der Stel, Jilt Sietsma, Rob Boom and Yongxiang Yang, "A comparative study of pellets, sinter and mixed ferrous burden behaviour in blast furnace conditions".

[2] Dharm Jeet Gavel, Allert Adema, Jan van der Stel, Jilt Sietsma, Rob Boom and Yongxiang Yang, "Ferrous raw material bed behaviour under nut coke mixed charge conditions".

7.1 Introduction

The iron produced from the blast furnace route is expected to continue to be utilised for the steel production [1]. Blast furnace ironmaking process is energy-intensive, and an increase in process efficiency is essential for sustainability. Due to the counter-current nature of the ironmaking from the blast furnace, the efficiency can be enhanced by improving the gas permeability.

It is well known that at the cohesive zone of the blast furnace, significant resistance to the gas flow occurs due to the softening and melting of the ferrous raw materials [2]. Therefore, to minimize the resistance, a low-temperature difference between the softening and melting of the ferrous burden is desired [2]. This can be achieved by proper selection of the ferrous raw material for metal production [3].

In the blast furnace generally, a mixture of two or three types (iron ore, pellets and sinter) of ferrous materials is used for the metal production. The mixing proportions of these ferrous raw materials are adjusted based on the chemical and economic offset. Generally, olivine fluxed pellets are used for its superior properties [4-5] and lower slag volume operations [6]. The iron ore sinter is added to improve the physical (strength) and chemical (basicity) property of the ferrous raw material bed [7]. Furthermore, the ferrous burden chemistry and mixing proportion are varied to adjust the slag composition, which controls the metal composition (carbon, silicon and sulphur). Various studies have been performed to understand the effect of basicity and MgO on the physicochemical properties of the ferrous burden [8-11]. However, only a few report the interactions among different type of ferrous raw materials [12].

Additionally, the nut coke mixed charging with ferrous burden has gained industry and researcher attention for increasing the permeability in the blast furnace [13-15]. Also, nut coke mixing with ferrous burden has assured higher reduction kinetics, longer thermal reserve zone, and improved high temperature bed properties. However, these studies are limited to either one burden type or have been performed maximum up to 1250 °C, which is lower than melting temperature in the blast furnace [14,16]. Thus, there is limited understanding about the permeability, melting and dripping properties of the mixed ferrous burden under nut coke mixed charge conditions at temperatures of interest.

In the present study, a thorough investigation is performed to understand the high temperature interaction among different types of the ferrous burden (pellet and sinter) in the absence and presence of nut coke. The study also includes the investigation of the melting and dripping behaviour of nut coke mixed ferrous raw material bed.

7.2 Materials and method

7.2.1 Raw materials

Commercially supplied iron ore pellets and sinter of size range 10-13 mm are utilised in the present study. Two types of fluxed pellets (type 1 and 2) and one type of iron ore sinter are mixed in 40:20:40 ratio to form a ferrous raw material bed. During the test, the coke of size 10-15 mm and 20-25 mm are utilised as the nut coke and regular coke, respectively. The chemical analysis of the ferrous burden is given in Table 3.1.

Figure 3.1 depicts the schematic of the sample bed arrangement inside the graphite crucible. In the sample without nut coke, the ferrous layer is sandwiched between the two regular coke layers (Fig. 3.1a). In the case of sample mixed with nut coke, the regular coke layer is proportionally removed. Consequently, the layer thickness of the regular coke decreases (Fig. 3.1b). In the experiments with nut coke, a maximum of 40 wt% replacement of the normal coke is used in the mixture to avoid critical thinning of the regular coke layer.

7.2.2 Experimental conditions

Two sets of experiments were performed to understand the melting behaviour of the ferrous bed with and without mixed nut coke. The experiments were performed on the Reduction Softening and Melting (RSM) apparatus under simulated blast furnace conditions. Detail information about the experimental set-up is given in Chapter 3 and references [15,17-18].

7.2.2.1 Smelting experiments

High temperature (20-1550 ^{o}C) experiments are carried out in RSM to realise the smelting of the ferrous raw material. The thermal and gas profile followed during the smelting experiments are given in Table 7.1. The smelting experiments are performed without and with nut coke replacement ratio of 20 wt% and 40 wt%.

The dripped samples collected in the cup are removed. Thereafter, a portion of the sample is pulverised and magnetically separated (slag and metal). The slag (non-magnetic portion) is analysed (XRF, X-ray fluorescence, Panalytical, Axios Max) for the present elements, and metal (magnetic portion) is analysed for the carbon content.

7.2.2.2 Quenching experiments

The quenching temperature for the sample bed was decided after a series of smelting experiments. In order to understand the prime reason for the ferrous bed melting, samples are quenched close to the bed melting temperature (T_m). For the ferrous bed with and without nut coke (40 wt%), the bed is quenched at 1445 ^{o}C and 1505 ^{o}C, respectively. After cooling, the sample crucibles are cast using cold mounting resin and cut vertically into two halves for further analysis.

Table 7.1 Thermal and gas profile followed during the experiments.

Step	Temperature range (^oC)	Heating rate (^oC/min)	CO(%)	CO_2 (%)	H_2 (%)	N_2 (%)	Gas flow rate (LPM*)
Step 1	20 – 400	7.0	0	0	0	100	5
Step 2	400 – 600	5.0	25	20.5	4.5	50	15
Step 3	600 – 950	5.0	30	15.5	4.5	50	15
Step 4	950 – 1050	1.2	33	12.0	5.0	50	15
Step 5	1050 – 1445	5.0	42	0	8.0	50	15
Step 6	1445 – 1505	5.0	42	0	8.0	50	15
Step 7	1505 – 1550	5.0	42	0	8.0	50	15
Step 8	1550 – 20	-5.0	0	0	0	100	5

*LPM- Litre per minute

7.2.3 Analysis

The cross-sections of the selected ferrous raw materials are visualised by using an optical microscope (Keyence VHX-5000). The chemical analysis of the pellets, sinter, dripped metal and slag are measured with XRF, and the results are given in Table 3.1 in Chapter 3.

The elemental distribution present in the quenched sample is investigated using Energy Dispersive X-ray analysis (SEM-EDS, JSM-IT100). For the estimation of carbon in the dripped metal, the combustion infrared detection technique (LECO, Carbon-Sulphur analyser, CS744) is employed.

7.3 Results and discussion

7.3.1 Typical ferrous bed characteristics

A typical trend of ferrous sample bed contraction and gas permeability under simulated blast furnace conditions is shown in Figure 3.9 and Fig. 3.10, respectively. Various stages of bed contraction and pressure drop are described in Table 3.6 and Table 3.8, respectively. Under the blast furnace conditions, the bed contraction of the ferrous raw material evolves through three distinct stages [19-20].

Generally, the three principal phenomena responsible for bringing these three stages are; indirect reduction, softening and melting. The complete list of different physicochemical phenomena which occurs at these stages is given in Table 3.7.

7.3.2 Iron ore pellet bed characteristics

The characteristic pellet (type 1) bed contraction and pressure drop behaviour under blast furnace condition are shown in Figure 7.1. In the first stage, about 14 % of bed contraction occurs (Fig. 7.1). The first stage of contraction occurs primarily due to shrinkage of individual pellets as a result of the gaseous (indirect) reduction. Then the iron starts to form on the pellet surface due to the complete reduction of iron oxide. These reduction reactions proceed topo-chemically on individual pellets [20-21]. Then as the temperature increases, sintering within and among the pellets occurs [20,22]. These make it difficult for the gas to flow into the interior of the bed and cause the melting of FeO-rich regions inside the pellets. Consequently, the pellets start to soften under the load. Then the melting starts based on the carburisation level achieved on the pellet shell. This is noted by a drastic increase in the rate of bed displacement to start the third stage of bed contraction (Fig. 7.1).

As described, the second stage of bed contraction occurs due to the localised liquid formation, which results in the pellet softening. The formed liquid is mostly entrapped in the pellet core and in the micro-pores present on the pellet. The inter pellet voids are available for the gas flow. As a result, no significant change in the pressure drop occurs during the second stage of bed contraction. As the pellet melting and breakout start, these voids start to get filled up by the liquid (iron and slag) [23]. Consequently, a sharp rise in the pressure drop occurs at about 1480 °C (Fig. 7.1). The formed liquid floods (at T_f) the pellet bed, to reach the maximum pressure drop (P_{Peak}).

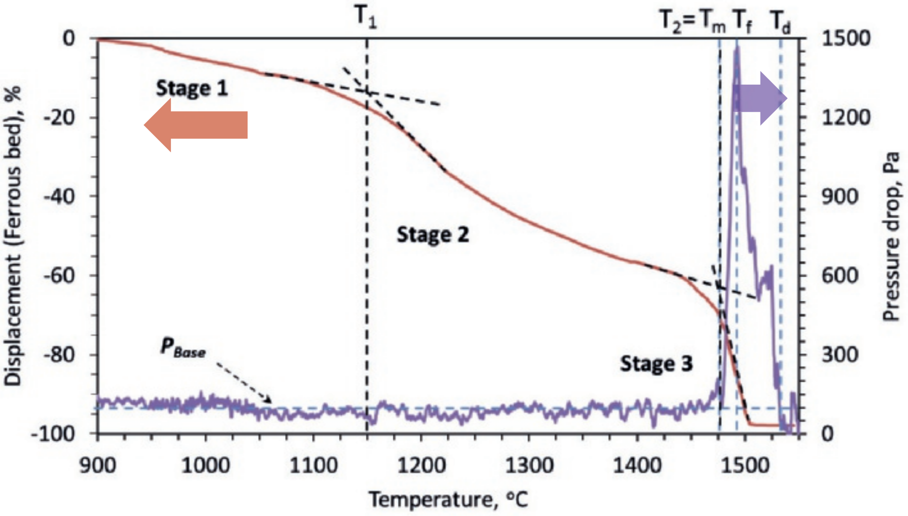

Fig. 7.1 Characteristic behaviour of the iron ore pellet bed under blast furnace conditions.

The internal state of the pellet bed is visualised by sample bed quenching at the start of melting (at 1480 ^{o}C) (Fig. 6.2). In the quenched bed, the first layer of the pellet is found broken at the bed melting temperature (region A, Fig. 6.2). On the other hand, the pellets present in the other layers appeared solid. This suggests layer-wise melting of the pellet bed, in the absence of nut coke. Furthermore, the EPMA analysis on the first (region A, Fig. 6.4) and second layer pellet (region B, Fig. 6.6) showed a significant difference in carbon concentration. This proves that the pellet in the first layer melts due to high carburisation induced by direct contact with the top layer regular coke. After melting the first layer of the pellet, the regular coke layer moves to the next pellet layer to carburise and to continue the melting. This layer-wise melting results in the longer high-pressure drop regime after the start of melting in the pellet bed. After significant liquid draining from the bed, the pressure drop value recovers back to the P_{Base} value at T_d.

The characteristics of pellet bed melting and dripping behaviour in the presence and absence of nut coke is discussed in detail in Chapter 6. The description in this chapter aims to provide a reference case for the case of sinter and pellet-sinter mixture.

7.3.3 Characteristics of sinter bed

The characteristics of the iron ore sinter bed contraction and pressure drop under simulated blast furnace condition are shown in Figure 7.2. In the first stage, a limited bed contraction (3.4 %) occurs in the sinter bed. Compare to the iron ore pellets; sinter has a stronger and more stable structure [24], which results in limited shrinkage of the sinter bed in the first stage temperature range. Additionally, due to irregular structure, sinter does not shrink uniformly across the bed to show less contraction.

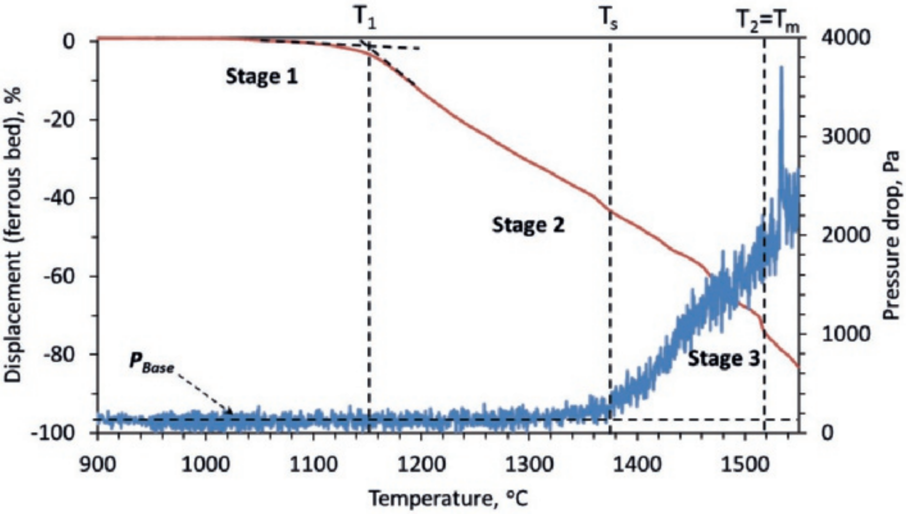

Fig. 7.2 Characteristic behaviour of iron ore sinter bed under blast furnace conditions.

Now, with the increase in temperature and reduction degree, the metal formation occurs in the sinter. Then due to the heat and pressure (load), particles start to get compacted among each other (second stage of contraction). Thereafter, the FeO rich region melts, which start to hinder the gas flow across the sinter bed. As a result, the pressure drop gradually starts to increase above the P_{Base} value after softening temperature (1375 °C).

As the reduction reaction proceeds further, sinter gets leaner in the FeO content. Consequently, the melting point of the slag increases drastically [25] (FeO <60 %, Fig. 7.3). The fluxes and gangue start to precipitate out from the melt. Correspondingly, the viscosity of the melt increases [8, 25-26]. This continues until the start of iron melting in the bed at ˜1520 °C, which is noticed by a sharp increase of pressure drop across the sample bed. The iron (melt) along with slag and precipitated solid particles (slag and gangue) forms a semi-fused mass, which exerts a strong resistance against the gas flow. Consequently, the pressure drop continues to increase even after bed melting temperature (T_m). Since there is no liquid dripping from the bed, no significant change in the bed contraction is observed in the third stage. After attending 1550 °C, the sample bed is quenched and afterwards cut vertically in two half's to visualise and characterise the internal state of the bed (Fig. 7.4).

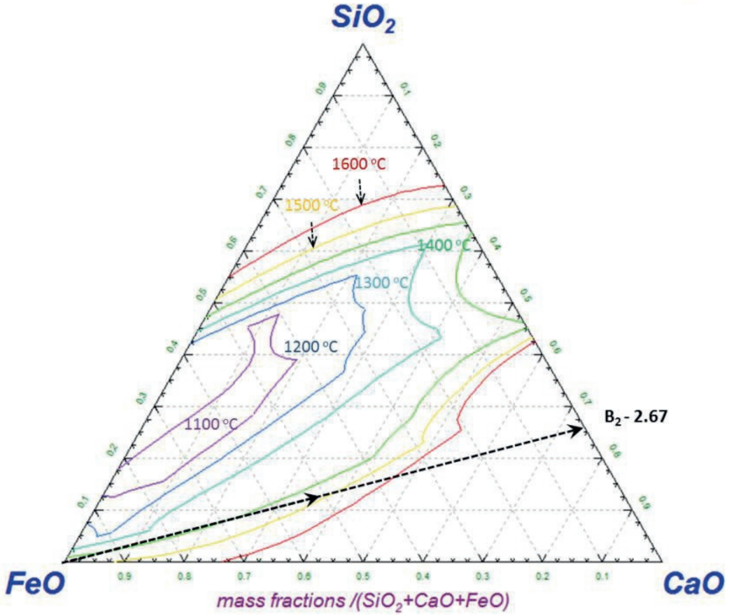

Fig. 7.3 SiO_2-CaO-FeO-(5%) MgO phase diagram with slag liquidus temperature projections (Factsage).

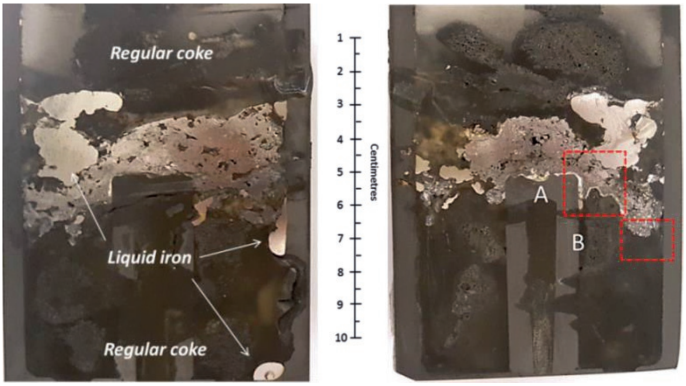

Fig. 7.4 Quenched iron ore sinter bed at 1550 ^{o}C.

The quenched bed photograph is shown in Figure 7.4. The photograph shows regions of liquid iron above and below (shiny area) the fused bed. The optical microscopy is performed on this selected metal region, which reveals the presence of iron in the form of grey cast iron (2.5-4.0 wt% C, 1-3 wt% Si) [27]. This is formed due to the carburisation of the liquid iron, which is in contact with the coke present in the top layer. However, such microstructure is not observed in the iron nuclei present inside the fused mass (Fig. 7.5e), due to lower iron carburisation.

Selected regions on the quenched bed are shown in Figure 7.5. The slag forming mineral rich interface between the regular coke and the fused layer is apparent from region A (Fig. 7.5a). The solid slag and disperse liquid metal is apparent from region B (Fig. 7.5d and 7.5e). EDS scan of a section in region B further confirms the distribution of calcium-rich slag around the metal droplet (Fig. 7.6). This forms a viscous semi-fused metal and slag region to resist the liquid dripping [28] and gas flow at high temperature.

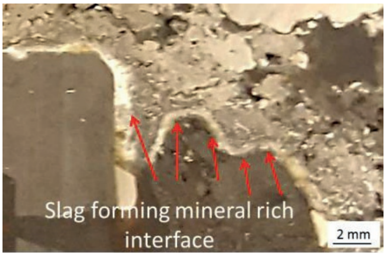

(a) Photograph of region A shown in Fig. 7.4

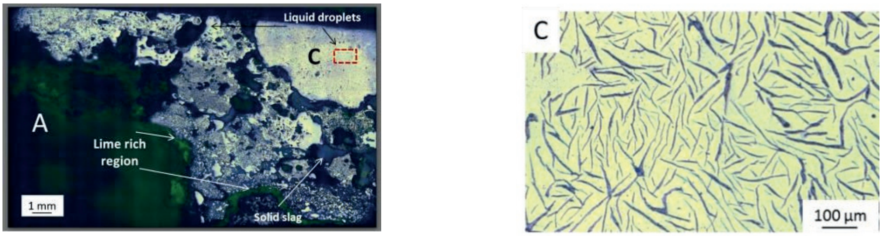

(b). Fused bed of liquid and solid slag forming mineral particles

(c). Microstructure of the metal in contact with coke (formed grey cast iron), region C shown in Fig. 7.5b

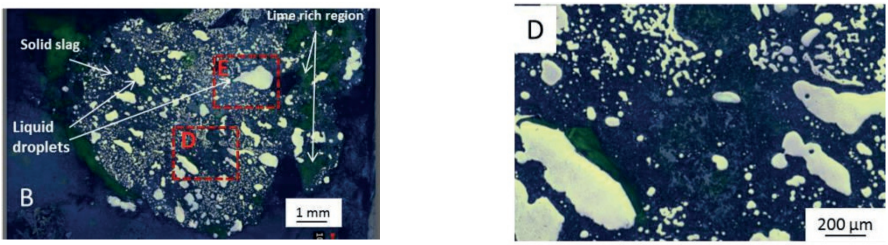

(d). Semisolid particle evolved from the iron ore sinter, region B from Fig. 7.4

(e). Iron micro-droplet dispersed in the semisolid slag forming mineral-rich region, shown in Fig. 7.5d

Fig. 7.5 Microstructure of the selected regions from quenched (at 1550 ^{o}C) iron ore sinter bed.

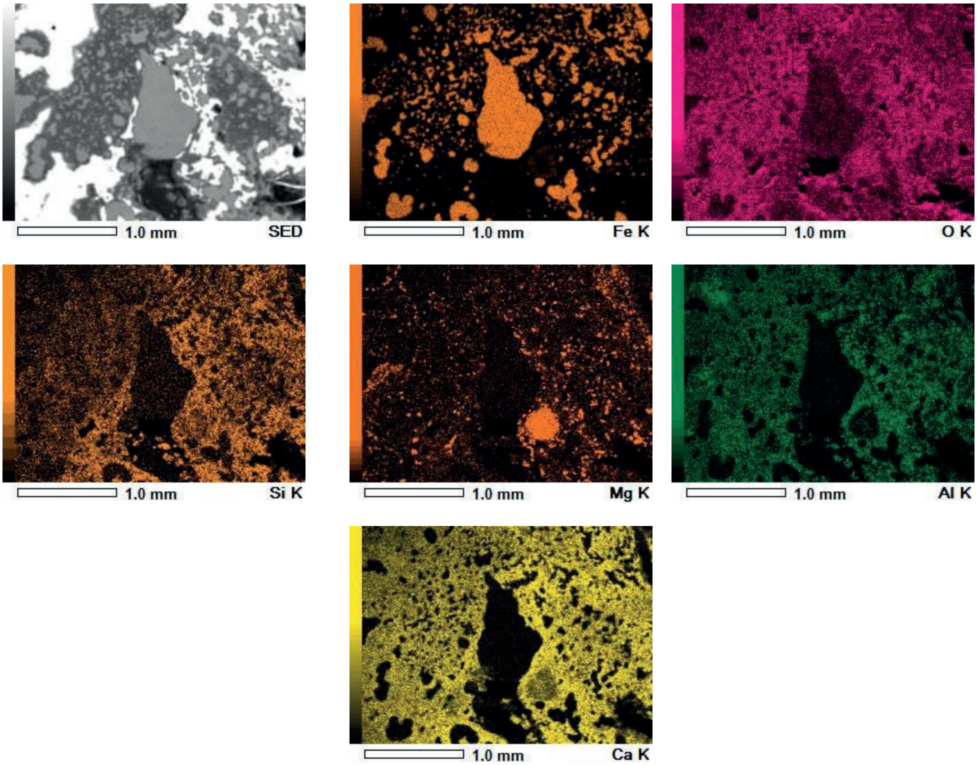

Fig. 7.6 EDS scan of a selected region E from quenched iron ore sinter bed (Fig. 7.5d). An entrapped liquid iron droplet present inside the bed.

An estimation was performed with Factsage to investigate the amount of liquid slag at 1550 °C. The results reveal that only ˜35 % of the slag is liquid at 1550 °C. Furthermore, estimation shows that for the complete melting of the slag forming mineral present in sinter (if FeO is completely reduced), a very high temperature of about 1940 °C is required (Fig. 7.7). This is the prime reason for the presence of solid slag forming minerals within the molten iron in the quenched bed, which forms a fused mass of metal and slag to resist (S_{value}= 0.65 MPa.°C) the gas flow across the bed.

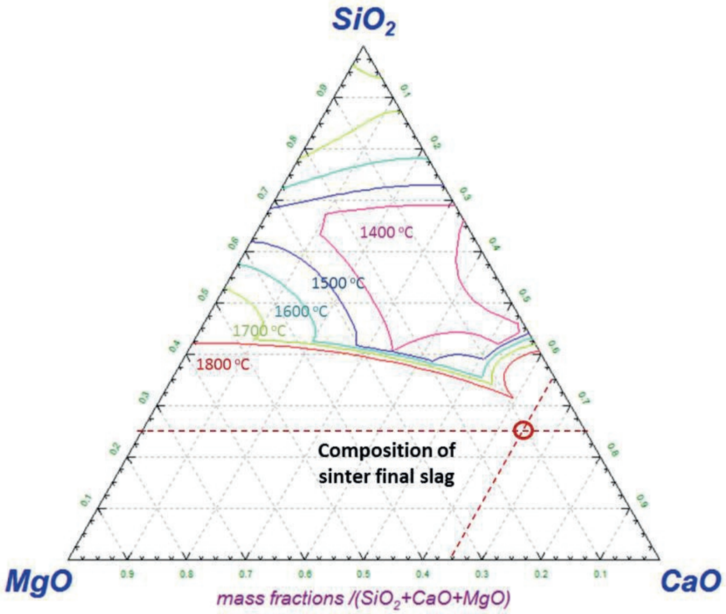

Fig. 7.7 Phase diagram (SiO_2- CaO-MgO-(6.25%) Al_2O_3) with liquidus temperature projections.

7.3.4 Characteristics of mixed ferrous burden (pellet and sinter mixture)

7.3.4.1 Ferrous bed contraction

The ferrous burden is a mixture of iron ore pellets (40 % pellets type 1: 20 % pellets type 2) and sinter in 60:40 ratio. The chemistry of the ferrous burden is given in Table 3.1. The ferrous bed contraction is shown in Figure 7.8. During the experiments under simulated blast furnace conditions, similar to pure pellet and sinter cases, three distinct stages of the bed contraction are observed. In the first stage, the mixture bed shows the contraction properties between the pure sinter and pure pellet bed. However, the shape of the curve in this region appear close to the case of iron ore pellet only bed (Fig. 7.1). This indicates that the bed contraction in the first stage occurs predominantly due to the shrinkage of the individual pellets in the bed, which is a result of the indirect reduction reactions [19-20].

Then the second stage of bed contraction starts with the rapid shrinkage similar to that of the pellet only bed. This occurs due to the start of pellet softening and sintering (within and among each other). Thereafter, the bed contraction curve changes its nature from pellet type to sinter type to continue the contraction with a gradual rate. Then, the second stage ends at ~1505 °C (T_2) with a bed displacement of 81 % (D_2). The T_2 temperature is higher by 25 °C compare to the pellet only case (1480 °C), which is primarily due to the poor reducibility and melting properties of the sinter. Furthermore, the high degree of shrinkage occurs in the ferrous bed is due to the poor high temperature strength of the sinter.

The shift from the second stage to the third stage is gradual, which is contrary to the case of pellet only burden. The bed contraction characteristic at the third stage is close to that of the sinter only bed (Fig. 7.2). This indicates that when sinter and pellet are mixed charged, the bed properties in the first and third stage is dominated by pellet and sinter, respectively. However, in the second stage, the bed shrinkage profile is governed by pellets initially then it is dominated by the sinter softening behaviour.

It is known that the rate of pellet bed melting (stage 3) is higher than that of the sinter bed (Fig. 7.8). The iron ore pellets contain low amount of impurities and fluxes. Thus, the melting temperature of the pellet is controlled by the level of iron (pellet shell) carburisation. However, the sinters are rich in gangue (SiO_2 and Al_2O_3) and fluxes (CaO and MgO) contents (Table 3.1), which certainly affects its melting behaviour. Among these, the melting of the calcium-rich oxide (CaO) is known to occur at very high temperatures [29] (Fig. 7.7). Thus, when the melting of iron from pellets and sinter starts, the flow of liquid is retarded due to the presence of the solid slag forming mineral particles (Fig. 7.5a). Consequently, the rate of mixed bed melting is gradual than that of the pellet only case.

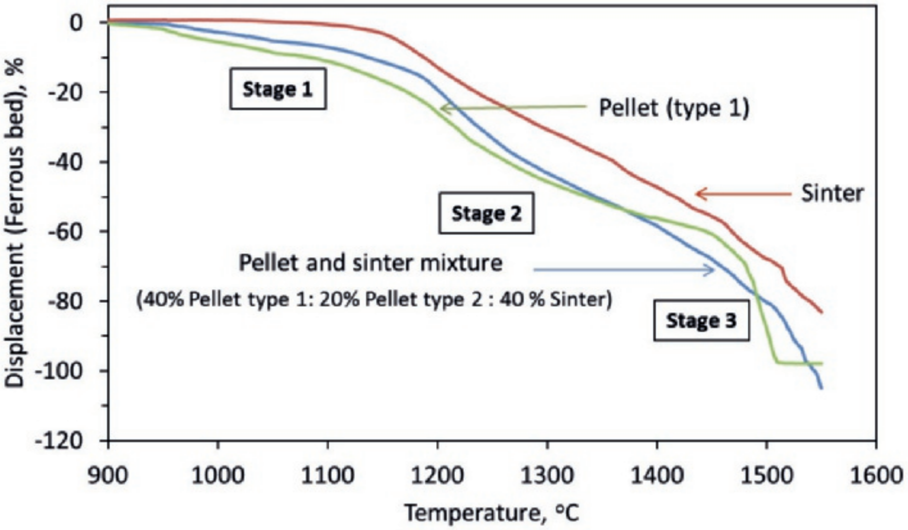

Fig. 7.8 Bed contraction profile for ferrous raw materials.

7.3.4.2 Ferrous bed permeability

The gas permeability profile during the softening and melting of the ferrous raw material bed is shown in Figure 7.9. The pressure drop across the bed starts to increase from P_{Base} at

1375 °C, which is close to the bed softening temperature (T_s) of the iron ore sinter (Fig. 7.2). Thereafter, the pressure drop continues to increase gradually. However, due to the presence of pellets in the bed, the magnitude of the pressure drop is observed lower than the case of sinter only burden. The slag in the pellet is mostly entrapped in the micro pores present in the metallic shell, and/or it is distributed in the core [22]. Consequently, at the time of bed softening, the interstitial voids around the pellets are open for the gas flow across the bed.

However, when the pellet melting starts, the slag and metal fill-up the inter-particle voids to mark the drastic increase in the pressure drop. The ferrous bed melting is observed to start at 1505 °C, which is in between the pellet and sinter only bed melting temperature of 1480 °C and 1520 °C, respectively. In the previous chapter, it is discussed that the carburisation achieved on the reduced iron controls the bed melting temperature. Now, considering the poor gas permeability compared to the pure pellet bed and higher permeability compared to the pure sinter bed, the iron carburisation is expected to be in between the pellet and sinter bed. Furthermore, two regimes of high-pressure drop are observed for the mixed burden after the start of bed melting, which indicates the melting of two different burden types. Then once P_{Peak} is achieved, the pressure drop is observed to decrease similar to the case of pure pellet bed. These suggest that layer-wise carburisation, melting and dripping of the ferrous burden occur in the bed.

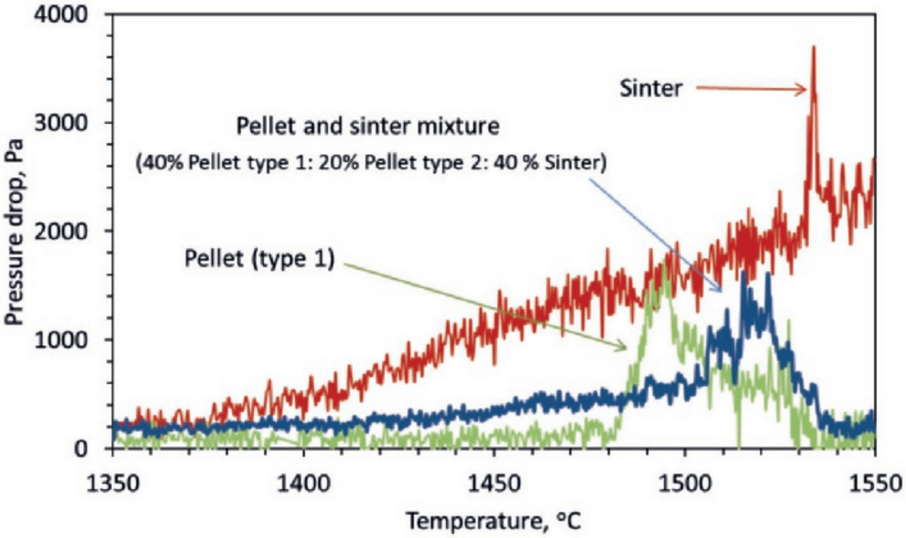

Fig. 7.9 Pressure drop profile for ferrous raw materials bed under simulated blast furnace conditions.

7.3.5 Effect of nut coke addition on ferrous bed (pellet and sinter mixture) contraction

The influence of nut coke addition (20 wt% and 40 wt%) on the ferrous bed (60 % pellet and 40 % sinter mixture) shrinkage is shown in Figure 7.10. The effect on the first stage of bed shrinkage is limited. A strong effect of the nut coke addition is observed in the second (softening) and third (melting and dripping) stage of bed contraction. The characteristics effect of nut coke addition on different stages is discussed below.

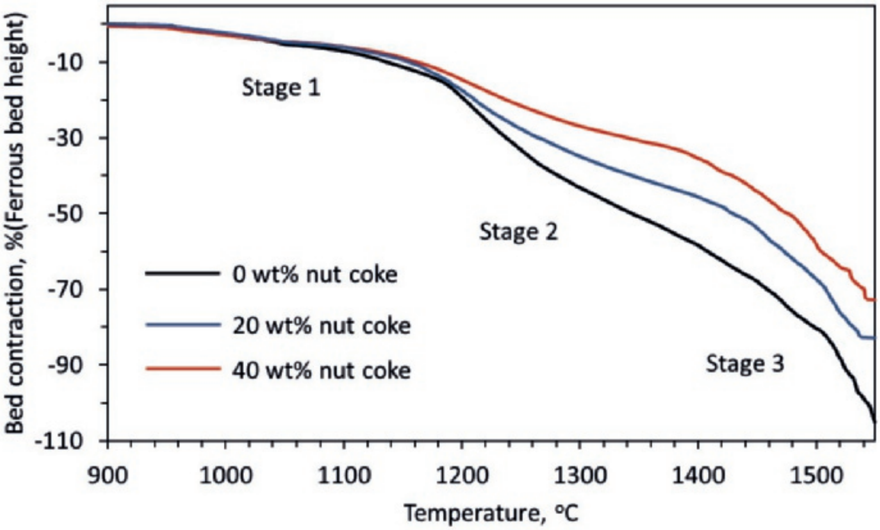

Fig. 7.10 Effect of nut coke addition on the ferrous bed (pellet (40% type 1: 20% type 2) and sinter (40 %) mixture) contraction.

7.3.5.1 Effect of nut coke addition on stage 1 behaviour

In the temperature range of the first stage, around 1000 ^{o}C, iron ore pellet swelling might occur [20,30-31]. However, in the examined case of ferrous burden (pellet and sinter mixture) due to the load (9.8 N/cm^2) on the sample top and use of H_2 gas for reduction, a limited swelling (less than 1 %) is observed (Fig. 7.11). Due to the close range, a clear effect of nut coke addition on the swelling is not established.

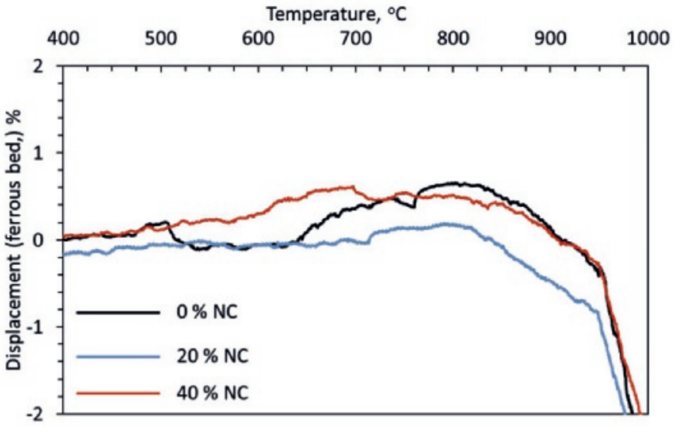

Fig. 7.11 Effect of nut coke addition on the swelling behaviour of the ferrous bed (pellet and sinter mixture).

The end temperature of the first stage (T_1), which represents the start of ferrous burden softening increases from 1157 °C to 1163 °C with 40 wt% nut coke addition (Fig. 7.12). The nut coke enhances the reduction degree of the ferrous burden to result in lower liquid (slag) formation, which shifts the T_1 to a higher temperature.

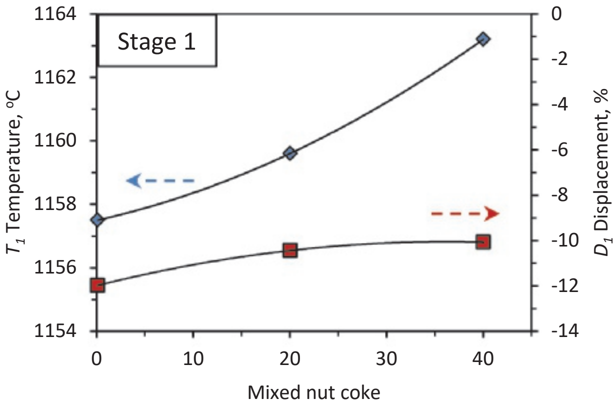

Fig. 7.12 Effect of nut coke addition on the first stage of bed characteristics temperature (T_1) and contraction (D_1).

Despite the higher reduction degree achieved on the burden, the first stage bed contraction (D_1) is observed to decrease from 12 % to 10 % with the increase in nut coke addition (Fig. 7.12). The presence of nut coke in the bed supports the structure and limits the sintering among the ferrous raw materials to undergo less contraction. Now, considering the trend of measured data, a non-linear relationship is recognised between nut coke addition and the first stage bed characteristic (T_1 and D_1).

7.3.5.2 Effect of nut coke addition on stage 2

The nut coke mixing with the ferrous burden (pellet and sinter mixture) has a substantial effect on the second stage of bed contraction (softening stage) (Fig. 7.13). The second stage end temperature (T_2), which represents the start of melting and the collapse of the individual ferrous burden, decreases by 98 ^{o}C (1505 ^{o}C to 1407 ^{o}C) upon 40 wt% nut coke addition (Fig. 7.13). The T_2 temperature is observed to decrease with an increase in added nut coke concentration. A non-linear relationship is found between the nut coke addition and the second stage end temperature (T_2) (Fig. 7.13).

The bed contraction in the second stage is observed to decrease from 81 % to 36 % upon 40 wt% nut coke addition with the ferrous burden (Fig. 7.12). Similar to the T_2 temperature, a non-linear relationship is found between the decrease in D_2 bed displacement and nut coke addition. One of the principal reasons for the bed shrinkage in the second stage is sintering among the ferrous burden [19,22]. Along with higher bed contraction, sintering results in slowing down of the reduction reaction by hindering the gas access to the unreduced portion of the ferrous burden (pellet and sinter). Consequently, the large volume of unreduced iron oxide (FeO) is left inside the ferrous burden. Now, as the temperature increases, the melting of the FeO rich portion starts along with gangue (SiO_2 and Al_2O_3) to cause the 'reduction retardation' phenomena [32-34]. This melt lowers the strength of the ferrous burden, which causes softening of the ferrous burden bed.

However, when nut coke is mix charged with ferrous burden, it hinders the sintering among the ferrous burden, which allows the CO-rich gas to reach the interior of the burden to result in higher reduction degree. Consequently, the 'reduction retardation' phenomena are minimised under nut coke nut mixed charge condition [32]. Now, as a result of formed metal on the ferrous raw materials, the bed strength increases to undergo comparative less contraction in the second stage [22].

In the nut coke mixed ferrous bed, due to the direct contact between coke and freshly reduced iron on the ferrous burden, the degree of the iron carburisation is high. As a result, the melting temperature [35] of the reduced ferrous burden is observed to decrease with the nut coke addition (Fig. 7.10 and Fig. 7.13). Therefore, the nut coke enhances the kinetics of metal formation and carburisation to lower the melting temperature of the ferrous bed. Consequently, the temperature and displacement range of the second stage is reduced with the increase in nut coke addition.

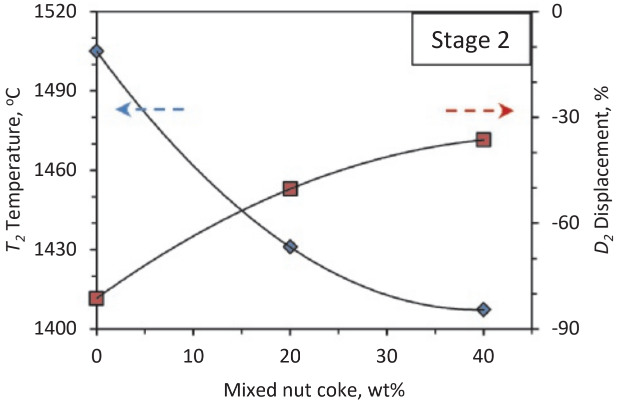

Fig. 7.13 Effect of nut coke addition on the second stage bed characteristics temperature (T_2) and contraction (D_2).

7.3.5.3 Effect of nut coke addition on stage 3

The third stage ends with melting and draining out of the liquid from the bed, which is noticed from the maximum possible bed contraction achieved during the experiment (Fig. 3.9). The end temperature for the third stage (T_3) is observed to decrease from 1550 °C to 1539 °C with 40 wt% nut coke addition (Fig. 7.10 and Fig. 7.14). Similar to the T_1 and T_2 temperature, a non-linear relationship is found between T_3 and added nut coke concentration. Due to the early start and strong drainage rate in the presence of nut coke, the T_3 temperature decreases with nut coke addition.

At the end of the third stage, liquid drains out to leave the unconsumed coke in the bed. Now due to the presence of unconsumed nut coke, the final bed displacement (D_3) is observed to decrease with the nut coke addition. Similar to D_2, a non-linear relationship is observed between D_3 and added nut coke concentration (Fig. 7.14).

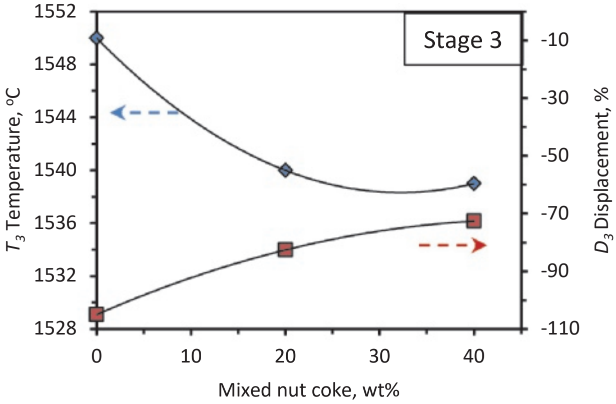

Fig. 7.14 Effect of nut coke addition on the third stage bed characteristics temperature (T_3) and contraction (D_3).

7.3.5.4 Bed displacement and temperature range

The first (ΔT_a) and third (ΔT_c) stage temperature range is observed to increase with the nut coke addition (Fig. 7.15a). However, the highest impact of nut coke addition is on the second stage (softening stage) (Fig 7.10 and 7.15a). The second stage temperature range is driven by the kinetics of iron oxide reduction and carburisation of the reduced iron [19]. Presence of nut coke in the bed not only improves the reduction kinetics of the ferrous raw materials but also improves the carburisation of the freshly reduced iron. Consequently, the melting of the ferrous burden shifts to the lower temperature [19,35], which results in shortening of the second stage temperature range (ΔT_b). ΔT_b is shortened by 103 °C (347 °C to 244 °C) upon 40 wt% nut coke addition. Additionally, nut coke limits the sintering among the ferrous raw material particles by physically hindering the contact among them [22]. Moreover, nut coke acts as a frame at the time of burden softening to undergo less contraction. Consequently, in the second stage, the displacement range (ΔD_b) is decreased by 43 % (69 % to 26 %) upon 40 wt% nut coke addition (Fig. 7.15b).

Nut coke enhances the reduction degree of the ferrous burden to increase the first stage temperature range (ΔT_a). ΔT_a is marginally increased by 6 °C (157 °C to 163 °C) with 40 wt% nut coke addition in the ferrous bed (Fig. 7.15a). Despite higher reduction on the ferrous burden due to the support provided by the nut coke in the bed, in the first stage, a decrease in the bed shrinkage range (ΔD_a) is observed. Similarly, the third stage displacement range (ΔD_c) is observed decreasing with nut coke addition. ΔD_c is decreased by 12.5 % (36.2 % to 23.7 %) with 40 % nut coke addition in the ferrous bed (Fig. 7.15b). The unconsumed nut coke present in the bed is the prime reason for the decrease in ΔD_c.

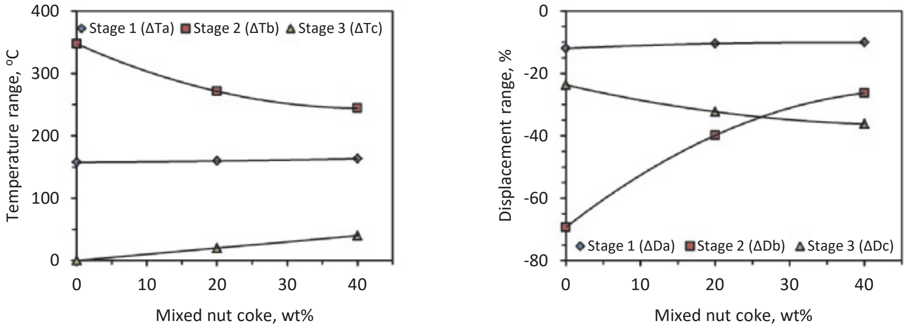

(a). Temperature range

(b). Displacement range

Fig. 7.15 Effect of nut coke addition on temperature and displacement ranges of different stages.

7.3.6 Effect of nut coke addition on ferrous bed (pellet and sinter mixture) gas permeability

Effect of nut coke addition on gas permeability (pressure drop) is shown in Figure 7.16. Various effects of the nut coke addition on the bed characteristic derived from pressure drop curves are discussed below.

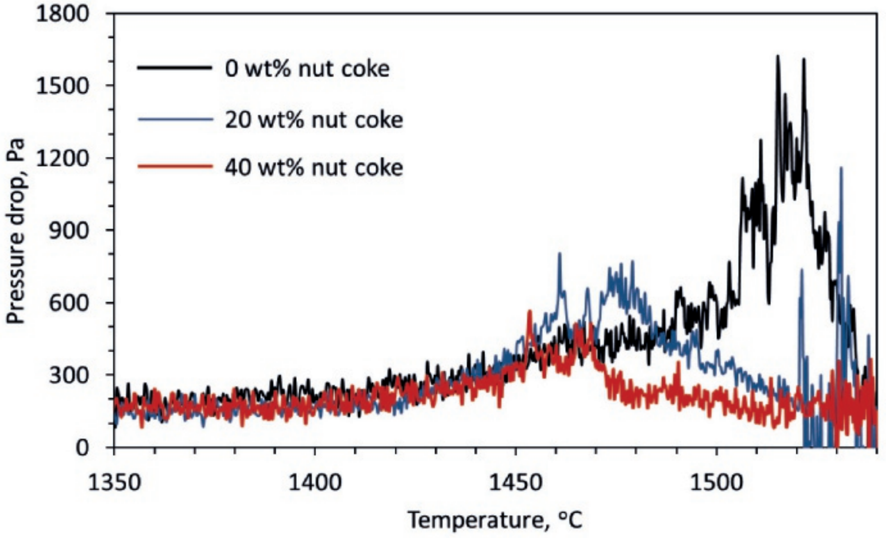

Fig. 7.16 Effect of nut coke addition on the ferrous bed gas permeability (represented by the pressure drop across the sample bed).

7.3.6.1 Effect on the bed characteristic temperatures

The characteristic bed temperatures are examined from the measured pressure drop profiles according to the definition laid in Figure 3.10 and Table 3.8. The bed softening temperature (T_s) is observed to increase by 44 °C (1374 °C to 1418 °C) upon 40 wt% nut coke addition with the ferrous raw materials. The increase in softening temperature (T_s) is due to the higher reduction degree achieved on the ferrous burden [22]. Additionally, the nut coke provides interstitial voids to accommodate the softening burden to delay the rise in a pressure drop across the bed.

The bed melting (T_m) and dripping (T_d) temperatures are noticed to decrease by 54 °C (1505 °C to 1451 °C) and 33 °C (1539 °C to 1506 °C), respectively, upon 40 wt% nut coke addition. In the presence of nut coke, the higher carburisation achieved on the reduced ferrous burden is the principal reason for the decrease in the bed melting (T_m) temperature [19]. The accessible pores and voids for gas flow due to the presence of nut coke in the bed facilities lower pressure drop (P_{peak}) and faster recovery to the P_{Base} value (Fig. 7.15 and Fig. 7.16). Consequently, T_d temperature decreases with nut coke addition.

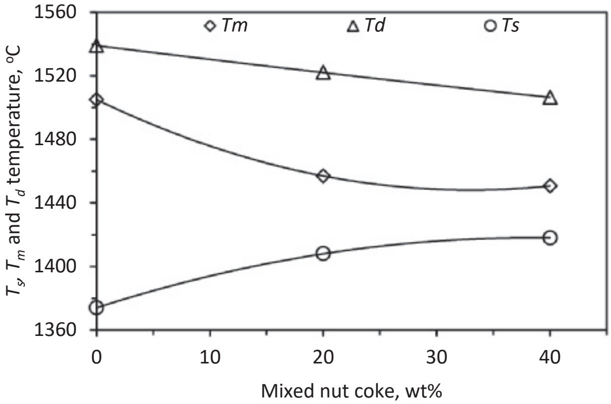

Fig. 7.17 Effect of nut coke addition on the ferrous bed characteristic temperatures.

7.3.6.2 Effect on S and S_p-value

During softening and melting of the ferrous raw materials, the pores in the bed are filled up to exert resistance against the gas flow. As a result, the pressure difference across the bed increases [36]. The area under the pressure drop curve till the start of bed melting (T_m), represents the resistance exerted to the gas flow due to the softening of ferrous burden (S_p value). And the complete area (S-value) under the pressure drop curve represents the total resistance exerted to gas flow during softening and melting of the ferrous burden (Fig. 3.10).

The S_p and S values are observed to decrease with the nut coke addition (Fig. 7.18). The nut coke present inside the bed remains solid at the cohesive zone temperature conditions. These provide pores (on nut coke) and voids (interstitial) for the gas flow to undergo less pressure drop at the time of bed softening and melting (Fig. 7.18). Thus, the gas permeability (S_p and S-value) improve exponentially with the nut coke addition in the ferrous raw materials bed.

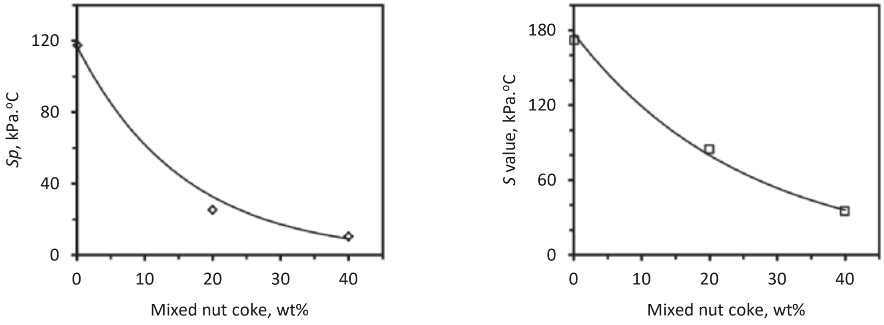

(a) S_P value (b). S-value

Fig. 7.18 Effect of nut coke addition on gas permeability (a) S_p value (a measure of resistance to gas flow during ferrous burden softening), (b) *S-value* (a measure of resistance to the gas flow during ferrous burden softening and melting)

7.3.7 Individual ferrous burden melting and bed melting

It is realised that for the ferrous bed mixed with nut coke, the melting (T_2) temperature of the individual particles of ferrous raw material (pellet or sinter) is different from the melting (T_m) temperature of the whole bed (bulk). The difference between the T_m and T_2 temperature increases non-linearly by 43 °C with 40 wt% nut coke addition (Fig. 7.19). At T_2 temperature, the melting of individual ferrous material starts and by T_m temperature, the melt spreads substantially in the bed to cause a sharp increase in the pressure drop across the bed. As discussed before, the nut coke remains solid at the time of ferrous bed melting, and accommodates the liquid in the interstitial voids to increase the bed melting temperature. However, in the absence of nut coke in the ferrous bed, T_2 and T_m occur at the same temperature (Fig. 7.19). A non-linear relationship is found between the melting temperature difference (T_m-T_2) and the nut coke addition.

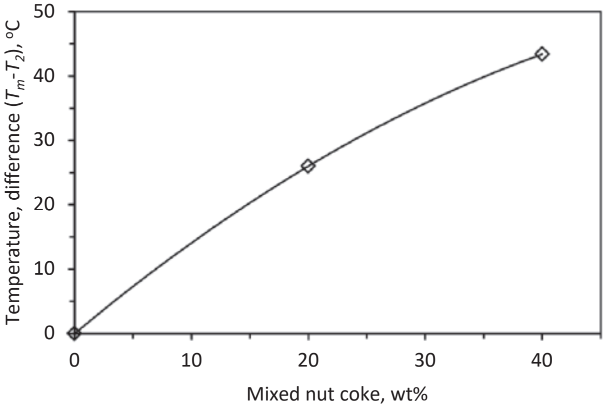

Fig. 7.19 Effect of nut addition on the temperature difference between individual burden melting (T_2) and bed melting temperature (T_m).

7.3.8 Effect of nut coke on softening and melting temperature range

The cohesive zone starts with the softening of the ferrous burden and ends with the melting and liquid dripping [2]. Thus during this process, limited pores are available in the bed for the gas flow. Consequently, reduced permeability occurs in the cohesive zone. In general, a narrow cohesive zone is desired for efficient blast furnace performance [36].

In the experiments under simulated blast furnace conditions, the ferrous burden softening starts at T_1 temperature, which is due to the start of in-situ melt formation [33] and sintering among the ferrous burden [22]. Initially, due to the lower rate of softening, a significant change in the pressure drop is not observed. However, once the ferrous raw material bed shrinks substantially (Fig. 7.10), the passage for the gas flow starts to get blocked. This is observed by a gradual rise in the pressure drop at the bed softening temperature T_s. Then, ferrous burden melts (T_m) and starts to drain out of bed. Consequently, the pressure drop recovers back to the P_{Base} value at dripping (T_d) temperature.

Considering the high-pressure drop regime spread between the T_s and T_d temperature, it is expected that this temperature range will be close to the real cohesive zone in the blast furnace. The softening temperature increases and the dripping temperature decreases with the nut coke mixing with the ferrous burden (Fig. 7.20). Thus, the difference between the T_d and T_s temperature is decreased by 77 °C (165 °C to 88 °C) upon 40 wt% nut coke addition in the ferrous bed (Fig. 7.19). Due to the non-linear relationship of T_s and T_d temperatures with the nut coke addition, a similar relationship is also found between the cohesive zone temperature range and added nut coke content (Fig. 7.19). Increased gas permeability and higher iron carburisation are the principal reasons, which narrows the cohesive zone temperature range.

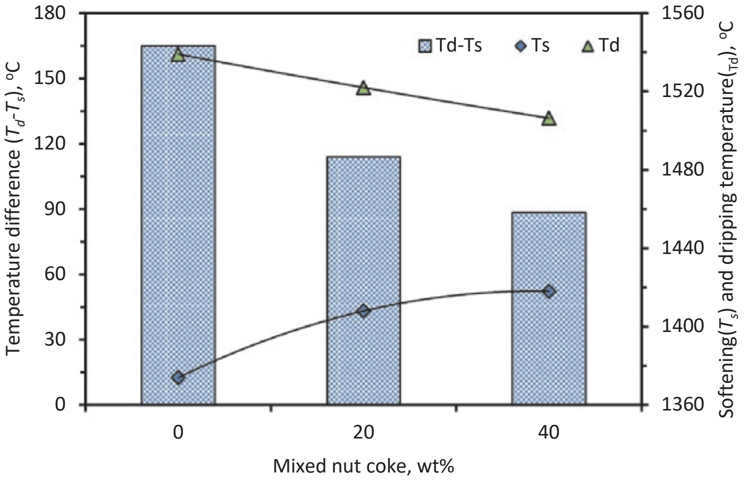

Fig. 7.20 Effect of nut coke addition on cohesive zone temperature range (T_s to T_d).

7.3.9 Effect of nut coke addition on iron carburisation

The melting temperature of the iron-carbon alloys decreases with the increase in the carbon concentration (for C < 4.3%) [35]. In the experiments under simulated blast furnace conditions, the freshly reduced iron gets carburised by CO gas [2] and mixed nut coke present in close vicinity [37]. Now, melting occurs in the bed based on the carburisation achieved on the freshly reduced iron. In the ferrous burden mixed with nut coke, iron carburisation is expected to be higher due to the increased gas permeability and presence of carbon (nut coke) inside the bed. Consequently, the melting temperature (T_2) of the ferrous burden decreases with the increase in nut coke addition.

It is usually considered that various reactions that occur in the blast furnace are close to the equilibrium [2]. Thus, the liquidus and solidus carbon content at the start of melting can be estimated from the iron-carbon equilibrium diagram. Under the assumption that T_2 is the ferrous burden melting point, the equilibrium liquidus and solidus carbon concentration are estimated using Factsage 7.0 (Fig. 7.21). When 40 wt% nut coke is added, an increase in the liquidus carbon content by 1.26 wt% (0.40 wt%C to 1.66 wt%C) is estimated. Similarly, the solidus carbon content is estimated to increase by of 0.51 wt%C (0.07 wt%C to 0.58 wt%C) upon 40 wt% nut coke addition in the ferrous bed. At the start of ferrous burden melting, to have sufficient fluidity for the deformation and liquid flow, the carbon content is expected to be close to the liquidus concentration instead of solidus concentration.

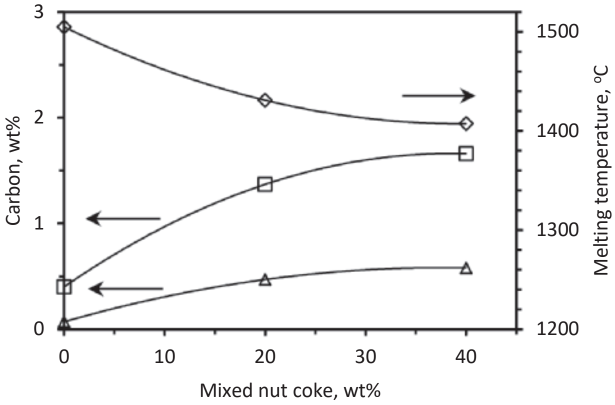

Fig. 7.21 Effect of nut coke addition on liquidus and solidus carbon concentration (estimated).

Table 7.2. Relationship summary on the effect of nut coke addition on the ferrous bed characteristics.

Parameters	**Unit**	**Relationship**	**Equation** **x = nut coke concentration (wt%)**	R^2
Stage 1 temperature (T_1)	°C	non-linear	$0.0019x^2 + 0.068x + 1157.5$	1.00
Stage 1 displacement (D_1)	%	non-linear	$-0.0015x^2 + 0.1071x - 11.991$	1.00
Stage 2 temperature (T_2)	°C	non-linear	$0.0635x^2 - 4.9949x + 1505.5$	1.00
Stage 2 displacement (D_2)	%	non-linear	$-0.0216x^2 + 1{,}9924x - 81.499$	1.00
Stage 3 temperature (T_3)	°C	non-linear	$0.0113x^2 - 0.725x + 1550$	1.00
Stage 3 displacement (D_3)	%	non-linear	$-0{,}0155x^2 + 1.43x - 105$	1.00
Bed melting temperature (T_m)	°C	non-linear	$0.0521x^2 - 3.4425x + 1505$	1.00
Flooding temperature (T_s)	°C	non-linear	$-0.03x^2 + 2.3x + 1374$	1.00
Dripping temperature (T_d)	°C	non-linear	$0.0017x^2 - 0.885x + 1539$	1.00
Dripping temperature (T_{xf})	°C	non-linear	$0.0012x^2 - 0.7566x + 1528.1$	1.00
(T_m-T_2)	°C	non-linear	$-0.0107x^2 + 1.515x - 1E-14$	1.00
(T_d-T_s)	°C	non-linear	$12.7x^2 - 89.1x + 241.4$	1.00
Permeability resistance during softening (S_p)	Pa.°C	exponential	$117e^{-0{\cdot}064x}$	0.97
Permeability resistance (S-value)	Pa.°C	exponential	$177.37e^{-0{\cdot}04x}$	1.00

Based on the series of experiments under simulated blast furnace conditions, the effect of nut coke addition on various process parameters is studied in detail. As discussed earlier, a non-linear relationship is found for various key temperatures and displacement with the nut coke addition. Interestingly, gas permeability (P_{Peak} and S-value) is improved drastically with the nut coke addition. The key relationships are summarised in Table 7.2.

For all the characteristic temperature and the displacement range, a non-linear relationship is found with the nut coke addition. This relationship is governed by the chemical function of coke (nut coke), which is utilised for the reduction of the ferrous burden (iron oxide) and iron carburisation. For the given iron oxide content, with an increase in mixed nut coke, the demand for reducing and carburising agent decreases. Additionally, the nut coke particle arrangement around the ferrous burden has an effect on the physicochemical properties of the bed. Once the ferrous raw material particle (pellet or sinter) is surrounded by one layer of nut coke, the second layer of nut coke around the ferrous particle will have a limited effect on the bed characteristics.

7.3.10 Morphology studies of the ferrous bed (pellet and sinter mixture)

7.3.10.1 Ferrous bed quenching

As discussed earlier, the permeability and cohesive zone properties improve with nut coke addition in the ferrous raw material bed. In order to understand and visualise the prime reason for such improvement, ferrous beds are quenched at the start of bed melting. The ferrous bed with (40 wt%) and without mixed nut coke are quenched at 1445 °C and 1505 °C, respectively, according to Fig. 7.22.

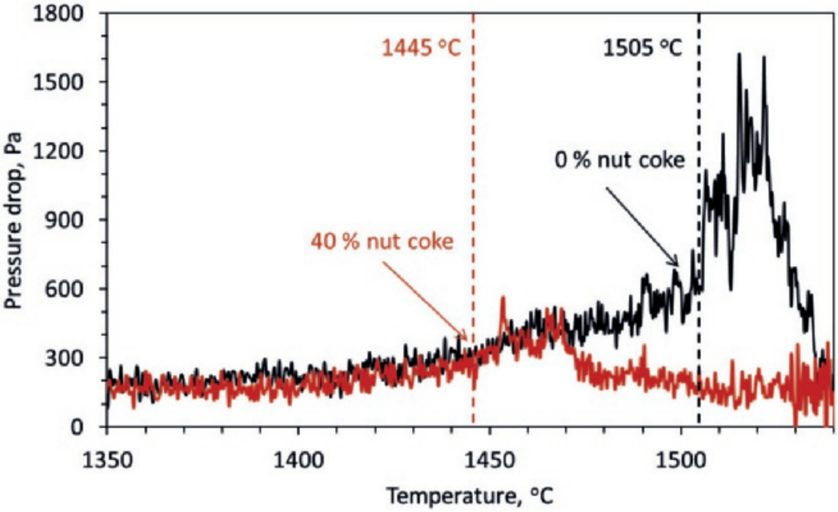

Fig. 7.22 Pressure drop profiles and identified quenching temperatures for the ferrous bed with 40 wt% nut coke (1445 °C) and without mixed nut coke (1505 °C).

7.3.10.2 Ferrous bed in the absence of nut coke

Photographs of the ferrous bed quenched at 1505 °C, just at the start of the bed melting, are shown in Fig. 7.23. A high degree of compaction achieved on the ferrous bed can be seen from the bed. The deformed first layer of the ferrous burden is apparent (Fig. 7.23). The ferrous burden present in other layers is solid and able to hold their shape. The iron ore sinter occupied the interstitial space around the pellets to close the inter-pellet voids. Additionally, close contacts among the sinter and pellets are observed (Fig. 7.23). Furthermore, no macroscopic melting is witnessed in the quenched bed.

Sections (region A and B) of the quenched bed are selected to visualise the internal state of the ferrous burden (Fig. 7.23 and Fig. 7.24). A sintered structure of the ferrous raw material is investigated under the microscope. Close contact among the ferrous burden can be seen in Figure 7.24. A clear interface is observed between the sinter and pellet (Fig. 7.25).

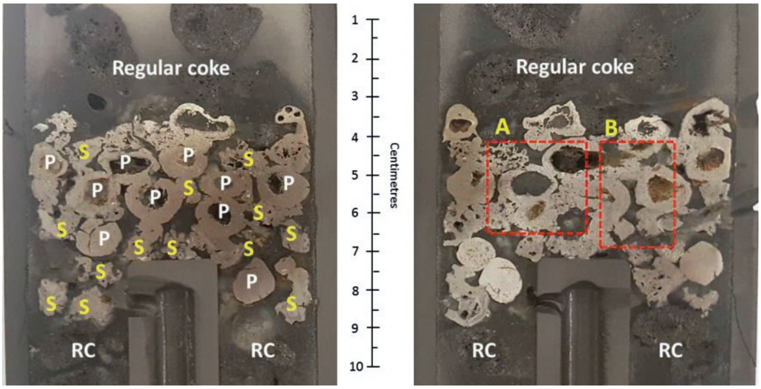

Fig. 7.23 Two halves of the sample bed without nut coke quenched at 1505 °C (P-Pellet, S-Sinter, RC- Regular coke).

To investigate the extent of interaction between the pellet and sinter, an SEM-EDS analysis is performed at a selected interface (Fig. 7.26). A clear difference in the present phases between the sinter and pellet is observed (Fig. 7.25d and 7.26). In the pellet region, along with the dense reduced iron layer, a slag rich in magnesium and silicon (olivine-type slag) is observed. And in the sinter region, dispersed iron nuclei in calcium and silicon rich slag matrix can be seen. These indicate that the interaction between the sinter and pellet is limited to the surface region only. No bulk melting and intermixing between the sinter and pellet is observed till the bed melting temperature (1505 °C). However, the surface pores of the sinter and pellets are blocked by slag. The close contact and sintering among the ferrous burden prevents the slag to flow away from the interface and limit the interaction close to the surface region only [11].

As discussed in Chapter 6, in the pellet bed without nut coke layer-wise melting occurs. Similarly, in the quenched ferrous burden bed, the iron ore pellet burden present in the top layer are observed to be significantly deformed (Fig. 7.23). However, due to the heterogeneous shape of sinter particles, the deformation is not apparent. Nevertheless, similar to the pellet-only burden, in the ferrous burden without nut coke, layer-wise carburisation and melting are also expected to occur.

Additionally, the melting of the pellets is faster compared to the sinter burden (Fig. 7.8). As discussed earlier, the pellets are low in impurities and flux content. Thus, the melting and dripping of the pellets are controlled by the pellet shell (iron) carburisation. However, the sinters are rich in gangue (SiO_2 and Al_2O_3) and flux (CaO and MgO) contents (Table 3.1). Among these, the melting of the CaO rich oxides is known to occur at higher temperatures [29]. Thus, when the melting of reduced iron in sinter starts, the flow of liquid is restricted by the presence of solid slag forming mineral particles. Consequently, the melting rate of sinter is retarded. Thus, when ferrous burden (sinter and pellet) are mixed together, melting and dripping behaviour is controlled by sinter present in the bed.

The top regular coke layer carburises and melts the first layer of ferrous burden. Then the regular coke moves to the second layer of ferrous burden to carburise and melt thereafter. The presence of sinter in the ferrous bed retards the overall melting rate of the burden. Consequently, the melting phenomena proceed with a slower rate than compared with the pellet-only case (Fig. 7.8). Additionally, at the end of the experiment, some non-dripped material (NDM) is left inside the crucible due to its high melting point.

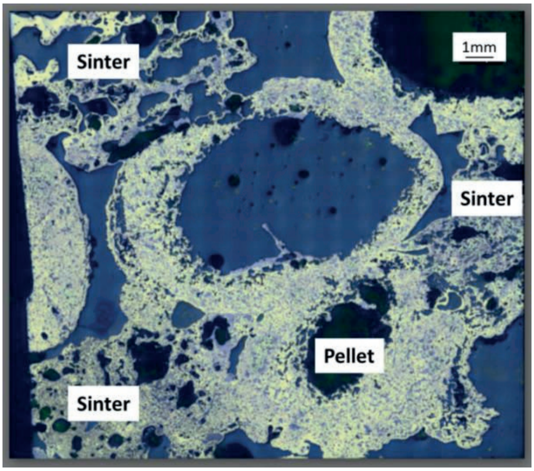

Fig. 7.24 Selected section (region A) from the ferrous bed quenched at 1505 °C without nut coke (Fig. 7.23).

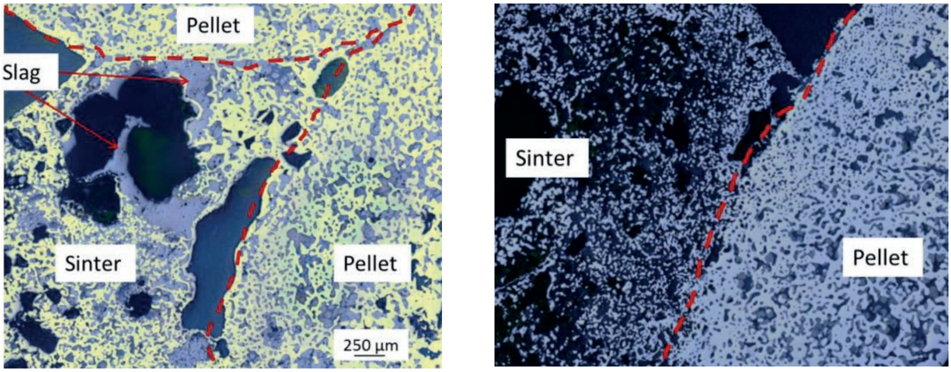

(a) Optical micrograph of an interface between sinter and pellet, from region A (Fig. 7.23)

(b) Optical micrograph of an interface between sinter and pellet from region B (Fig. 7.23)

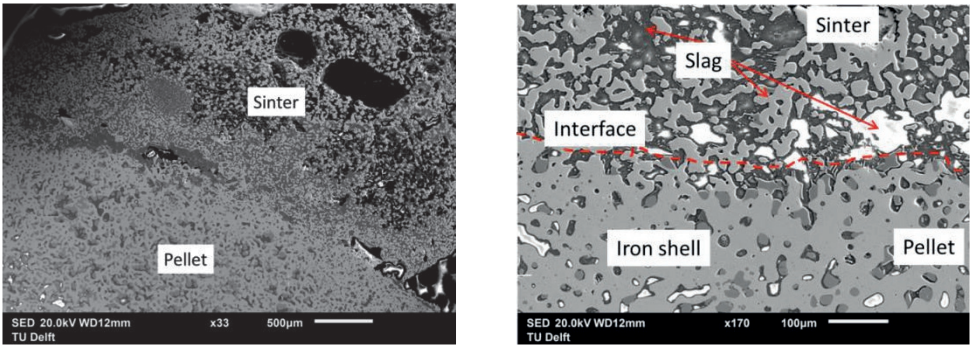

(c) SEM-EDS of pellet sinter interface, from region B (Fig. 7.23)

(d) Close up of SEM-EDS of pellet sinter interface, from region B (Fig. 7.23)

Fig. 7.25 SEM-EDS micrograph of an interface between pellet and sinter.

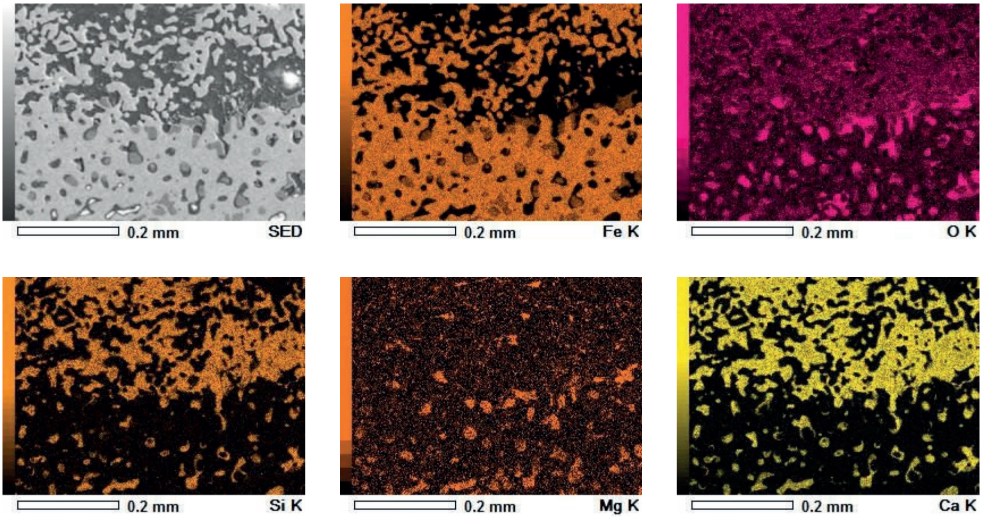

Fig. 7.26 SEM-EDS elemental scan at the pellet-sinter interface (Fig. 7.25d).

7.3.10.3 Ferrous bed mixed with nut coke

The ferrous sample bed mixed with 40 wt% nut coke is quenched close to the bed melting temperature (1445 ^{o}C). The photograph of the quenched sample bed is shown in Figure 7.27. It is evident from the photograph that the nut coke acted as a frame to provide support to the ferrous bed. Additionally, the nut coke hindered the contact among the sinter and pellets to avoid the tight packing of the bed due to sintering and softening of the ferrous burden. Consequently, the pores and the voids are open for reducing gases to reach the unreduced regions in the ferrous bed.

Inside the bed, the presence of a thicker rim of the metallic shell on the pellets and sinter, clearly indicates that a higher degree of reduction is attained on the ferrous burden under nut coke mixed charge conditions. However, a few particles of sinter are found hollow on the top layer of the ferrous raw material bed. Sinter segregation could result in a lower degree of reduction.

To examine the effect of nut coke on the ferrous raw materials, representative samples located close to the nut coke are selected from the quenched bed (Fig. 7.27). The SEM-EDS analysis is performed on these samples. In the sinter sample located close to the nut coke, nuclei of the iron can be seen on the surface (Fig. 7.28). The nuclei are lean in slag content compared to the rest of the sinter (Fig. 7.28b). This nucleus is about to melt and drop out of the sinter. This is a typical pattern of sinter melting; the reduced iron-rich region coalesces to form an iron nucleus, which will melt based on the carburisation level and attained temperature. At another location on the same sinter particle, due to the higher reduction achieved on the surface, the slag is pushed inside the sinter (Fig. 7.27c). This restricts the sinter slag to get in contact with the pellet surface pores to limit the reduction reactions.

On the pellet close to the nut coke, a metal-rich shell and core are obtained (Fig. 7.27). These are due to the higher degree of reduction achieved in the interior of the pellet. Similarly, in another sample piece, the sintering among the ferrous burden is avoided by the presence of the nut coke (Fig. 7.28a). The reduced sinter and pellet shell can be seen in the micrograph (Fig. 7.28). The nut coke added inside the bed is clearly seen to restrict the direct contact among the ferrous burden. The nut coke acted as a barrier to stop the slag from filling up the pores of other ferrous burdens. Additionally, the carbon (nut coke) placed in close vicinity of the ferrous burden provides reducing gas for higher reduction of the burden. Thus, the gas diffusion and chemical reaction are enhanced in the presence of nut coke in the bed [32]. Moreover, due to the direct contact of ferrous burden with nut coke, the higher degree of iron carburisation occurs. Thus, the melting of the ferrous bed occurs simultaneously in the nut coke mixed ferrous bed.

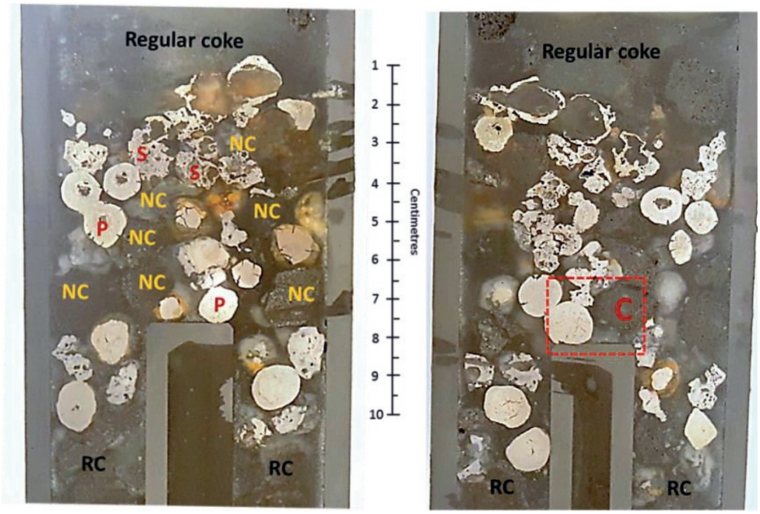

* NC- Nut Coke

Fig. 7.27 Two halves of the sample bed with nut coke (40 wt%) quenched at 1445 ^{o}C (P-Pellet, NC – Nut Coke).

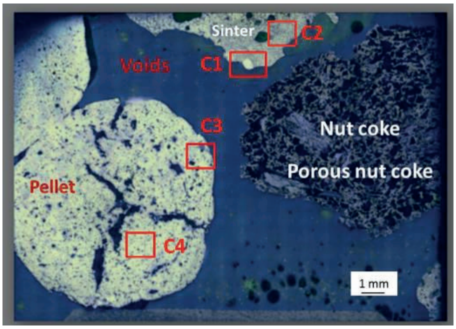

(a) Optical micrograph of region C from the quenched ferrous bed (from Fig. 7.27)

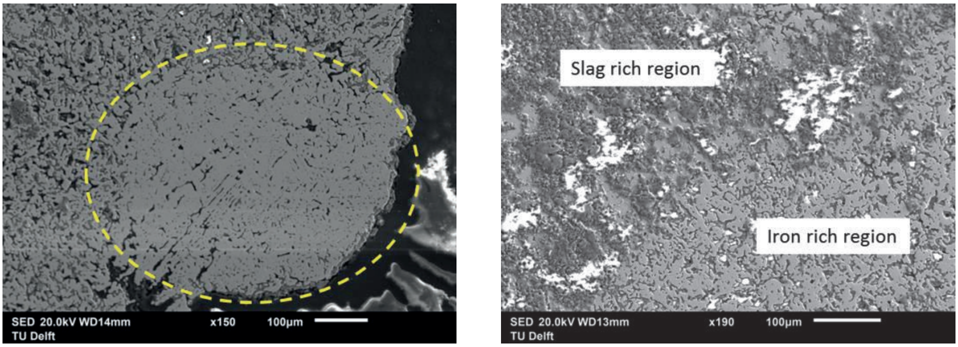

(b) Region C1 on the sinter surface (SEM)

(c). Region C2 in the interior of the sinter (SEM)

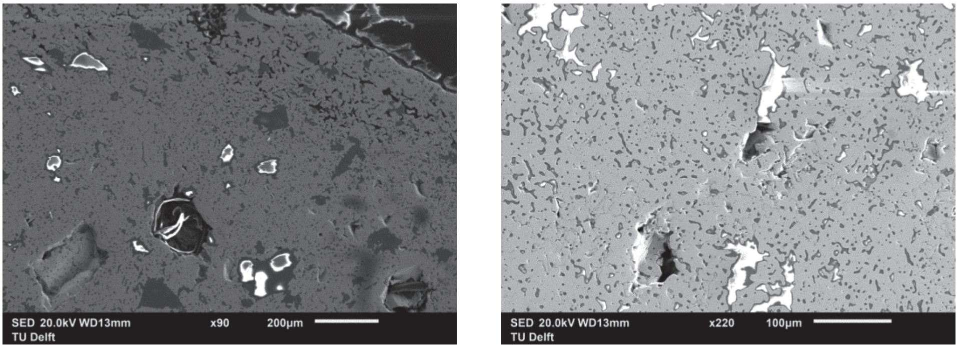

(d) Region C3 on the pellet surface (SEM)

(e) Region C4 on the pellet core (SEM)

Fig. 7.28 Micrograph of the ferrous burden mixed with (40 wt%) nut coke.

7.3.11 Effect on first liquid drop temperature (T_{xf})

The liquid drips out of the sample crucible and gets collected at the cups located in the sample receiver (Fig. 3.8). The time and the temperature (T_{xf}) of the first liquid drop are marked after visualising the event from the glass window located at the receiver (Fig. 3.8). The liquid is observed to drip in the form of rivulets. The inconsistency in liquid dripping could also be a result of the liquid (slag and metal) and solid coke interaction (Fig. 6.9) [26,38]. For example, the liquid iron turns from wetting (50^o for 0 wt%C) to non-wetting (130^o for 5 wt%C) with an increase in the carbon concentration [38].

In the examined cases of ferrous burden, the temperature T_{xf} decreases with nut coke addition (Fig. 7.29). The nut coke enhances the degree of iron carburisation to lower the melting point [35] of the reduced iron [19]. The temperature T_{xf} is witnessed to decrease by 29 ^oC (1528 ^oC to 1499 ^oC) upon 40 wt% nut coke addition in ferrous bed.

Additionally, the presence of a thinner regular coke layer in the case of nut coke mixed ferrous burden supports the earlier dripping of liquid from the bed. Once the liquid drop is formed in the bed, then while crossing the thinner regular coke layer, the probability of liquid hold up is low. As a result, the first liquid drop appearance temperature (T_{xf}) will decrease with nut coke addition in the ferrous bed.

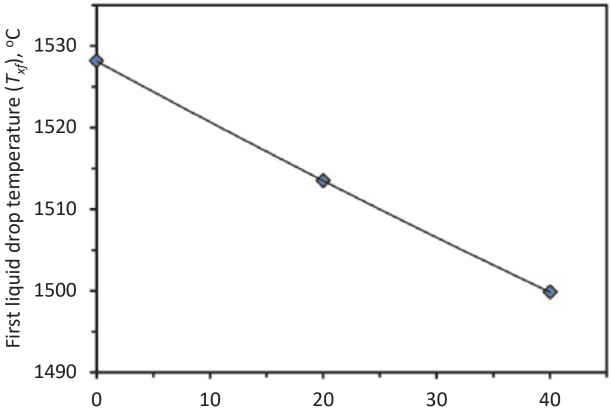

Fig. 7.29 Effect of nut coke addition on the first liquid drop temperature (T_{xf}).

7.3.12 Coke consumption

The mass of the coke before and after the experiment is measured to calculate the amount of the coke utilised. No clear trend in the total coke utilisation is observed, which might be a result of the irregular shape (surface area) and stochastic nature [39] of liquid interaction with the coke. Moreover, a slight increase in total coke consumption is observed with nut coke mixing in the ferrous raw material. The gas permeability is increased by the nut coke mixing in the bed (Fig. 7.16 and Fig. 7.18). Consequently, the kinetics of the reduction and iron carburisation is increased, which can increase the total coke utilisation in the bed.

This is contrary to the pellet-only burden, in which the total coke consumption is decreased with the nut coke addition. This is due to the low interaction of the liquid with the nut coke. The formed liquid drained out quickly after passing the thinner regular coke layer. However, in the case of ferrous burden (pellet and sinter) mixed with nut coke, a higher interaction between the coke and liquid occurs to result in high coke consumption. This is also evident with the increase in nut coke replacement ratio, the degree of reduction increases (Fig. 7.30).

Nevertheless, the nut coke is able to utilise in place of the regular coke (Fig. 7.30). Very importantly, the weight (%) of the regular coke consumed is observed to decrease with the nut coke addition in the ferrous raw materials bed. This indicates that the nut coke is preferentially utilised to fulfil the chemical functions (reductant and iron carburiser) of the coke in the blast furnace conditions. Thus, the regular coke will be able to retain its big particle size due to its lower utilisation, which when reaching the blast furnace hearth will support the liquid permeability.

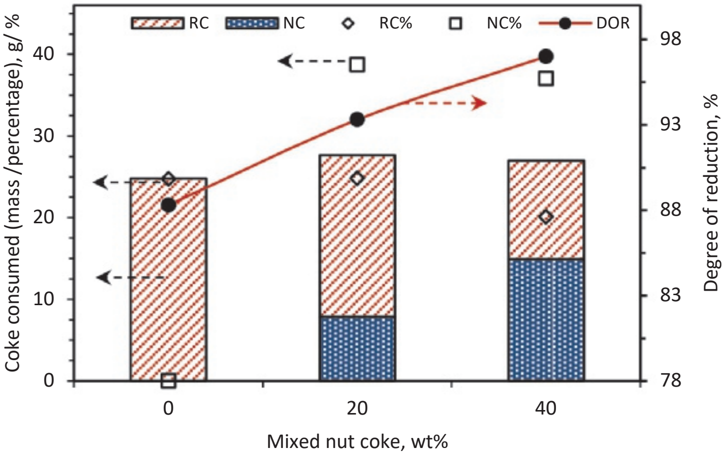

Fig. 7.30 Coke utilisation and degree of reduction in smelting experiments.

7.3.13 Drip liquid chemistry

In the blast furnace, the liquid drips out of the cohesive zone to flow through the active coke zone. While the melts flow over the coke, many vital reactions occur, such as the direct reduction of FeO-rich slag, liquid iron carburisation [12], sulphur and silicon transfer [2]. Furthermore, the dripping pattern of the liquid is also strongly linked to the gas intake capacity and therefore, to the productivity of the blast furnace [2].

On the one hand, nut coke enhances the iron and carbon (coke) contact in the bed. On the other hand, the regular coke layer gets thinned, as the nut coke is added as the replacement of the regular coke. This might affect liquid interaction, hold-up and dripping characteristics. Therefore, it is important to understand the effect of nut coke addition on the chemistry of the dripped liquid (metal and slag).

7.3.13.1 Effect of nut coke addition on liquid iron carburisation

The carbon content in the dripped iron increases by 0.71 wt% (from 2.78 to 3.49 wt%) upon 40 wt% nut coke addition in the ferrous bed (Fig. 7.31). As discussed before, the liquid iron is carburised during its flow over the coke bed [28]. In spite of thinner regular coke layer present in the case of nut coke mixed ferrous burden, the carbon content in the dripped iron is observed to be higher than the iron produced in the absence of nut coke.

This is contrary to the case for the pellet-only burden (Fig. 6.13). In the case of the pure pellet burden, the rate of the third stage (Fig. 7.8) of the bed contraction is high. Consequently, once the melting and dripping start, the liquid passes through the regular coke bed quickly and is carburised in a relatively short time [28]. As a result, the liquid iron carburisation is controlled by the regular coke layer thickness. Therefore, for the pellet-only bed, the carbon content in the liquid dripped iron is observed to decrease with the nut coke addition.

However, in the case of sinter and pellet mixed ferrous burden, the third stage of contraction is gradual (Fig. 7.8). The presence of sinter in the ferrous burden slows down the melting and dripping of liquid from the bed. Thus, the reduced iron stays in the bed for a longer time to interact with the nut coke. Thus, in the case of nut coke mixed ferrous burden, the presence of carbon (nut coke) in contact with the liquid iron enhances the iron carburisation.

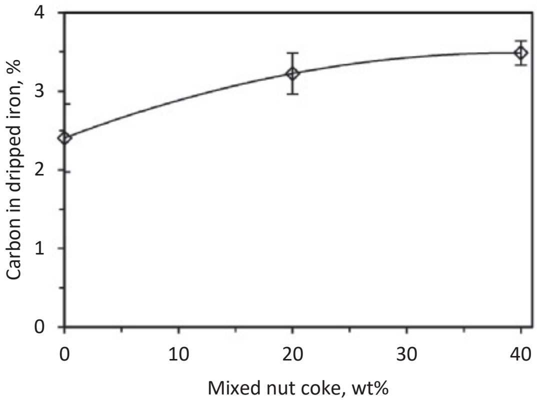

Fig. 7.31 Effect of nut coke addition on carbon in the dripped metal.

7.3.13.2 Dripped slag chemistry

Dripped slag chemistry is shown in Table 7.3. The FeO content in the dripped slag for all examined cases is noticeably very low (0.8 to 1.8 wt%). No apparent effect of nut coke addition on the slag FeO content is observed. This might be a result of the stochastic nature of liquid dripping, which varies the solid-liquid interaction in the bed [12, 40-41]. The FeO content in the dripped slag is observed to be lower than that of the pellet only case (Fig. 7.8). This is due to the presence of sinter in the ferrous burden, which retards the rate of melting and dripping. As a result, high interaction between the coke and ferrous material occurs at the time of melting and dripping (stage 3) (Fig. 7.8).

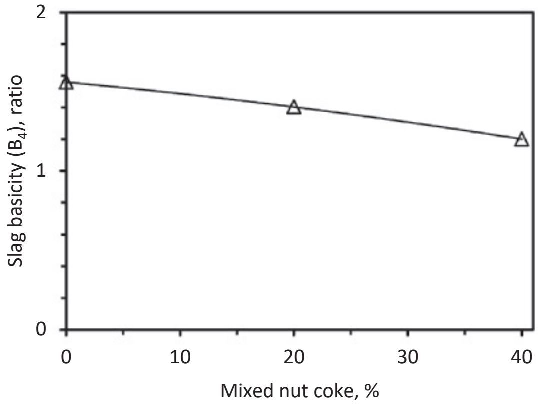

Fig. 7.32 Effect of nut coke on dripped slag basicity.

Table 7.3. Dripped slag chemistry.

NC	FeO, %	CaO, %	MgO, %	SiO_2,%	Al_2O_3,%	B_2, ratio	B_3, ratio	B_4, ratio
0	1.1	45.6	10.7	28.9	7.2	1.6	1.9	1.6
20	0.8	43.9	11.1	31.9	7.2	1.4	1.7	1.4
40	1.8	38.7	11.9	34.2	7.9	1.1	1.5	1.2

A decrease in the dripped slag basicity [B_4= (CaO + MgO)/(SiO_2 + Al_2O_3)] is observed with the nut coke addition. This occurs due to the increase in silica and alumina content of the slag. As the total coke utilisation is increased with the nut coke addition (Fig. 7.30), this can increase the coke ash (SiO_2 and Al_2O_3) content in the slag which decreases the slag basicity.

However, for certainty, this needs to be checked with total slag (dripped and non-dripped) and metal collected from the experiments.

The non-dripped material (NDM) is collected after the experiments from inside the crucible. A very high basicity (Table 7.4) is the reason for the non-dripping nature of this slag forming minerals, which has a high liquidus temperature [26,28-29]. Consequently, these minerals are not able to melt and flow out of bed. The NDM from the ferrous bed without nut coke is observed to be high in silica. However, no apparent effect of nut coke addition is observed on the non-dripped slag chemistry. A typical XRD of the non-dripped material is shown in Figure 7.33.

Table 7.4. Non dripped material (NDM) chemistry.

NC, wt%	FeO, wt%	CaO, wt%	MgO, wt%	SiO_2, wt%	Al_2O_3, wt%	B_2, C/S ratio	B_3(C+M)/S ratio	B_4 (C+M)/(S+A) ratio
0	1.21	50.03	11.38	29.39	5.31	1.70	2.09	1.77
20	0.92	56.79	6.1	26.87	6.99	2.11	2.34	1.86
40	0.93	56.66	6.02	26.6	7.35	2.13	2.36	1.85

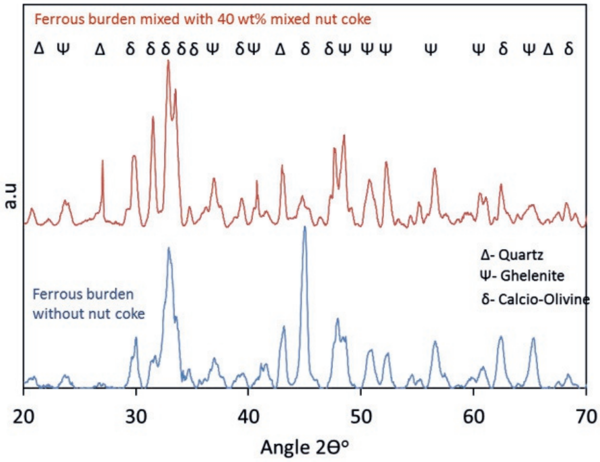

Fig. 7.33 X-ray diffraction pattern of the non-dripped slag.

7.3.14 Gas profile

A typical profile of the evolved gases during the smelting of the ferrous burden under simulated blast furnace conditions is shown in Figure 7.34. A significant difference between the gas inlet and outlet chemistry clearly indicates that a strong interaction between the gas and sample occurs during the experiment. It can be seen that CO_2 gas measured in the outlet is always observed to be higher than in the inlet. Conversely, the CO gas in the outlet profile is observed to be lower than the inlet profile, below 1450 ^{o}C. In the high temperature range (> 1450 ^{o}C), a regime of high CO gas concentration is marked in the outlet profile, which falls inside the third stage (melting and dripping stage) of the bed contraction (Fig. 7.8). As a result of melting and dripping of the ferrous raw materials, a direct interaction of the liquid (slag and metal) with the carbon (coke) occurs (5.6 and 5.12). Consequently, a sharp rise in the CO gas concentration is observed. Furthermore, it is apparent from the equilibrium diagram that at high temperature, the CO gas is more stable than the CO_2 gas in the presence of solid carbon due to the Boudouard reaction (Fig. 5.18). Thus the evolved CO gas is not regenerated to the CO_2 gas (reaction 5.6 and 5.12).

Similar to the CO gas, H_2 also interacts with the ferrous sample, participating in reduction reactions. Consequently, evolved water vapour (H_2O) is detected in the gas outlet, which is also observed to vary during the experiment (Fig. 7.34). Possible reactions for bringing the changes in the outlet gas chemistry are discussed in section 5.6.2.1.

The ferrous raw materials (iron oxides) interact with the reducing gas to form metallic iron. As a result, the oxygen present in the ferrous raw materials evolves in the form of CO, CO_2 and H_2O gas. These off-gas chemistry profiles are later analysed to determine the degree of reduction of ferrous raw materials and carbon utilisation during the experiment.

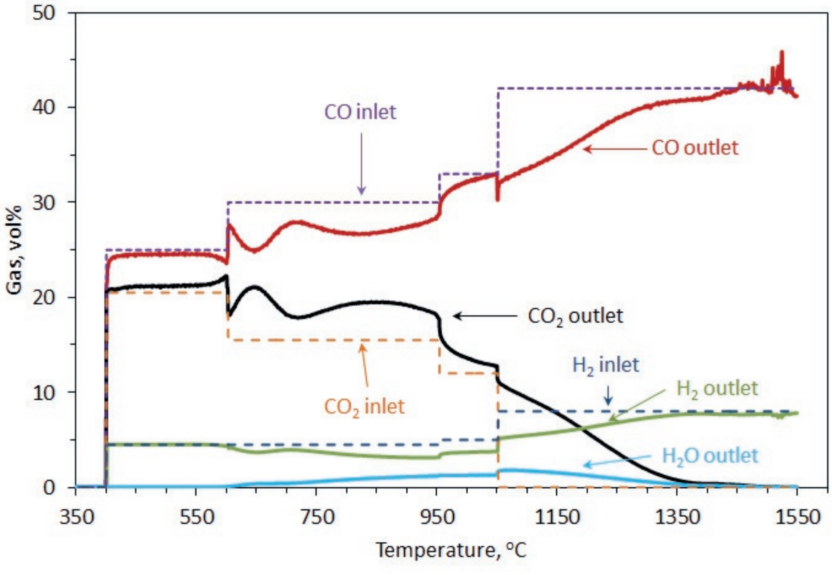

Fig. 7.34 A typical gas inlet and outlet profile during the experiments in RSM.

7.3.14.1 Effect of nut coke addition on evolved gas chemistry

The nut coke, being carbonaceous material actively involves in the reduction and carburisation reactions of the ferrous raw materials (iron oxide), which affects the off-gas composition. Furthermore, when nut coke is added as a replacement of the regular coke, the off-gas chemistry might also be affected by the thinning of the regular coke layers. Figure 7.35 shows a comparison of the evolved gas profiles during the experiments for the ferrous raw material bed without and with (40 wt%) mixed nut coke (as a replacement of the regular coke). For a given gas inlet profile, the difference in the off-gas composition is observed between the sample bed with and without mixed nut coke. In spite of having thinner regular coke layer (top layer) for regeneration of the evolved CO_2 gas, in the high temperature range (>1200 ^{o}C), a regime of accelerated CO gas evolution is apparent. This is generated due to the presence of nut coke in the ferrous bed, which actively participate in the reduction and regeneration of CO by Boudouard reaction (5.1). Furthermore, the CO_2 off-gas profile is also affected due to the nut coke participation in the carburisation of the freshly reduced iron (reaction 5.11). However, the two cases are very close to each other for the major part of the process.

In order to quantify the effect of nut coke addition on the degree of reduction (DOR) and the carbon utilisation, these off-gas profiles are further analysed.

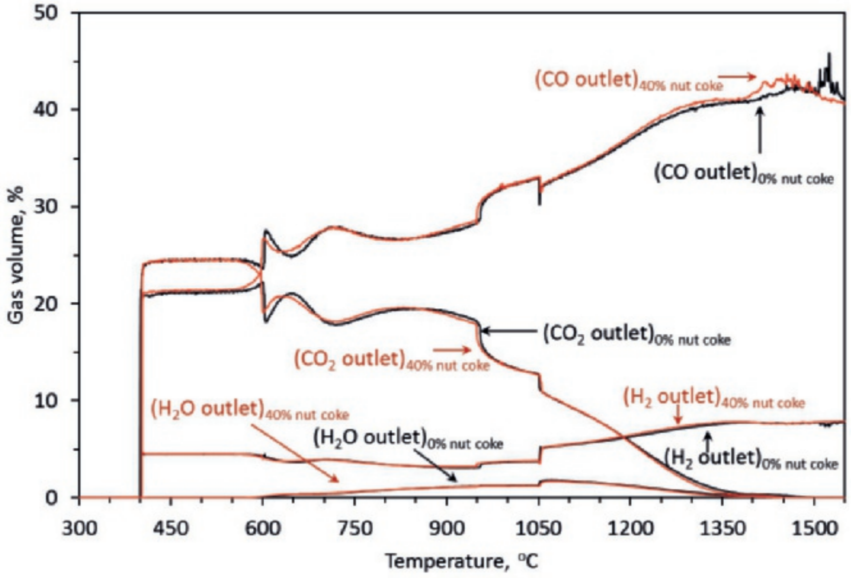

Fig. 7.35 Effect of nut coke (40 wt%, replacement of regular coke) addition on the gas outlet profile.

7.3.14.2 Degree of reduction

The degree of reduction (DOR) is estimated by the loss of oxygen to the original oxygen present in the ferrous raw materials (equation 3.1). The DOR profile for the ferrous burden (pellet and sinter mixture) under simulated blast furnace conditions is shown in Figure 7.36. It should be noted that the reduction takes place under non-isothermal conditions. Several shifts in the slope of the DOR curve are observed, which is due to the change in the heating rate at different temperature intervals (Table 3.4), which affects the reduction kinetics of the ferrous burden.

However, an apparent increase in the DOR is observed with the increase in temperature from 400 ^{o}C to 1250 ^{o}C for the ferrous bed without mixed nut coke. The ferrous raw materials are reduced topo-chemically to form a metallic shell on the surface. Now, as a result of sintering of iron, it becomes difficult for the reducing gas to reach the interior of the ferrous burden (pellets and sinter). Consequently, a regime of sluggish DOR appears from 1250 ^{o}C – 1500 ^{o}C. Then, with the increase in the temperature (above 1500 ^{o}C), a drastic increase in the DOR is observed as a result of melting in the bed. As a result of melting, the FeO-rich slag gets in contact with the carbon (coke) for direct reduction (5.6). The final reduction degree of the ferrous burden (88 %) is observed lower than that of the pellet-only case (93 %) (Fig. 5.20 and Fig. 7.36). This is primarily due to the presence of sinter in the ferrous bed mixture (40 wt%), which has lower reducibility than pellets due to the dense structure (low pore density).

Effect of nut coke addition (20 wt% and 40 wt%) on the degree of reduction (DOR) is shown in Figure 7.36. A higher DOR is observed for the sample bed mixed with nut coke. Furthermore, an accelerated rate (slope) of DOR is apparent for the sample bed mixed with nut coke in the temperature range from 450 ^{o}C to 1550 ^{o}C. The improved gas permeability (Fig. 7.16) in the presence of nut coke enhances the reduction kinetics of the ferrous raw materials. The nut coke supports the bed structure to limit the sintering among the ferrous raw materials [22]. Consequently, the pores are open to reducing gases to reach the interior of the ferrous raw material. Thus, an accelerated rate of reduction is noticed in the high temperature regime for ferrous bed mixed with the nut coke (Fig. 7.36). Additionally, the reaction product of iron oxide reduction, i.e. CO_2, is regenerated by its reaction with nut coke in the mixed bed. Thus, the reduction potential of the gas is enhanced in the presence of nut coke in the bed.

However, in the absence of nut coke, evolved CO_2 gas might not be able to regenerate as CO gas inside the ferrous bed. Thus, while passing across the top regular coke layer, this CO_2 rich gas is regenerated. Now, in spite of the thicker regular coke layer for the sample bed without nut coke, a comparatively lower CO concentration in the off-gas profile is observed, especially in the high temperature range from 800 ^{o}C to 1500 ^{o}C (Fig. 7.35). This indicates an accelerated rate of iron oxide reduction and CO_2 regeneration occurs in the presence of nut coke in the ferrous raw material bed. In the absence of nut coke, iron present in the ferrous raw material periphery sinters to form a dense shell, which is difficult for the reducing gas to penetrate. Thus, the reduction reaction in the absence of nut coke is diffusion-controlled [16].

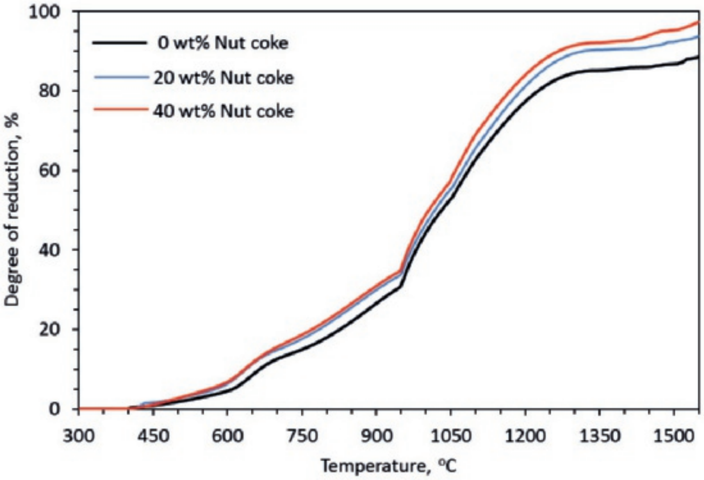

Fig. 7.36 Effect of nut coke addition on an estimated degree of reduction (DOR).

7.3.13.3 Carbon utilisation

The carbon utilised or consumed during the experiment is estimated by mass carbon balance between the gas inlet and outlet (3.5). Accumulated mass of carbon lost from the sample bed during the experiment is shown in Figure 7.37. Similar to the DOR, several shifts in the curve for carbon loss (utilised) is apparent due to the change in heating rate, which changes the reaction kinetics (Table 3.4). Nevertheless, an increase in carbon consumption is noticed with an increase in temperature (Fig. 7.37).

Effect of nut coke (20 wt% and 40 wt%) addition on the carbon utilisation is shown in Figure 7.37. A higher degree of carbon utilisation is noticed with the increase in the nut coke addition in the ferrous raw material bed. In the temperature range from 500 °C to 1550 °C, an accelerated rate of carbon consumption is observed (Fig. 7.37). The presence of carbon in the form of nut coke in the ferrous raw material bed accelerates the kinetics of the reduction reactions. Thus, carbon (nut coke) utilisation is enhanced by the Boudouard (5.1), water gas reaction (5.10) and by direct reduction of the FeO-rich slag (5.6). Furthermore, before the bulk melting in the bed, the coke is also consumed in the carburisation (solid-state) of iron present as the metallic shell [19]. Since the CO_2 gas evolves during this carburisation reaction, it is accounted for in the carbon loss estimated by the gas analysis. It can also be clearly seen that nut coke addition leads to a higher total reduction degree, which will consume more carbon or CO gas.

However, the carbon loss due to the liquid state iron carburisation cannot be estimated by the mass balance of carbon between the inlet and evolved gas. The liquid state carburisation occurs once the liquid iron flows over the solid coke particle, which occurs at high temperature (>1400 °C) towards the end of the heating cycle (Table 3.4). Thus, an exact amount of the coke utilised by the liquid state carburisation is difficult to estimate by the gas analysis.

However, an approximation can be made by comparing weight difference between the carbon loss from the gas analysis (Fig. 7.36) and the actual weight of coke loss (Fig. 7.30) from the collected coke after the experiments. It can be seen that compared to the estimated weight loss (gas analysis), more carbon is lost during the experiments (Fig. 7.38). This unaccounted carbon loss is found high for the case of 0 wt% and 20 wt% mixed nut coke ferrous bed. Then it is observed to decrease for 40 wt% mixed nut coke scenario. This trend is in line with the carbon level in the dripped liquid metal from the ferrous bed (Fig. 7.31).

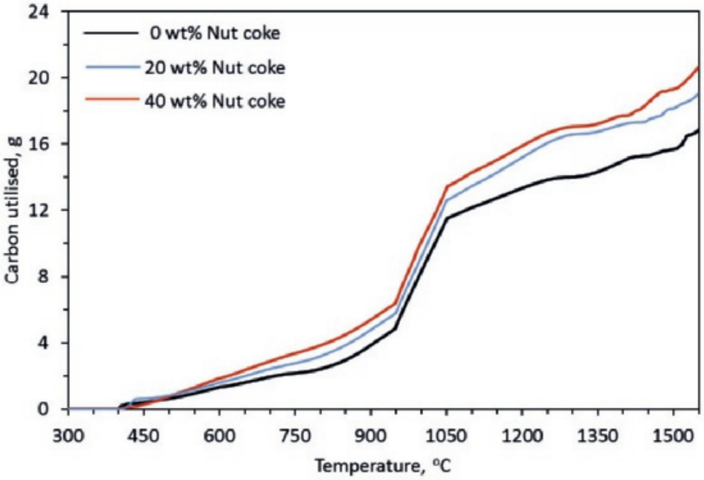

Fig. 7.37 Effect of nut coke addition on the carbon utilisation.

Furthermore, a contrasting difference is observed for the carbon loss for the liquid state carburisation between the pellet bed and ferrous raw material bed. For the ferrous raw material, the carbon level in the dripped iron is found to be higher for the nut coke mixed scenario (Fig. 7.31). Whereas, for the pellet bed, the carbon level in the dripped metal is found to be lower for the nut coke mixed pellet bed (Fig. 6.13). This is primarily due to the presence of sinter in the ferrous raw material bed. The iron ore sinter, melting and dripping is gradual compared to the drastic nature of pellet melting and dripping (Fig. 7.8). Consequently, during the third stage of bed contraction at high temperature, the liquid iron and slag interact strongly with the coke (regular and nut coke) for the case of a ferrous burden to be reduced and carburise thereafter. However, in the case of pellet-only bed, the liquid state carburisation is dependent on the regular coke layer thickness. As a result, with the decrease in the regular coke layer thickness with nut coke addition, the iron carburisation decreases.

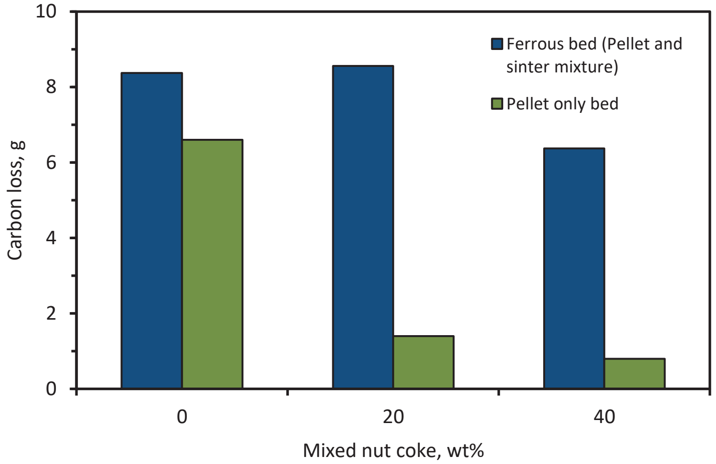

Fig. 7.38 Effect of nut coke addition on the carbon loss due to the liquid state carburisation (calculated).

7.4 Conclusions

The effect of nut coke addition on the ferrous raw material mixture (60% pellet: 40% sinter) bed is studied under simulated blast furnace conditions in the reduction, softening and melting (RSM) apparatus. After a series of smelting and quenching experimental investigations, the following conclusions can be drawn.

1) The contraction of the ferrous raw material mixture bed evolves through three distinct stages. The first stage of bed shrinkage occurs due to the indirect reduction of ferrous burden. The second stage of bed contraction occurs due to the softening and sintering of the ferrous burden. The third stage of bed contraction occurs due to the melting and dripping of the reduced ferrous burden.
   In the ferrous bed, the first and third stage behaviour is controlled by pellet and sinter, respectively. The second stage showed mixed properties of the pellet and sinter.
2) Nut coke mixing with the ferrous burden affects all the three stages of bed shrinkage. The impact of nut coke addition is significant in the second stage. As the nut coke mixing enhances the reduction of ferrous burden and carburisation of freshly reduced iron, the second stage is shortened by 98 ^{o}C for 40 wt% nut coke.

3) In the absence of nut coke, sintering among the ferrous burden (pellet and sinter) is observed to restrict the gas flow, which causes a gradual loss of permeability in the bed. Then, until the start of bed melting (T_m), the interaction between the sinter and pellet is limited to the surface region only. No bulk intermixing and melting is realised.
4) Nut coke physically hinders the contact among the ferrous burden to limit the sintering. Consequently, the bed softening temperature (T_s) increases (44 °C for 40 wt% nut coke) with the nut coke addition.
5) The cohesive zone temperature (T_s to T_d) range is decreased by 77 °C upon 40 wt% nut coke mixing with the ferrous burden.
6) At the time of softening and melting of ferrous burden, the nut coke acted as a frame to provide the pores and voids for the gas flow. An exponential relationship is found between the nut coke addition and an increase in the gas permeability (inverse of S_p and S-value).
7) A simultaneous and layer-wise melting occurs in the ferrous bed with and without mixed nut coke, respectively. The iron carburisation occurs by direct contact with the coke. In the case of nut coke mixed ferrous burden, freshly reduced iron get carburised simultaneously to melt thereafter. However, when nut coke is absent, iron carburisation and melting proceeds layer-wise.
8) Due to the higher iron-carburisation in the presence of nut coke, the melting and dripping of ferrous material starts at low temperature compared to the case when nut coke is absent in the bed.
9) A non-linear relationship is found between the added nut coke replacement ratio and various bed characteristics.
10) In the presence of nut coke due to the enhanced kinetics of reduction reactions and iron carburisation, the degree of reduction (DOR) and carbon utilisation increases.

7.5 References

[1] J.P. Birat, Global technology roadmap for CCS in industry: Steel sectoral report, Amsterdam, 2010.

[2] A.K. Biswas, Principles of blast furnace iron making - theory and practice, Cootha Publishing House, Brisbane, Australia, 1981.

[3] X.W. An, J.S. Wang, R.Z. Lan, Y.H. Han, Q.G. Xue, Softening and melting behavior of mixed burden for oxygen blast furnace, J. Iron Steel Res. Int. 20 (2013) 11–16.

[4] A. Kemppainen, K. Ohno, M. Iljana, O. Mattila, T. Paananen, E. Heikkinen, T. Maeda, K. Kunitomo, T. Fabritius, Softening behaviors of acid and olivine fluxed iron ore pellets in the cohesive zone of a blast furnace, ISIJ Int. 55 (2015) 2039–2046.

[5] P. Kaushik, R.J. Fruehan, Mixed burden softening and melting phenomena in blast furnace operation Part 3 – Mechanism of burden interaction and melt exudation phenomenon, Ironmak. Steelmak. 34 (2007) 10–22.

[6] P. Semberg, C. Andersson, B. Björkman, Interaction between iron oxides and olivine in magnetite pellets during reduction to wüstite at temperatures of 1000 – 1300 °C, ISIJ Int. 53 (2013) 391–398.

[7] C.E. Loo, L.T. Matthews, D.P. O'dea, Lump ore and sinter behaviour during softening and melting, ISIJ Int. 51 (2011) 930–938.

[8] Y.S. Lee, D.J. Min, S.M. Jung, S.H. Yi, Influence of basicity and FeO content on viscosity of blast furnace type slags containing FeO, ISIJ Int. 44 (2004) 1283–1290.

[9] S. Dwarapudi, T.K. Ghosh, A. Shankar, V. Tathavadkar, D. Bhattacharjee, R. Venugopal, Effect of pellet basicity and MgO content on the quality and microstructure of hematite pellets, Int. J. Miner. Process. 99 (2011) 43–53.

[10] P.F. Nogueira, R.J. Fruehan, Blast furnace burden softening and melting phenomena: Part II. Evolution of the structure of the pellets, Metall. Mater. Trans. B. 36 (2005) 583–590.

[11] W.T. Guo, Q.G. Xue, Y.L. Liu, X.F. She, J.S. Wang, Microstructure evolution during softening and melting process in different reduction degrees, Ironmak. Steelmak. 43 (2016) 22–30.

[12] V. Shatokha, O. Velychko, Study of Softening and melting behaviour of iron ore sinter and pellets, High Temp. Mater. Process. 31 (2012) 215–220.

[13] D.J. Gavel, A review on nut coke utilisation in the ironmaking blast furnaces, Mater. Sci. Technol. 33 (2017) 381–387.

[14] E.A. Mousa, A. Babich, D. Senk, Effect of nut coke-sinter mixture on the blast furnace performance, ISIJ Int. 51 (2011) 350–358.

[15] Q. Song, Effect of nut coke on the performance of the ironmaking blast furnace, PhD Thesis, Delft University of Technology, 2013.

[16] E.A. Mousa, D. Senk, A. Babich, Influence of nut coke on iron ore sinter reducibility under simulated blast furnace conditions, Ironmak. Steelmak. 37 (2010) 219–228.

[17] D.J. Gavel, A. Adema, J. van der Stel, J. Sietsma, R. Boom, Y. Yang, Physicochemical behaviour of olivine iron ore pellets mixed with nut coke under simulated blast furnace conditions, Proc. 8th Int. Cong. On Sci. and Tech. of ironmaking (ICSTI), ASMET, Vienna, (2018), 523-529..

[18] Q. Song, Y. Yang, R. Boom, Effect of nut coke on the reduction behavior in iron-making blast furnace, Baosteel Tech. Res. 9 (2015) 8–16.

[19] D.J. Gavel, A. Adema, J. van der Stel, J. Sietsma, R. Boom, Y. Yang, Effect of nut coke addition on physicochemical behaviour of pellet bed in ironmaking blast furnace, ISIJ Int. 59 (2019) 778–786.

[20] J. Sternel, A.K. Lahiri, Contraction and meltdown behaviour of olivine iron ore pellets under simulated blast furnace conditions, Ironmak. Steelmak. 26 (1999) 339–348.

[21] M. Iljana, A. Kemppainen, T. Paananen, O. Mattila, E. Heikkinen, Evaluating the reduction-softening behaviour of blast furnace burden with an advanced test, ISIJ Int. 56 (2016) 1705–1714.

[22] D.J. Gavel, Q. Song, A. Adema, J. van der Stel, J. Sietsma, R. Boom, Y. Yang, Characterization of the burden behaviour of iron ore pellets mixed with nut coke under simulated blast furnace conditions, Ironmak. Steelmak. (2018) 1–8.

[23] J. Ishii, R. Murai, I. Sumi, Y. Yongxiang, R. Boom, Gas permeability in cohesive zone in the ironmaking blast furnace, ISIJ Int. 57 (2017) 1531–1536.

[24] T. Nishimura, K. Higuchi, M. Naito, K. Kunitomo, Evaluation of softening, shrinking and melting reduction behavior of raw materials for blast furnace, ISIJ Int. 51 (2011) 1316–1321.

[25] P.A. Tanskanen, S.M. Huttunen, P.H. Mannila, J.J. Härkki, Experimental simulations of primary slag formation in blast furnace, Ironmak. Steelmak. 29 (2002) 281–286.

[26] M. Hino, T. Nagasaka, A. Katsumata, K. Higuchi, K. Yamaoshi, N. Kon-no, Simulation of primary-slag melting behaviour in the cohesive zone of a blast furnace, considering the effects of Al_2O_3, FeO and basicity in the sinter ore, Metall. Mater. Trans. B. 30B (1999) 671–683.

[27] D. Gross, Fatigue design and safety factor for scroll compressor wraps, Woodhead Publishing Limited, 2013.

[28] V. Shatokha, O. Velychko, Study of softening and melting behaviour of iron ore sinter and pellets, High Temp. Mater. Process. 31 (2012) 215–220.

[29] M. Allibert, H. Gaye, J. Geisler, D. Janke, B.J. Keene, D. Kirner, M. Kowalski, J. Lehmann, K.C. Mills, D. Neuschutz, R. Parra, C. Saint Jours, P.J. Spencer, M. Susa, M. Tmar, E. Woermann, Slag atlas, 2nd ed., Verlag Staheisen, Dusseldorf, 1995.

[30] T. Sharma, R.C. Gupta, B. Prakash, Effect of reduction rate on the swelling behaviour of iron ore pellets, ISIJ Int. 32 (1992) 812–818.

[31] F.W. Frazer, H. Westenberger, K.H. Boss, W. Thumm, The relationship between basicity and swelling on reduction of iron-ore pellets, Int. J. Miner. Process. 2 (1975) 353–365.

[32] E. Mousa, D. Senk, A. Babich, Reduction of pellets-nut coke mixture under simulating blast furnace conditions, Steel Res. Int. 81 (2010) 706–715.

[33] T. Bakker, Softening in the blast furnace process: local melt formation as the trigger for softening of ironbearing burden materials, PhD Thesis, Delft University of Technology, 1999.

[34] A. Kemppainen, K. Ohno, M. Iljana, O. Mattila, T. Paananen, E. Heikkinen, T. Maeda, K. Kunitomo, T. Fabritius, Softening behaviors of acid and olivine fluxed iron ore pellets in the cohesive zone of a blast furnace, ISIJ Int. 55 (2015) 2039–2046.

[35] O. K. Goldbeck, Iron-Carbon, in: Iron-binary phase diagrams, Springer, Berlin, 1982: pp. 23–26.

[36] B. Nandy, S. Chandra, D. Bhattacharjee, D. Ghosh, Assessment of blast furnace behaviour through softening–melting test, Ironmak. Steelmak. 33 (2006) 111–119.

[37] K. Nagata, R. Kojima, T. Murakami, M. Susa, H. Fukuyama, Mechanisms of pig-iron making from magnetite ore pellets containing coal at low temperature., ISIJ Int. 41 (2001) 1316–1323.

[38] M. Humenik, D.W. Hall, R.L. Van Alsten, Graphite-base cermets- a new material for bearing, electrical high temperature applications, Met. Progr. 81 (1962) 101.

[39] W. Husslage, Dynamic distribution - sulphur transfer and flow in a high temperature packed coke bed, PhD Thesis, Delft University of Technology, 2004.

[40] M. Hayashi, K. Suzuki, Y. Maeda, T. Watanabe, Microstructure change and primary slag melting of sinter in the cohesive zone of a blast furnace, 55 (2015) 1223–1231.

[41] W.M. Husslage, M.A. Reuter, R.H. Heerema, T. Bakker, A.G.S. Steeghs, Flow of molten slag and iron at 1500 °C to 1600 °C through packed coke beds, Metall. Mater. Trans. B. 36B (2005) 765–769.

8. Complete replacement of the regular coke with nut coke

Chapter 7 showed the beneficial effect of nut coke mixing on the ferrous burden (pellet and sinter) properties. In the experiment with 40 wt% mixed nut coke, the negative impact on the gas permeability was expected due to the thinning of the regular coke layer; conversely, no negative impact was observed. In fact, the bed permeability was improved substantially with the nut coke addition in the ferrous bed. Therefore, it will be interesting to study the raw material bed behaviour, when all regular coke is replaced with the nut coke to completely mixed charge in the blast furnace.

Thus, in this chapter, the effect of complete mixing of nut coke with the ferrous burden (pellet and/or sinter) is examined. The chapter is concluded with a discussion on the practical implications of full replacement of the regular coke with nut coke in the ironmaking blast furnace.

This chapter is based on a prepared manuscript for submission in a peer-reviewed international journal.

Dharm Jeet Gavel, Allert Adema, Jan van der Stel, Jilt Sietsma, Rob Boom and Yongxiang Yang, “Effect of complete replacement of regular coke with nut coke on the physicochemical properties of ferrous bed”, 2019.

8.1 Introduction

Nut coke addition to the ferrous burden (pellet and sinter) is shown to be beneficial for the ironmaking blast furnace (Chapter 7). Continuous improvement of the physicochemical properties of the bed is observed with the nut coke addition, as a replacement of regular coke [1-2]. However, an optimum nut coke replacement ratio for the ferrous raw material bed is not known. Additionally, with the increasing trend of auxiliary injections fuel (coal, natural gas, fuel oil, coal tar, plastics and hydrogen gas) in the blast furnaces for the partial fulfilment of the thermal and reducing conditions, the total coke demand for iron production is decreasing [3-5]. This could result in a critical thinning of the regular coke layer, which may lead to complete mixing of the ferrous burden with coke in the blast furnace.

Historically, the ironmaking process started with the completely mixed burden of reductant (mostly charcoal) and fine iron ore particles for metal production. For example, in ancient “Tatara” furnace, metal was produced by reducing the iron ore fines (called ironsand) in the charcoal bed [6]. However, after the discovery of coke, charcoal is substituted and the bigger blast furnaces are developed. The coke has a much higher strength than charcoal. To further improve the blast furnace permeability and productivity, coke and iron ore in agglomerated form are charged in alternate layers due to their different particle sizes.

In case of emergence of complete mixing of reductant and the ferrous raw materials in the blast furnace, nut coke size (8-40 mm) being close to the ferrous burden size range, it can be a reductant of the first choice to replace the regular coke (40-80 mm). Thus, an understanding of the ferrous burden behaviour under complete nut coke mixed-charged conditions is vital. Hence, it is explored and discussed in the current chapter. The experimental investigations are performed to understand the physicochemical behaviour of the ferrous raw material bed (pellet and/or sinter) under complete (100 %) nut coke mixed-charged condition as a replacement of the regular coke.

8.2 Materials and methods

8.2.1 Raw materials

Commercially supplied iron ore pellets and sinter of size range 10-13 mm are used in the present study. In the case of pellet-only burden, iron ore pellet (type 1) is utilised for the experimental studies. In the case of the mixture ferrous burden, the pellet type 1, pellets type 2 and sinter are mixed in 40:20:40 ratio. The coke of size 10-15 mm (small) and 20-25 mm (large) is utilised as the nut coke for the smelting experiment. The chemical analysis of the ferrous burden is given in Table 3.1. The chemical analysis of the coke and ash are given in Table 3.2 and Table 3.3, respectively.

Figure 8.1 shows the schematic of the sample bed arrangement inside the graphite crucible. Nut coke is added as a complete replacement (100 %) of the regular coke. Consequently, regular coke layers are absent in the sample bed (Fig. 8.1). Experiments for fully mixed conditions are carried out with a constant bed weight of ferrous burden (pellet and/or sinter mixture) of 500 g and coke weight of 100 g, which represents a coke ratio of 300 kg/t of hot metal (kg/tHM) in the blast furnace equivalent. The blast furnace is assumed to operate with a pulverised coal injection (PCI) rate of 200 kg/tHM.

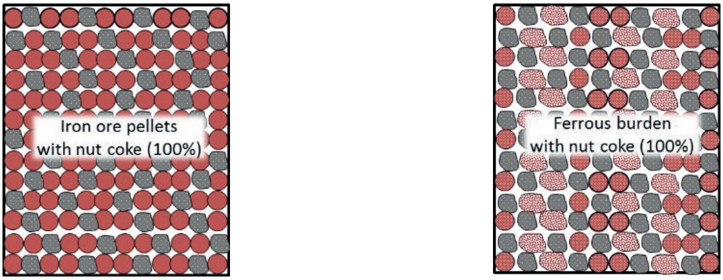

(a). Iron ore pellet mixed with 100 % nut coke

(b). Ferrous burden of pellet and sinter mixed with 100 % nut coke

Fig. 8.1 Schematic of the sample bed arrangement inside the crucible (internal diameter 64 mm).

8.2.2 Experimental procedure

The Reduction Softening and Melting (RSM) apparatus is utilised to perform the experiments (Fig. 3.1). The sample bed arranged in a graphite crucible is placed inside the RSM furnace (Fig. 3.1) and the smelting experiments are performed under the simulated blast furnace conditions. The detailed experimental procedure is given in section 3.4-3.5. The list of the experiments (Series E) performed with 100 % mixed nut coke is given in Table 3.5. Dripped sample characterisation is performed as discussed in section 3.6.

8.3 Result and discussion

8.3.1 Characteristics of the iron ore pellet bed completely mixed with nut coke

The characteristics of the iron ore pellet bed mixed with nut coke (100 %), as a replacement of the regular coke is discussed in this section. Various parameters for the bed contraction and pressure drop are defined in Table 3.6 and Table 3.8, respectively.

Characteristics of the pellet bed mixed with 100 % nut coke (10-15 mm), is shown in Figure 8.2. Similar to the pellet bed without nut coke, three distinct stages of the bed contraction are observed for the fully mixed bed. Interestingly, only a marginal increase in the pressure drop value is observed (˜100 Pa) during the melting and dripping (stage 3) of the iron ore pellets (Fig. 8.2). This occurs due to the presence of a high density of pores, which allow the gas to easily flow across the bed.

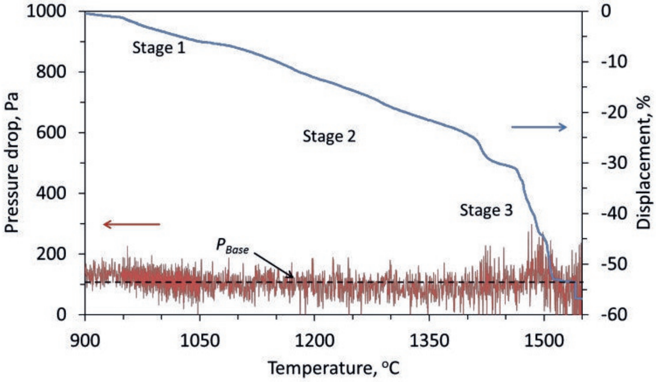

Fig. 8.2 Characteristics of the iron ore pellet bed mixed with 100 % nut coke (10-15 mm).

When the materials of two different sizes are mixed, the particle of smaller size will align around the bigger sized particles (Fig. 8.3). As a result, the interstitial voids are occupied. In the case of pellets (10-13 mm) and regular coke (40-80 mm), the iron ore pellet will occupy the voids around regular coke. Now, when this material bed reaches the high temperature zone in the blast furnace, the pellet will soften and melt to block the passage for the gas flow. Consequently, the gas permeability will be hampered, which will negatively affect the productivity of the blast furnace.

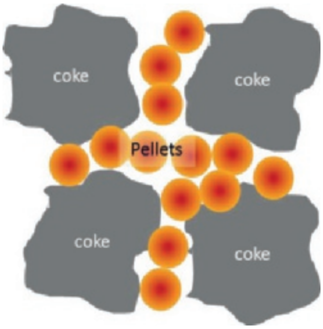

Fig. 8.3 Schematic of particle arrangement when bigger size coke and smaller iron ore pellets are mixed.

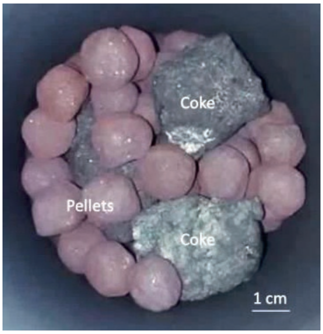

Fig. 8.4 Photograph of the sample bed from the crucible top, before experiment (pellets 10-13 mm and coke 20-25 mm).

Considering the particle size difference between the iron ore pellet (10-13 mm) and bigger sized nut coke (20-25 mm), poor permeability might occur. Thus, to investigate the bed behaviour when bigger sized nut coke (20-25 mm) is completely mixed with the small-sized iron ore pellet, smelting experiments are conducted in the RSM. The sample arrangement (top view) inside the crucible before the experiment is shown in Figure 8.4. The alignment of the pellet around the coke is apparent from Figure 8.4.

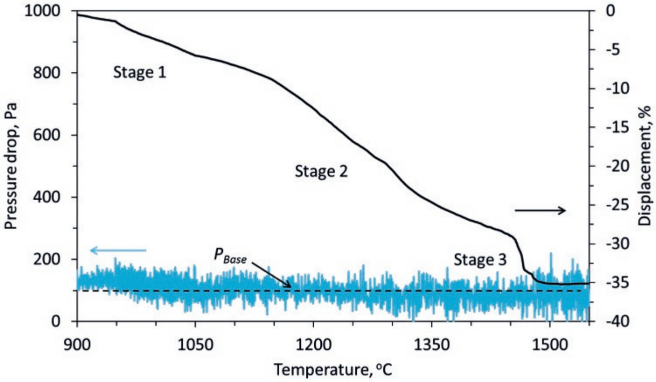

Fig. 8.5 Characteristics of the iron ore pellet bed mixed with 100 % nut coke (20-25 mm).

The characteristics of the iron ore pellet bed, completely mixed with nut coke of size 20-25 mm is shown in Figure 8.5. Similar to the pellet bed without nut coke, three stages of the bed contraction are observed. Furthermore, no rise at all in the pressure drop is observed at the time of burden melting and dripping (stage 3). This indicates that during the pellet melting, the inter-particle voids and pores are open for the gas flow. Consequently, the gas permeability is maintained across the bed.

8.3.1.1 Comparison of bed contraction characteristics

The effect of nut coke addition on the bed contraction characteristics is shown in Figure 8.6. Nut coke increases the reduction degree and iron carburisation of the iron ore pellets (Chapter 6). Consequently, for the pellet bed mixed with nut coke (10-15 mm), the softening (T_1) and melting (T_2) temperature linearly increases and decreases, respectively (Fig. 8.6b). However, a limited effect of nut coke addition is observed on the dripping temperature (T_3). Similarly, with marginal effect on the first stage of bed contraction, in the second and third stage, the bed contraction decreases linearly with the nut coke addition. In the presence of nut coke due to the higher degree of iron carburisation achieved on the pellets, the bed melting temperature decreases to shorten the second stage regime. The third stage of bed contraction decreases due to the support provided by the left-over nut coke inside the bed.

A similar effect of nut coke mixing occurs for the pellet bed mixed with 20-25 mm size nut coke. However, only a limited effect is observed on the bed characteristics temperature. This is due to the bigger size of mixed nut coke, which has a lower surface area. Consequently, a limited contact among the pellet and coke occurs, which results in lower chemical interaction (reduction and iron carburisation). Furthermore, due to the support provided by the unconsumed nut coke, a marginal bed contraction (8 %) occurs in the third stage.

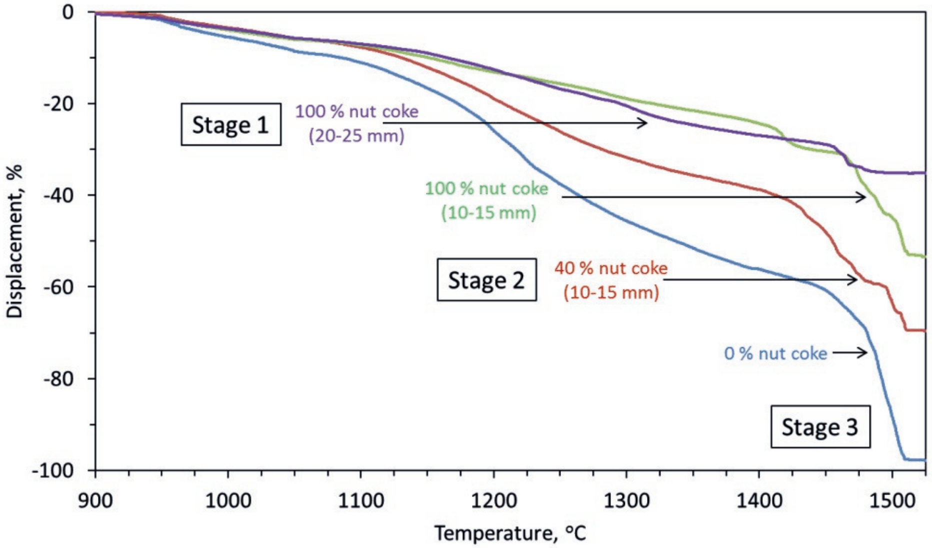

(a) Bed contraction profile

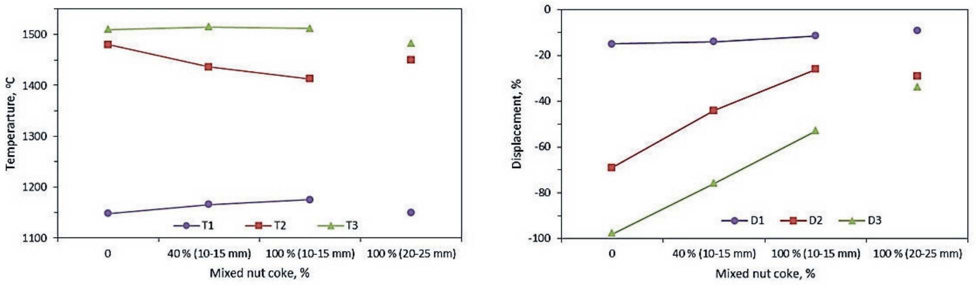

(b) Bed characteristics temperature (c) Bed characteristics displacement

Fig. 8.6 Effect of nut coke addition on iron ore pellet bed contraction characteristics.

8.3.1.2 Comparison of bed permeability characteristics

Measured pressure drop profiles for the iron ore pellet bed mixed with different nut coke sizes (10-15 mm and 20-25 mm) and concentration is shown in Figure 8.7. The nut coke provides the pores and voids for the gas to flow across the pellet bed. Thus, the gas permeability increases with the nut coke addition in the pellet bed (Fig. 8.8). Strikingly, for the pellet bed completely mixed with nut coke(10-15 mm and 20-25 mm), no significant rise in the pressure drop occurs at the time of pellet softening, melting and dripping (Fig. 8.7).

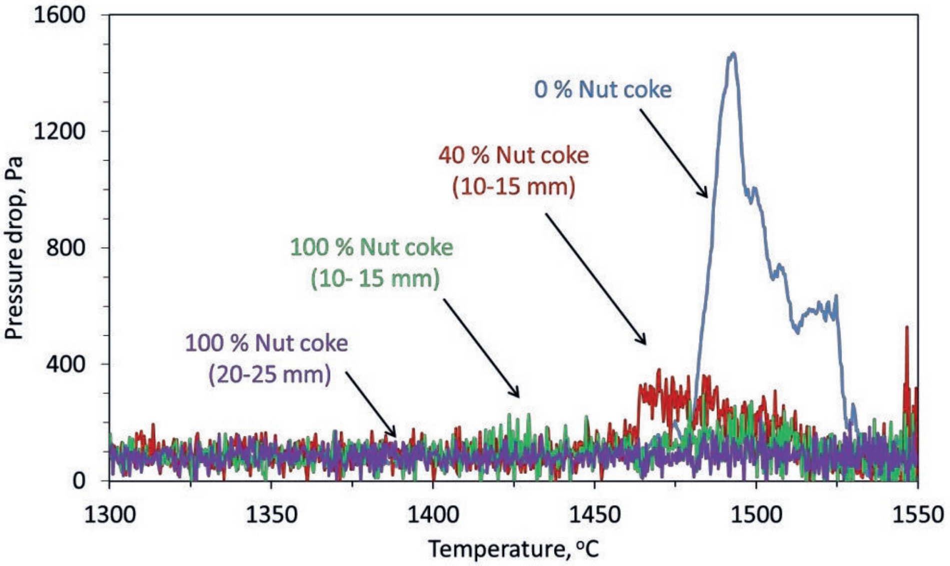

Fig. 8.7 Effect of nut coke addition on pressure drop profile (gas permeability).

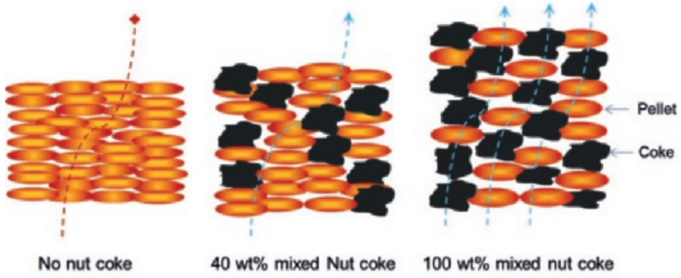

Fig. 8.8 Schematic of effect of nut coke addition on the gas permeability during softening and melting.

8.3.1.3 Gas profile

Effect of complete replacement of regular coke with nut coke: The gas inlet composition followed during the smelting experiments is given in Table 3.4. The off-gas profile from the sample bed mixed with (100 wt%) and without nut coke is shown in Figure 8.9. Several shifts in the gas outlet profile are due to the change in the gas inlet composition (Table 3.4). However, a difference in the off-gas composition between the bed with and without mixed coke can be seen (Fig. 8.9). This difference in the gas outlet composition is apparent, especially for CO and CO_2 gas (Fig. 8.9). A schematic of various reactions occurring in the sample bed is shown in Figure 5.23.

In the absence of the nut coke in the bed, the inlet gas mixture (CO, CO_2, H_2 and N_2) first interacts with the lower regular coke layer (Fig. 3.7a). Consequently, the concentration of carbon monoxide (CO) gas increases (5.1), which flows upward to reduce the iron ore pellet (iron oxide). As a result of the iron-oxide reduction, carbon dioxide (CO_2) gas evolves (5.2-5.5), which with its interaction with the upper regular coke layer gets regenerated to carbon monoxide (CO) (5.1). At high temperature, as the iron ore melting occurs, the FeO-rich slag flows over the incandescent coke to instantaneously reduce to iron and release CO gas. As a result, a CO gas rich regime is observed to mark the melting of the pellets in the bed (Fig. 8.9).

When the small nut coke (10-15 mm) is utilised as a complete replacement of the regular coke, the coke layer present above and below the iron ore pellet layer is absent. Thus, for given inlet gas, the iron oxide reduction and CO gas regeneration (5.1) occur simultaneously inside the sample bed. Due to the close contact between the nut coke and pellets, intensive reduction and iron carburisation reactions occur. Now, due to the absence of top regular coke layer, the gas evolving out of the sample bed will not be able to regenerate. Consequently, a lower concentration of the CO gas is noticed from the pellet bed mixed with 100 % nut coke in temperature range from 650 °C to 1400 °C. This indicates a higher efficiency of the gas (CO) utilisation in the presence of the nut coke in the pellet bed. Due to the high iron carburisation achieved on the pellet shell, the melting of the pellet starts earlier compared to the case without nut coke. This is evident from the earlier appearance of CO gas rich regime during the heating cycle of the sample bed (at 1400 °C).

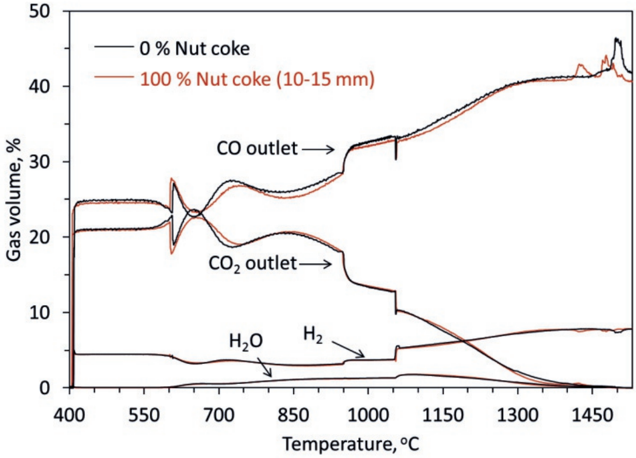

Fig. 8.9 Effect of complete (100 %) replacement of regular coke with nut coke (10-15 mm) on the evolved gas profile.

Effect of mixed nut coke size on evolved gas composition: Effect of mixed nut coke size (10-15 mm and 20-25 mm) on the off-gas profile can be observed in Figure 8.10. The specific surface area of the coke decreases with the increase in the particle size. Consequently, the chemical interaction between the pellets and coke decreases with the increase in the coke size, resulting in a lower CO gas regeneration. This in turn will slow down the rate of reduction and iron carburisation. This is indicated by the late appearance of CO gas rich regime for pellet bed mixed with 20-25 mm nut coke, which denotes that the melting of the pellets occurs at high temperature (at 1510 °C). This further suggests that the chemical function of the nut coke to reduce and carburise the iron ore pellets decreases with the increase in size.

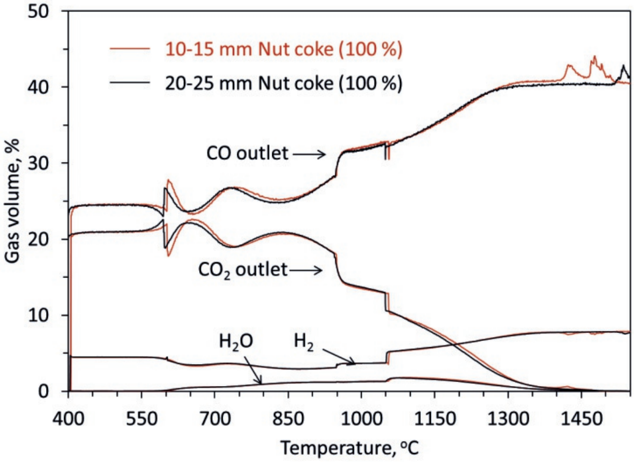

Fig. 8.10 Effect of nut coke particle size on off-gas profile.

8.3.1.4 Degree of reduction and carbon utilisation

Based on the off-gas profile, the degree of reduction (DOR) and carbon utilisation is estimated (3.1 and 3.7). An improved DOR profile is observed with added nut cokeof size 10-15 mm.

However, for the pellet bed completely mixed with 20-25 mm sized nut coke, a lower DOR is realised compared to all other examined cases. This can be a result of segregation of the iron ore pellets in the bed, which provides a preferential flow path for the gas across the bed. Consequently, the gas flows across the bed without sufficient interaction with the coke and iron ore pellets. Although the pressure drop measurement across the pellet bed mixed with 20-25 mm nut coke suggested improved gas permeability (Fig. 8.11), the efficiency of the gas distribution is not known. Furthermore, the late appearances (at high temperature) of the bed melting (T_2) and CO gas rich regime indicate a limited reduction and iron carburisation in the presence of bigger sized nut coke (Fig. 8.6 and 8.10). Thus, for effective utilisation of the nut coke, particle size should be kept close to the size of the iron ore pellet.

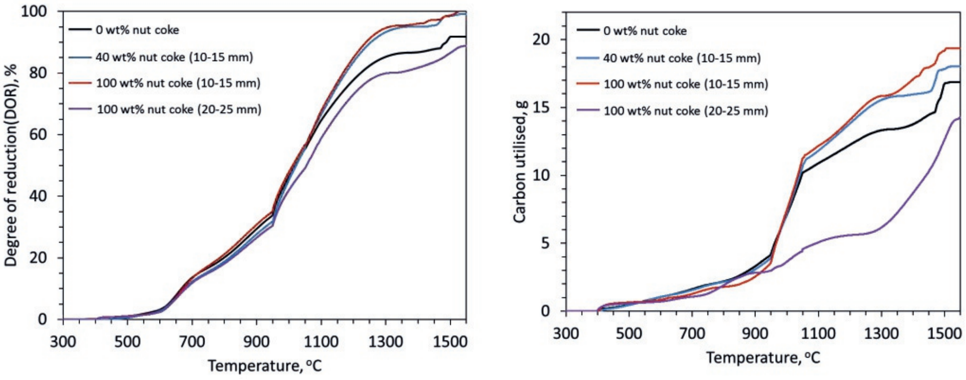

(a) Degree of reduction

(b) Carbon utilisation

Fig. 8.11 Effect of nut coke addition on the estimated degree of reduction (DOR) and carbon utilisation of the iron ore pellet bed.

Similarly, the carbon utilisation is observed to increase with the added nut coke of size 10-15 mm (Fig 8.11b). For a similar reason discussed for the DOR, the carbon utilisation is decreased for the pellet bed mixed with 20-25 mm sized nut coke (Fig. 8.11b).

8.3.1.5 Coke consumption in the smelting of iron ore pellet bed

After the smelting experiments, the remaining coke is collected from inside the crucible and weighed to calculate the amount of coke consumed. The amount of coke consumed along with the final degree of reduction achieved on the iron ore pellet is shown in Figure 8.12. A high degree of reduction (˜99 %) is observed for the case of pellet bed fully mixed with nut coke of size 10-15 mm (Fig. 8.12). Mixed nut coke of size 10-15 mm was able to efficiently utilise as a replacement of regular coke. However, in the case of pellets fully mixed with 20-25 mm sized nut coke, less coke is consumed. This might be the result of segregation of small sized pellets takes place around the coke,which results in the gas flow in some preferred channels (Fig. 8.4). As a result, adequate interaction between the pellets and coke does not occur, which results in the lower degree of reduction achieved on the pellets (Fig. 8.12).

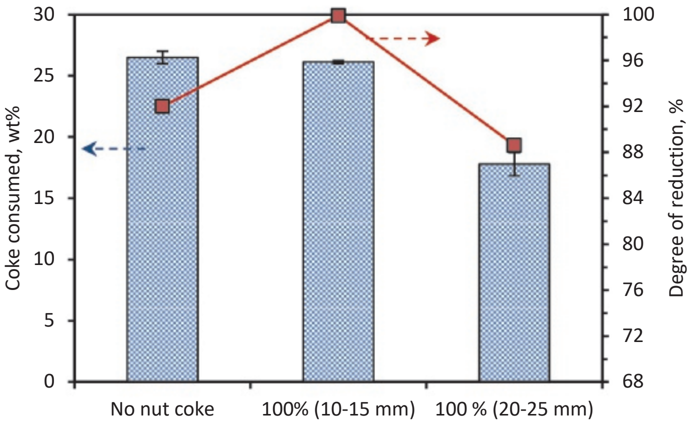

Fig. 8.12 Coke consumed in the smelting of pellet with and without mixed nut coke (measured).

8.3.1.6 Carbon in dripped iron

After melting, when the liquid iron flows over the incandescent coke, iron carburisation occurs. For the smelting experiments with 100 wt% mixed nut coke (10-15 mm and 20-25 mm), the carbon concentration in dripped metal is observed in the range of 2.5 to 3.5 wt% (Fig. 8.13). Considering the high carbon concentration in the pellet quenched in the presence of mixed nut coke (Fig.6.6 and 6.8), the dripped liquid iron was expected to have higher carbon content. However, no clear trend on the carbon content of the dripped metal is observed. Also, the carbon content in iron is observed in the similar range as in the absence of nut coke, which suggests that no negative impact on the carbon content of the dripped metal will occur as a consequence of the complete replacement of the regular coke with the nut coke.

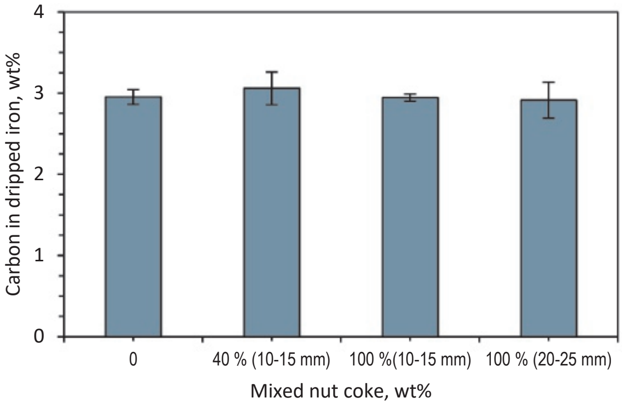

Fig. 8.13 Effect of nut coke addition on the carbon in dripped iron.

8.3.2 Characteristics of ferrous burden of pellet and sinter mixed with 100 wt% nut coke

Considering the poor interaction between the gas and sample in the pellet bed completely mixed with 20-25 mm sized nut coke, smelting experiments with the ferrous raw materials are performed only with 10-15 mm sized nut coke.

The effect of nut coke (10-15 mm) addition (replacement of the regular coke) on the ferrous (pellet and sinter mixture) bed contraction characteristics is shown in Figure 8.14. The ferrous bed characteristics without and with 40 wt% mixed nut coke are discussed in section 7.3.5. The bed contraction profile for the ferrous raw material completely mixed with nut coke (100 %) evolves through three distinct stages. The nut coke increases the kinetics of the reduction reaction and iron carburisation to shrink the second stage between the first and third. The profile of the first and second stage appear smooth. However, the third stage of bed contraction occurs in a stepwise manner, which is due to the resistance offered by the solid nut coke at the time of ferrous burden melting and dripping.

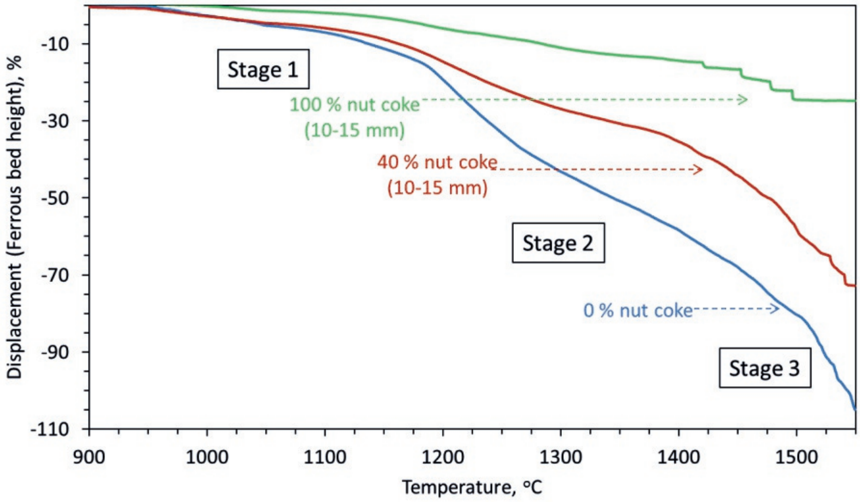

Fig. 8.14 Effect of nut coke addition on bed contraction characteristics of ferrous burden (pellet and sinter mixture).

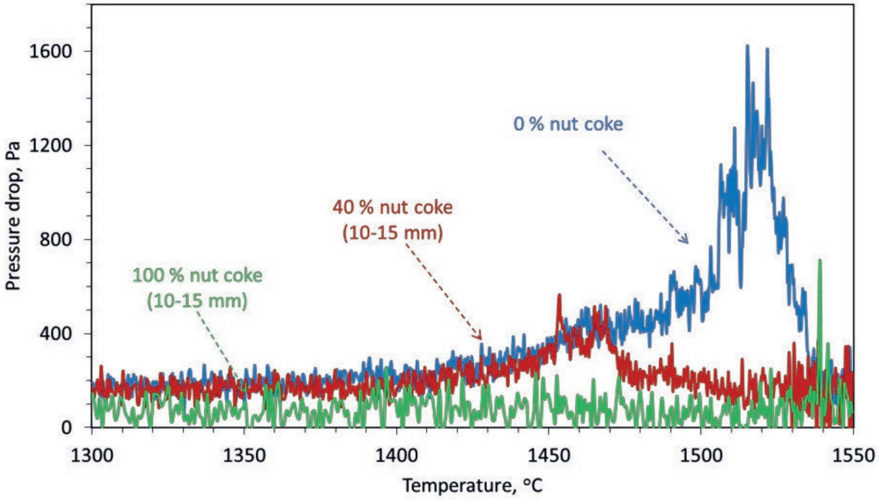

Fig. 8.15 Effect of nut coke addition on the pressure drop profiles (gas permeability) for the ferrous burden (pellet and sinter mixture).

The effect of nut coke mixing (replacement of the regular coke) on the measured pressure drop profile is shown in Figure 8.15. The ferrous bed permeability characteristics without and with 40 wt% mixed nut coke are discussed in section 7.3.6. For the ferrous bed completely mixed with nut coke (100 wt%), the measured pressure drop across the bed is observed in a narrow range. Interestingly, no rise in the pressure drop occurs at the time of softening, melting and dripping. The pores and voids provided by the nut coke allow the free movement of the gas across the ferrous raw material bed during softening and melting. Therefore, a high degree of gas and raw material interaction occurs in the presence of nut coke in the bed, thereby enhancing the kinetics of reduction and iron carburisation of the ferrous raw materials.

8.3.3 Ferrous burden gas outlet profile with 100 % mixed nut coke

8.3.3.1 Gas outlet profile

Compared to the ferrous bed without nut coke, the CO and CO_2 concentration of the outlet gas is observed to be lower and higher, respectively, for the ferrous bed mixed with nut coke (Fig. 8.16). This indicates a higher utilisation of the reducing gas (η_{CO}) under the nut coke mixed charge conditions.

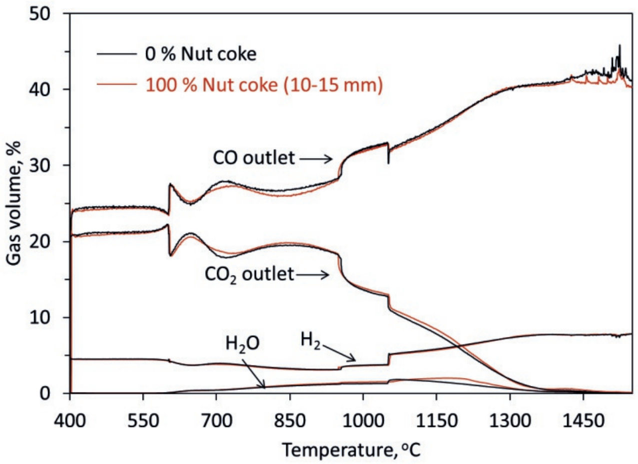

Fig. 8.16 Effect of nut coke mixing on off-gas profile from ferrous bed (pellet and sinter mixture).

8.3.3.2 Degree of reduction and carbon utilisation

Based on the off-gas profile, the degree of reduction (DOR) and carbon utilisation is calculated (3.1 – 3.7). An increased DOR profile is observed with the nut coke addition (Fig. 8.17a). However, a regime of lower DOR is observed below 1000 °C for the complete nut coke mixed ferrous bed, which might be the result of the absence of lower regular coke layer. The inlet gas interacts with the regular coke layer present at the bottom of the crucible to increase the reduction potential of the gas (CO gas content), which flows inside the sample bed. Furthermore, the coke gasification is known to occur at high temperature, which could limit the reduction degree of the ferrous raw materials (Fig. 5.18). Once the temperature is high (above 1000 °C), the DOR is observed to increase continuously due to the simultaneous reduction and regeneration of the reducing (CO) gas. Similarly, the rate of carbon utilisation is observed to increase above 1000 °C, which is due to the higher kinetics of the reduction and carburisation reactions (5.4 and 5.11) (Fig. 8.17b). The presence of the nut coke in the close proximity of the ferrous raw material increases the kinetics of these reactions.

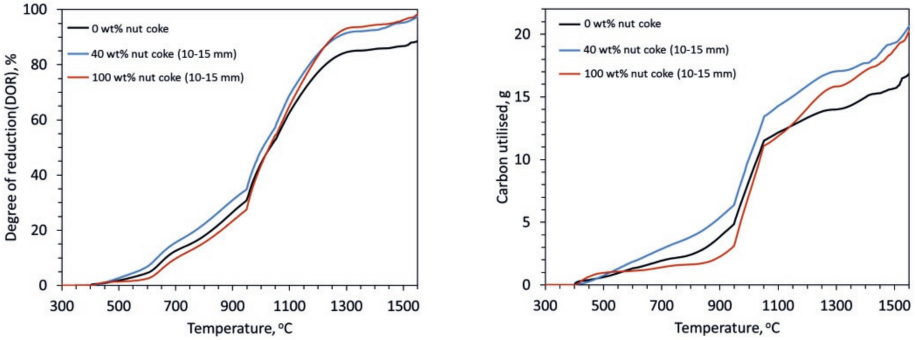

(a) Degree of reduction profiles

(b) Carbon utilisation profiles

Fig. 8.17 Effect of nut coke addition on the degree of reduction (DOR) and carbon utilisation of ferrous raw material bed.

8.3.3.3 Dripped metal and slag composition

The carbon content in the dripped iron increases with the nut coke mixing (Fig. 8.18). As discussed before (Section 6.3.4.2), the liquid iron is carburised during its flow over the coke bed [7]. In spite of the absence of a regular coke layer, a higher carbon content is observed in the dripped iron (Fig. 8.18), in the case of complete replacement of regular coke by the nut coke. This shows that due to the direct contact between the nut coke and the ferrous burden, the simultaneous melting and iron carburisation is promoted.

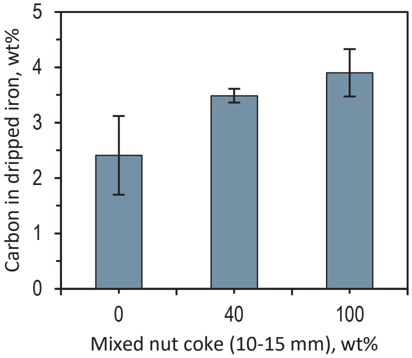

Fig. 8.18 Effect of nut coke mixing on the carbon in dripped iron.

The composition of the slag dripped from the ferrous bed completely mixed with nut coke is given in Table 8.1. A low FeO content (0.83 %) is observed in the dripped slag, which shows that in the presence of mixed nut coke, a high reduction degree is achieved on the ferrous burden.

Table 8.1: Effect of nut coke addition on dripped slag composition.

Nut coke	FeO, %	CaO, %	MgO, %	SiO_2, %	Al_2O_3, %	B_2	B_3	B_4
0	1.1	45.6	10.7	28.9	7.2	1.6	2.	1.6
40	1.8	38.7	11.9	34.2	7.9	1.1	1.5	1.2
100	0.8	41.1	11.7	31.9	8.8	1.3	1.7	1.3

8.3.3.4 Melt dripping profile of the ferrous burden

Dripping experiments are performed to understand the liquid dripping behaviour when regular coke is completely replaced with mixed nut coke in the ferrous burden (pellet and sinter mixture). The dripped liquid is collected in different cups to understand the effect of dripping time and temperature on the chemistry and weight distribution (Fig. 8.19). The temperature range and collected dripped liquid weight are given in Table 8.2.

During the experiment, it is observed that at first only the molten metal drips out of the bed. This indicates that the melting and dripping phenomena are initially controlled by the melting of the metal (iron). Thereafter, the metal and slag simultaneously drip out of the bed. Dripping from the sample bed starts at 1531 ^{o}C and continues till 1550 ^{o}C(Fig. 8.19).

Due to the high interaction between the nut coke and ferrous burden, a high carbon (> 3 wt%) is found in the dripped iron. It is observed that with the temperature, the carbon content in the dripped iron increases. However, for liquid iron dripped around 1544 ^{o}C lower carbon content in the liquid is observed, which is due to the higher volume of the liquid dripping at that temperature range. This could limit the coke and liquid interaction in order to decrease the carbon content in the dripped iron.

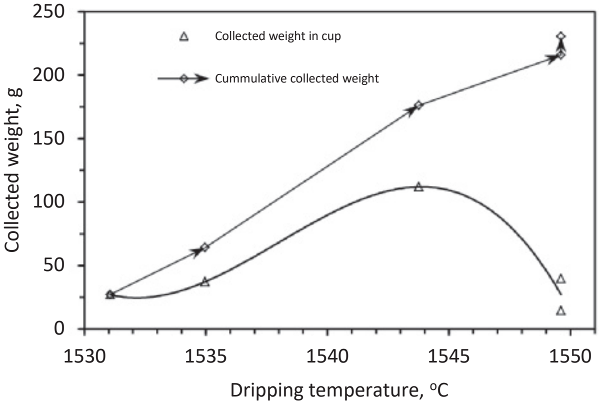

(a). Collected dripped liquid during the smelting experiment

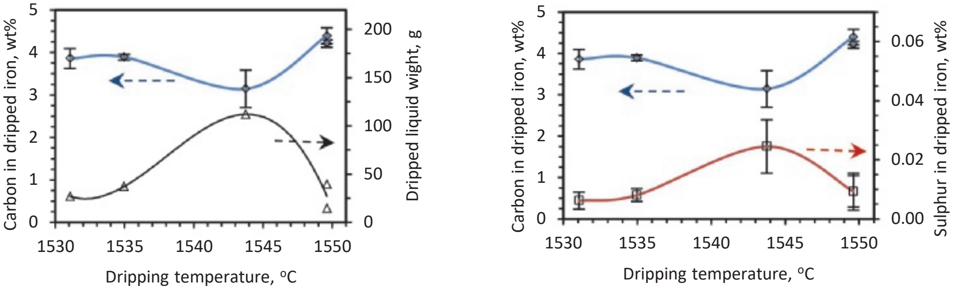

(b). Carbon content in the dripped metal and amount of the dripped metal

(c). Carbon and sulphur content in the dripped metal

Fig. 8.19 Effect of complete replacement of regular coke with mixed nut coke on the liquid dripping profile from ferrous burden (pellet and sinter).

Table 8.2. Liquid dripping profile from fully nut coke (10-15 mm) mixed ferrous bed.

Cup no.	Sample bed temperature, °C	Weight, g	Metal or Slag	Flow type
1	1531	27	Metal	Rivulets
2	1535	37	Metal	Rivulets
3	1544	112	Metal and Slag	Rivulets
4	1550	40	Metal and Slag	Rivulets
5	1550 (Hold 5 min)	15	Metal and Slag	Droplets

Consequently, a high sulphur content is also observed due to the lower interaction between the slag and metal around 1544 °C. Also, the low carbon content in the dripped metal favours the conditions for the presence of sulphur in the metal [8].

An effect of temperature and dripped liquid volume is apparent from the dripped slag composition (Table 8.3). As the temperature increases, CaO-rich phases melt from the ferrous burden to drip out of the crucible. In addition, a decrease in the FeO content of the slag is a result of higher reduction degree achieved at high temperature.

Table 8.3. Effect of temperature on the dripped slag composition from ferrous burden fully mixed with nut coke (10-15 mm)

Dripping Temperature, °C	FeO, %	CaO, %	MgO, %	SiO_2, %	Al_2O_3, %	B_2	B_3	B_4
1544	1.1	39.2	12.2	32.8	8.9	1.2	1.6	1.2
1550	0.6	43.1	11.2	31.0	8.7	1.4	1.8	1.4

8.3.3.5 Coke consumption in the ferrous bed

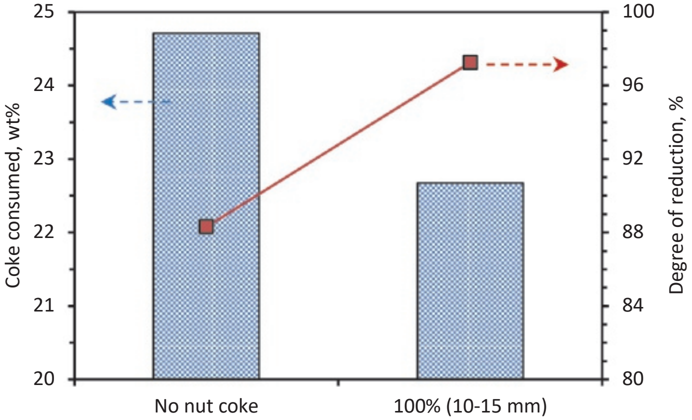

Fig. 8.20 Coke consumed during the experiments with the ferrous burden (pellet and sinter mixture).

The fraction of coke consumed in the smelting of ferrous burden (pellet and sinter mixture) is shown in Figure 8.20. For the ferrous bed fully mixed with nut coke (10-15 mm) a higher degree of reduction (97 %) is observed. Interestingly, in spite of the higher reduction degree achieved, a low amount of coke is consumed, which is primarily due to the high gas utilisation in the ferrous bed fully mixed with nut coke (Fig. 8.17). This shows the potential of nut coke to decrease the reductant consumption in the iron making blast furnace process.

8.3.4 Discussion

The various roles played by the metallurgical coke in the ironmaking blast furnace are shown in Figure 8.21. These roles can be divided into three main categories of chemical, mechanical and thermal functions. The chemical function is to produce the reducing gas for the reduction of iron oxide and to provide carbon for the carburisation of the reduced iron. The thermal function is to provide the thermal energy to sustain the reduction reactions, heating and melting of the ferrous materials. The mechanical function is to provide support for the raw material burden to maintain adequate gas permeability throughout the blast furnace.

The counter-current nature of the ironmaking blast furnace requires an adequate gas permeability. It is one of the principal reasons for alternate charging of the regular coke (40-80 mm) and the ferrous raw materials (10-30 mm) in the blast furnace. Furthermore, to sustain the load, high temperature and gas conditions, metallurgical coke is utilised, which other reductants like coal and charcoal cannot. Along with the mechanical function, the chemical and thermal requirement for the iron production is easily met with the alternate charging of the coke and the ferrous raw materials in the blast furnace.

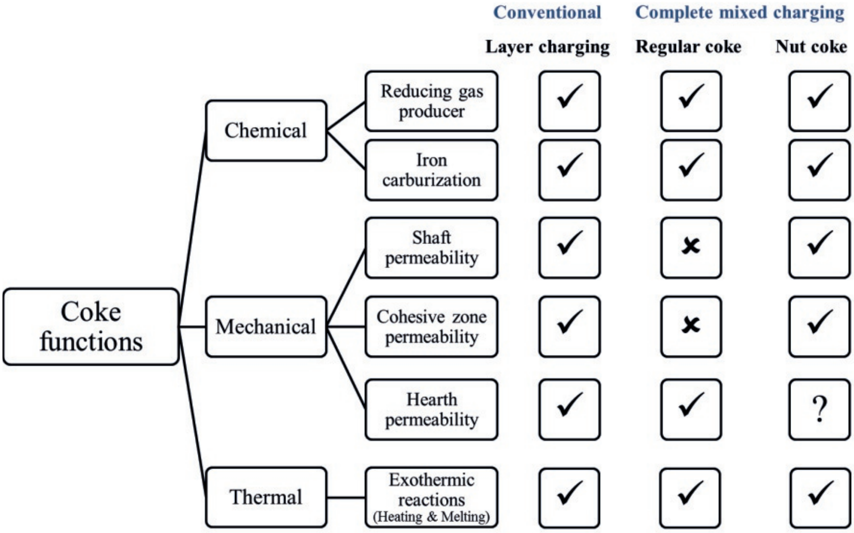

Fig. 8.21 Functions of the metallurgical coke with the burden charging method in the iron-making blast furnaces.

When the regular coke (40-80 mm) and the ferrous burden (10-30 mm) are completely mixed charged, the chemical and the thermal requirements of the coke can be met. Still, the efficiency of the heat and mass transfer is questionable. However, the most important function of maintaining the gas permeability in the blast furnace cannot be met with this charging method. This is due to the tight packing of the small ferrous raw materials around the bigger regular coke. This will hamper the permeability in the shaft region of the blast furnace. Furthermore, when this mixed burden reaches the high temperature zone, it will soften and melt to clog the bed. The gas permeability will then be hampered dramatically in the furnace, resulting into the channelling, hanging, slip and other irregularities in the blast furnace. This is not desirable for the stable operation of the blast furnace. Thus, the regular coke and the ferrous raw material are not mixed charged in the blast furnace.

Traditionally, the iron making process started with the mixed charging of the ferrous raw materials with the reductant (charcoal, coal, etc.). For example, in the ancient Japanese process for iron production called “Tatara”, the fine-sized (less than 1 mm) ferrous raw materials (magnetite called ironsand, size) are mixed charged with the charcoal [6,9]. Here, the fine iron ore powder gets reduced, softened and molten to flow over the stationary bed of charcoal. However, this is a batch process for the production of solid iron, in which the clay vessel (height 1.1 m, length 3 m, width 1.1 m) is broken to remove the metal product [6]. The efficiency of the process was very poor as it requires the time of about 72 hours, 10 tonnes of iron ore and 12 tonnes of charcoal for the production of 2.5 tonnes of the metal. This gives a clear message that mixing materials of two different particle size is not desirable for the process efficiency.

Nevertheless, considering the similar size ranges for the nut coke and ferrous raw materials completely mixed charging in the blast furnace can enhance the process efficiency. Thus, a series of smelting experiments are performed in the RSM to understand the physicochemical behaviour of the bed, especially when nut coke is completely mixed charged (as a replacement of the regular coke) with the ferrous raw materials. This reveals that the chemical function of coke is increased and efficiently meets requirements under mixed charge conditions. Furthermore, the mechanical role of maintaining the gas permeability in the shaft and the cohesive zone can be increased by nut coke mixed charging. This can result in efficient gas utilisation (Fig. 8.17), which can also lower coke consumption in the blast furnace (Fig. 8.20).

In the RSM, the blast furnace hearth condition cannot be simulated. Thus, knowledge of the nut coke behaviour in the hearth cannot be generated from the smelting experiments in the RSM. Considering that about 75 wt% of the smaller sized nut coke remains unconsumed to report in the hearth (Fig. 8.20), it could cause irregular liquid flow. However, a lower concentration of nut coke is expected to reach the hearth of the blast furnace as in the RSM experiments; the sample bed is externally heated. Thus, the coke required to maintain the thermal conditions for reduction, heating and melting of the raw materials is not predicted by the RSM experiments.

A detailed understanding of the nut coke behaviour in the blast furnace hearth is required before using nut coke as a complete replacement of the regular coke. Furthermore, various burden distribution strategies can be devised to effectively utilise the nut coke in the blast furnace. For example, the blast furnace can be charged with big (larger than 40 mm) regular coke to form the central coke column, which when reaching the hearth forms a permeable deadman. Whereas, nut coke completely mixed with ferrous raw material can be charged in the mid radial and peripheral location in the blast furnace to improve the gas permeability.

8.4 Conclusions

The physiochemical properties of the ferrous raw materials bed are investigated for the case when regular coke is completely (100 %) replaced by the nut coke (10-15 mm and 20-25 mm). After a series of smelting experiments with nut coke mixed with the iron ore pellets and ferrous burden mixture (60% pellet: 40% sinter), the following conclusions can be drawn.

(1) The ferrous bed of nut coke (10-15 mm) mixed with iron ore pellet also evolves through three distinct stages of the bed contraction. The impact of complete replacement is significant in the second stage, which is shortened due to a higher reduction and iron-carburisation rate achieved on the iron ore pellets and sinter.
(2) Under completely mixed charge conditions, due to the pores and inter-particle voids provided by the nut coke, gas permeability (pressure drop) in the bed is increased at the time of softening, melting and dripping of the ferrous materials.
(3) When nut coke (10-15 mm) is added as the complete replacement of the regular coke, the gas utilisation is enhanced to increase the degree of reduction and carbon utilisation in the bed of iron ore pellets and ferrous burden (pellet and sinter mixture).
(4) The chemical, thermal and mechanical functions performed by the coke in the blast furnace can be improved under complete mixed charge conditions. However, for higher chemical utility, the mixed nut coke size should be kept similar to that of the ferrous raw materials size range.

Nut coke mixing as a complete replacement of the regular coke has shown potential to increase the physicochemical properties of the ferrous raw material bed. Smelting experiments performed in the RSM indicate that a significant fraction of unconsumed nut coke can reach the blast furnace hearth. Thus, a thorough understanding of the unconsumed nut coke behaviour in the blast furnace hearth is required. Furthermore, various burden distribution strategies can be explored for more effective utilisation of the nut coke in the iron making blast furnace.

8.5 References

[1] D.J. Gavel, A. Adema, J. van der Stel, J. Sietsma, R. Boom, Y. Yang, Effect of nut coke addition on physicochemical behaviour of pellet bed in ironmaking blast furnace, ISIJ Int. 59

(2019) 778–786.

[2] D.J. Gavel, A. Adema, J. van der Stel, C. Kwakernaak, J. Sietsma, R. Boom, Y. Yang, Melting behaviour of iron ore pellet bed under nut coke mixed charge conditions, ISIJ Int. 60 (2020).

[3] H. Ahmed, New trends in the application of carbon-bearing materials in blast furnace iron-making, Minerals. 8 (2018) 561-580.

[4] Z. Liu, J. Zhang, T. Yang, Low carbon operation of super-large blast furnaces in China, ISIJ Int. 55 (2015) 1146–1156.

[5] A. Minoru, T. Kaneo, I. Takanori, T. Nobuhiro, Development of waste plastics pulverization for blast furnace injection, JFE Tech. Rep. 19 (2014) 110-117.

[6] T. Inoue, Tatara and the Japanese sword : the science and technology, Acta Mech. 214 (2010) 17–30.

[7] V. Shatokha, O. Velychko, Study of softening and melting behaviour of iron ore sinter and pellets, High Temp. Mater. Process. 31 (2012) 215–220.

[8] F.N.H. Schrama, E.M. Beunder, B. van den Berg, Y. Yang, R. Boom, Sulphur removal in ironmaking and oxygen steelmaking, Ironmak. Steelmak. 44 (2017) 333–343.

[9] H. Tanii, T. Inazumi, K. Terashima, Mineralogical study of iron sand with different metallurgical characteristic to smelting with use of Japanese classic iron- making furnace “Tatara", ISIJ Int. 54 (2014) 1044–1050.

9. Conclusions and recommendations

9.1 Conclusions

To investigate the effect of nut coke mixing with the ferrous raw materials (pellets and/or sinter), several series of smelting, quenching and dripping experiments were performed under simulated blast furnace conditions in the lab-scale Reduction Softening and Melting (RSM) apparatus. The physicochemical behaviour of the ferrous raw-material bed (pellets and/or sinter) mixed with nut coke were studied for various nut coke sizes (10-15 mm, 15-20 mm and 20-25 mm) and replacement ratios with regular coke (0 wt%, 10 wt%, 20 wt%, 30 wt%, 40 wt% and 100 wt%).

The physicochemical properties of the pellet bed are affected by the nut coke addition.

- The iron ore pellet bed contraction evolves through three distinct stages. The first stage of bed contraction occurs due to the indirect reduction of the pellets. Sintering, softening and carburisation of the iron shell evolve in the second stage. The third stage starts with melting and continues until all ferrous material has dripped out of the bed.
- All three stages of bed shrinkage are affected by the nut coke addition. The second stage is affected the most, in which the bed contraction and temperature range are shortened due to the enhanced reduction kinetics, limited sintering, lower softening and a higher degree of carburisation achieved on the pellets. As a result, the cohesive zone temperature range is narrowed by the nut coke addition.
- It is experimentally confirmed that the nut coke not only acts as a reducing agent when placed in close proximity of the pellets but also acts as a ‘spacer’ to physically hinder the contact among the pellets. Hence, it limits the sintering among the pellets, which will allow the reducing gas to reach the interior of the pellet.
- During the pellet softening, the pores and voids provided by the nut coke decrease the variation in the gas permeability (represented by the pressure drop and S-value). Furthermore, at the time of melting and dripping, the nut coke acts as a frame to keep the voids open for the gas flow. As a result, the gas permeability drastically increases with the nut coke addition in the pellet bed.
- The formed iron shell of the pellets carburises first and then eventually melts by direct contact with the coke. In the case of the pellet bed without nut coke, the process starts from the interface between the pellet layer and the regular coke layer, and progresses layer-wise. In contrast, in the case of the pellet bed mixed

with nut coke, melting proceeds simultaneously due to the multiple points of contact between the coke (nut coke and regular coke) and pellets across the bed.

- The higher iron carburisation achieved in the presence of the nut coke is the primary reason for the decrease in the melting temperature of the pellet bed. Thus, in the case of the pellet bed mixed with nut coke (40 wt%), the liquid dripping starts earlier, i.e., at a lower temperature (˜1500 °C) than the case when nut coke is absent (1518 °C). Additionally, in the nut coke mixed pellet bed, a steady rate of liquid dripping occurs, whereas from the pellet bed without nut coke a significant amount of liquid drops at the higher temperature (above 1542 °C).
- Substantial iron carburisation occurs in the liquid state, indicated by the difference in the carbon level of the quenched pellet and the dripped metal. In the case of the ferrous bed without nut coke, a high degree of iron carburisation takes place when liquid iron flows through the thicker regular coke layer. However, in the pellet bed mixed with nut coke, the degree of liquid state iron carburisation is observed to be lower due to the presence of a thinner regular coke layer.
- The addition of nut coke increases the kinetics of reduction and iron carburisation of the pellets. As a result, the degree of reduction (DOR) and gas (CO) utilisation increases with the nut coke mixing in the pellet bed. Furthermore, due to the limited liquid state carburisation, the total coke consumption decreases with the nut coke mixing in the pellet bed.
- The nut coke is effective as a replacement of regular coke for all investigated nut coke sizes and fractions. Also, the nut coke is consumed preferably compared to the regular coke.
- Similar physicochemical behaviour is observed for the pellet bed mixed with 15-20 mm and 20-25 mm sized nut coke. However, the ability to limit the bed contraction and to enhance the bed permeability increases with the nut coke size. It is also observed that the ability to reduce the iron oxide and to carburise iron, decreases with the increase in added nut coke size.

The experiment with the mixed ferrous burden of 60 % pellets and 40 % sinter revealed that the nut coke (20 wt% and 40 wt%) increases the permeability and high temperature properties of the ferrous bed.

- The mixed ferrous burden contraction also evolves through the three distinct stages, similar to the pellet only case. The first and third stage behaviour is dominated by both pellet and sinter, respectively. The second stage shows mixed properties of the pellet and sinter.
- In contrast to the pellet-only case, due to the sintering among the mixed ferrous burden (pellet and sinter), high resistance to the gas flow is observed. This results in a gradual loss of permeability across the bed, during softening (second stage of

contraction). Then, until the start of bed melting (T_m), the interaction between the sinter and pellet is seen to be limited only on the surface region. No bulk intermixing and melting are realised.

- In the presence of nut coke, the contacts within the ferrous burden (pellet and sinter) are physically hindered, limiting the sintering. Consequently, the bed softening temperature (T_s) increases (by 44 ^{o}C for 40 wt% nut coke). Also, due to the increased gas permeability in the presence of nut coke, the reduction degree of ferrous burden and carburisation of the freshly reduced iron decrease. As a result, the cohesive zone temperature range is decreased (by 77 ^{o}C for 40 wt% nut coke).
- Similar to the pellet-only bed, for the mixed ferrous burden, nut coke acts as a frame to substantially increase the gas permeability (inverse of S_P and S-value).
- A non-linear relationship is observed between the added nut coke concentration and various bed characteristics, like temperatures and contraction.

The development of physicochemical properties of the pellet and ferrous burden (pellet and sinter mixture) mixed with nut coke inspired the author to examine the effect of complete replacement of the regular coke with the nut coke. The behaviour of the pellet and ferrous burden is examined with a fully mixed nut coke of sizes 10-15 mm and 20-25 mm under simulated blast furnace conditions.

- Due to the intensified contact between the ferrous raw materials and nut coke, the degree of reduction and iron carburisation is enhanced.
- Interestingly, for the pellet and ferrous (pellet and sinter mixture) beds, fully mixed with nut coke (10-15 mm), no increase in the pressure drop is observed during the softening, melting and dripping of the ferrous material. The nut coke provides inter-particle voids, which allow the gas to flow freely across the bed. As a result, the bed permeability drastically increases under the fully mixed charged conditions.
- The chemical, thermal and mechanical functions performed by the coke in the blast furnace can be increased under complete mixed-charge conditions. However, for higher chemical utility, the mixed nut coke size should be kept similar to the size of the ferrous raw materials.

9.2 Recommendations for future work

- After the smelting experiments in the RSM with different nut coke replacement ratios, it was observed that a significant quantity of the nut coke is not consumed. Under the real blast furnace conditions, this unconsumed nut coke is expected to reach the hearth, which might affect the liquid permeability. Thus, thorough investigations (modeling and experimental) are required to understand the behaviour of unconsumed nut coke in the blast furnace hearth.

- The gas and thermal profiles vary also in the radial direction in the blast furnace, which might affect the rate and amount of nut coke utilisation. Therefore, a clear burden distribution scheme across the blast furnace radius and axis is required for the effective utilisation of the nut coke.
- A model can be devised with the help of reported data on bed characteristics to predict the physicochemical behaviour of the ferrous raw material bed mixed with nut coke in the real blast furnace.
- To increase the nut coke utilisation above and in the cohesive zone, methods such as enhancing the nut coke reactivity by doping it with fluxes (CaO, Fe_2O_3, etc.) can be investigated. Also, to limit the regular coke consumption, coke passivation with the use of reagents (B_2O_3, TiO_2, SiO_2, Al_2O_3, etc.) can be explored. Furthermore, the use of other carbon-rich agglomerates like briquettes and special pellets can be explored in combination with nut coke to increase reductant efficiency by increasing the length of the thermal reserve zone.
- Complete replacement of the regular coke with nut coke and mixing with the ferrous materials have shown the potential to improve the physicochemical properties of the ferrous raw material bed. However, understanding of the liquid dripping and hold-up behaviour is required, as the unsaturated liquid iron wets the coke surface, which might cause liquid accumulation inside the ferrous burden, i.e. the hold-up. Also, a detailed strategy is required to realise complete nut coke mixed charging in the blast furnace. For example, in the hearth to keep the deadman permeable, charging of the larger central coke can be tried along with the charging of fully nut coke mixed ferrous burden in the mid-radial and periphery area inside the blast furnace.

Summary

The principal objective of this work is to understand the physicochemical behaviour of the ferrous raw material (pellet and/or sinter) bed mixed with nut coke under the blast furnace conditions. To investigate this behaviour, a specially designed blast furnace simulator called the Reduction Softening and Melting (RSM) apparatus is utilised (Chapter 3). In the RSM, blast furnace conditions of gas (varying profile of CO-CO_2-H_2-N_2 gas mixture), load and temperature (20-1550 ^{o}C) were simulated for a stationary raw materials bed.

First, the pellet bed behaviour was investigated in the absence of nut coke. It was found that the shrinkage of the iron ore pellet bed evolves through three distinct stages. In the first stage, an indirect reduction takes place. Sintering, softening and iron carburisation evolve in the second stage. Then melting and dripping of the metal and slag occur at the third stage (Chapter 4 and 5).

After a series of experimental investigations, it was observed that mixing nut coke (10-15 mm) with the iron ore pellets affects all three stages of the bed contraction. The second stage temperature and displacement range are affected the most, being shortened due to enhanced reduction kinetics, limited sintering, less softening and a high degree of iron carburisation achieved in the pellets. Consequently, the cohesive zone temperature range is narrowed with the nut coke addition (10-40 wt%) in the pellet bed. Furthermore, during the pellet bed softening, melting and dripping, the pores and voids provided by the nut coke allow the gas flow across the bed to increase the gas permeability (represented by the inverse of area under the pressure drop curve). This increases the gas utilisation in the bed, increasing the degree of reduction (DOR) and iron carburisation of the pellets (Chapter 5).

To further understand the melting and dripping behaviour of the pellet bed in the presence of nut coke (40 wt%), a series of quenching and dripping experiments were performed in the RSM. It was confirmed that during the melting of the iron ore pellets, mixed nut coke acts as a frame to maintain the passage for the gas flow (Chapter 6).

Generally, the formed pellet shell (which is iron) in contact with the coke carburises, and eventually melts. In the absence of the nut coke, the contact between the pellet and coke occurs only at the layer interface. Consequently, the melting of the pellet occurs layer-wise. However, in a pellet bed mixed with nut coke, simultaneous melting of the layers occurs due to the multiple points of contact between the coke (nut coke and regular coke) and the pellets (Chapter 6).

Furthermore, the degree of iron carburisation (in solid state) is observed to be higher in the presence of nut coke. This results in a decrease of the melting temperature with an increased nut coke addition in the pellet bed. Thus, from the pellet bed mixed with nut coke (40 wt%), the liquid dripping starts earlier, i.e. at a lower temperature (˜1500 ^{o}C) compared

to the case when nut coke is absent (1518 ^{o}C). Additionally, from the nut coke mixed pellet bed a steady rate of liquid dripping occurs, whereas from the pellet bed without nut coke a significant amount of liquid drops at a higher temperature (above 1542 ^{o}C).

During the liquid dripping, a substantial degree of iron carburisation occurs, indicated by the difference in the carbon level in the iron of the quenched pellets and the dripped metal. In the case of a sample bed without nut coke, most of the carburisation takes place when liquid iron flows through the thicker regular coke layer. However, in the case of a pellet bed mixed with nut coke, due to the presence of a thinner regular coke layer, a lower degree of liquid state carburisation occurs. Interestingly, this also assists the lower (total) coke consumption from the bed mixed with nut coke. More importantly, the nut coke (10-15 mm) was observed to be utilised preferably instead of the regular coke (Chapter 5 and 6).

These investigations were extended for the pellet bed mixed with nut coke particle size of 15-20 mm and 20-25 mm as a replacement of the regular coke (10 wt% and 30 wt%). Similar physicochemical behaviour is observed for the pellet bed mixed with both additional size ranges. The ability to limit the bed contraction and to enhance the bed permeability increases with the nut coke size. However, the capacity of nut coke to improve the reduction kinetics and carbon utilisation decreases with the increase in the particle size (Chapter 5).

In an industrial blast furnace, based on the economical and chemical offset, a mixture of two or three types of iron-bearing raw materials is used (ferrous burden). Therefore, in the present work, the effect of nut coke addition is extended to the ferrous burden of the pellet (two types) and sinter mixture (60 % pellets, 40 % sinters). It is observed that the mixed ferrous bed contraction in this configuration also evolves through the three distinct stages. The first and third stage contraction behaviour are dominated by the pellets and sinter, respectively. The second stage shows mixed contraction properties, initially of the pellets and followed by that of sinter (Chapter 7).

In the absence of nut coke, it is observed that the sintering among the ferrous raw materials (sinter and pellets) restricts the gas flow, which results in a gradual loss of bed permeability. Then, a drastic increase in pressure drop occurs as a result of melting of ferrous raw materials. Nut coke physically hinders the contact among the ferrous burden, thus limiting the sintering, which increases the ferrous bed softening temperature (by 44 ^{o}C for 40 wt% nut coke). Further, the softening-melting temperature range (cohesive zone) decreases (by 77 ^{o}C for 40 wt%) with nut coke mixing (Chapter 7).

Due to the pores and the inter-particle voids provided by the mixed nut coke, a drastic increase in the gas permeability is observed. This increased permeability enhances the reaction kinetics to increase the degree of reduction (DOR) and carbon utilisation.

In general, the total coke requirement for the ironmaking blast furnace is decreasing with the increasing trend of auxiliary fuel injections (pulverised coal, natural gas, waste plastics, etc.). This may lead to the complete mixing of the coke with the ferrous raw materials. Foreseeing this, experiments with full nut coke mixed ferrous raw materials (pellet and/or sinter) were performed in the RSM, and the process promised the improved physicochemical properties for the mixed bed. Remarkably, during softening and melting of the ferrous burden no rise in the pressure drop occurs, when nut coke is mixed as the complete replacement of the regular coke. This shows that the pores and inter-particle voids provided by the nut coke could increase the gas permeability at the time of softening, melting and dripping of the ferrous material. The chemical, thermal and mechanical functions performed by the nut coke in the blast furnace can be increased under complete mixed charge conditions. However, for higher chemical utility, the mixed nut coke size should be kept similar to that of the ferrous raw materials size range (Chapter 8).

In conclusion, various experimental results give support for more extensive use of nut coke as a replacement of the regular coke in the ironmaking blast furnace.

Samenvatting

Het hoofddoel van dit werk is om het fysicochemische gedrag van kleintje kooks (Engels: nut coke) gemengd met ijzererts (in de vorm van pellets en/of sinter) te onderzoeken in een bed onder hoogovencondities. Om het gedrag van het ijzererts-pelletbed gemengd met kleintje kooks te onderzoeken is een speciaal ontworpen *Reduction Softening and Melting* (RSM; reductie, verweking en smelt) installatie gebruikt (Hoofdstuk 3). In deze RSM worden de hoogovencondities van gas (een veranderend profiel van CO-CO_2-H_2-N_2), mechanische belasting door de lading en de hoge temperaturen (20-1550 °C) gesimuleerd voor een stationair bed.

Als eerste is het pelletbed zonder kleintje kooks onderzocht. Daarbij is geconstateerd werd duidelijk dat het krimpen van het ijzererts-pelletbed in drie stappen verloopt. Eerst vindt indirecte reductie plaats. Daarna volgt sintering, verweking en opkolen van het ijzer in de tweede stap. In de derde stap smelt het metaal en druppelt het naar beneden (Hoofdstuk 3 en 5).

Uit de experimenten blijkt dat kleintje kooks (10-15 mm) gemengd met het ijzererts-pelletbed alle drie de stappen beïnvloedt. De temperatuur en de samendrukking in de tweede stap wordt het meest beïnvloed door kleintje kooks, vanwege verhoogde reductiekinetiek, beperkte sintering, verminderde verweking en de verhoogde opkolingsgraad van de pellets. Hierdoor wordt de bandbreedte van de temperatuur in de cohesieve zone versmald door de toevoeging van kleintje kooks (10-40 gew.%) aan het pelletbed. Ook wordt de gasdoorlaatbaarheid (in de vorm van drukval en de inverse S-waarde) verhoogd tijdens het verweken, smelten en de druppelvorming in het pelletbed, door de ruimtes en gangen veroorzaakt door kleintje kooks. Deze grotere gasbenutting in het bed verhoogt zowel de reductiegraad als de opkolingsgraad van de pellets (Hoofdstuk 5).

Om het smelt- en druppelgedrag van het pelletbed met kleintje kooks (40 gew.%) beter te begrijpen is een serie van afschrik- en druppelexperimenten uitgevoerd in de RSM. Hierbij is bevestigd dat tijdens het smelten van de pellets, kleintje kooks (dat in vaste vorm blijft) als het ware de doorstroomgangen voor het gas stut (Hoofdstuk 6).

In het algemeen zal de ijzeren schil van de pellet in contact met kleintje kooks opkolen en uiteindelijk smelten. Wanneer er geen kleintje kooks aanwezig is, zal zich een laag vormen tussen de kooks en de pellets. Hierdoor zal het smelten van de pellet laagsgewijs plaatsvinden. Wanneer echter kleintje kooks door het pelletbed gemengd wordt (40 gew.%), zal het smelten tegelijkertijd op meerdere contactpunten tussen de kooks (zowel kleintje kooks als reguliere kooks) en de pellets plaatsvinden (Hoofdstuk 6).

Het bleek dat de opkolingsgraad van het ijzerhoog is in de aanwezigheid van kleintje kooks. Dit betekent dat de smelttemperatuur van het pelletbed lager wordt naarmate er meer kleintje kooks aan wordt toegevoegd. Bij een pelletbed met kleintje kooks (40 gew.%) begint het druppelen eerder, bij een lagere temperatuur (˜1500 °C), dan bij een pelletbed zonder kleintje kooks, wat een smelttemperatuur van 1518 °C heeft. Bovendien is de druppelsnelheid stabiel bij een pelletbed met kleintje kooks, terwijl bij een pelletbed zonder kleintje kooks de druppelsnelheid significant toeneemt boven de 1542 °C.

Tijdens het druppelen vindt er een behoorlijke mate van opkolen van het ijzer plaats, hetgeen wordt aangetoond door het verschil in koolstofconcentratie tussen de afgeschrokken pellets en de ijzerdruppels. Bij een pelletbed zonder kleintje kooks vindt er verhoogde opkoling plaats als het vloeibare ijzer door de dikkere reguliere kookslaag stroomt. Doordat kleintje kooks een deel van de reguliere kooks vervangt, vindt er minder opkolen van het ijzer plaats in een pelletbed met kleintje kooks. Het is opvallend dat toevoeging van kleintje kooks aan het pelletbed ook leidt tot lagere kooksconsumptie in het algemeen. Nog belangrijker is dat uit de experimenten blijkt dat de reductiereactie en de opkolingsreactie in vaste vorm bij voorkeur plaatsvinden met kleintje kooks (10-15 mm) in plaats van met reguliere kooks (Hoofdstuk 5 en 6).

Het onderzoek is uitgebreid met het vervangen van de reguliere kooks in het pelletbed door kleintje kooks met een deeltjesgrootte van 15-20 mm en 20-25 mm (10 gew.% en 30 gew.%). In de pelletbedden met kleintje kooks van 15-20 mm en 20-25 mm groot, is een vergelijkbaar fysicochemisch gedrag geconstateerd. Naarmate de grootte van kleintje kooks stijgt, neemt ook de beperking van de samendrukking van het pelletbed en dus de permeabiliteit ervan toe. De mate waarin kleintje kooks de reductiekinetiek en koolstofbenutting verbetert neemt echter af bij een toenemende deeltjesgrootte (Hoofdstuk 5).

In een industriële hoogoven, gebaseerd op economische en chemische afwegingen, worden normaal gesproken twee of drie verschillende ijzerhoudende grondstoffen in gemengde vorm (de ijzermöller) gebruikt. Daarom is dit onderzoek uitgebreid met een ijzermöller van twee verschillende types pellets en van een mix van 60% pellets en 40% sinter. Ook hierbij is geconstateerd dat de samendrukking van het bed plaatsvindt in drie afzonderlijke stappen. De eerste en derde stap worden respectievelijk door de pellets en de sinter gedomineerd. De tweede stap laat de samendrukkingseigenschappen van beide zien, waarbij aanvankelijk de pellets en later de sinter domineren (Hoofdstuk 7).

In de afwezigheid van kleintje kooks blijkt dat samenklonteren (sinteren) van ijzerhoudend materiaal (zowel pellets als sinter) de gasstroom hindert, wat leidt tot een geleidelijke afname van de gasdoorlaatbaarheid van het bed. Vervolgens vindt er een enorme toename in drukval plaats wanneer de ijzerhoudende materialen beginnen te smelten. Doordat kleintje kooks het sinteren van ijzerhoudend materiaal fysiek hindert, wordt het sinteren beperkt en neemt de verwekingstemperatuur toe (met 44 °C bij 40 gew.%). Bovendien neemt de bandbreedte van de verwekings- en smelttemperatuur, de zogenaamde cohesieve zone, af als kleintje kooks wordt toegevoegd (met 77°C bij 40 gew.%) (Hoofdstuk 7).

Uit de experimenten blijkt dat, doordat kleintje kooks de doorgangen en de ruimtes tussen de deeltjes in het bed vergroot, de gasdoorlaatbaarheid (gemeten door de inverse S-waarde) significant toeneemt. Deze hogere doorlaatbaarheid verhoogt de reactiekinetiek, waardoor de reductie en de koolstofbenutting toenemen (Hoofdstuk 7).

De totale benodigde hoeveelheid kleintje kooks voor een hoogoven is omgekeerd evenredig met de hoeveelheid geïnjecteerde hulpbrandstoffen (zoals kolen, aardgas, gebruikt plastic, enz.). Dit kan leiden tot een volledige mix van de kooks en de ijzerhoudende grondstoffen. In de toekomst zal in hoogovens kleintje kooks mogelijk volledig worden gemengd met ijzerhoudende grondstoffen (pellets en/of sinter). Daarom zijn deze experimenten uitgevoerd in de RSM, waarbij geconstateerd is dat fysicochemische eigenschappen van het bed verbeterd worden. Opvallend is dat tijdens het verweken en smelten van de ijzermöller de drukval niet toeneemt, wanneer alle reguliere kooks vervangen worden door kleintje kooks. Dit laat zien dat de doorgangen en de ruimte tussen de deeltjes veroorzaakt door kleintje kooks de gasdoorlaatbaarheid verhoogt tijdens het verweken, smelten en druppelen van het ruwijzer. Wanneer de lading (kleintje kooks en ijzerhoudende grondstoffen) volledig gemengd wordt, kunnen de chemische, thermische en mechanische effecten van kleintje kooks nog worden vergroot. Voor een hogere chemische beschikbaarheid moet echter de stikgrootte van kleintje kooks gelijk worden gehouden aan de stukgrootte van de ijzerhoudende grondstoffen (Hoofdstuk 8).

Uit de verschillende experimentele resultaten blijkt dat er meer kleintje kooks kan worden gebruikt in plaats van de reguliere kooks in het hoogovenproces.

Curriculum Vitae

05/2019 - 12/2019	PhD Researcher Group of Metals Production, Refining and Recycling Materials Science and Engineering Delft University of Technology, The Netherlands
05/2015 - 05/2019	PhD Scholar Group of Metals Production, Refining and Recycling Materials Science and Engineering Delft University of Technology, The Netherlands
08/2011 - 04/2015	Researcher Iron and Ferro Alloys Research Group Research and Development, Tata Steel Jamshedpur, India
07/2009 - 07/2011	Masters of Engineering, Materials Engineering Indian Institute of Science, Bangalore, India
07/2005 - 06/2009	Bachelor of Technology, Metallurgical Engineering National Institute of Technology, Raipur, India

List of publications

Published journal articles

- Dharm Jeet Gavel, Allert Adema, Jan van der Stel, Jilt Sietsma, Rob Boom and Yongxiang Yang, *Melting behaviour of iron ore pellet bed under nut coke mixed charge conditions*, ISIJ International, 2020, 60 (3).
- Dharm Jeet Gavel, Allert Adema, Jan van der Stel, Jilt Sietsma, Rob Boom and Yongxiang Yang, *Effect of nut coke addition on the physicochemical behaviour of the pellet bed in ironmaking blast furnaces*, ISIJ International, 2019, 59 (5), 778-786.
- Dharm Jeet Gavel, Qingshi Song, Allert Adema, Jan van der Stel, Jilt Sietsma, Rob Boom and Yongxiang Yang, *Characterization of the burden behaviour of iron ore pellets mixed with nut coke under simulated blast furnace conditions*, Ironmaking and Steelmaking, 2018, DOI: 10.1080/03019233.2018.1510873.
- Dharm Jeet Gavel, *A review on nut coke utilisation in the iron-making blast furnaces*, Materials Science and Technology, 2017, 33, 381-387.

Conference articles in proceedings

- Yongxiang Yang, Dharm Jeet Gavel, *Fundamental studies on blast furnace and alternative ironmaking technologies towards reduced carbon footprint*, Innovation of ironmaking technologies and future international collaboration - the 54th committee on ironmaking of Japan society for promotion of science, Tokyo, November 2019.
- Dharm Jeet Gavel, Cees Kwakernaak, Allert Adema, Jan van der Stel, Jilt Sietsma, Rob Boom and Yongxiang Yang, *Carburisation and melting behaviour of iron ore pellet bed under nut coke mixed charge conditions*, Estad and Metec, Dusseldorf, June 2019.
- Dharm Jeet Gavel, Allert Adema, Jan van der Stel, Jilt Sietsma, Rob Boom and Yongxiang Yang, *Physicochemical behaviour of olivine iron ore pellets mixed with nut*

coke under simulated blast furnace conditions, ICSTI 2018, Vienna, September 2018, 523-529.

- Dharm Jeet Gavel, Qingshi Song, Allert Adema, Jan van der Stel, Jilt Sietsma, Rob Boom and Yongxiang Yang, *Characterisation of iron ore pellet behaviour under nut coke mixed charge conditions*, Science and technology of ironmaking and steelmaking, IIT Kanpur, December 2017, 315-318.
- Dharm Jeet Gavel, Qingshi Song, Jilt Sietsma, Jan van der Stel, Rob Boom, Yongxiang Yang, *Optimum nut coke for the blast furnaces*, Scanmet, Lulea, June 2016.

Acknowledgements

In the year 2015, I took two best decisions of my life. First, offcourse is of getting married and second to pursue this Ph.D. Both of these decisions have completely transformed my life. On one hand, after marriage, I am evolved as a better social person. On the other hand, Ph.D. has augmented my professional abilities. The Ph.D. journey was very pleasant because of the wonderful people around me. I would like to thank them all for being so kind and helpful to me.

First of all, I would like to thank my promotors dr. Yongxiang Yang and prof. Jilt Sietsma for their constant guidance and encouragement. I am grateful, especially to dr. Yang for giving me a lot of freedom and technical guidance during the course of this Ph.D. work. My sincere thanks to prof. Sietsma for improving my data interpretation skills by his critical views on my research data.

My acknowledgement to the mentor of our MPRR (Metals Production, Refining and Recycling) research group, prof. Rob Boom, for constantly motivating me and challenging me to repeat the experiments. I learned a lot about the steel industries (globally), from the rich knowledge and experience of prof. Boom.

This Ph.D. program is carried out in close collaboration with the M2i (Materials innovation institute) and Tata Steel Europe (Netherlands). I thank our research partner Tata Steel for their suggestions to increase the credibility and utility of our research apparatus and results. I especially thank Jan van der Stel (Knowledge group leader ironmaking, Tata Steel Europe) for constantly encouraging and challenging me, which helped me to scale up my technical abilities. I am thankful to Allert Adema and Lucas Bleijendaal of Tata Steel (IJmuiden) for coordinating the project and providing me the technical know-how of the process. I am grateful to Tim Peeters, Bert Gols, James Small, Varsha Pridhivi, Stefan Born, Johannes Hage, Jim Post, Yanping Xiao, Chris Treadgold and other members of Tata Steel (IJmuiden) for the fruitful discussions, which helped to increase my technical insight about the blast furnace process. I would like to extend my sincere gratitude to dr. Sanjay Chandra (CRDSS), dr. Samik Nag and my ex-colleagues of Tata Steel India (Jamshedpur) for providing me a very nice learning opportunity (at TSI) and motivating me to pursue the Ph.D. study. I acknowledge dr. Victoria Savran of M2i for smooth management of this project.

My sincere regards to Frank Schrama for being a very nice friend, colleague, officemate, paranymphs and introducing me with Dutch culture. I am indebted to Zhiyuan Chen for being very generous and always at my disposal for any kind of help. This Ph.D. study would have not been possible without the assistance of Sander van Asperen, Kees Kwakernaak, Remko Seijffer, Hans Hofman, Michel van den Brink, Ruud Hendrix, Niek van der Pers, Olaf Voorwinde, Prisca Koelman and Saskia Brandt Corstius, all of Delft university of technology.

I express gratitude to my colleagues and friends Prakash-Pavitra, Aida, Zhi-Xiaoling, Yang, Sebastian, Tim, Evangelos, Ashkan, Zhiyuan-Zhiyou, Chentang, Bala, Sudhindra, Ali, Qiang, Devi, Jantsje, Sylvia, Gautam-Sakshi, Syam-Ranjani, Shivraj-Rama, Chenna, Ankit, Srikanth-Jhilmil and Bapin-Sharmistha for being with me in my Ph.D. journey.

My greatest gratitude to my mother, who always inspired me to excel in life. I was able to do this because of you mummy, I miss you. I am grateful to my father, brother and to my in-laws, for being caring and supportive to me. Now, coming back to the first best decision of my life to marry Chandrakanta Gavel, thank you so much for your unconditional love for me.